UNIVERSIDADE FEDERAL DE SÃO CARLOS
CENTRO DE CIÊNCIAS EXATAS E DE TECNOLOGIA
DEPARTAMENTO DE QUÍMICA
PROGRAMA DE PÓS-GRADUAÇÃO EM QUÍMICA

"Synthesis, structural diversification, biological activities and biotransformation of dibenzylacetones: simple chemistry furnishing potent compounds"

Zia Ud Din*

Thesis Submitted to the Federal University of Sao Carlos for the Degree of Doctor of Science, in Organic Chemistry

Supervisor: Prof. Dr. Edson Rodrigues Filho
* Awardee (TWAS/CNPq)

São Carlos - SP
2016

UNIVERSIDADE FEDERAL DE SÃO CARLOS

Centro de Ciências Exatas e de Tecnologia
Programa de Pós-Graduação em Química

Folha de Aprovação

Assinaturas dos membros da comissão examinadora que avaliou e aprovou a Defesa de Tese de Doutorado do candidato Zia Ud Din, realizada em 23/02/2016:

Prof. Dr. Edson Rodrigues Filho
UFSCar

Prof. Dr. Edson Roberto da Silva
FZEA/USP

Prof. Dr. Tiago Venâncio
UFSCar

Profa. Dra. Cíntia Duarte de Freitas Milagre
UNESP

Prof. Dr. João Batista Fernandes
UFSCar

بِسْمِ اللهِ الرَّحْمٰنِ الرَّحِيمِ

IN THE NAME OF ALLAH

THE COMPASSIONATE

THE MERCIFUL

"We made every living thing from water,

Will they not then believe?"

(AL-QURAN, SURA ANBIYAH 21, AYAH 30).

AN ADORE TO

MY PARENTS

Memorandum

The research presented in this thesis has been carried out in Laboratório de Bioquímica Micromolecular de Microorganismos - LaBioMMi at the Department of Chemistry Federal University of São Carlos, São Carlos SP Brazil, between March 2012 and March 2016. This thesis presents the original work of the author unless stated elsewhere and otherwise. Additionally, none of this work has been submitted for any other degree prior to this.

Acknowledgement

Abbreviations

BA	Brønsted acid
COSY	Correlation spectroscopy
DMF	Dimethylformamide
DMSO	Dimethylsulfoxide
ee	Enantiomeric excess
HB	Hydrogen bonding
HSQC	Heteronuclear single-quantum correlation
HMBC	Heteronuclear multiple bond correlation
LB	Lewis base
NOE	Nuclear overhauser effect
NMR	Nuclear magnetic resonance
DIMCARB	Dimethyl ammonium dimethyle carbamate
1D	One-dimensional
2D	Two-dimensional
D_2O	Deuterium oxide
HPLC	High performance liquid chromatography
IR	Infrared
UV	Ultra Violet
Min	Minute
LC	Liquid chromotography
MW	Molecular weight
DFT	Density functional theory
HOMO	Highest occupied molecular orbitals
LUMO	Lowest unoccupied molecular orbitals
SAR	Structure activity relationship

IC$_{50}$ Half minimal inhibitive concentration

EC$_{50}$ Half minimal effective concentration

FMN   Flavine mano nucleotide

List of Tables

List of figures

List of Schemes

Abstract

"Synthesis, structural diversification, biological activities and biotransformation of dibenzylacetones: simple chemistry furnishing potent compounds"

The structural diversity of known compounds holding two benzene rings directly connected to each other (Bis-phenyl), or separated by a carbon-chain (Bis-arylalkane), is nowadays generated intensive scientific studies across the world. Some of them are very renowned for their important biodynamic activities for human beings. For instance, the natural occurring classes of substances Stilbene (Bis-arylethene), Chalcone (Bis-arylpropenone) and Curcumin (Bis-arylheptene) have been subject of deep studies in literature due to their pharmacological activities such as antimicrobial, anti-inflammatory, anti-tumor, antioxidant and anticancer. Almost all of these compounds have in common the amino acid phenylalanine as biosynthetic precursor. In this work, we seek to give a concise overview of their structures diversity, occurrence, chemistry and the bioactivities of dibenzylacetones established. The effort to synthesize these compounds and their congeners and its modification with good pharmaceutical profile were carried. We have studied the anti-parasitic activity of all these synthesized compounds and found some potent compounds. The mechanistic study show that enzyme inside parasite reduces the C=C bonds in synthesized dibenzylacetones and leading to more potency which alter redox system of parasite, which result increase of nitrogen and oxygen species and interfere mitochondria function, which ultimately causes death of parasite. Although the literature contains only limited computational studies on these compounds, it can be predicted good and differential π-π interactions of aromatic rings of these compounds with aromatic

amino acids in enzymes. We have made an effort to explain our results in the result of docking and DFT analysis.

Resumo

"Síntese, diversidade estrutural, atividade biológica e biotransformação dodibenzalacetona: química simples fornecendo compostos potentes"

A diversidade estrutural de compostos conhecidos contendo dois anéis de benzeno diretamente ligados uns aos outros (bis-fenil), ou separadas por uma cadeia de carbono (Bis-arylalkane), atualemente alvo de intensos estudos científicos em todo o mundo. Alguns deles são muito famosos por suas atividades biodinâmicas importantes para os seres humanos. Por exemplo, as classes que ocorrem naturalmente de substâncias Stilbene (Bis-arylethene), chalcona (Bis-arylpropenone) e curcumina (Bis-arylheptene) têm sido objeto de estudos aprofundados na literatura, devido às suas atividades farmacológicas, tais como antimicrobianas, anti-inflamatórias, anti-tumoral, anti-oxidante e anti-cancerígeno. Quase todos estes compostos têm em comum o aminoácido fenilalanina como precursor biossintético. Neste trabalho, procuramos dar uma visão concisa de suas diversidade estrutural, ocorrência, química e as atividades biológicas estabelecidas. O esforço para sintetizar estes compostos e os seus congéneres e sua modificação para uma variedade de novos heterociclos com bom perfil farmacêutico também são concebidos e discutidos à luz do nosso conhecimento atual. Nos temos estudado a atividade anti-parasitária de todos estes compostos sintetizados e encontramos alguns compostos potentes. O mecanismo do estudo demonstra que enzima dentro do parasita reduz as ligações C = C em curcuminoids sintetizados levando à uma maior potência capaz de alterar o sistema redox do parasita, que resultam aumento de espécies reatives de nitrogênio e oxigênio e interfere na função mitocôndria, causando a morte de parasita. Embora a literatura contenha apenas estudos computacionais limitados sobre estes compostos, é possível prever

boas e diferenciais interacções π-π de anéis aromáticos destes compostos com aminacidos aromáticos em enzimas. O separador inter aneis bisarylalkanoid é capaz de realizar esta interação porém limitada. Estas características foram discutidas neste estudo.

Summary

Part 1

1. INTRODUCTION

Natural substances containing benzene ring in their molecular structures are abundant in nature. Among them, bisarylalkanoids have generated intensive scientific studies. From structural point of view, these "Bisaryl" compounds are congeners of at least three classes of important natural products stilbenes, chalcones, and cucurmins. A good series of ArC_nAr', with n varying from zero to seven is formed (FIGURE 1.1) by grouping these compounds on the basis of carbon chain (C_n). The size of carbon chain (C_n), which acts as inter-ring spacer separates two benzenoid rings (Ar and Ar'). Numerous studies have been conducted, by various natural product chemist, synthetic organic chemist and pharmacologists, on the inter-ring spacer bisarylalkanoids.
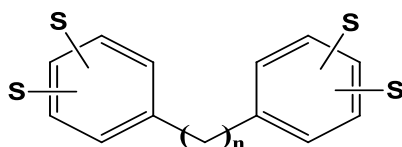
n = 0: Bisphenyls (ArC_0Ar')
n = 1: 1,1-Bisarylmethane (ArC_1Ar')
n = 2: Stilbenes (1,2-Bisarylethane, ArC_2Ar')
n = 3: Chalcones (1,3-Bisarylpropane, ArC_3Ar')
n = 4: 1,4-Bisarylbuthanes (ArC_4Ar')
n = 5: 1,5-Bisarylpenthanes (ArC_5Ar')
n = 6: 1,6-Bisarylhexanes (ArC_6Ar')
n = 7: Cucurmins (1,7-Bisarylheptanes, ArC_7Ar')

FIGURE 1.1- General formulas for Bisphenyl and Bisarylalkanoid.

All ArC_nAr' has a common biosynthetic origin from phenylalanine that leads to cinnamate cascade (SCHEME 1.1) except ArC_1Ar' and ArC_6Ar' series. ArC_1Ar' series is probably formed in nature by reductive ring opening of xanthones, while ArC_6Ar' are not found as a natural compound instead is synthesized from inspiration by gingerol. Gingerols are another very important bioactive natural products produced by *Zingiber* species. Stilbenes (ArC_2Ar'),

chalcones (ArC$_3$Ar´), gingerols and cucurmins (ArC$_7$Ar´) seem to be biosynthesized during anabolic phase from phenylalanine. Phenylalanine has benzene ring which oxidize generally at C-4 and C-5, and thio esterified by coenzyme-A, generating a key intermediate 4-cinnamate-SCoA (4CSCoA). In almost all plants, the intermediate 4CSCoA is converted into flavonoids. Flavonoid is one of the most abundant classes of natural product which can be enzymatically accumulated as chalcones (ArC$_3$Ar´). Depending on the producing organism, 4CSCoA can be further attached to polyketide chains of different sizes or other thioacyl groups to form stilbenes, gingerols and cucurmins. Compounds ArC$_0$Ar´ (Bisphenyl) are generally lignans, and the rare ArC$_4$Ar´ and ArC$_5$Ar´ appear to be formed during catabolism by decarboxylations of lignans or lignans-intermediaries.
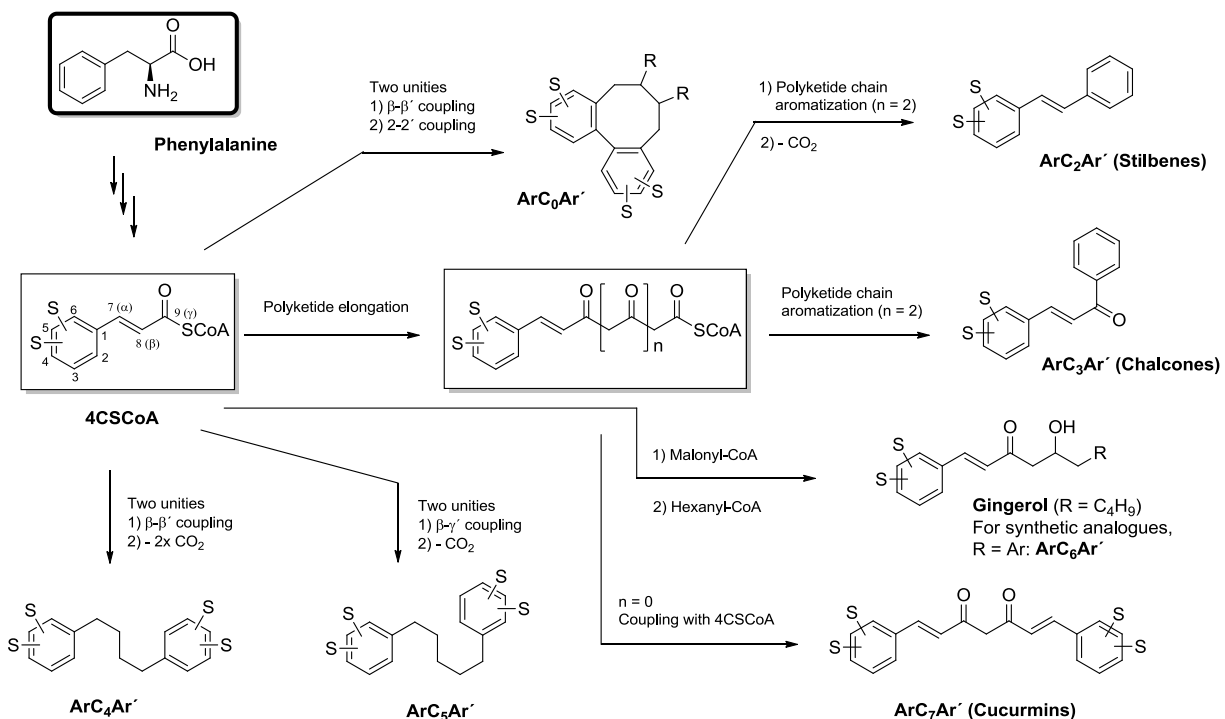
Scheme 1.1- Summary of biosynthetic pathway for compounds ArC$_n$Ar´.

The objectives of this research are to highlight the significant and ongoing body of research on inters-ring spacer diarylalkanoids. A detailed literature about some individual classes has been focused which covers all aspects of these classes and their bioactivity. The future of inter-ring spacer diarylalkanoids produced by natural sources or synthesized is bright and iridescent due to its attractive chemistry and pharmacophoric potential. The new compounds will offer a host of exciting direction for both pure and applied research.

1.1 Chalcone

Chalcone (FIGURE 1.2) consist of two aromatic rings connected by a three carbon α, β -unsaturated carbonyl group. Chalcones considered as the precursor of flavonoids and isoflavonoids abundantly found in plants, and also have been shown to exhibit a diverse array of pharmacological activities. The enone linkage presents in basic structure play crucial role for the activity of chalcone and chalcone derivatives. Chalcone attracted attention because of their pharmacological activities such as Antiangiogenic effects (MOJZIS et al., 2008), anti-tumor (QI et al., 2014), anti-viral (DE CAMPOS-BUZZI et al., 2006), anti-inflammatory (BANDGAR et al., 2010), anti-fungal (LAHTCHEV et al., 2008), anti-cancer (MAI et al., 2014), anti-nematodal (ATTAR et al., 2011), anti-plasmodial (WU et al., 2006), anti-tuberculosis (MASCARELLO et al., 2010), anti-platele (ZHAO et al., 2005), and Anti-HIV (WU et al., 2003). Several review has been published about the chemistry, synthesis and medicinal properties of chalcone (AKSÖZ et al., 2011). Which explain several pharmaceutical activity of chalcone and its derivatives. Researchers are very interested in such a structure because it has magic property due to special

conjugation. Phenyl alanine is the precursor of chalcone and leads the basic skeleton of it.

1.1.1. Synthesis of Chalcone

Chalcone can be synthesized in different synthetic methodology from various aldehyde and ketone. A number of synthetic routes have been described for synthesis of chalcone. The general synthesis involves Claisen Schmidt and aldol condensation (SHEME 1.2). Condensation takes place under homogeneous conditions in the presence of acid or base (IRANPOOR; KAZEMI, 1998). Traditionally, strong alkaline media including natural phosphates, $Ba(OH)_2$, have been employed for their synthesis (SEBTI et al., 2002). The use of several acids and bases has also been demonstrated. Ultrasound radiation and solvent free condition is also been used for pharmacological chalcone building block (LI et al., 2002).
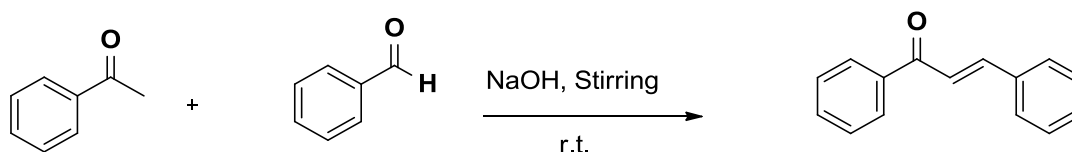
SCHEME 1.2- General procedure for chalconesynthesis

Different researcher are trying in modification of existing synthetic methods by changing catalyst, solvent or using other catalytic moiety. S Kumar et al. applied simple, rapid, efficient and environmentally benign procedure for the synthesis of pharmaceutically important chalcone (SCHEME 1.3). The synthesis is carried by grinding aryl aldehydes and acetophenones with anhydrous barium hydroxide (C-200) in the absence of solvent (KUMAR;

LAMBA; MAKRANDI, 2008). The use of organic solvent for extraction of compound is also avoided. This methodology is highly useful for the synthesis of 2-hydroxy chalcones.
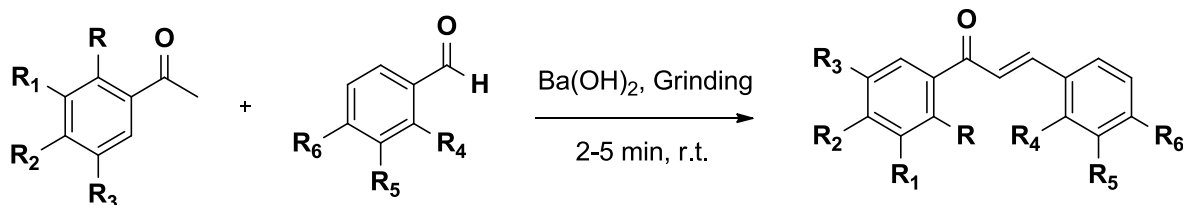
SCHEME 1.3 - Procedure for the synthesis of chalcone derivatives.

This methodology is preferred on the other conventional method due to reaction time. The reaction time is significantly less as compared to other method. Edmont V. Stoyanov *et al.* condensed 20-hydroxyacetophenone with aromatic aldehydes in a well closed vessel using microwave irradiation or classical heating at 132 C°, affords a fast and simple method for the liquid-phase synthesis of 20-hydroxychalcones (STOYANOV; CHAMPAVIER; BASLY, 2002).

Adding more about the effect and medium of reaction amino propylated nanosilica was prepared by a simple sol–gel process from tetraethyl orthosilicate (TEOS) and then it was functionalized with different quantities of 3 amino propyltriethoxysilane (APS) under toluene reflux. The materials were used as catalyst in the Claisen–Schmidt preparation of chalcones for the reaction of substituted acetophenones and benzaldehydes under solvent-free conditions (SCHEME 1.4). The result exhibited that the presence of a high amount of aminopropyl groups was significant for a very good performance of the catalyst in the substrate conversion (ROMANELLI et al., 2011).
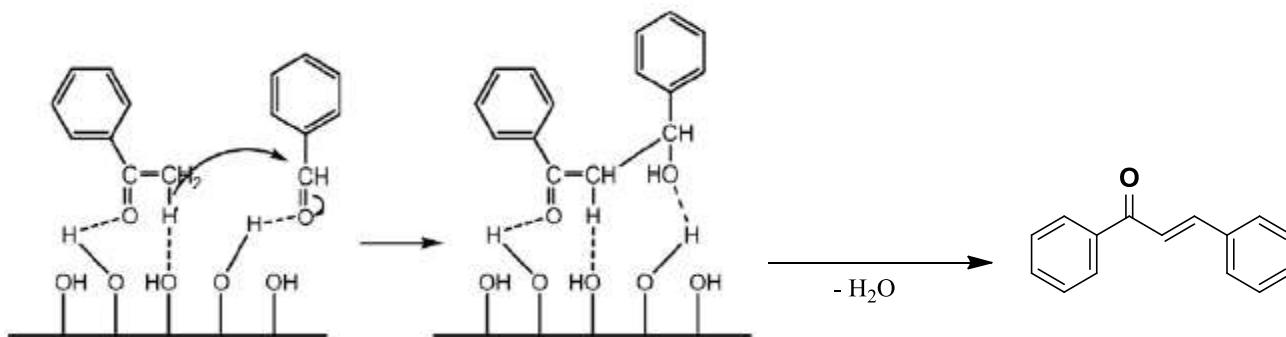
SCHEME 1.4- Proposed mechanism of chalcone synthesis catalyzed by silica-sol gel.

Ognyan Petrov *et al*. used thionyl chloride in ethanol as a catalytic for the synthesis of chalcone. In this method various substituted chalcone were synthesized by aldol condensation. The HCl is produced in situ by the reaction of $SOCl_2$ with absolute ethanol (PETROV; IVANOVA; GEROVA, 2008). Nasser Iranpoor and Foad Kazemi used metal catalyst (Anhydrous $RuCl_3$) for aldol condensation of aldehyde and ketone for getting chalcone analogous (IRANPOOR; KAZEMI, 1998). Regio selective self condensation reaction of some ketones and aldehydes were also described. The catalytic effect of Ru(III) is shown by performing similar reactions under thermal conditions without catalyst.

Said Eddarir *et al*. produced a general method for the synthesis of chalcones based on the Suzuki reaction between cinnamoyl chlorides and phenylboronic acids or between benzoyl chlorides and phenylvinylboronic acids (EDDARIR et al., 2003). The reaction is not affected by substituents found either on the acyl chloride or on the boronic acid which opens the way to

a general synthesis of chalcones. The whole synthetic procedure is shown (SCHEME 1.5).
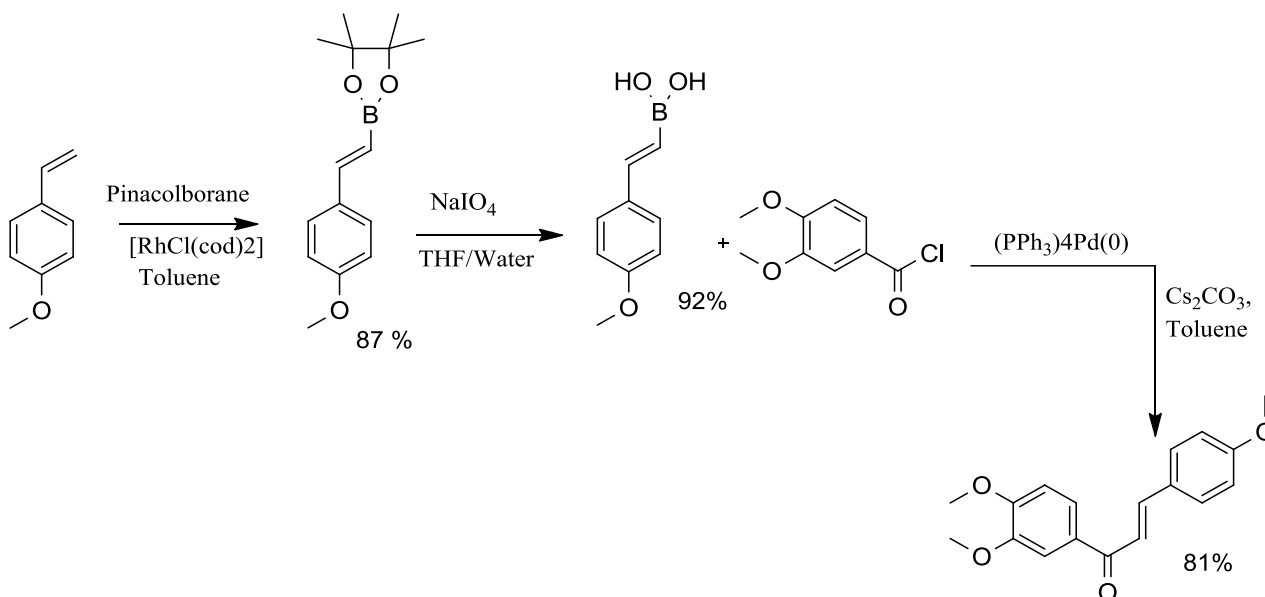
SCHEME 1.5 - Synthesis of chalcone by Suzuki Coupling.

1.1.2. Biological activity of Chalcone

1.1.2.1 Anti-Malarial activity

In developing countries protozoal diseases such as malaria, amoebiosis, sleeping sickness, leishmaniasis and others are prevailing and are of great concern. The malarial diseases are still a devastating disease due to unsuitable medication, especially *Plasmodium malaria*, *Plasmodium ovale*, *Plasmodium falciparum*, and *Plasmodium vivax*. Among all these agents, *P. falciparum* resistance to common antimalarials is a major obstacle for malaria control (NOWAKOWSKA, 2007a). Licochalcone A isolated from Chinese liquorice roots, has been studied in literature (CHEN et al., 1994) as highly effective in

an in vitro screen against chloroquine-susceptible (3D7) and chloroquine-resistant (Dd2) *P. falciparum* strains in a [3H] hypoxanthine uptake assay.

Parvesh Singh *et al.* synthesized acridinyl chalcone derivative by refluxing in alcohol (TOMAR et al., 2010). In a result a series of novel chalcones bearing acridine moiety attached to the amino group in their ring A was prepared. The reaction is non catalyzed nucleophilic aromatic substitution between various 30-amino chalcone or 40-amino chalcones and 9-chloro acridine (SCHEME 1.6). Although, all the synthesized compounds inhibited full parasite growth at micro-molar concentration, Compound **1**, **2** and **8**, bearing -OCH3 substituent at ring A inhibited 86%, 71% and 14.3% parasite maturation at concentrations 2 mg/mL, 0.4 mg/mL and 0.08 mg/mL, respectively. The most potent compounds did not show activity against *P. yoelii* under in vivo conditions.

1. R_2 = H
2. R_2 = 4-OCH$_3$
3. R_2 = 4-Cl

4. R_2 = H,   5. R_2 = 3-NO$_2$
6. R_2 = 3-CH$_3$,   7. R_2 = 4CH$_3$
8. R_2 = 4-OCH$_3$, 9. R_2 = 3,4,5-OCH$_3$
10. R_2 = 4-Cl
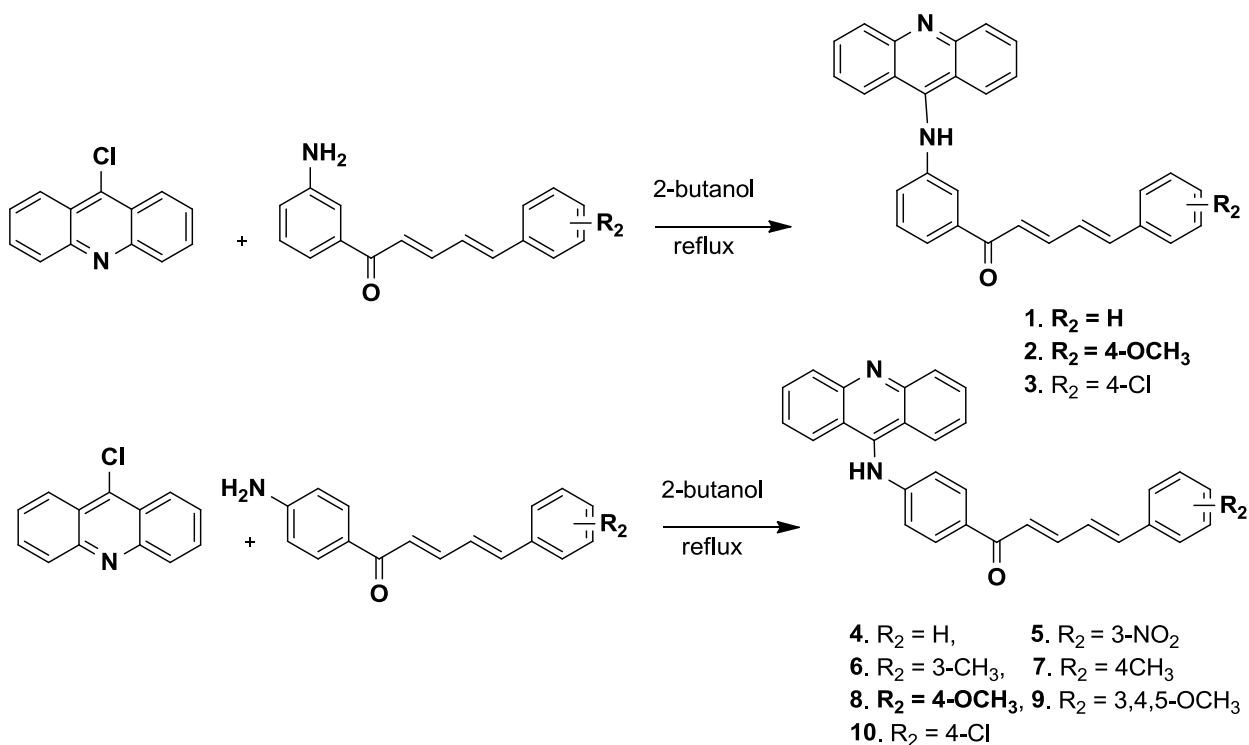
SCHEME 1.6 - Synthesis of 1-(4-(9-acridinylamino)phenyl)-3(substituted) phenylprop-2-en-1-one.

Compounds **1**, **2** and **8** compounds showed potent activity. These new chalcone derivatives showed much enhanced activity relative to other chalcone derivatives. Three compounds (**16**, **17** and **23**) were further screened for in vivo efficacy against a chloroquine-resistant rodent malaria parasite *Plasmodium yoelii* (strain N-67) in Swiss mice model. In the potent compounds it is observed that two compounds **2** and **8** having methoxy substituent's, significantly increases the activity.

1.1.2.2 Anti-Inflammatory activity

Many research explain the synthesis and anti-inflammatory activity of chalcone (BANDGAR et al., 2010). While various chalcones like naturally occurring, sappan chalcone (**11**), licochalcones (**12**) and butein (**13**) (Fig 37) are known to exhibit potent anti-inflammatory activity (NOWAKOWSKA, 2007b; BANDGAR et al., 2010). Chalcone having cyclohexyl group **14** (FIGURE 1.3) showed potent anti-inflammatory activity due to the formation of hydroperoxides. The computational studies of these compounds having more electron donating potentials (higher HOMO) are better inhibitors of hydro peroxides as exhibited by 63% as compared to aspirin (66%) (ACCHE et al., 2008).
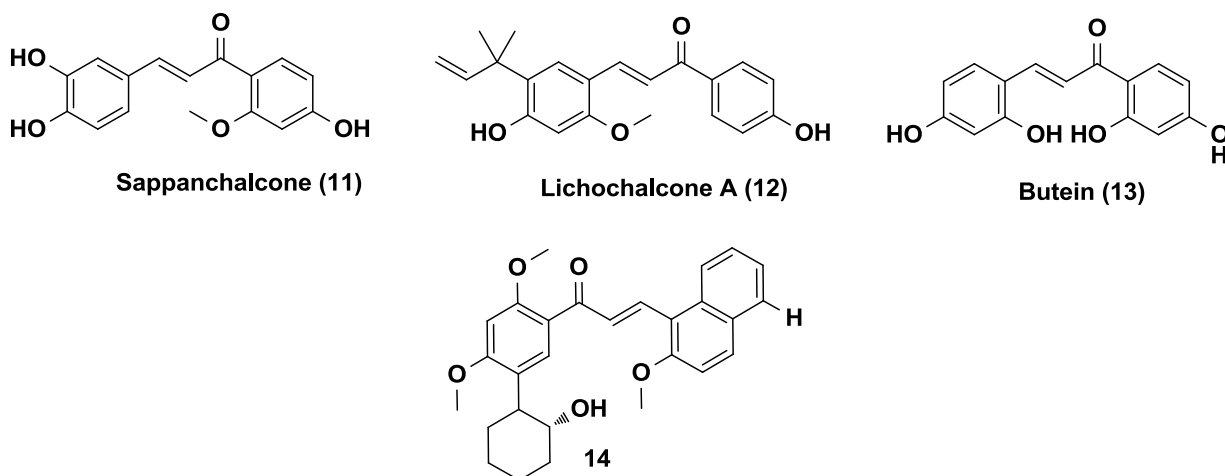
FIGURE 1.3 - Electron donating chalcone as potent active moiety.

Further studying the structure activity relationship it is observed that various substitution on chalcone also play a key role in anti-inflammatory activity. The SAR studies on Chalcone derivatives related to electron donating moiety on chalcone demonstrated that the inhibitory activity was due to the 4-hydroxy group and the possible co-planarity between the phenyl rings and the adjacent conjugated ketone (SHIGEO et al., 2001). Cheng *et al.* reported that broussochalcone A (FIGURE 1.4) silent up concentration-dependent production of NO, with an IC_{50} value of 11.3 µM in LPS-activated macrophages. The experimental data proposed that this compound exerted potent inhibitory effects on NO production facilitated by its suppression of IkBα phosphorylation, IkBα degradation, NF- kB activation and iNOS expression rather than openly on the enzymatic activity of iNOS (CHENG et al., 2001). The in-vitro experiments pointed out those compounds **15-17** to be an inhibitor of the NF-kB pathway of cellular activation in macrophages. A therapeutic oral administration of compound (25 mg/kg) on days 17–24 after adjuvant injection, in the rat adjuvant-induced arthritis model, gave a mass of effects including significant

inhibition of paw oedema, defense from weight loss and reduction of the levels of inflammatory (ROJAS et al., 2003).
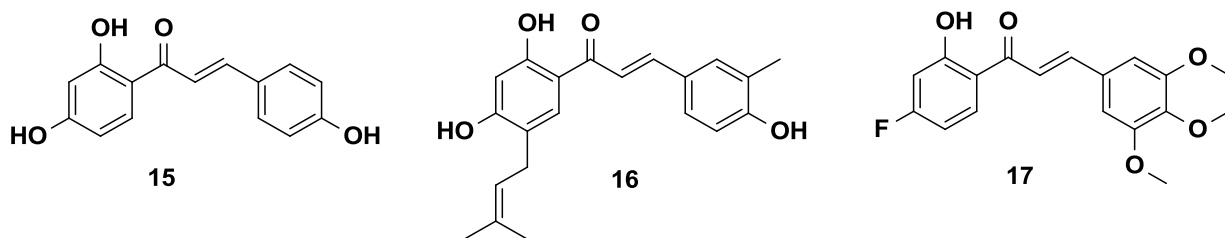
FIGURE 1.4 - Effect of substituents on activity of chalcone.

1.1.2.3 Anti-Cancer activity

Chalcones have attracted much attention due to their diverse range of biological activities including anti-cancer. Cancer is one of the major roots of death worldwide. The number of patients diagnosed with different types of cancer has almost doubled in last three decades, and is expected to increase even higher in coming years if new efficient treatment methods were not developed. As chalcones consist of two aromatic rings connected by an α,β-unsaturated carbonyl group and it has been shown that the elimination of α,β -unsaturated carbonyl system could hinder their biological activities (SAHU et al., 2012). A number of synthetic modifications, such as oxathiolone fused (KONIECZNY et al., 2007), monosubstituted, methoxylated substituted, boron substituted (ACHANTA et al., 2006), heterocyclic infused (REDDY et al., 2008), biphenyl based (SHARMA et al., 2010), imidazolones linked, coumarin based chalcones (SASHIDHARA et al., 2010) or other substitutions chalcone have also reported to affect the biological activities including anticancer activities of chalcones. Sashidhara *et al.* synthesized a series of coumarin–

chalcone hybrids and evaluate it for their in vitro cytotoxicity against a panel of four human cancer cell lines and normal fibroblasts (NIH3T3). Among 21 compounds screened, three compounds (**18-20**) (FIGURE 1.5) showed IC_{50} range from 3.59 to 8.12 µM. The most promising compound showed around 30 fold more selectivity towards C33A (cervical carcinoma) cells over normal fibroblast NIH3T3 cells with an IC_{50} value of 3.59 µM. The presence of ester moiety, especially methyl ester at position 3 and coumarin ring were believed to be crucial for the anti-cancer activity of these compounds. From this work it is observed that pharmacophore such as α,β unsaturated system and coumarinemoiety is crucial for activity. Therefore, a single molecule containing more than one pharmacophore, each with different mode of action could be beneficial for the treatment of cancer (SOLOMON; HU; LEE, 2009).
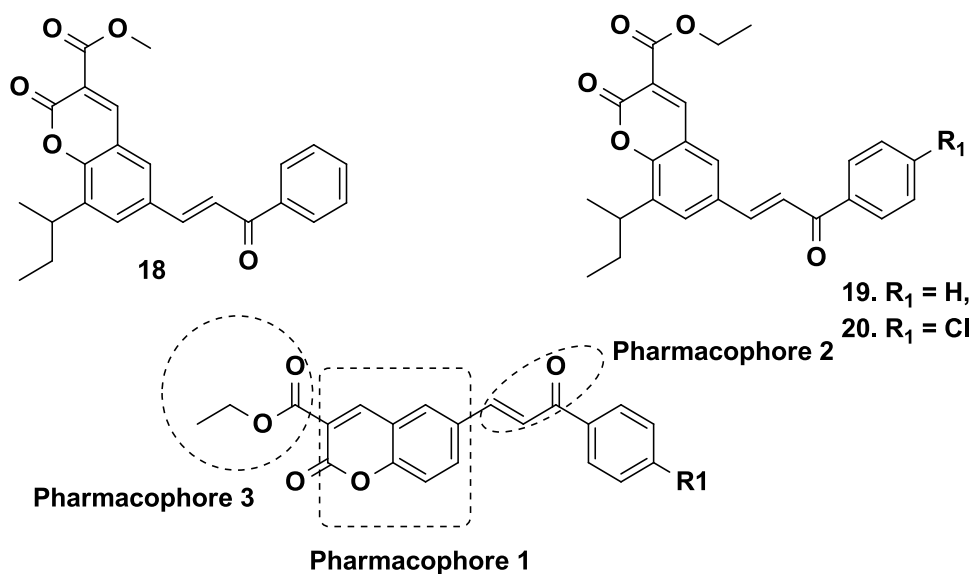
FIGURE 1.5 - Compounds showing potent anti-cancer activity.

Further study revealed that the cytotoxicities correlate moderately well with their NF-κB inhibitory activities, suggesting that suppressing NF-κB

activation is likely responsible for at least some of the cytotoxicities. Balasubramanian Srinivasan *et al.* explored the structure-activity relationship (SAR) of a series of chalcone-based compounds regarding their NF-κB inhibitory activities by using a luciferase- based in vitro NF-κB reporter assay with the objective to determine the essential functionalities on the chalcone core for NF-κB inhibition. The lead compound with low micro molar inhibitory activity was evaluated for its inhibitory activities against kinases upstream of NF-κB and in vitro and in vivo anticancer activities. One lead compound **21**, (FIGURE 1.6) directly inhibits the kinase activities of I kappa B kinase 2 (IKKβ) and interleukin-1 receptor-associated kinase 4 (IRAK4), potentially responsible for its NF-κB inhibitory activities (SRINIVASAN et al., 2009).
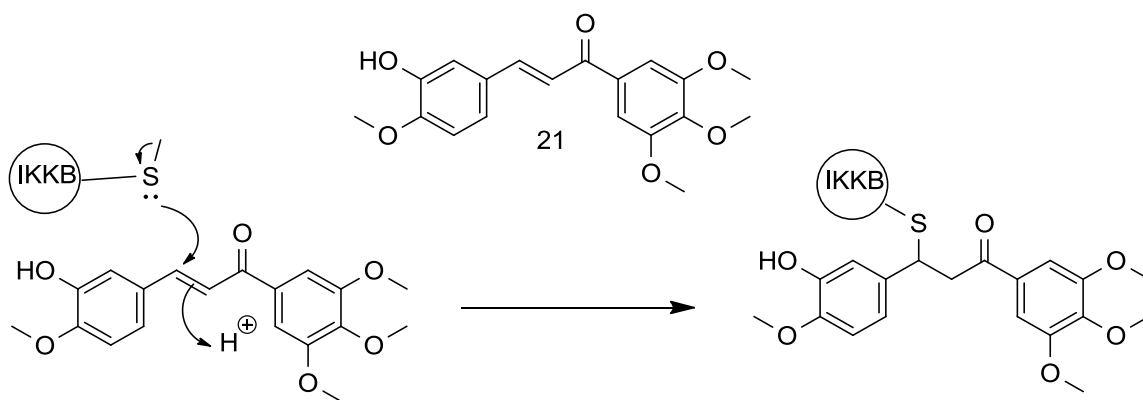
FIGURE 1.6 - Mechanism of chalcone to inhibit NF-κB via covalent modification of IKKβ.

The cytotoxicity and anti-cancer activity of substituted chalcone and their various modified form have also been studied in literature. The effect of substitution and different electron donating and withdrawing group has significant influence on cyto-toxicity.

1.1.2.4 Anti-Oxidant

As we know the substitution of one group of atom in a molecule significantly modify the biological activity. Padhye et al. synthesized fluorinated chalcones and studied its anti-oxidant properties (FIGURE 1.7) (PADHYE et al., 2010). All synthesized molecules were subjected to superoxide dismutase (SOD) scavenging assay in count to their anti-cancer activity evaluation. All synthesized compounds showed good anti-oxidant activity with IC_{50} values ranging between 5.27 and 13.68 mM. Compound **22** with two fluorine atoms and one hydroxyl group (ortho, ring A) exhibited maximum anti-oxidant activity with IC_{50} value 5.27 mM, even better than the standard molecule, ascorbic acid (IC_{50} ¼ 5.43 mM).

X = H, OH, F
Y = OH, F, H
Z = OH, F
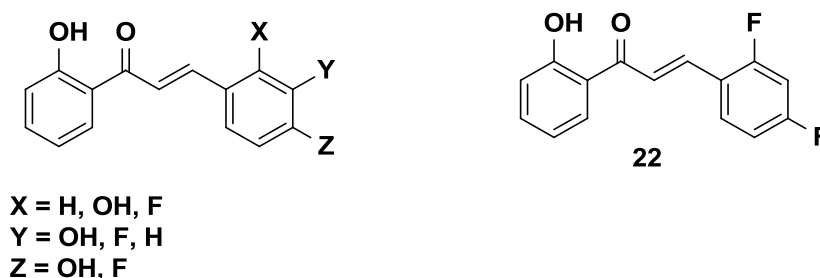
FIGURE 1.7 - Flourinated chalcone.

Yi-Ping Qian *et al.* synthesized Hydroxychalcones (**23–28**) (FIGURE 1.8) with different numbers and positions of hydroxyl groups on the two aromatic rings, and their antioxidant activities against the stable galvinoxyl (GO) radical in ethanol and ethyl acetate, and free radical-mediated lipid peroxidation of human red blood cells and DNA strand breakage were systematically examined. It was observed that structure and the reaction medium are two important factors affecting the antioxidant mechanism and

activity. In addition, the antioxidant activity of hydroxychalcones depends considerably on the position and number of the hydroxyl groups, the lipophilicity of the molecules and the reaction medium.
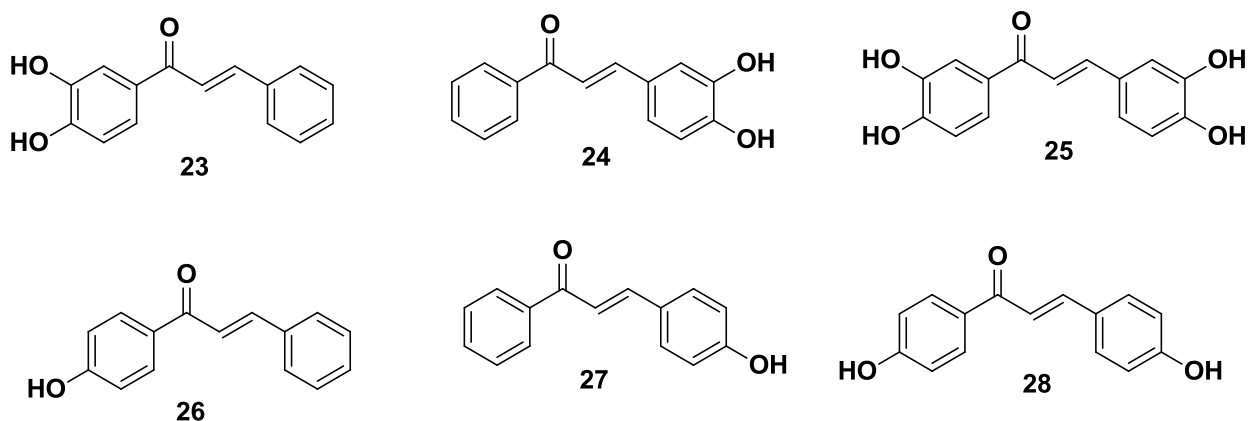
FIGURE 1.8 - Structures of hydroxylated chalcones.

1.2 Bisarylpentane

The class of biaryl in which the two moiety is seperated by 5 corbon system is called bisaryl pentane. Dibenzylideneacetones is the general examples, in which the moiety is seperated by α,β-unsaturated carbonylic system (FIGURE 1.9).
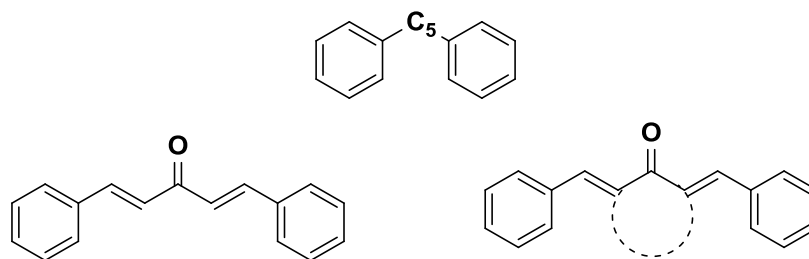
FIGURE 1.9 - General structure of bisaryl pentane.

Due to its interesting conjugated system in the whole skeleton it shows a broad rang of pharmacological activities.

1.2.1 Synthesis of Bis aryl pentane

Various research groups have tried to synthesized it by different methods. Aher et al. synthesized a series of dibenzylideneacetones (SCHEM 1.7) from simple classical condensation of various aldehydes having different substitution with acetone (AHER et al., 2011).
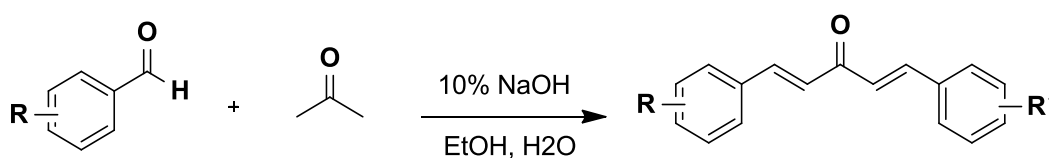
SCHEME 1.7 - Synthesis of biaryl pentane.

The simple condensation is an easy method for preparation of DBA but the chances of reversible reaction increases in some cases (HATHAWAY, 1987). More study reveals that some time self-condensation is also possible and it is one of the drawback of classical aldol condensation for the preparation of biaryl pentane (NAKANO et al., 1987).

Adding more a methods developed to carry aldol reaction catalyzed by salt ammonium chloride (TEIMOURI; et al., 2009), and magnesium hydrogen sulphate (SALEHI et al., 2002). Salt is an efficient and readily available reagent and inexpensive catalyst in cross aldol condensations of different ketones with various aromatic aldehydes to prepare the α,α'-bis(substituted benzylidene) cycloalkanones. The methodology is a green procedure avoiding the use of toxic solvents and acid liquids. Other chemical reagent is also used like NaOAc

in acetic acid (MOTIUR et al., 2007), Polymer-supported sulphonic acid (NKC-9), aqueous micellar media (SHRIKHANDE; GAWANDE; JAYARAM, 2008), iodine (DAS et al., 2006), microwave synthesis with aluminium oxide and modified-phosphate.

Different catalyst is also used for the preparation of bisaryl pentane. Peyman Salehi et al. showed that aromatic aldehydes undergo crossed-aldol condensation with ketones in the presence of silica sulfuric acid under solvent-free conditions to afford the corresponding α, β-unsaturated aldol products in excellent yields (SCHEME 1.8) (SALEHI et al., 2004). The catalyst is extended for use in cyclic ketones. The reagent (catalyst) is reusable for several times without any decrease in the yield of the reactions.
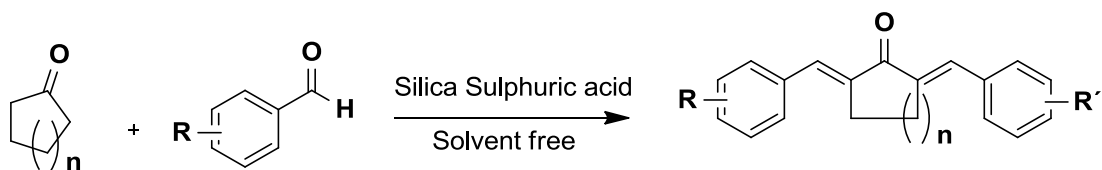
SCHEME 1.8 - Synthesis of DBA in solvent free condition.

Other metal hydroxide was also used to catalyze cross aldol reaction. Srikant Bhagat et al. synthesized a series of bisaryl pentane by usage hydroxide of lithium (BHAGAT; SHARMA; CHAKRABORTI, 2006). The rate of the cross-aldol condensation was affected by the nature of the ketone and electronic and steric factors associated with the aldehyde (SCHEME 1.9). The reaction rate was faster for acyclic ketone than that for cyclic ketone (e.g., cyclohexanone). In case of cycloalkanones, the rate of the reaction was also dependent on the size of the ring of the cycloalkanone. The rate of cross-aldol condensation of cyclopentanone was faster than that of cyclohexanone for a common aldehyde.
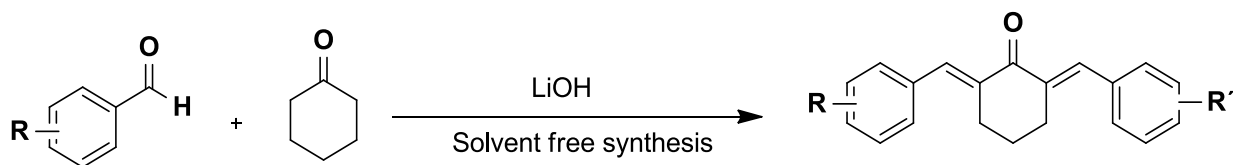
SCHEME 1.9 - Dual activation role of LiOH during tandem cross-aldol condensation between a ketone and an aldehyde.

From this work it is clear that the method is a very efficient and selective protocol for crossed-aldol condensation of ketones with aromatic aldehydes and high yield synthesis of α,α'-bis(substituted benzylidene)cycloalkanones in the presence of a reusable and ecologically benign catalyst. Easy and Simple work-up procedure, including washing the mixture followed by evaporation of the solvent, is another advantage of this methodology.

Several method adopted for synthesis of unsymmetric bisaryl pentane. The methodology is efficient when unsymmetric ketone is used. For example acetone is an symmetrical ketone so mostly its condensation give a symmetric products too, because both carbon are equivalent and nucleophilc formation take place equally on both carbon. For unsymmetrical bisaryl pentane unsymmetrical ketone is first treated with various aldehydes in the presence of HCl gas to give monoaldehydic product (Intermediate), further reaction of other aldehyde in normal base catalyse condition give desired product (MURTHY et al., 2008).
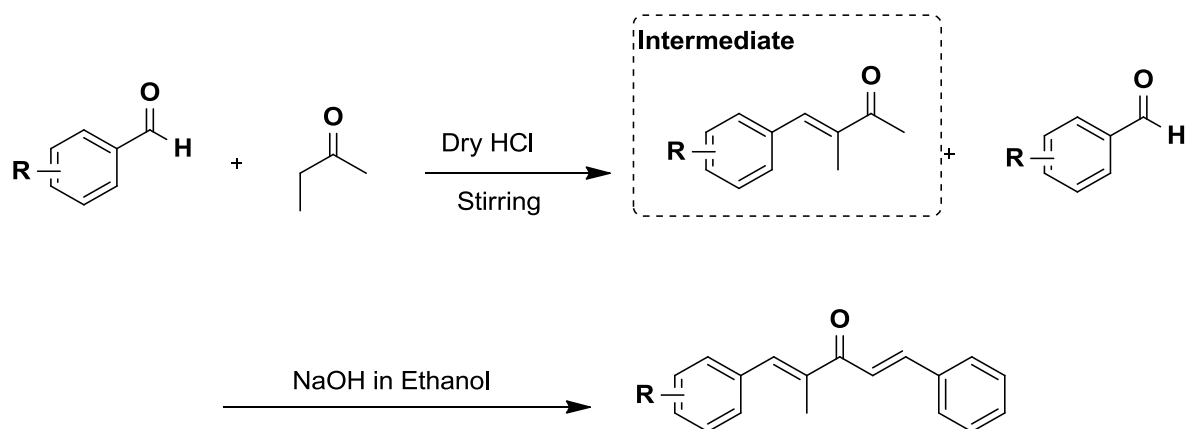
SCHEME 1.10 - Sythesis of unsymmetrical bisaryl pentane.

Guillem Valero *et al.* carried the enentioselective synthesis of bisaryl pentane (VALERO; RIBÓ; MOYANO, 2014). The use of the enantiomeric catalyst (*R,S*)-**8** allowed to obtain enantiomerically enriched (*S,S*)-anti-7 (78% ee), also in a 3:1 anti/syn mixture with syn-7 (SCHEME 11). Together with chiral HPLC analysis, which suggested that product, is either formed in a non-enantioselective fashion or that it has racemised during the course of the reaction.

13% yield, 3:1 anti/syn, 80% ee (anti)
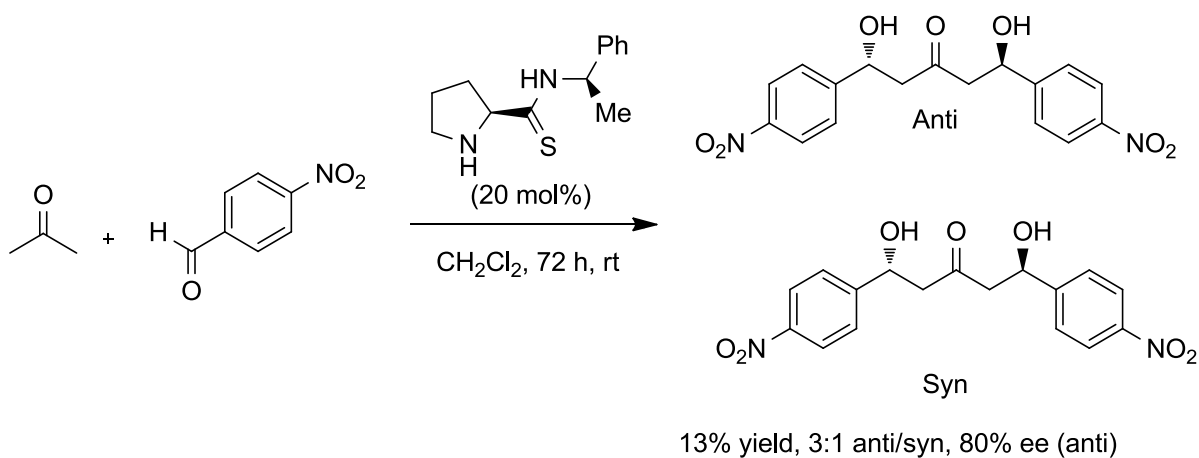
SCHEME 11 - Enantioselective preparation of double aldol product.

Then the catalytic role of bis aldol product were experimented in presence of appropriate solvent.
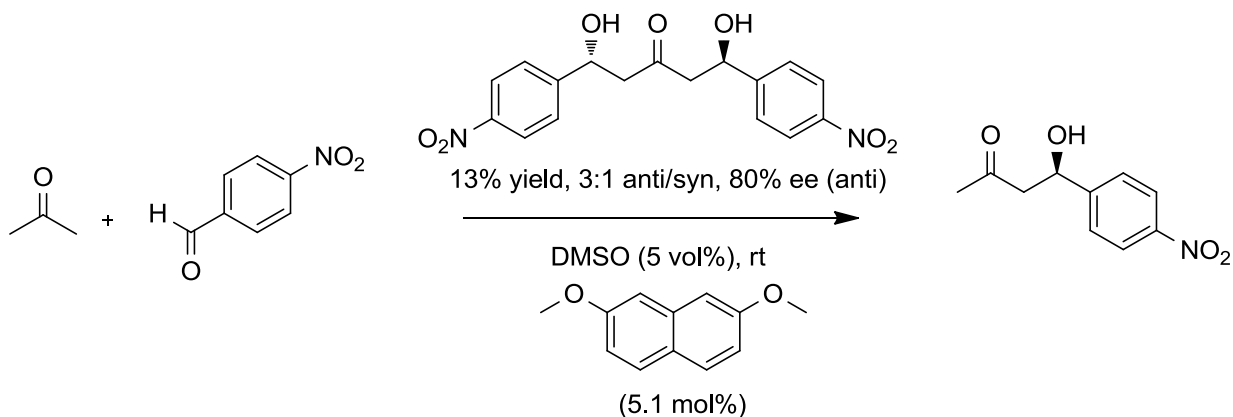
SCHEME 1.11 - Study of the catalytic role of biaryl pentane in the aldol reaction between acetone and nitro-benzaldehyde.

Firstly, as depicted in (SCHEME 1.11), it was assumed that the oxygenated functional groups of the bis(aldol) product interact with both the aldehyde and enol form of ketone. So it shows the role of bis aryl pentane as a catalyst for the synthesis of aldol products.

1.2.2 Biological activity of bisaryl pentane

Due to promising moities bisaryl pentane show various biological activity.

1.2.2.1 Anti-Parasitic activity

Braga *et al.* recently synthesized a series of symmetrical bisaryl pentane anologues and studied its anti-leishmanial activity (S.F.P. BRAGA et al., 2014).

The result of this work showed that bis aryl pentene moiety has the potential to be constructed for its action against parasite. Manohar *et al.* studied the anti-malarial activity of bisarylpentane against the two strains of *P. falciparum*, and found that the compounds exhibited good anti-malarial behavior in an *in vitro* activity (MANOHAR et al., 2013). Twenty different compounds were tested against *P. falciparum* cultures and six of them were found to provide excellent inhibition of both CQ-R and CQ-S (IC50 < 1 Mm. (FIGURE 1.10).
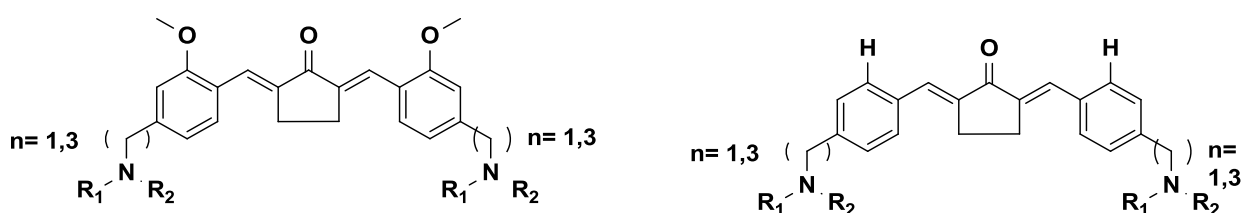
FIGURE 1.10 - Potent *in vitro* CQ-R and CQ-S inhibitors of the *P. falciparum* parasite.

We synthesized a series of un-symmetrical biaryl pentane by aldol and cross aldol condensation from 2- butanone and various para substituted aromatic aldehyde. In the study four aldehyde having different electron donating and withdrawing substitution were used. All compounds were evaluated for in vitro anti-leishmanial activity.

1.2.2.2 Cyto-toxic activity

Bis aryl pentane show various activty due to its structural motiff. Dimmock et al. synthesized different bis aryl pentane analogs by varying substitution at para position of cyclohexyl ring and evaluated for its cyto-toxic activity (JONATHAN et al., 2003). The compounds were cytotoxic to a number

of human tumours in vitro, mainly towards colon cancer and leukemic cells. The activity is due to the main skeleton of compounds which was confirmed from other work of Dimmock and his colleagues. They synthesized a number of 1,3-arylidene-2-tetralones (DIMMOCK et al., 2002). The most enones were more cytotoxic than the traditional anticancer agent melphalan and some demonstrated selective toxicity towards leukemic and colon cancer cells (FIGURE 1.11). Studying the mechanism showed that the modes of action of representative compounds interfering with the biosyntheses of nucleic acids and proteins and also altering redox potentials.
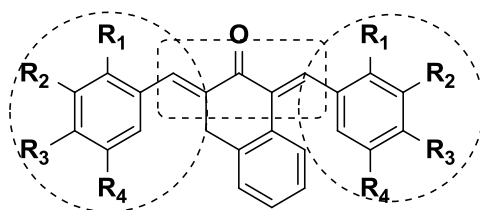
1,5-diaryl pentene moiety

FIGURE 1.11 - Dimmock synthesis of diaryl pentene having stilbene moiety

Study reveals that 1,5-diaryl-3-oxo-1,4-pentadienyl pharmacophore can be influenced by the substitution on aromatic ring. Nitro group has a greater effect on activity because it can be reduced in the tumor (DIMMOCK et al., 2005). The activity of 2-arylidenecyclohexanones and 2,6-bis(arylidene)cyclohexanone were also compared (JONATHAN et al., 2000). It was found that bis(arylidene)cyclohexanone **29** was 3 times more active than its corresponding mono arylidene **30** (FIGURE 1.12).
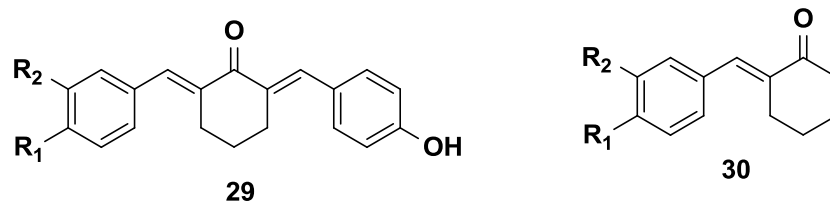
FIGURE 1.12: Mono and bi arylidene and its cyto-toxic comparison.

Literature survey confirmed that 1,5-diaryl-3-oxo-1,4-pentadienyl is pharmacophore which is considered to interact at a complementary binding site in susceptible neoplasms (DAS et al., 2007a). The presence of an acyl group has been attached to the piperidyl nitrogen atom in order to interact with an additional binding site thereby to enhance cytotoxic potencies (FIGURE 1.13). Longer substitution increases the activity significantly.
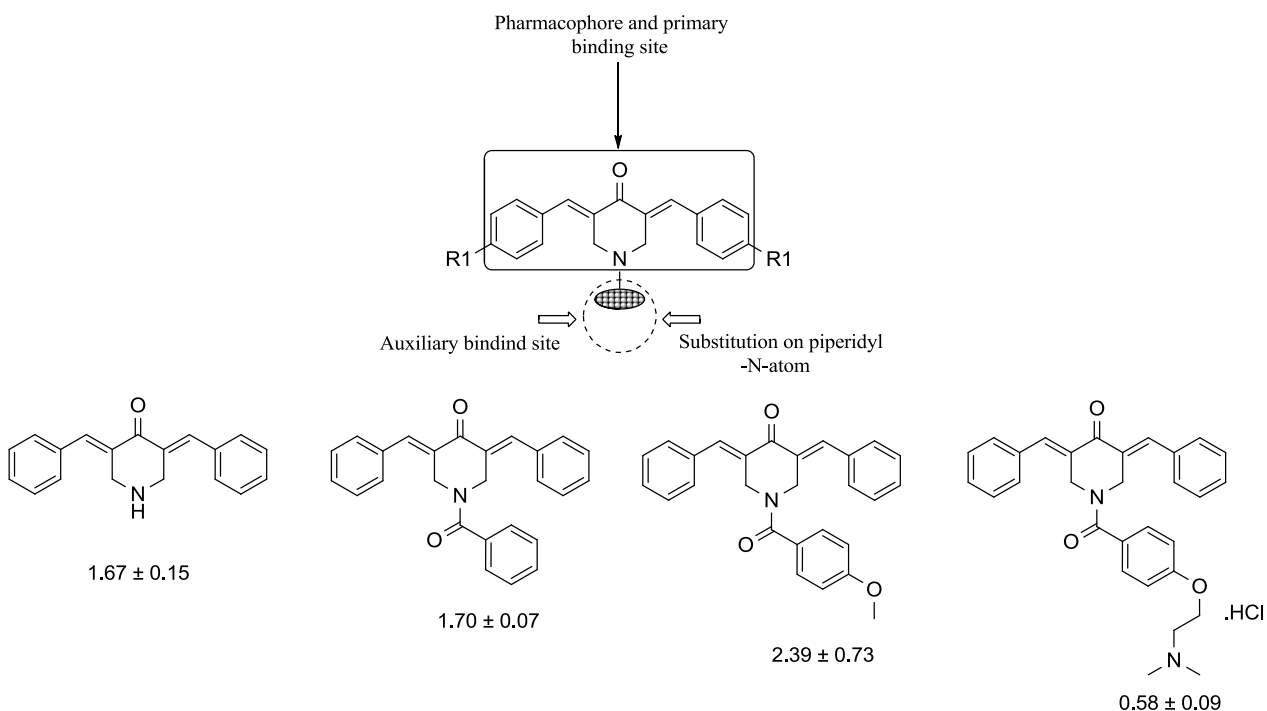
FIGURE 1.13 - Structures with IC_{50} values in µM.

1.2.2.3 Anti-Oxidant actvity

Bisaryl pentane also show anti-oxidant activity. Weber *et al.* synthesized and evaluate bisaryl pentane for its anti-oxidant potential (W.M. WEBER, L.A. HUNSAKER, S.F. ABCOUWER, L.M. DECK, 2005). Most of the analogues with anti-oxidant activity retain the phenolic ring substituents. It is also proposed that bisarylpentane attenuates H_2O_2 -induced apoptosis through direct and indirect scavenging of ROS, leading to inhibit the mitochondria-mediated apoptotic pathway. The results suggest the potential for bisarylpentane to be used in treating diseases in which free radical and oxidative damage are involved. So this class provides significant moiety and future plane to be research more for its potential to treat to disease related to unbalance anti-oxidant.

1.2.2.4 Anti-tubercular activity

Singh *et al.* synthesized symmetrical bisaryl pentane analogs and studied its anti-tubucular activity (SINGH et al., 2009). Several compounds showed moderate antitubercular activity with MIC = 12.5–1.56 µg/mL. Various 2,6-bis(arylidene)cyclohexanones were trailed against *Mycobacterium tuberculosis* $H_{37}Rv$ (DIMMOCK et al., 2004). The compounds inhibited the growth of the microorganism by 21-66%. Other study suggest that trimethoxy group on one of the aromatic ring enhance the activity (DAS et al., 2007b). Analogs of trimethoxy moiety is 30 times more potent than verapamil. The effect were observed by studying electron donating moiety on aromatic ring and other side electron withdrawing group on aromatic moiety. These two types of system are crucial to enhance the activity (FIGURE 1.14).
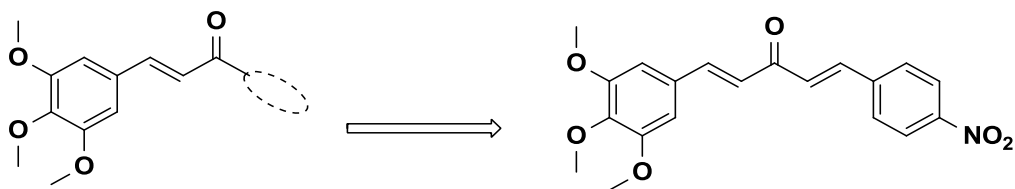
FIGURE 1.14 - Nitro group on benzene significantly enhance its potential.

1.3 Diarylheptanoids

The **diarylheptanoid** are a class compounds consist of two aromatic rings (aryl groups) joined by a seven carbons chain (heptane) and having various substituents (FIGURE 1.15). They can be classified into linear (curcuminoids) and cyclic diarylheptanoids (KESERÜ; NÓGRÁDI, 1995). There natural analogs mainly extracted from plants (PER et al., 2002). There is unsaturation in the main skeleton of curcumin. This unsaturation in the main unit has an E-configuration (trans C=C bonds). The aryl rings may be symmetrically or unsymmetrically substituted; the most common natural substituent's are of the oxy type, such as hydroxy or methoxy elements (BAIRWA et al., 2014).
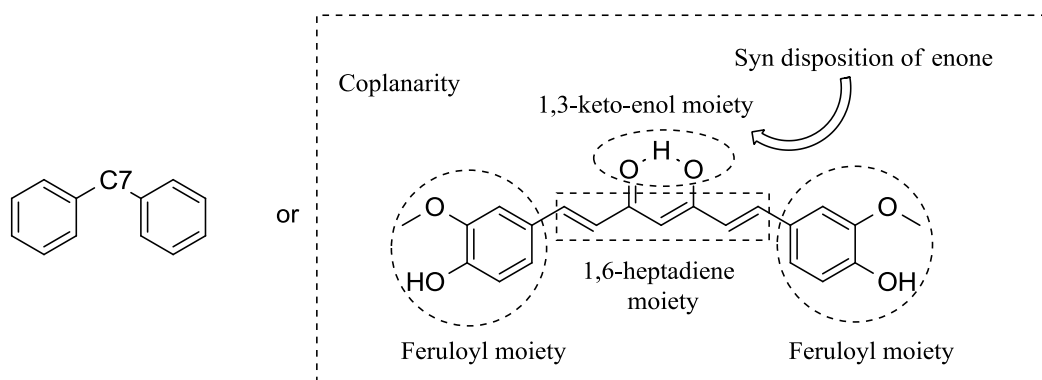
FIGURE 1.15 - General structural representation of Curcuminoids.

Curcumin, 1,7-bis-(4-hydroxy-3-methoxy-phenyl)- hepta-1,6-diene-3,5-dione (FIGURE 1.16), is a main compound of these series is polyphenolic compound naturally present in the Curcuma longa plant, also known as tumeric. It is present in keto enol isomeric form. It was used primarily as a coloring agent and additive in food, and is the main constituents of food in many countries. Francese *et al*. did experiment to use curcumin as a matrix medium in MALDI-MS (FRANCESE et al., 2013). In the result curcumin is revealed to be a versatile and multipurpose matrix. It has been applied successfully for the analysis of different pharmaceuticals and drugs, for imaging lipids in skin and lung tissues, and for the analysis of a number of compound classes in finger marks. In each experiment, the curcumin is shown to promote analyte ionization very capably as well as provide brilliant mass spectral image quality. The synthetic curcumin were preferred for the study then commercially available one. Curcumin has also long been used for its therapeutic properties in a number of medical scenarios.
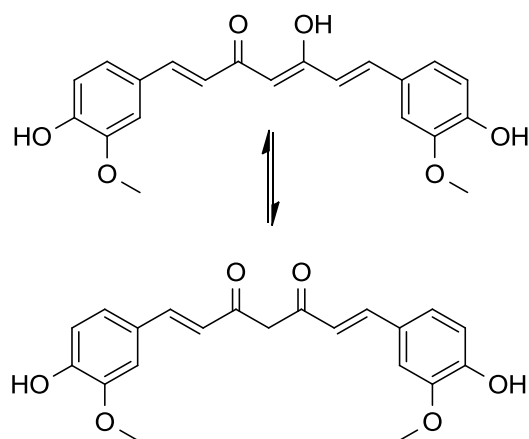
FIGURE 1.16 - Curcumine, keto enol form.

Structurally curcuminoids are very important due to pharmacological activity. It shows biological activity (GOEL; KUNNUMAKKARA;

AGGARWAL, 2008) like anti-cancer, anti-microbial, anti-viral, anti-fungal, anti-oxidant, anti-inflammatory, anti-tumor, anti-diabetic, neuro-protective activity, anti-aging and anti-platelet . It is also measured that curcumin play an important role in spinal injury recovery. Curcumin also inhibit human recombinant cytochrome P450s, show unique binding site of tubulin and telomerase inhibiting activity. In order to explain its anti-oxidant activity Sun et al. did theoretical calculation base on DFT study. It was found that H-atom abstraction from the phenolic group, not from the central CH_2 group in the heptadienone link take place.

The natural curcumin and its metabolites are shown (FIGURE 1.17) and explained in literature (ANAND et al., 2007) and can be purified from turmeric powder. Turmeric contains three important analogues, curcumin, demethoxycurcumin (DMC), and bisdemethoxycurcumin (BDMC). Collectively all these three is known as curcuminoids. The three compounds differ in methoxy substitution on the aromatic ring. Curcumin has two symmetric o-methoxy phenols linked through α, β-unsaturated diketone moiety. The other form (BDMC) is also symmetric, having deficient in two o-methoxy substitutions, while DMC has an asymmetric structure with one of the phenyl rings having o-methoxy substitution. Among the three curcuminoids, curcumin is the most abundant in turmeric, followed by DMC and BDMC. Commercially available curcumin mixture contain 77% curcumin, 17% DMC, and 3% BDMC.
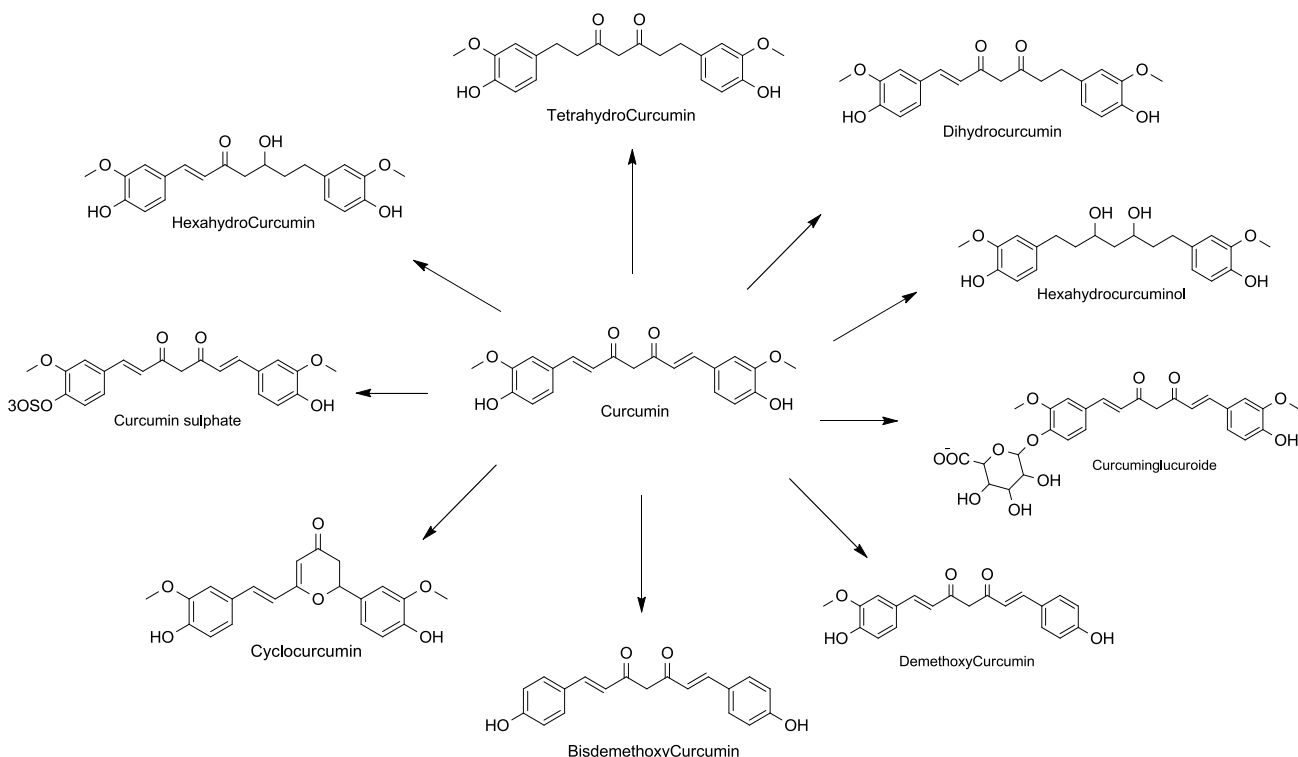
FIGURE 1.17 - Natural curcumin and its metabolits.

Shen and Ji tried to evaluate the similarities between the biological activities of curcumin and its degradation products against diseases such as Alzheimer's disease and cancer; it was observed that the bioactive degradation products may contribute to the pharmacological effects of curcumin. This possibility needs more experimental trial for elucidating the pharmacology of this promising natural product for various diseases. So Shen and Ji discussed the hypothesis that metabolites of curcumin, specifically vanillin and ferulic acid, could account for its striking poly pharmacology as well as for the enigmatically low levels of curcumin in animal and human plasma upon dietary administration (SHEN; JI, 2012). So this need more experiment to test this hypothesis that the degradation products are positively identified, such that the correct products are considered for activity. So Odaine *et al.* (FIGURE 1.18)

29

observed that the widely held notion that vanillin, ferulic acid, and feruloyl methane are abundant products of the non enzymatic degradation of curcumin (SCHNEIDER, O. N.; GORDON, 2012). So in the result of experiment it is determined that vanillin, ferulic acid, and feruloylmethane are not abundant degradation products of curcumin. They may very well be bioactive compounds in their own right, but should not be used to determine whether metabolites of curcumin account for its polypharmacology.
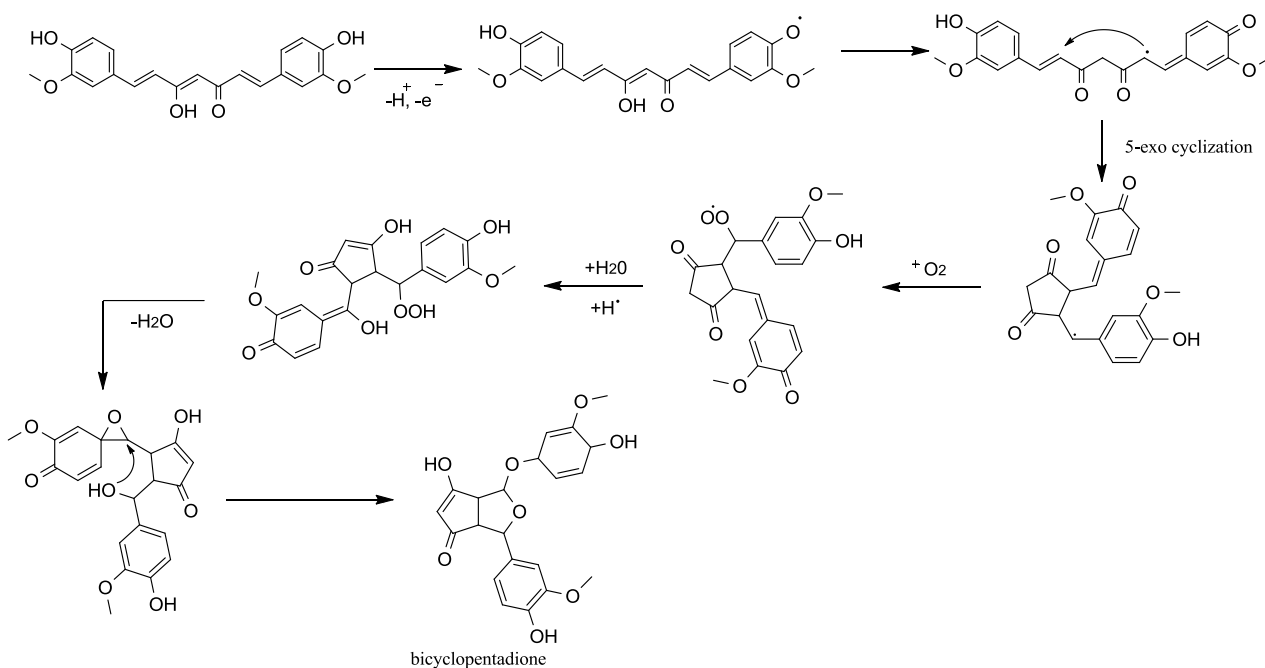
FIGURE 1.18 - Degradation products of curcumin.

The biosynthetic pathways for curcuminoids (KATSUYAMA et al., 2009) initially, the phenylpropanoid diketide intermediate is formed from the condensation of phenylpropanoid-CoA and malonyl-CoA in the presence of diketide-CoA synthase. The corresponding curcuminoids are obtain from this intermediate through reaction with a further molecule of phenylpropanoid-CoA catalyzed by the enzyme curcumin synthase. Hydroxylases and O-

methyltransferases then convert the mentioned bisdemethoxycurcumin into demethoxycurcumin and curcumin (SCHEME 1.12).

Roughley and Whiting reported feeding experiments with ^{14}C-labelled compounds, and proposed two pathways for the formation of the curcuminoid skeleton (ROUGHLEY; WHITING, 1973) . One of the pathways involved cyclization of a polyketide chain consisting of a phenylpropanoid starter unit and five C_2 units derived from malonic acid, presumably via malonyl CoA, to give a second aromatic ring, and the other involved the condensation of two phenylpropanoids to a central carbon provided by a malonic acid molecule . They could not, however, determine experimentally which pathway represented the actual pathway of curcuminoid formation.
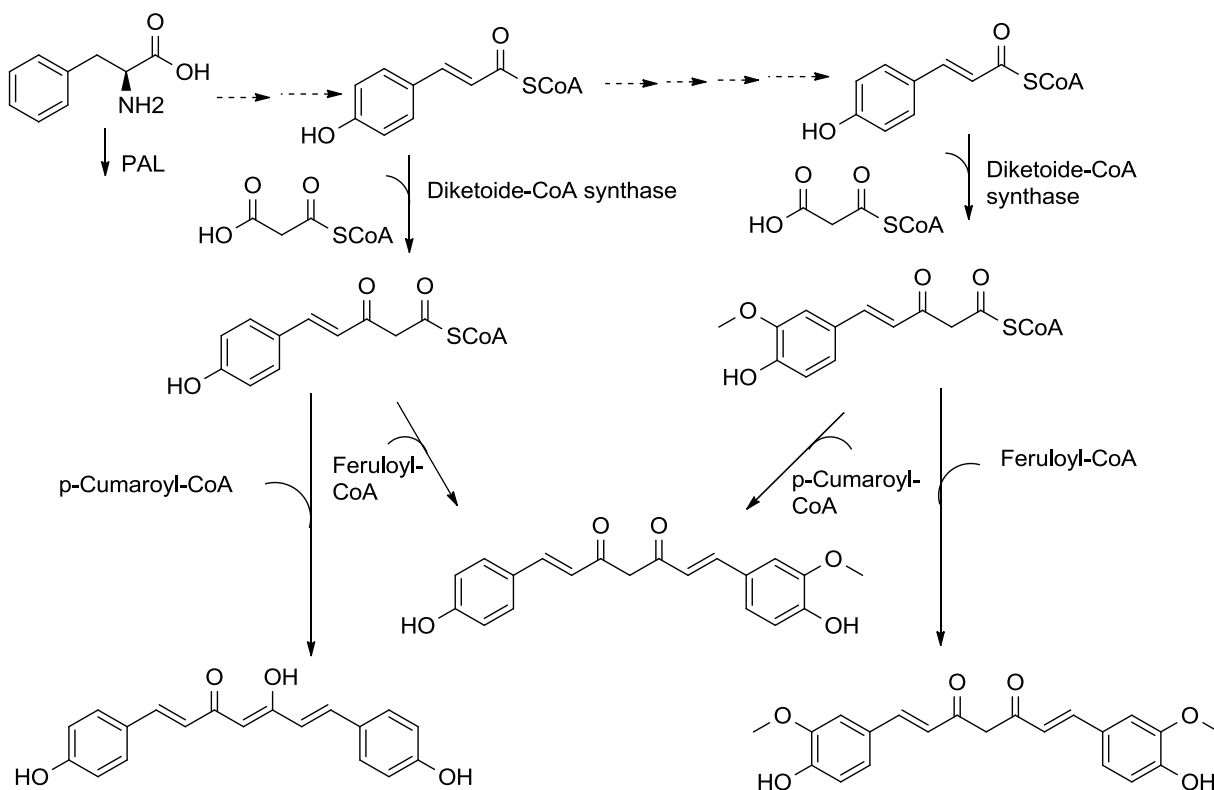
SCHEME 1.12 - Representation of biosynthetic pathway for curcumin.

Diaryl heptanoids show potent biological activity for a series of diseases, but its oral use face problem due to its less solubilty in water. So researcher are trying to improve its solubility and bioavailability.

1.3.1 Synthesis of Curcumin

In 1937, Pavolini *et al.* carried out a one-step synthesis of curcumin using 2,4-pentanedione (SCHEME 1.13), vanillin and boric anhydride, but the yield was only 10% (PAVOLINI, 1937). Then Lampe in 1918 synthesized curcumin in five steps starting from ethyl acetoacetate and carbomethoxy feruloyl chloride (SCHEME 1.14). After condensation, saponification and decarboxylation, the intermediate product was again exposed to carbomethoxy feruloyl chloride. The consequential condensation product was then cleaved under acidic conditions. Curcumin was generated after saponification and decarboxylation (V. LAMPE, 1918). Ferrari *et al.* synthesized symmetrical new curcumin analogues (SCHEME 1.15) with the aim to improve the chemical stability in physiological conditions and potential anticancer activity (FERRARI et al., 2011).
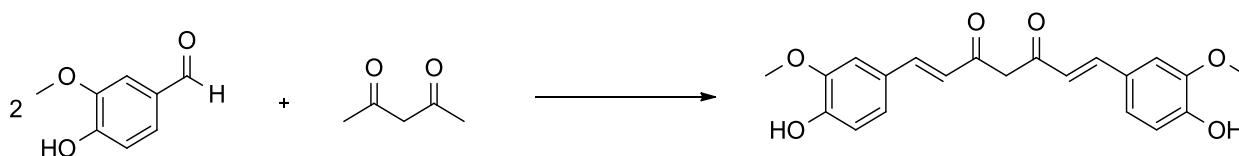
SCHEME 1.13 - Synthesis of curcumin according to Pavolini.
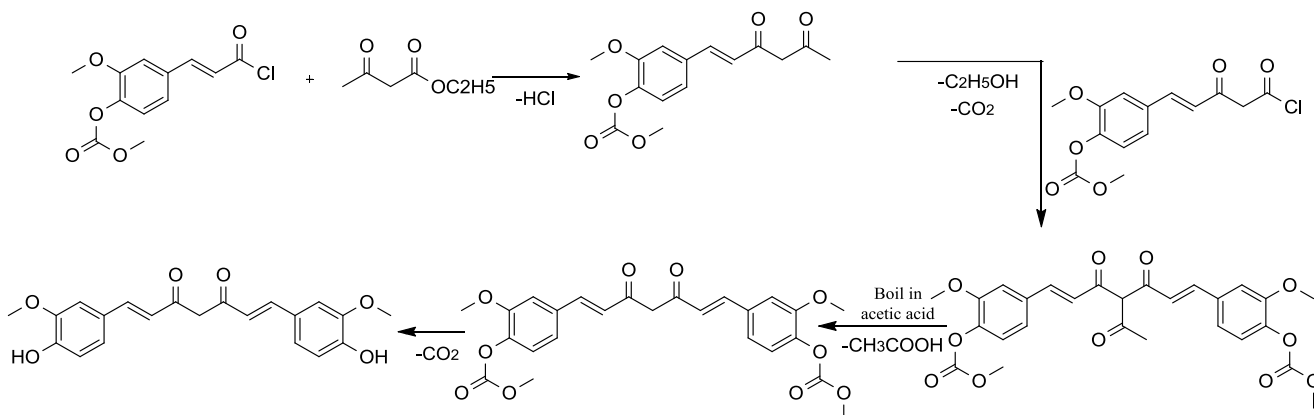
SCHEME 1.14 - Synthesis of curcumin according to Lampe.
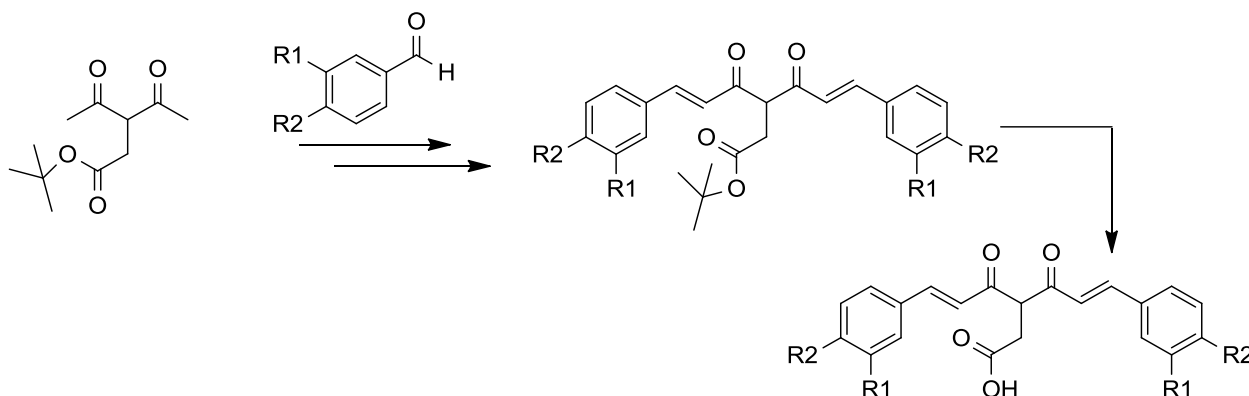
SCHEME 1.15 - Synthesis of symmetrical curcumin anologues.

Pabon *et al.* (SCHEME 1.16) reported different approach toward curcumin synthesis of 1,7-bis(4-methyl)-1,6-heptadiene-3,5-dione, according to the reported method, 4-methly-benzaldehyde and tributyl borate were dissolved in dry ethyl acetate and were heated to 100°C. Subsequently the reaction product of 2,4-pentadione and boric anhydride was added and the mixture heated for 30 min, while stirring, in order to achieve a homogeneous mixture. Finally, after having been maintained for 30 min at 100 °C, while stirring, the mixture turned brown. After cooling to 50°C hydrochloric acid was added

33

leading to the addition of ethyl acetate. The layers were separated, and the aqueous layer was extracted once with ethyl acetate. The residue was dissolved in chloroform/methanol and subsequently cooled, after which the crystals were sucked off resulting curcumin (PABON, 2010).
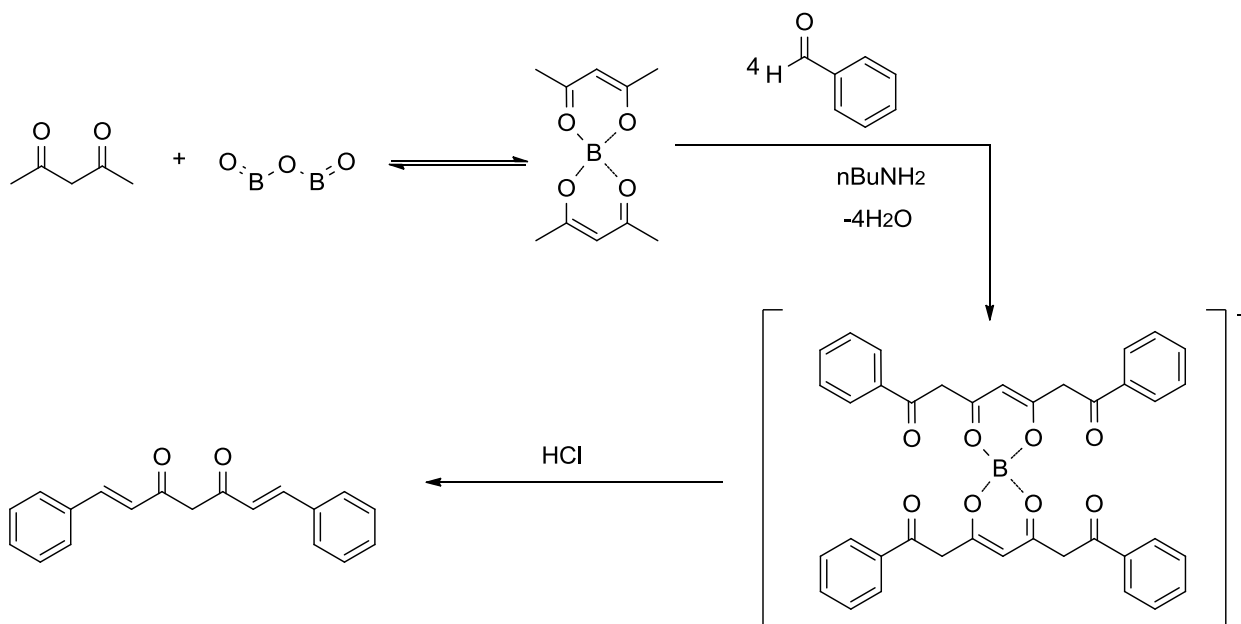
SCHEME 1.16 - Synthesis of curcumin by Pabon et al method.

Soumyananda Chakraborti *et al.* attempted to increase the stability of curcumin. Several analogues were synthesized in which the diketone moiety of curcumin (**31)** was replaced by isoxazole (compound **32**) and pyrazole (compound **33**) groups (FIGURE 1.19). Isoxazole and pyrazole curcumins were found to be enormously stable at physiological pH (SOUMYANANDA et al., 2013).
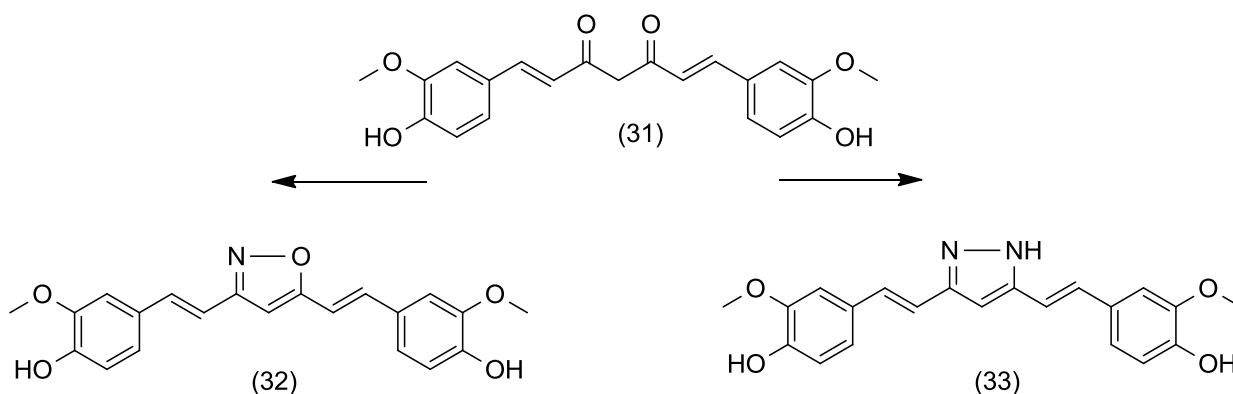
FIGURE 1.19 - Synthesis of curcumin and its analogues.

Luo *et al.* prepared monoalkyne derivative of curcumin by applying click chemistry approach (LUO; TIKEKAR; NITIN, 2014). Modification of curcumin to its monoalkyne derivative (SCHEME 1.17) did not impact its apoptotic activity in cells. Further DSPE-PEG micelles labeled with Alexa-647 were used as a representative nanoscale carrier to improve the solubility and delivery of monoalkyne curcumin (**34**).
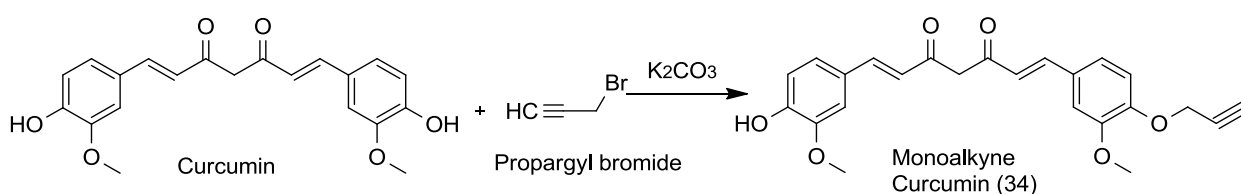
SCHEME 1.17 - Synthesis of Monoalkyne curcumin.

The approach of substitution was extended to get more substituted form (compounds **34-38**) in order to get the desired solubility and bioavailability result (FIGURE 1.20) (DOLAI et al., 2011) .
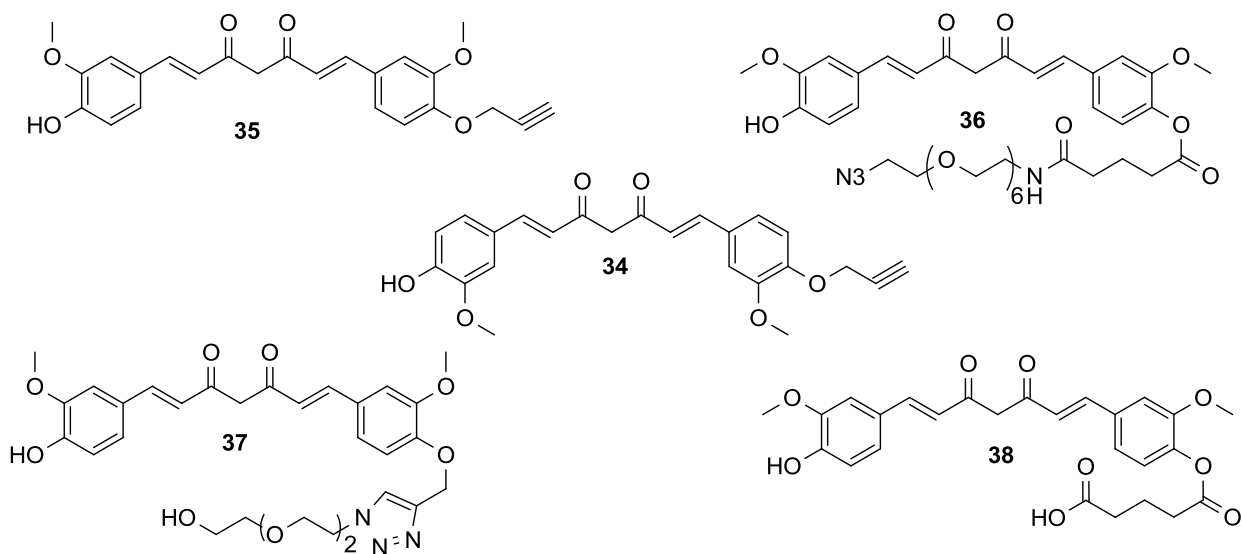
FIGURE 1.20 - Mono functional curcumin derivatives.

Shi *et al*. converted curcumin to active monofunctional derivatives (SHI et al., 2007). The derivatives were employed to produce a 3 + 2 azide-alkyne "clicked" curcumin dimer and a poly(amidoamine) (PAMAM) dendrimer-curcumin conjugate (SCHEME 1.18). The monofunctional curcumin derivatives keep its biological activity and are proficient for labeling and dissolving amyloid fibrils. It also selectively destroys human neurotumor cells. The synthetic methodology developed affords a general strategy for attaching curcumin to various macromolecular scaffolds.
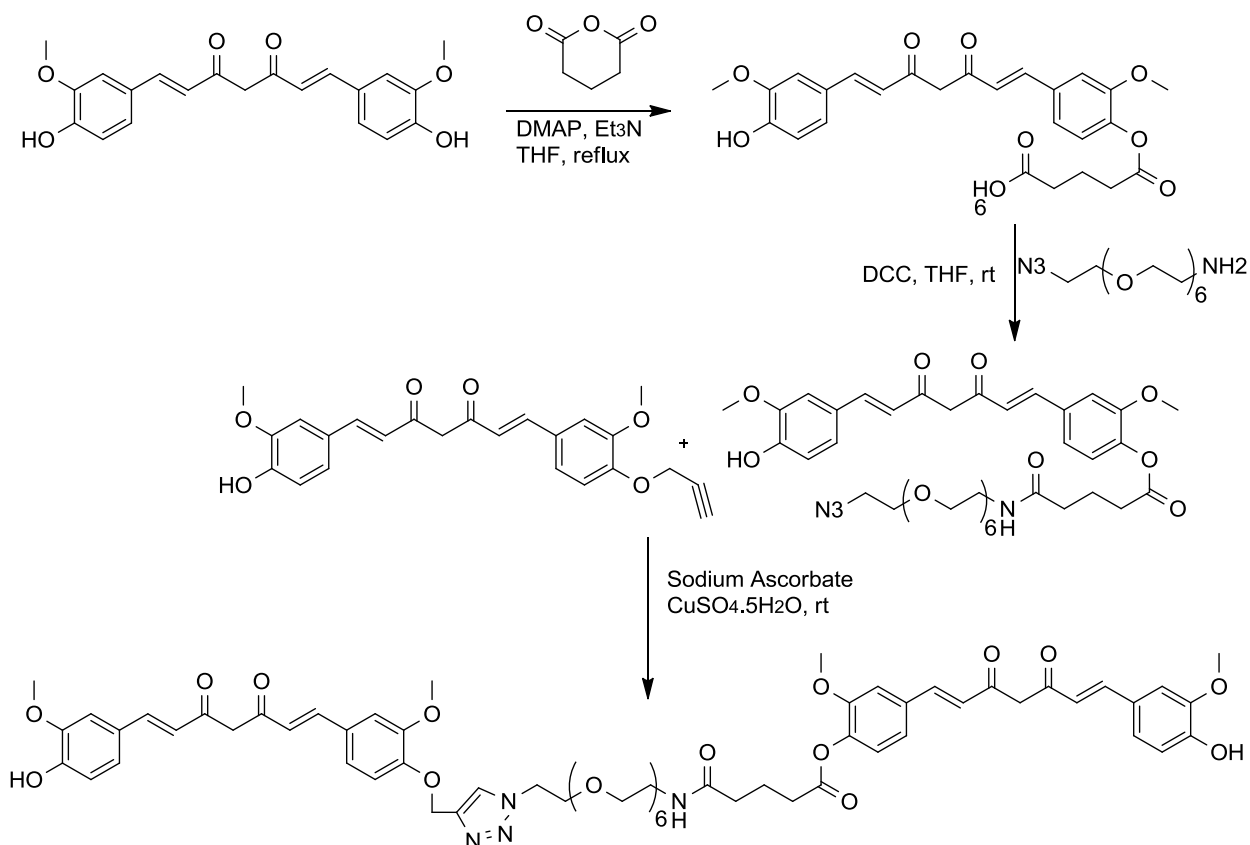
SCHEME 1.18 - Synthesis of mono functional curcumin derivatives.

Many research data appeared to increase the solubility, stability and bioavailability and also deal with rapid metabolism of curcumin. So in order to get the desired results curcumin is combined with BSA/ι-carrageenan complexes, cocrystalization with hydrophobic moieties, encapsulation in casein nanocapsules, nanoparticle, bixin and curcumin with β-cyclodextrin, potassium norbixinate by microencapsulation with maltodextrin DE20 and freeze-drying, encapsulation in artificial seed oil bodies, silica nanoparticles , conjugation with poly(ethylene glycol), polyelectrolyte-coated curcumin nanoparticles, biocompatible microparticles, solid lipid nanoparticles, encapsulation of curcumin, nanostructured lipid carriers and gold nanoparticles functionalized with cyclodextrin curcumin complexes.

1.3.2 Biological Activity of diaryl haptanoids

1.3.2.1 Anti-Microbial activity

Curcumin along with other activities also show anti-microbial activity. Curcumin based metallo curcumin having amino acid has been evaluated for their anti-microbial potential (CHANDRASEKAR; PRAVIN; RAMAN, 2014). In the result it was observed that complexes exhibit better activity against bacteria and fungi than the curcumin. Curcumin-encapsulated nanoparticles were also evaluated. Curcumin exhibited immense therapeutic potential against *H. pylori* infection (DE et al., 2009). Micro capsulated curcumin increase the solubility and bioavailability as well its anti-microbial activity against various fungi and bacteria and also play its role in the preservation of food. Ascorbic acid mixed with curcumin increases its microbial activity. Conjugation of the phenolic hydroxyl group of curcumin to a sugar moiety or amino acid renders it water-soluble while enhancing its *in vitro* antibacterial properties. The combination of curcumin and other antibiotic improve the activity significantly. It is also the inhibitor for *Staphylococcus aureus* sortase A and *Streptococcus mutans* by photodynamic potential.

1.3.2.2 Anti-Oxidant activity

Antioxidants are compounds which protect the cell membranes against auto-oxidation. The basic moiety in curcumin (phenolic, N-diketone, as well as the methoxy groups) contributes to the free-radical-scavenging activity. But phenolic group has a greater effect on radical-scavenging properties of

curcumin. Other study suggests that demethoxylation derivatives of curcumin are the most potent inhibitors of lipid peroxidation. Curcumin inhibit the generation of hydroxyl radicals (·OH) and iron-catalyzed lipid peroxidation. The bis-demoxycurcumin was observed to be the most potent anti-oxidant. It means hydroxyl group at para position is crucial for activity. It was also observed that methylation depresses the anti-oxidant activity. Further sterically hindered phenolic group by the introduction of two methyl groups at the ortho position increases the activity (VENKATESAN; RAO, 2000). The curcumin extract was also studied for their anti-oxidant activity. Extracts from recently dried tissue were significantly more potent than extracts from aged commercially available turmeric powder. Curcumin is also able to effectively quench singlet oxygen at very low concentration in aqueous systems (DAS; DAS, 2002).

There is different proposition about the mechanism of anti-oxidant behavior of curcumin. Gorman *et al*. report that curcumin radical reacts with ascorbate ion in acetonitrile:water, and lead to the regeneration of curcumin (GORMAN et al., 1994). Other mechanism explains the binding of curcumin with lysozyme. Jovanovic *et al*. reported that ph 7 and below the keto form dominates, and curcumin acts as an extraordinarily potent H-atom donor while the enolate form of the heptadienone link predominates at ph 8 and above. Masuda *et al.* reported that curcumin reduces about 50% of the lipid hydroperoxide formation (SCHEME 1.19) relative to that of the control experiment (MASUDA et al., 2002). Conjugation of curcumin with amino acid also enhances its anti-oxidant activity significantly.
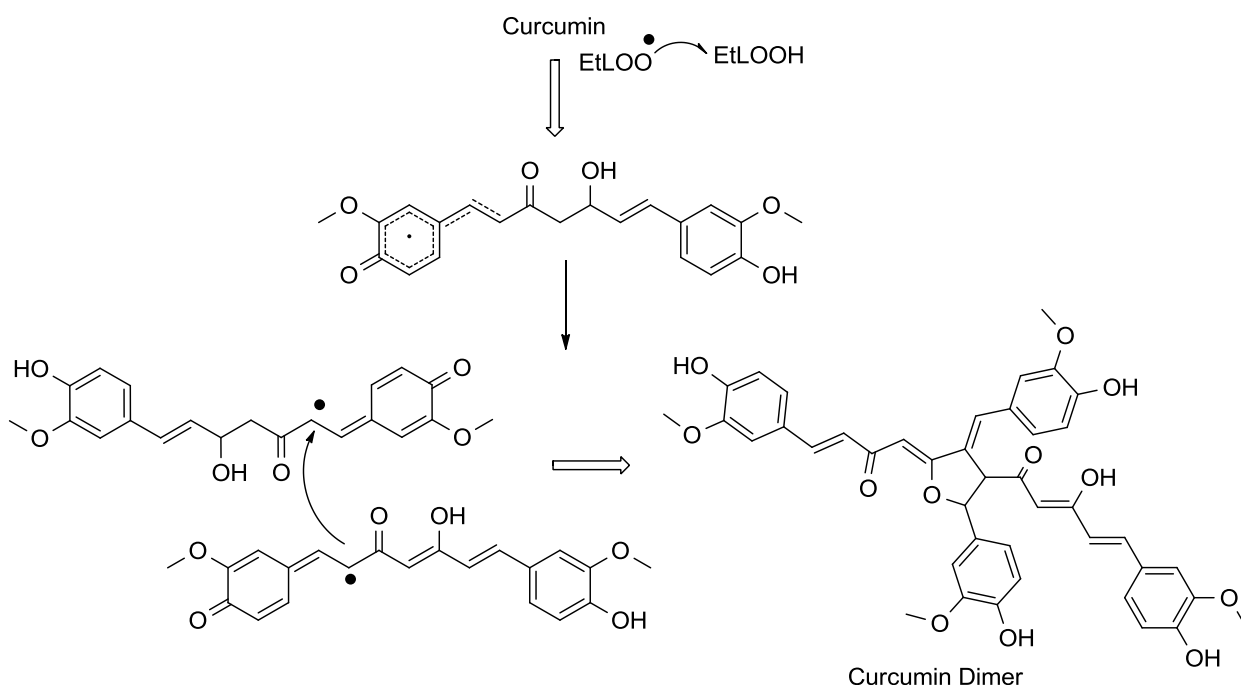
SCHEME 1.19 - Antioxidant mechanism of curcumin against the oxidation of ethyl linoleate.

1.3.2.3 Anti-Cancer Activity

Curcumin is a promising anticancer agent for various cancer types. Different curcumin analogs has been synthesized and evaluated for their anti-cancer potential. Yallapu *et al.* evaluated therapeutic potential of novel poly(lactic-*co*-glycolic acid)- curcumin nanoparticles for prostate cancer treatment (YALLAPU et al., 2014). Curcumin loaded PHEMA nanoparticles also show good results (KUMAR et al., 2014). Other study reported that curcumin is a favorable compounds that has demonstrated extraordinary therapeutic potential for prostate cancer (AGGARWAL, 2014). Yu and Huang encapsulated curcumin with starch in order to enhance its solubility and bio availability and in the result encapsulated curcumin exihibited enhanced in vitro anti-cancer activity compared to free curcumin (YU; HUANG, 2010).

Curcumin in AIN 76A diet on carcinogen-induced tumorigenesis in the fore stomach, duodenum, and colon of mice were also trailed (HUANG et al., 1994). It was observed that curcumin inhibit the number of tumors per mouse and the percentage of mice with tumors but it also reduces tumor size. Basile *et al.* studied anti-cancer effect of bis demethoxy curcumin and diacetyl curcumin (BASILE et al., 2009). It was revealed that bDMC induces rapid DNA double-strand breaks. Curcumin, demethoxy curcumin and bisdemethoxy curcumin was also studied for their antimetastasis activity. Demethoxy curcumin and bisdemethoxy curcumin showed better antimetastasis activity then curcumin. Simon *et al.* studied the effect of curcumin and cyclo curcumin on the proliferation of MCF-7 human breast tumor cells (SIMON et al., 1998). Curcuminoids (**39-41**) appear to be potent inhibitors, while Cyclocurcumin **42** was less inhibitory (FIGURE 21). Bioconjugation with curcumine also enhances its activity (MISHRA et al., 2005). Further study explains that diketone moiety in the curcumin molecule seems to be essential for the inhibiton activity. Computational study showed that curcumin inhibits breast cancer cell lines though inhibiting of HER2-TK (YIM-IM et al., 2014) and epidermal growth factor receptor tyrosine kinase (EGFR-TK).

39. R$_1$ = R$_2$ = OMe
40. R$_1$ = H, R$_2$ = OMe
41. R$_1$ = R$_2$ = H

42. Cyclo Curcumin
Less potent
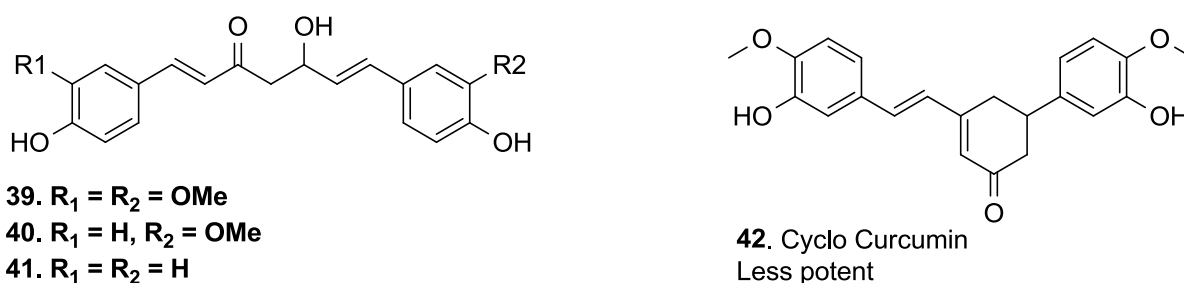
FIGURE 1.21 - Structure of curcuminoids and cyclo curcuminoids.

Mechanism of curcumin to act as anti-cancer was reported by Singh R.P *et al.* According to this study curcumin induces apoptosis through a number of different molecular targets and inhibits metastasis, invasion and angiogenesis (SINGH; AGARWAL, 2006). Other study suggests that curcumin suppresses FTC133 cell invasion and migration by inhibiting PI3K and Akt signaling pathways, and in the result produce anti-metastatic activity. It is also investigated that cytotoxity is related to the cellular uptake of curcuminoids and does not depend on p21 status.

1.3.2.4 Neuro-protective activity

Petr *et al.* synthesized some curcuminoid analogs and evaluate it for their potential as neuron protector (JIRÁSEK; AMSLINGER; HEILMANN, 2014). Compounds **43** and **44** were found important feature for protection against glutamate-induced neurotoxicity (FIGURE 1.22).
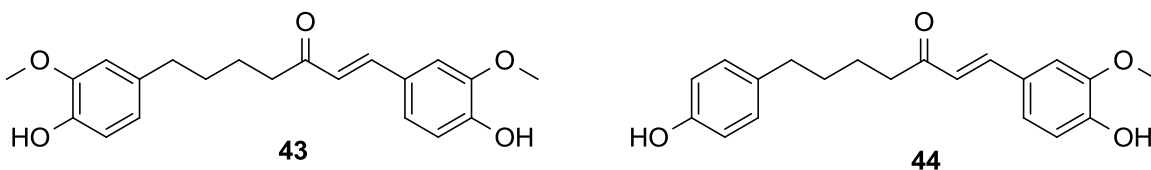
FIGURE 1.22 - Potent neuro protective compounds.

Methoxy group is crucial for activity. Other compounds substituting methoxy has lower activity compared to compounds **43** and **44**. But hydroxyl has also significant effect upon activity. The importance of hydroxy has explained by studying the effect of bisdemethoxy curcuminoids, which enhances Aβ phagocytosis and play a role to control neurological diseases

(FIALA et al., 2007). Other work shows that curcumin has an intracellular action mediating a protective effect against iAβ-induced neurotoxicity (QIN; CHENG; YU, 2010). Curcumin also protects against the Aβ-induced toxicity on neurons of the central nervous system (CNS) (QIN et al., 2009). It also help to cure Alzheimer's disease.

1.4 Interaction Study or *In-silico* study

1.4.1 Hydrogen bonding interaction

The most important interaction between two compounds or between compound and protein is H-bonding interaction. The interaction is very important for inhibiting specific enzymes or inhibiting growth of infected site. The binary interaction between protein protein pair is reported extensively (JONES; THORNTON, 1996). There is vast detail about the interaction of natural products and protein. Jiang et al. studied the interaction between stilbenoids and Vam3 and Sky (SAIJUN, F.; PEIXUN, 2014). The two hydrogen bonds with Glu449 and Phe382 of Syk were observed along with arene-cation interaction between that of Vam3 and Lys402 of Syk was also observed. It was also observed that stilbene induce gene expression changes in Mtb that resemble those induced by HU deficiency resulting HU a potential target for the development of therapies against tuberculosis (TUHIN et al., 2013). The literature study show that there is π-π interaction between the phenyl system of stilbene with phenyl system of amino acids (MIKSTACKA et al., 2014). This interaction is important for the discovery of new drugs. The π-π interaction is also present in chalcone (SUN et al., 2012). It is responsible for binding and protect cell against various diseases. Hydrogen bond and van der

waal interactionis seen in curcumin to have affinity toward amino acid. The hydrophilic and hydrophobic interactions with stronger affinity were also found. Hydrogen bonding along with salvation effect was observed by studying different solvents (SUSRUTA, S.; DANILO, 2013). Also hydrogen bonding and charge interactions were seen between curcumin and collagen. Metal in our body interact with curcumin and play important role in the anti-oxidant activity. The interaction is shortly shown (FIGURE 1.23).
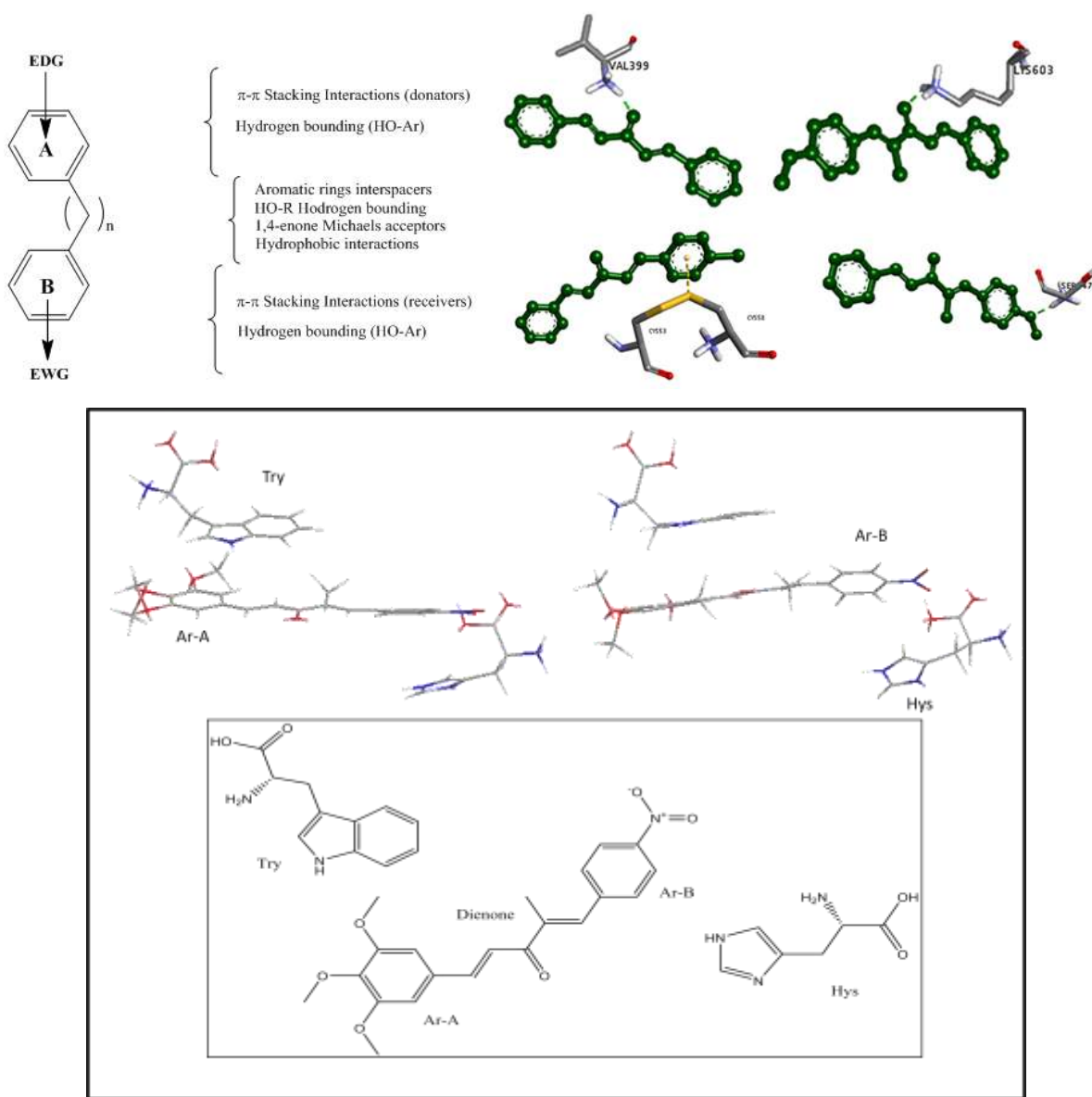
FIGURE 1.23 - Interaction representation of biphenyls.

❖ 2

Objective – Part 1

2 Objectives

Main objective of the work include.

- ✓ The synthesis of natural products analogous having anti-parasitic activity.
- ✓ The focus was given to compounds derived or based on chalcone and curcumin basic structures.
- ✓ The synthesized technique used by following green chemistry principle by using acid, base or ionic liquid (DIMCARB) as a catalyst.
- ✓ The evaluation of all these compounds for their potential against *Trypanosoma cruzi* and *Leishmania amazonesis*.
- ✓ The structural modification of active compounds for more potent compounds.

❖ 3

Results and Discussion

Part 1

3.1 Synthesis

The reaction of benzaldehyde and three *p*-substituted benzaldehydes with 2-butanone, using gaseous HCl as catalyst as outlined (SCHEME 3.1), produced the 4-aryl-3-methylbutenone **45**-**48**, which were isolated and characterized by spectroscopic data. These reactions were performed at room temperature by stirring the reaction mixture and passing dry gaseous HCl until the reaction mixture turned to red. Stirring continued until the completion of starting materials, which was monitored by TLC.
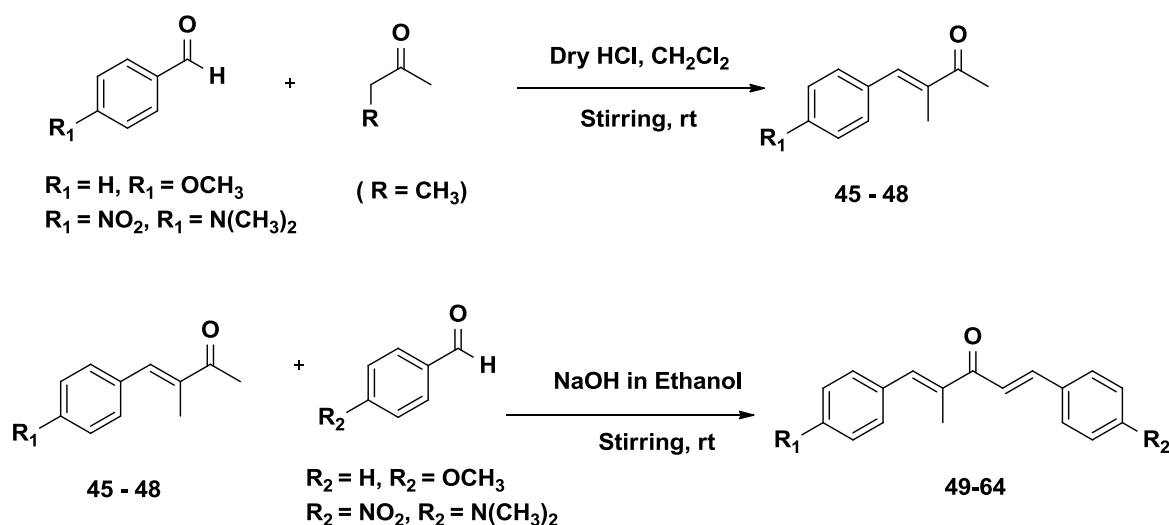
Scheme 3.1 - Reaction conditions for the synthesis of compounds **45-48** and ultimate synthesis of **49-65** from intermediate compounds **45-48**.

The reaction was very clear giving yields of 48-61 % of **45-48**, which were analyzed by NMR as follows: compound **45** showed two characteristic signals of two methyl groups in the shielded region at δ 2.06 and 2.47, whereas one =CH signal was displayed at δ 7.39 as singlet; additionally three aromatic signals having integration for five proton were detected at δ 7.32, 7.41 and 7.52. ^{13}C NMR spectra of **45** showed signals for two methyl groups at δ 13.0

and 25.9, and six peaks from δ 128-139 for eight carbons, with two of these peaks having double intensity for aromatic carbons. The characteristic peak at δ 200.3 is due to carbonyl carbon. The ^{1}H NMR spectra of compounds **46**, **47** and **48** are similar each other. Only compound **46** showed an extra signal at δ 3.85 due to OCH$_3$ substitution on benzene, and a signal at δ 3.02 for compound **48** due to N(CH$_3$)$_2$ substitution in benzene ring. By reacting each of the intermediary compounds **45**-**48** systematically with benzaldehyde (**A1**), anisaldehyde (**A2**), *N*,*N*-dimethylebenzaldehyde (**A3**) and nitrobenzaldehyde (**A4**) the respective sixteen dibenzylidene ketones **49**-**65** were produced in 45-93 % yield after re-crystallization from ethanol. All these reactions were carried in basic medium in ethanol, and their progress was monitored by TLC. The reaction time varied for each unsymmetrical product and depended on the nature and reactivity of the aldehyde used. Thus, as expected for aldol condensations, electron donors (amine and methyl-ether) at *para*-position in the benzene rings decreases the reaction time, while nitrobenzaldehyde reacted very fast. The aldol-dehydrated products are preferably *E* regeoisomers but *Z* isomers were also obtained in 1-5 %. The structures of these new compounds were determined by ^{1}H and ^{13}C NMR, HMQC and HMBC spectra.

Compounds **49**-**52** were synthesized from **45**, by treating it with benzaldehyde, anisaldehyde, *N*,*N*-dimethylebenzaldehyde and nitrobenzaldehyde in basic conditions in ethanol. The presence of a pair of doublets at δ 7.53 and 7.69, with a coupling constant of c.a. 16 Hz, typical for a *trans* two spins system, clearly confirms that the aldol condensation with the second aldehyde did occur. Also, extra signals in the aromatic region were noted in the ^{1}H spectra and the signal for methyl ketone group disappeared, showing that an aromatic ring had been added and the methyl group had been substituted to a significant extent. The major peaks in the NMR spectra of these

compounds are almost the same except from an additional signal in compounds **49**, **50** and **52.** Compound **49** has benzene ring with no substituent, while in compound **6** the *para* hydrogen of benzene is substituted by a OCH$_3$ group, showing a singlet at δ 3.85 ppm in ^{1}H NMR, and a peak at δ 55.4 ppm in ^{13}C NMR. Compound **51** shows an extra signal at δ 3.06 due to N(CH$_3$)$_2$, and **52** is prompt recognized by the strong deshieleding effect caused by NO$_2$ group to the orto hydrogen's (δ 8.27). Compounds **53-64** were similarly synthesized from compound **46-48**, so the spectroscopic study is comparable to that of compounds **49-52**, showing approximately the same signals shifts as shown in the compounds derived from **45**. The structures of all compounds were further identified using FTIR, UV-Vis and mass spectrometric analysis.

3.2 Biological evaluation

The synthesized compounds **45-64** were evaluated against promastigote forms of *L. amazonensis* and epimastigote and trypomastigote forms of *T. cruzi*. The intermediaries compounds (**45-48**) were found inactive in the bioassays, indicating that the second aldol reaction is important since it introduces groups that contribute to bioactivity. The more active compounds against epimastigotes of *T. cruzi* were **51, 61, 62, 63, 64** exhibiting an IC$_{50}$ value (inhibitory concentration for 50% of the parasites) of 13.3, 1.8, 10.0, 14.0 and 1.8 μM, respectively (TABLE 3.1). For trypomastigotes of *T. cruzi* the substances that showed greater activity were **62** and **64**, showing an EC$_{50}$ (effective concentration for 50% of the parasites) of 15.4 and 17.5 μM, respectively. Considering the evaluation of activity against promastigotes of *L. amazonensis* it was observed that substances **52**, **61**, **63** and **64** are the most active, with IC$_{50}$ values of 11.6, 13.4, 12.0 and 3.4 μM, respectively.

Table 3.1 - Antiparasitary and citotoxicity activities of 1, 5-diaryl-3-oxo-1, 4-pentadienyl derivatives **45-64**.

Compounds	Epimastigote IC_{50} (µM) Average±SD	Trypomastigote EC_{50} (µM) Average ± SD	Promastigote IC_{50} (µM) Average±Sd	LLCMK$_2$ CC_{50} (µM) Average± SD	M. J774A1 CC_{50} (µM) Average± SD
(**45**)	> 100	>100	>100	687.5 ± 17.68	742.5 ± 81.32
(**46**)	> 100	>100	>100	280.0 ± 28.28	240.0 ± 14.14
(**47**)	> 100	>100	>100	150.0 ± 0.00	160.0 ± 14.14
(**48**)	82.2 ± 7.42	>100	>100	266.0 ± 12.73	70.5 ± 16.26
(**49**)	15.9 ± 1.34	71.7 ± 2.33	15.3 ± 0.35	33.6 ± 5.28	34.5 ± 7.78
(**50**)	14.3 ± 5.13	>100	20.4 ± 3.32	93.0 ± 9.90	51.0 ± 11.31
(**51**)	13.3 ± 2.90	>100	20.0 ± 2.83	53.0 ± 4.24	20.2 ± 3.96
(**52**)	16.9 ± 0.00	65.0 ± 7.07	11.6 ± 1.70	43.3 ± 4.16	26.0 ± 1.41
(**53**)	16.7 ± 1.41	73.3 ± 4.67	22.3 ± 1.77	44.0 ± 0.00	54.0 ± 8.49
(**54**)	23.6 ± 2.33	>100	21.8 ± 0.28	75.0 ± 7.07	34.1 ± 1.75
(**55**)	21.3 ± 0.00	>100	18.0 ± 0.00	411.0 ± 55.15	36.2 ± 4.35
(**56**)	25.2 ± 4.60	>100	14.8 ± 1.77	20.1 ± 6.80	30.0 ± 6.56
(**57**)	24.1 ± 2.62	78.3 ± 2.40	21.5 ± 0.71	191.0 ± 12.73	28.5 ± 0.71
(**58**)	>100	>100	20.1 ± 1.48	285.1 ± 81.81	34.3 ± 5.13
(**59**)	25.1 ± 1.27	>100	20.5 ± 2.12	314.3 ± 0.00	10.0 ± 0.00
(**60**)	>100	>100	>100	167.0 ± 8.49	966.6 ± 57.74
(**61**)	3.5 ± 0.35	17.5 ± 2.05	13.4 ± 1.98	264.3 ± 3.25	47.3 ± 4.16
(**62**)	10.0 ± 0.00	73.3 ± 0.00	15.5 ± 1.70	172.1 ± 15.77	36.6 ± 1.15
(**63**)	14.0 ± 0.00	>100	12.0 ± 0.71	25.9 ± 9.50	24.7 ± 2.52
(**64**)	1.8 ± 0.21	15.4 ± 4.10	3.4 ± 0.07	32.5 ± 1.20	43.0 ± 4.24
PC1	6.5±0.7	34.5±7.6		614.7±115.2	
PC2			0.06 ± 0.00		3.7 ± 0.31

PC1: Benznidazol, PC2: Amphotericin B

The literature concerning antiparasitary activities of curcuminoids and chalcones reports results with IC_{50} around those we found in the present work

(CHANGTAM et al., 2010). Symmetrical dibenzylideneketones made using cyclic ketones gave antileishmanial activity with lower IC_{50} values. A recent study showed that both electrons withdraw or donator groups at the aryl part of symmetrical dibenzylideneacetones, made from propanone and two equivalents of substituted aldehydes, affect positively the bioactivity compared with nonsubstituted compounds. Our results, using the series of asymmetrical dibenzylydeneketone compounds (TABLE 3.1), shows that the strong electron attractor NO_2 substituent is the most responsible for the great activity observed. Compounds **52** and **61** differ only in the aromatic ring, where the NO_2 is attached, but their bioactivity is significantly different. This result indicates that introducing the electron-attracting group during the first reaction results in better activity of the final compounds. Thus, nitro compounds **61** and **64** were found to be the most active anti-parasitics in the three assays performed (TABLE 2.1), and indeed compound **64**, with two NO_2 groups, is the most active amongst the twenty tested substances. These results parallels those recently published by others researchers, which found that nitroreductase enzymes, present in *Leishmania danovani* but not in the mammal cells, activate NO_2-containing drugs into a more active form (WYLLIE; PATTERSON; FAIRLAMB, 2013).

The mechanism by which drugs act against parasites have been studied by many groups around the (OUELLETTE; DRUMMELSMITH; PAPADOPOULOU, 2004). Many of these studies suggest that drugs can bind to nucleic acids and cell wall components, or inhibit enzymes activity in the parasite. Along with the presence of NO_2 group in our compounds that putatively can be reduced/activated by parasite reductases our nitrobenzylideneketones **61** and **64** may be good electrophiles to bind some parasite cells components. These molecules were studied using a computational

method, in order to see possible binding points. The molecular geometry that came out from these calculations shows that the presence of the methyl group at C-2 of the 1,4-pentadienyl-3-one chain disturbs the first enone π system (1-en-3-one), while the second part, formed by the benzene ring bound to C-5 and the 4-en-3-one, is planar with an almost perfect parallelism of the *p*-orbitals (FIGURE 2.1). As a result, carbon C-1 contains only small electron density compared with C-5. These observations may have some relationship with our bioactivity results, which showed that electron attractor group present in the aromatic ring connected to C-1 contributes for greater bioactivity. Probably C-1 is a good electrophilic center to bind parasite cell components.
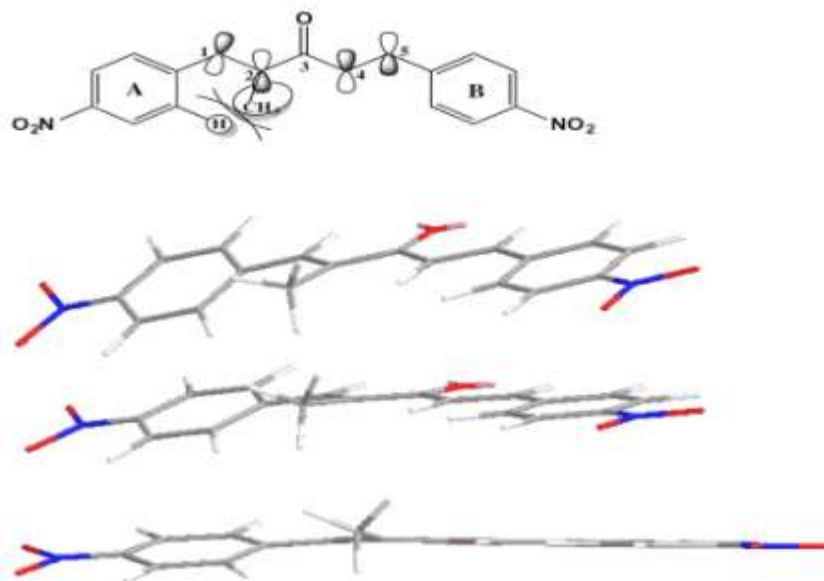
Figure 3.1 – Computational optimization show that ring A become out of the plane due to steric hinderance caused by CH3 group close to Ar-H on ring A.

In addition, we also evaluated the cytotoxicity of the compounds against LLCMK$_2$ cells (kidney epithelial cells from *Macaca mulatta*) and macrophages J774A1. The results showed that the active substances were more toxic against

the parasites than for the cell lines tested. Finally, our results demonstrated that compounds **61** and **64** proved to be the most active against this trypanosomatids and may become promising compounds for treatment of leishmaniasis and Chagas disease.

3.3 Transformation of compound 61 and 64 by *T. cruzi*

Compounds **61** and **64,** these two nitro group containing substances were very active when tested against different forms of *T. cruzi* and *L. amazonensis* [10]. Metabolomic profile of these compounds by *T. cruzi* was studied. Epimastigote forms were exposed to 20 μM of **61** and **64** over six hours and then metabolites were extracted. After this treatment, approximately 90% of the parasites were found died. Parasites that were not exposed to compounds **61** and **64** were used as control for mass spectrometric analysis of both samples in parallel with reference compounds.

Cultivation medium containing *T. cruzi* with and without test substances were lyophilized prior to extraction. Extractions were performed by partitioning with ethyl acetate after suspending lyophilized powder in water successively at pH 7, 3 and 8, in order to cover the possibility of forming acid or basic compounds. Biotransformation products were detected only in the neutral extract.

Each of compounds **61** and **64** were consumed completely (not detected in the LC-UV-MS analysis) and produced only one metabolite. Compound **61** ($C_{18}H_{15}NO_3$, 293 Da) and **64** ($C_{18}H_{14}N_2O_5$, 338 Da) exhibited [M-H]$^-$ peaks at *m/z* 292 and 337 in their respective APCI$^-$ mass spectrum, and showed a cinnamoyl UV absorption band with λ_{max} at 318 and 323 nm, respectively. In both metabolites detected, the cinnamoyl absorption was substituted by a λ_{max} at

277 (metabolite **67**, from **61**) and 279 (metabolite **68**, from **64**), and the molecular masses increased by 4 Da (*m/z* 296 and 341 for **67** and **68** respectively). These data in conjunction clearly indicated reduction of the two C-C double bond (SCHEME 3.2, FIGURE 3.2). Metabolite **67** and **68** were also characterized by ESI$^+$ HRMS, showing [M+H]$^+$ at 298.1443 ($C_{18}H_{20}NO_3$, cal. 298.1443) and 343.1301 ($C_{18}H_{19}N_2O_5$, cal. 343.1294) respectively.

61. R = H
64. R = NO$_2$

67. R = H
68. R = NO$_2$
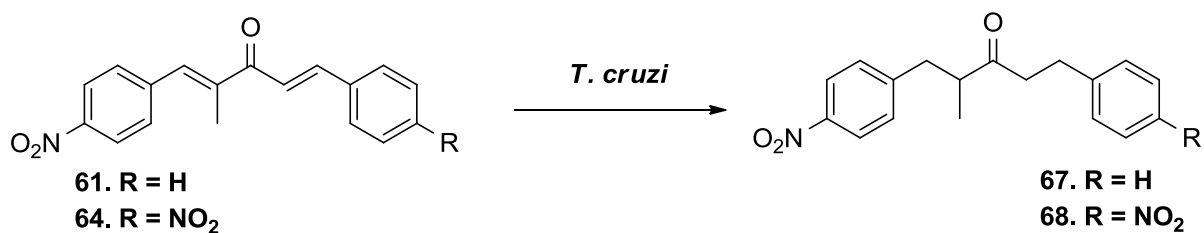
Scheme 3.2 - Unsymmetrical 1,5-diaryl-3-oxo-1,4-pentadienyls **61** and **64** derived metabolites. The action of parasite reduced both double bonds.

3.4 Synthesis of compounds 65-72

Based on the above shown reductive biotransformation of the active compounds by *T. cruzi*, a series of substances derived from **61** and **64** was produced, all of them containing hydrogenated positions compared with precursors. These reduced compouds were all tested for *T. cruzi* inhibition. Compounds **65-72** (SCHEME 3.3, FIGURE 3.3) were obtained by chemical or microbiological methods. Hanzsch ester hydrogenation (HEH) produced compounds **65** and **66**, with reduction only at the less substituted C-C double-bound, while the whole cells of the fungus *Penicillium brasilianum* reduced both double-bounds resulting in **67** and **68**. Sodium borohydride was used for

carbonyl reduction of **61** and **64** producing the alcohols **69** and **70**. When **61** and **64** were treated with H_2 on Pd/C the double bonds and nitro groups were reduced forming compounds **71** and **72**.

The ^{1}H NMR spectra of compound **61** and **64** shows the presence of a pair of doublets at δ_H 7.53 and 7.69, with a coupling constant of c.a. 16 Hz, typical for a *trans* two vinylic spins system. The ^{13}C NMR of both compounds show the characteristics C=O signal at c.a. δ_C 190. Compounds **65-72** completely lose these signals because all these groups were reduced by specific reagents. The ^{1}H NMR spectra of compounds **65** and **66** show the appearance of methylene protons at nearly δ_H 3.0, while disappearing CH=CH signal at δ_H 7.53 confirm the reduction of one CH=CH selectively. The ^{1}H NMR spectra of **67** and **68** show the disappearance of 2 double bonds representative signal between δ_H 7-8, while the appearance of new methylenic signals between 2-3 ppm confirm the reduction of both double bonds in compounds **61** and **64**. The ^{13}C NMR spectra shows the disappearing of two signals between δ_C 120-140 and the appearance of two new signal between 30-40 ppm confirm the reduction of CH=CH. The ^{1}H NMR spectra of compounds **69** and **70** shows the appearance of doublet nearly δ_H 4.80, proving the reduction of carbonyl group. The ^{13}C NMR confirms the reduction of carbonyl by dis-appearing the carbonylic signal at δ_C 190 and appearing of carbinolic signal for C-OH at δ_C 77.0. The ^{1}H NMR of compounds **71** and **72** show the disappearance of all CH=CH signals at δ_H 7.53 and 7.69, while appearing signal between 3-4 ppm confirm the reduction of olefinic system. The detection of four signals in ^{13}C NMR appeared due to methylenic carbons. The up-field shift in ^{1}H NMR was observed in aromatic signals, which was due to the reduction of nitro to amino group. The Pd/C on hydrogen reduces double bonds along with nitro groups.

The structures of all compounds were further established using UV-Vis and mass spectrometric analysis.
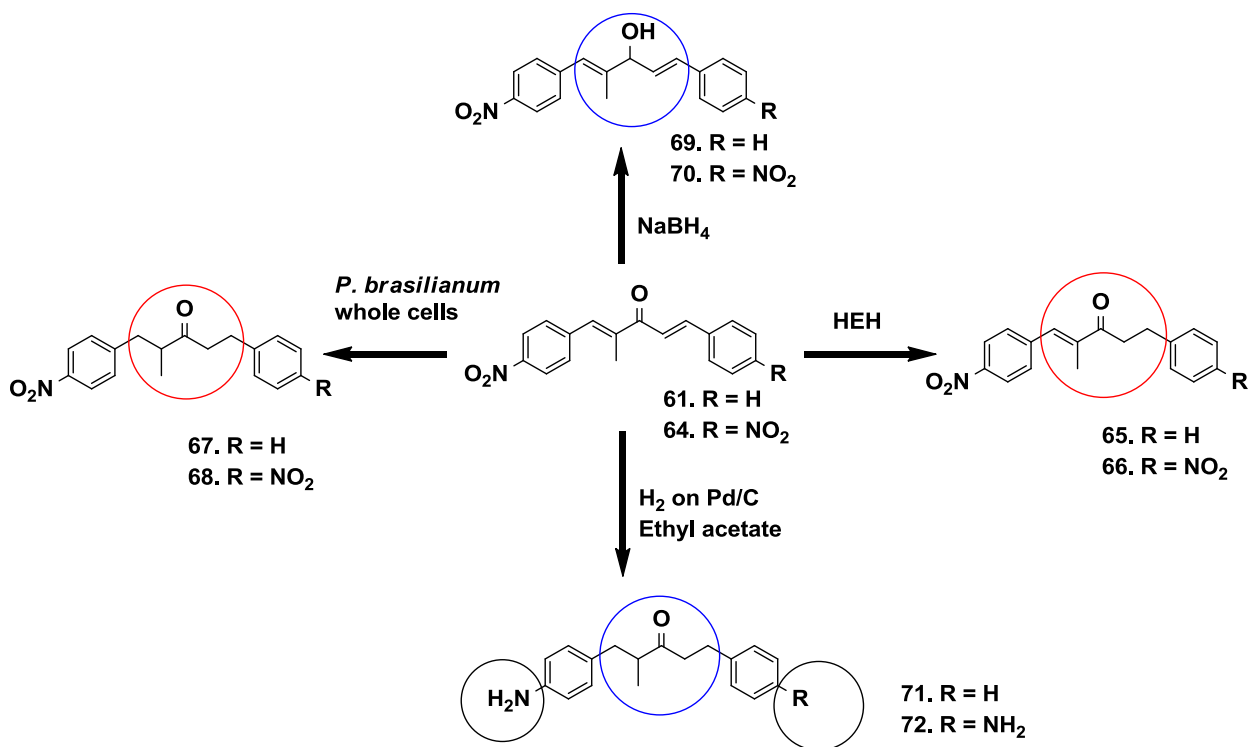
Scheme 3.3 - Selective reduction of different groups by selective reagent and catalyst.

3.5 Metabolism and bioactivity study

Compounds **61** and **64** showed great antiparasitary activities against *T. cruzi* and *L. amazonensis* (TABLE 3.1). They inhibited epimastigotes forms of *T. cruzi* exhibiting an IC_{50} value (inhibitory concentration for 50% of the parasites) of 3.5 and 1.8 µM respectively (ZIA et al., 2014). Recently, we studied how these drugs acts in *T. cruzi* and found that they cause an intense oxidative stress resulting in cell death by necrosis, autophagy and apoptosis. It was also observed that DNA fragmentation, intensification of lipid per

oxidation, and reduction of free thiols levels occurred (BIDÓIA et al., 2016). In the present work we found that *T. cruzi* reduces the double-bonds of the dienone system present in **61** and **64**. This finding can be close related to the diminishing amount of free thiols groups in the parasite cells. Thiols groups are part of important cysteine containing co-enzymes in many organisms. Trypanothione (N1,N8-bis(glutathionyl)spermidine or $T(SH)_2$) is the major redox mediator in *T cruzi*. $T(SH)_2$ can react with Michael acceptors like enones and other α,β-unsaturated carbonyl groups containing substances. The scheme shown in Figure 3.4 below could explain the observed physiological effects that **61** and **64** causes in *T. cruzi*, as well as the reduction of their C-C double bonds. Carbons C-1 in **61**, and C-1 and C-5 in **64** are strongly electrophylic because they are β-enone and due the presence of the electron withdrawing NO_2 group at *para* position in the aromatic ring. Thus, **61** and **64** can be attacked by the thiols from $T(SH)_2$, producing a $T(S)_2$ - drug covalent complex. This explains the diminishing of free SH groups in *T. cruzi* cells after exposed to **61** and **64**. The efforts of the cell machinery to regenerate the redox mediator $T(SH)_2$ may result in disruption of a portion of the covalent complex, producing an amount of reduced compounds **67** and **68**. Usually the reducing agent is NADPH (SCHEME 3.4, FIGURE 3.4).
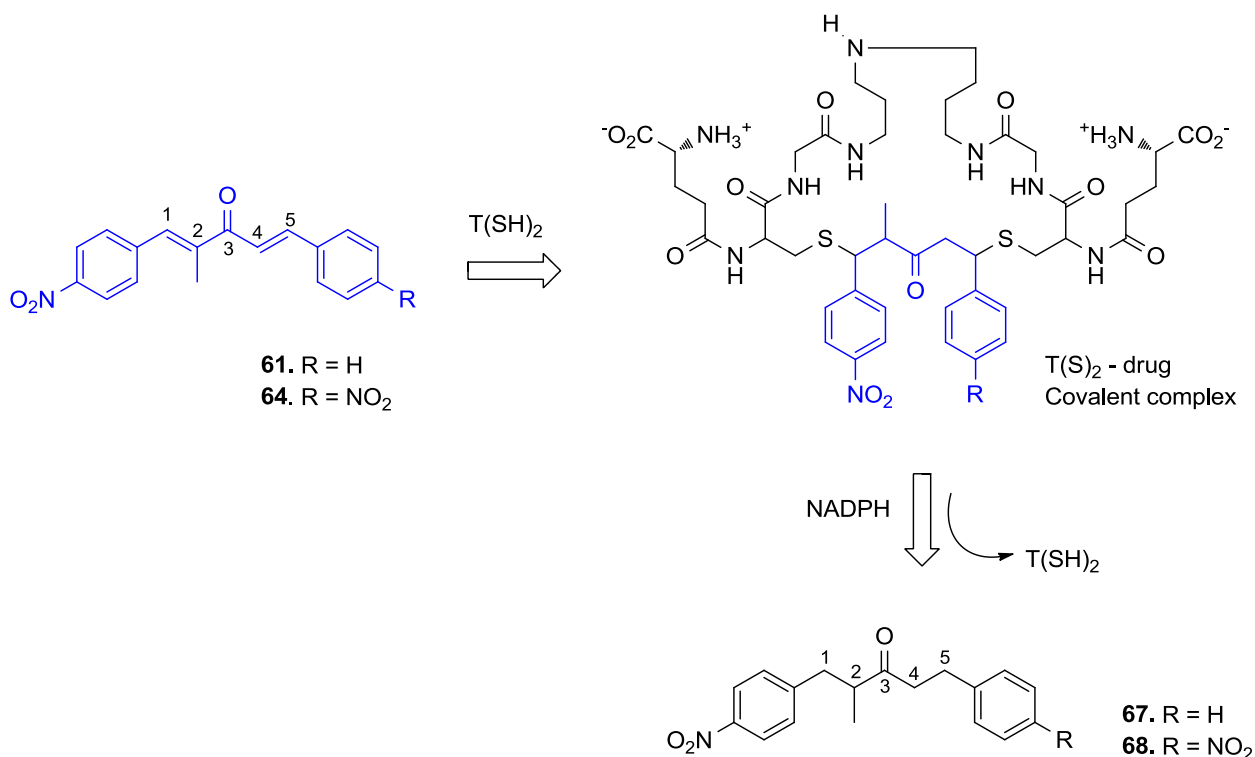
Scheme 3.4 - Formation of covalent complex of **61** and **64** with trypanothione redox system and reduction by NADPH.

In order to check the structural requirements for the activity of these diarylpentadienones some derivatives reduced at different positions were prepared by chemical and microbiological methods. Among compounds **65-72**, **67** and **68** were obtained by bio-catalytic method using whole cells of *Penicillium brasilianum* as biocatalyst, because all synthetic catalyzing agents used failed to selectively reduce both double bonds. In *P. brasilianum* the enzyme OYE (old yellow enzyme) plays an important role in the reduction of double bonds.

T. cruzi and *L. amazonensis* were treated with **65-72**, which are different reduced form of potent compound **61** and **64**. In general the IC_{50} values enhanced significantly for both parasites in comparison with activity observed

for parent compounds (TABLE 3.2). It means that double bonds are crucial for activity. In general it was seen that potency decreases by reducing any of the moiety of compounds **61** and **64**. Compounds having one bond reduced (**65** and **66**) faces reduction in the potency and exhibit IC_{50} 52.2 ± 1.6 and 11.9 ± 0.6 µM against epimastigote. By reduction the two double bonds we get the compounds obtained by the metabolomic study, compounds **67** and **68**. These compounds also loss their potency and its IC_{50} decreases to 58.1 ± 0.9 and 15.3 ± 2.1 µM against epimastigote. Compounds **69** and **70** undergone reduction of carbonyl and IC_{50} reaches to > 100 and 22.4 ± 1.62 respectively. Compounds **71** and **72** which were obtained by the reduction of double bonds and NO_2 exhibit a complete loss of potency by showing IC_{50} 89.8 ± 6.94 and 42.7 ± 4.45 µM respectively. These results are contrary to those published by others researchers, which found that nitroreductase enzymes present in *T. cruzi* and in *Leishmania danovani*, but not in the mammal cells, activate NO_2-containing drugs into a more active form. In those organisms, the trypanocidal activity of nitro compounds is depend on nitroreductase enzymes (NTR) that converts them to amines, enhancing their activity.

In all the reduced products **65-72** it was observed that compounds derived from **64** maintain their activity up to little extent as compared to that derived from compounds **61**. By losing potency the cytotoxicity against normal cell lines improved and it is also not harmful for it in high concentration. Greater the selectivity index (SI) value, better the drug candidate. The SI value of compound **64** is better than compound **61**, being better candidate than **61**. All other reduced products **65-72** shows poor selective index as related to their biological activity. In similar pattern the activity of compounds **65-72,** also show reduction for *L. amazonensis* (promastigotes), except for compound **65**,

derived from **61**, which shows IC$_{50}$ value c.a. half of the parent compound, but with selectivity ten times better (TABLE 3.2).

Table 3.2 - Antiparasitary and cytotoxicity activities of compounds **61, 64-72**.

S. No	*T. cruzi* epimastigote	SI in epimastigotes	*L. amazonensis* promastigotes	SI in promastigotes	*VERO* cells
	IC$_{50}$ (µM)		IC$_{50}$ (µM)		CC$_{50}$ (µM)
61	3.5 ± 0.4	13.5	13.4 ± 2.0	3.5	47.3 ± 4.2
64	1.8 ± 0.2	23.9	3.4 ± 0.1	10.1	43.0 ± 4.2
65	52.2 ± 1.6	4.8	6.8 ± 0.0	36.5	248.1 ± 15.3
66	11.9 ± 0.6	12.8	24.4 ± 2.4	6.3	152.7 ± 3.9
67	58.1 ± 0.9	2.4	20.2 ± 2.2	7.0	140.4 ± 5.2
68	15.3 ± 2.1	7.2	16.6 ± 1.8	6.7	110.9 ± 4.3
69	> 100	-	74.0 ± 4.0	4.4	323.8 ± 13.3
70	22.4 ± 1.6	13.5	23.7 ± 2.4	12.7	302.1 ± 15.8
71	89.8 ± 6.9	3.2	21.0 ± 1.8	13.8	260.3 ± 1.3
72	42.7 ± 4.5	10.0	21.0 ± 3.7	20.3	426.3 ± 8.2
PC1	6.5±0.7				614.7±115.2
PC2			0.06 ± 0.00		

SI: Selectivity index; PC1 (positive control 1): Benznidazole; PC2 (positive control 2): Amphotericin B

3.6 Molecular Docking

3.6.1 Optimization of ligands

The structure of all compounds **61, 64-72** were analyzed for their stability and optimized energy using software Avogadro 1.1.1 which is an advanced semantic chemical editor, visualization, and analysis platform (HANWELL et al., 2012). Several calculations were carried to know the best stable structure of compounds. Lower energy conformers were selected for docking calculation. It was observed that the planarity of compounds changed completely by reducing one or more bonds (FICURE 3.2). Thus, in case of compounds **65-72**, the aromatic rings go out of the plane, and the molecules gain conformational flexibility.
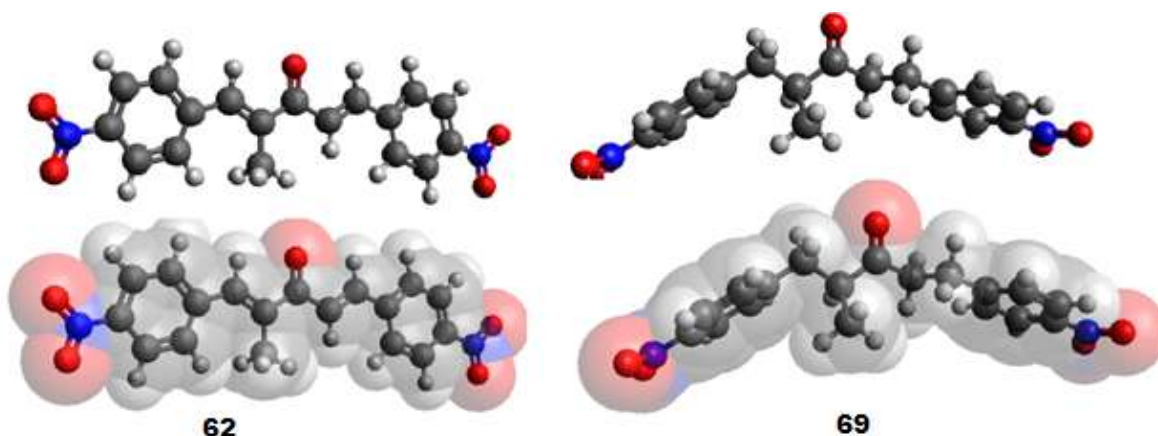
Figure 3.2 - Planarity loses as the result of reduction of double bonds in compound **64**, calculated by software Avogadro 1.1.1.

3.6.2 *In-silico* interaction studies

All compounds were analyzed for their binding possibility to enzyme trypanothione reductase *Pdb* code 1BZL and the result obtained were tabulated

in Table 3.3. Active site calculation was performed on the basis of crystallized ligand in its crystal structure. Centroid of the active site was calculated and then all compounds were evaluated for their *in-silico* inhibition study. The amino acids which contribute actively are Gly-12, Gly-14, Ser-15, Gly-16, Asp-36, Val-37, Ser-47, Ala-48, Gly-51, Thr-52, Cys-53, Val-56, Cys-58, Lys-61, Gly-126, Gly-128, Ala-160, Ser-161, Gly-162, Arg-288, Arg-291, Gly-326, Asp-327, Met-333, Leu-334, Thr-335, Pro-336, Ala-338. Compounds **61, 64-72** have interaction with amino acid in the active sites of 1BZL, depend on the structure and pharmacophoric sites. Compound **61**, which is second potent compound, has interaction with amino acids Lys-61 by forming H-bond between Oxygen of nitro having bonded distance 2.5 Å. H-bond *pi* interaction between aromatic ring and Gly-16 by distance of 1.65 Å were also observed. Compound **64**, which are most potent in the series, show a good interaction with amino acids of the active site of enzyme. Several bonding interaction were calculated including H bond between Carbonyl and that of Thr-335 by distance 2.93 Å, H-bond between Gly-128 with oxygen of nitro group by distance of 3.16 Å, 2H bonds between Thr-335 with oxygen of nitro group by distance of 2.49 and 3.06 Å respectively. Also 1H bond between Gly-51 with oxygen of carbonyl by bonding distance of 3.40 Å along with 1 sigma pi interaction between Thr-52 and aromatic ring of ligand by distance of 3.4 Å were calculated (FIGURE 3.3).

Compound **64** and their derivatives has two nitro groups show greater interaction then compound **61** derivatives having one nitro group. Extra nitro group significantly increases all type of interaction including Van der Waals, hydrogen bonding, water interaction, electrostatic and covalent bond interaction (FICURE 3.4).

Compounds exhibited potency *in-silico* was also active in wet lab experiment like compounds **61**, **64**, **65**, **66**, **68**, and **70**. The docking result is in agreement with in-vitro assay results except compound **66** and **70**, which show great inhibition *in-silico* than wet lab experiment (TABLE 3.3). Compound **66** having one bond and compound **70** having carbonyl reduced may probably give space to enzyme to be interacting more strongly. After reduction of these moieties it still maintains some degree of planarity, but when both double bonds are reduced the planarity loses completely. So the interaction forces become weak. These results showed that there is maximum probability that these compounds inhibit trypanothione reductase.

Table 3.3 - Docking results of compounds **61, 64-72** docked on to trypanothione reductase (1BZL).

Compounds	Binding energy (kcal mol^{-1})	Inhibition constant (Temp = 298.15 k) ki µM	Calculated RMS from reference (Å)
61.	-8.51	0.58	32.72
64.	-10.26	0.03	32.46
65.	-8.36	0.75	33.70
66.	-8.96	0.27	26.46
67.	-7.04	6.90	35.85
68.	-7.86	1.72	32.75
69.	-7.50	3.19	27.47
70.	-8.74	3.92	29.44
71.	-4.54	473	26.59
72.	-4.64	396	28.00
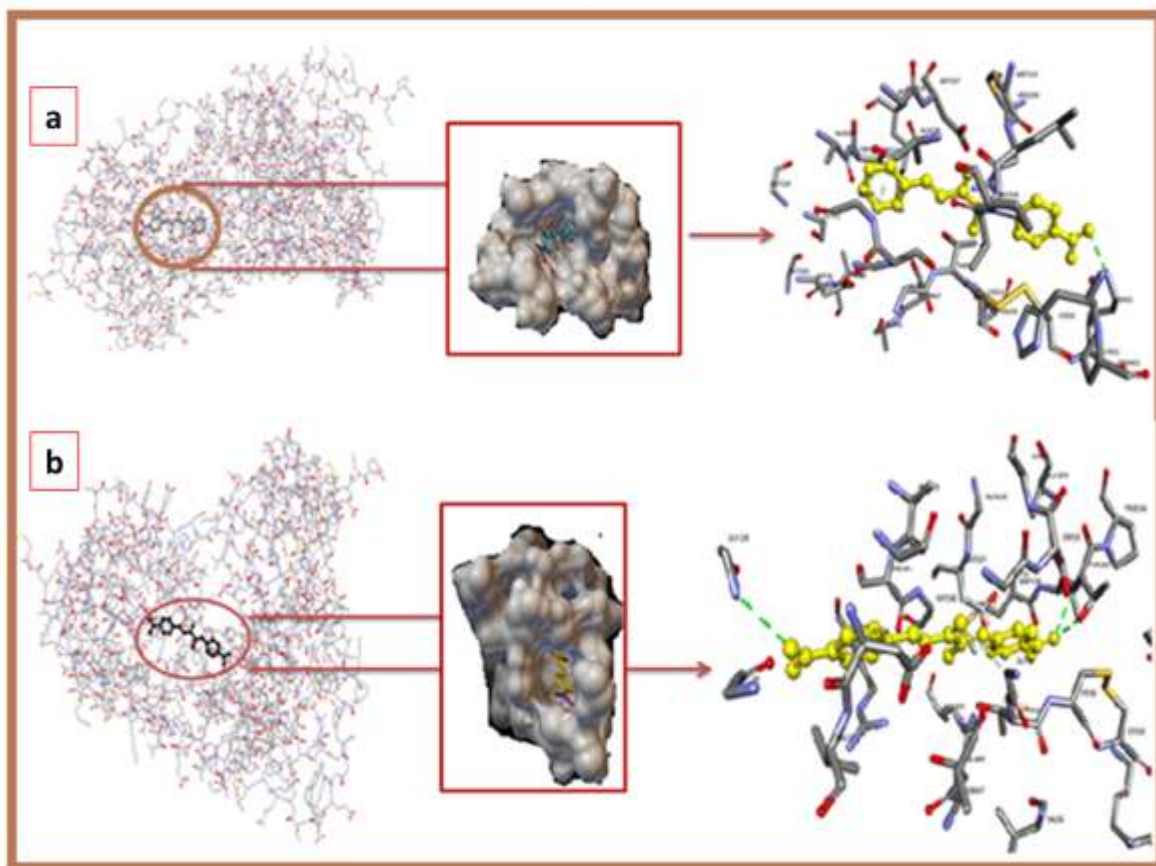
Figure 3.3 - *In-silico* analysis of the interaction of compounds **61** (above) and **64** (below) with active site of 1BZL.
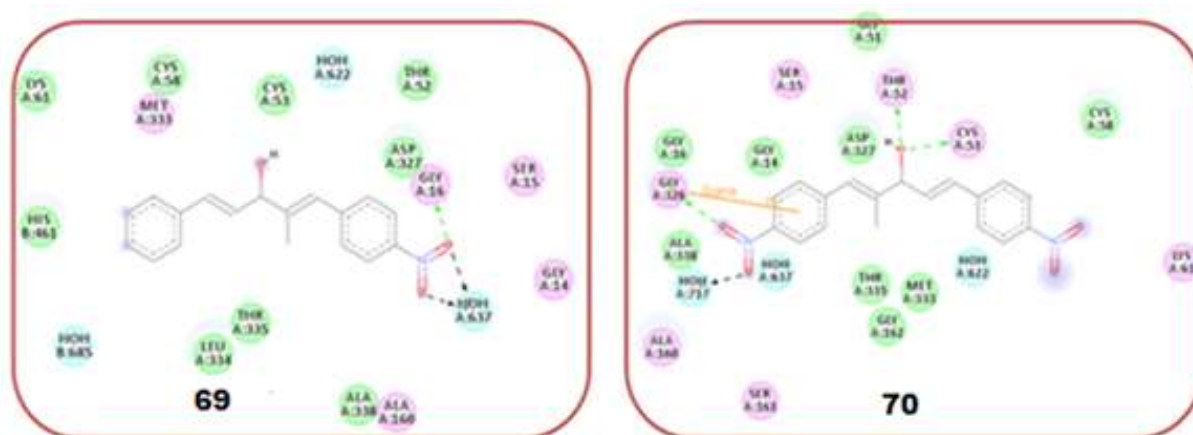
Figure 3.4 - Comparison of compound **69** and **70** interactions in 2D.

3.6.3 Studies on molecular orbitals by computational analysis

The highest occupied molecular orbital (HOMO) and lowest unoccupied molecular orbital (LUMO) for compound **64** (FIGURE 3.5), and compounds having no nitro were also analyzed by Gaussian (HEHRE; DITCHFIELD; POPLE, 1972). It is observable that the charge density in HOMO is mainly localized on the ring A of compound **64** with little charge density on one double bond. The figure show that compound **64** has LUMO which represent that the double bonds are more susceptible to reduction so can be reduced by the action of enzyme trypanothione reductase. The stability of all compounds were also calculated by Avogadro (HANWELL et al., 2012).
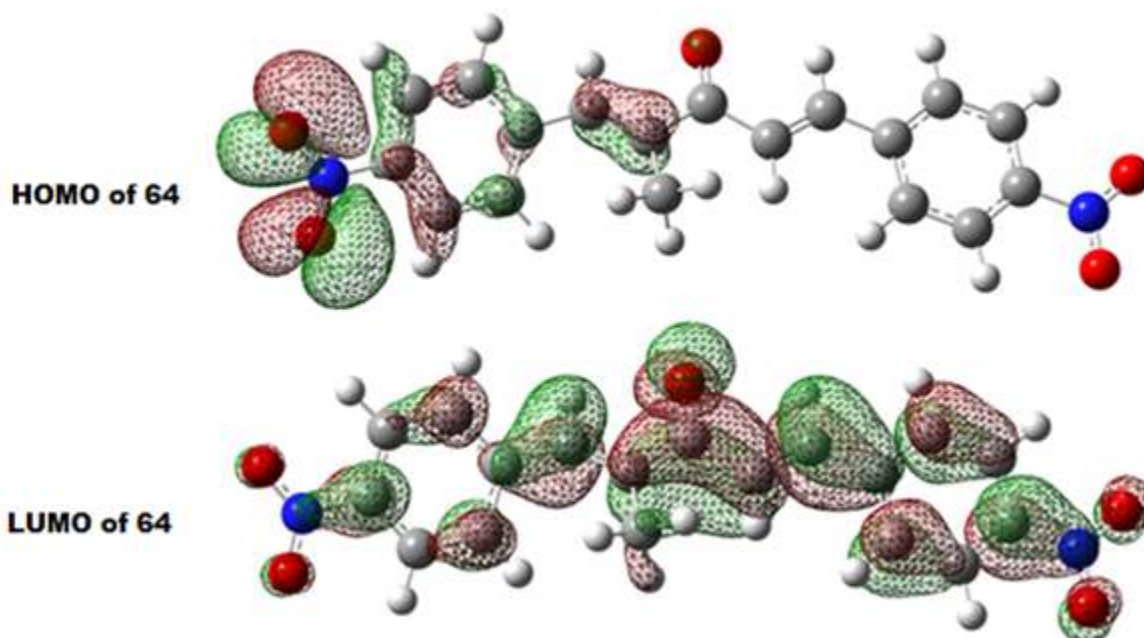
Figure 3.5 - Electronic distributions for for compound **64** [(1E,4E)-2-methyl-1,5-bis(4-nitrophenyl)penta-1,4-dien-3-one]. Semi-empirical calculations were performed using the Gaussian software package with the semi empirical B3LYP/6-31G(d,p) method and full geometric optimization.

Previously (ZIA et al., 2014), a series formed of 20 compounds inspired from chalcone and curcumin structures was synthesized and tested against *Trypanosoma cruzi* and *Leishmania amazonensis*. Among these substances, 2-methyl-1-(4-nitrophenyl)-5-phenylpenta-1,4-dien-3-one (**61**) and 2-methyl-1,5-bis(4-nitrophenyl)penta-1,4-dien-3-one (**64**) showed impressive results, with IC_{50} lower than the commercial drug benznidazole. During following studies, it was observed that these compounds induces oxidative stress in three different forms of *T. cruzi*, causing damage in essential cell structures, reflecting in lipid peroxidation and DNA fragmentation (FIGURE 3.6) (BIDÓIA et al., 2016).
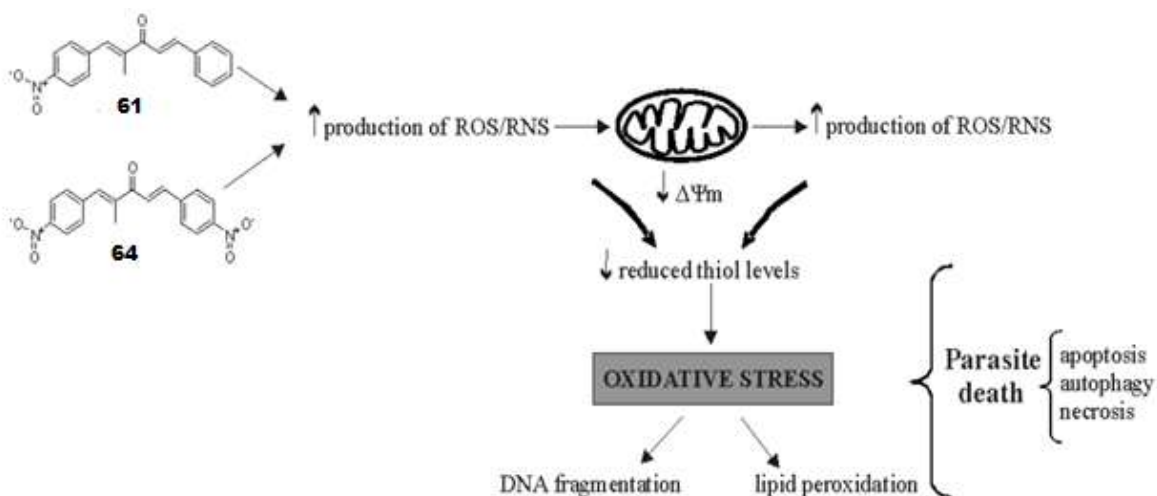
Figure 3.6 – Inhibition mechanism of compounds **61** and **64**.

3.7 Synthesis of compounds 73-93

In order to increase the search for anti-parasitic compounds, different moiety having methoxy and halogen were synthesized. Compounds **73** and **74** were synthesized by the condensation of anisaldehyde and chloro benzaldehyde

with 2-butanone and 2-pentanone respectively, using gaseous HCl as catalyst. Intermediate compounds **73** and **74** were isolated and characterized by spectroscopic data. Then the intermediate yields compounds **75-93** by treating with various aromatic aldehydes in base catalyzed condition. The synthesis, characterization and spectroscopic date of compounds **73-93** are included in supplementary section. The targeted diarylpentanoids were synthesized to see the effect of substitution on aromatic rings. Previously symmetrical diarylpentatanoids were found to have potency to treat leishmaniasis (S.F.P. BRAGA et al., 2014). In our project we focused to prepare unsymmetrical diarylpentanoids of various substitution patterns, to explore more the effect of different aryl groups upon activity (SCHEME 3.5 and TABLE 3.4).
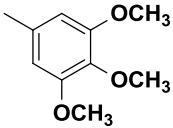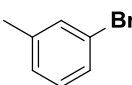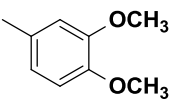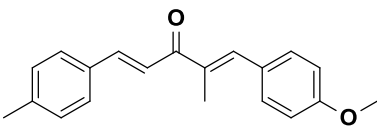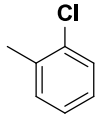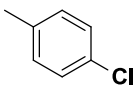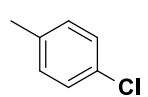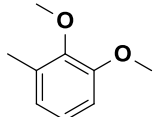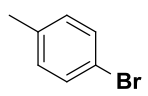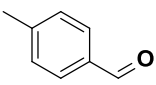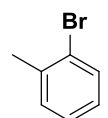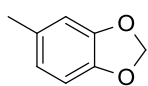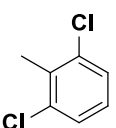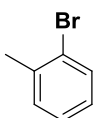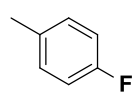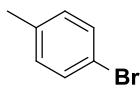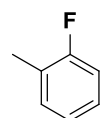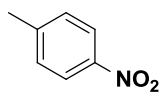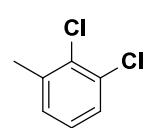
NMR data of compound **73** showed two characteristic signals of two methyl groups in the shielded region at δ_H 2.07 and 2.45, whereas one methoxy signal at δ_H 3.85. Double bond (=CH) signal was appeared at δ_H 7.47 as singlet. Two aromatic doublet displayed at δ_H 6.95 and 7.41 having spin coupling constant of approximately 8 Hz. ^{13}C NMR spectra of **73** showed signals for two methyl groups at δ_C 12.9 and 25.8 ppm, and a methoxyl at δ_C 55.3, and six peaks from δ_C 113-159 for eight carbons, with two of these peaks having double intensity for aromatic carbons. The characteristic peak appeared at δ_C 200.2 is due to carbonyl carbon. Compound **74** exhibits similar NMR spectra except one extra signal of CH$_2$ at δ_H 2.43 and its ^{13}C NMR signal at δ_C 26.1. Compounds **75-86** were produced by reacting compound **74** with different aldehydes having electron donating and electron withdrawing moieties. It was successfully completely characterized by NMR. One double bond and aromatic moiety has added, so ^{1}H NMR has two more doublet for -CH=CH- having coupling constant of approximately 16 Hz which is characteristic of H-H trans coupling system. The aromatic signals appeared at δ_H 6.5-7.8 depend on the substitution

attached to it. Compounds **87-93** were prepared from the reaction of compound **74** with different aldehyde. These compounds were characterized by ^{1}H NMR and ^{13}C NMR having similar spectral signals as for compounds **75-86** except one extra quartet signal of CH_2 groups at δ_H 2.64. The quartet appearance is due to the coupling of CH_2 with neibouring CH_3 group..
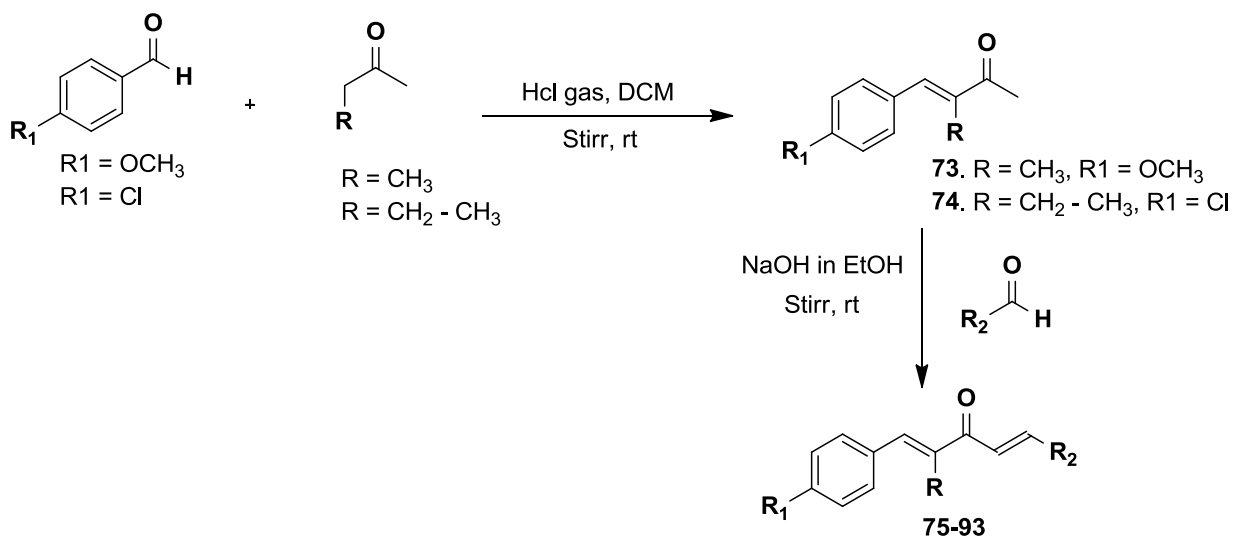
Scheme 3.5 - Synthesis of intermediate compounds **73** and **74** and their unsymmetrical diaryl analouges. Compounds **75-86** is derived from **73** while **87-93** is derived from intermediate **74.**

Table 3.4 - Unsymmetrical diraylheptanoids analogues substitution. Compounds **75-86** are derived from **73** while **87-93** are derived from intermediate **74.**

Compounds	R$_2$	Compounds	R$_2$
75	3,4,5-trimethoxyphenyl (OCH$_3$, OCH$_3$, OCH$_3$)	85	3-bromophenyl (Br)
76	3,4-dimethoxyphenyl (OCH$_3$, OCH$_3$)	86	(diarylheptanoid structure with O, and two aryl groups, one bearing O)
77	2-chlorophenyl (Cl)	87	4-chlorophenyl (Cl)
78	4-chlorophenyl (Cl)	88	2,3-dimethoxyphenyl (O, O)
79	4-bromophenyl (Br)	89	4-formylphenyl (O)
80	2-bromophenyl (Br)	90	benzo[d][1,3]dioxol-5-yl (O, O)
81	2,6-dichlorophenyl (Cl, Cl)	91	2-bromophenyl (Br)
82	4-fluorophenyl (F)	92	4-bromophenyl (Br)
83	2-fluorophenyl (F)	93	4-nitrophenyl (NO$_2$)
84	2,3-dichlorophenyl (Cl, Cl)		

3.8 Biological Evaluation of compounds 73-93

3.8.1 Antiproliferative assay

The unsymmetrical curcuminoids were evaluated for their antiparasitary potential against epimastigote and trypomastigote of *T. Cruzi* and promastigote of *L. amazonesis* (TABLE 3.5). Synthesized compounds were more potent than benznidazole showing IC_{50} and EC_{50} value in milli molar range. Moreover, the results showed that the compounds were more toxic against the parasites than to Vero cells (kidney epithelial cells from African green monkey). This research opened a way to explore the promising activity of diraylheptanoids analogues for the development of effective drugs for the treatment of parasitic diseases.

Table 3.5 - Antiparasitary and citotoxicity activities of biarylalkanones **73-93.**

Compounds	Epimastigote IC_{50} (µM) Average ± SD	Trypomastigote EC_{50} (µM) Average ± SD	Promastigote IC_{50} (µM) Average ± SD	Vero cells CC_{50} (µM) Average ± SD
73	> 100	>100	>100	240.0 ± 14.1
74	> 100	>100	58.0 ± 4.2	135.9 ± 2.6
75	6.1 ± 1.0	69.2 ± 0.9	3.7 ± 0.4	21.4 ± 2.0
76	9.7 ± 0.8	66.7 ± 1.7	9.8 ± 2.4	74.2 ± 2.5
77	17.8 ± 1.0	21.8 ± 0.1	19.5 ± 2.1	74.3 ± 3.0
78	18.9 ± 0.0	23.0 ± 0.6	13.8 ± 1.1	87.0 ± 3.0
79	20.0 ± 2.6	21.1 ± 1.8	17.3 ± 1.1	31.2 ± 5.0
80	21.7 ± 3.4	25.0 ± 2.6	21.7 ± 3.6	71.0 ± 2.4
81	19.6 ± 0.5	27.9 ± 3.8	8.2 ± 1.1	65.7 ± 1.4
82	15.1 ± 0.4	19.7 ± 2.8	19.3 ± 1.1	68.1 ± 5.2
83	15.2 ± 1.8	67.6 ± 0,5	32.2 ± 3.6	81.2 ± 2.9
84	16.8 ± 0.4	14.8 ± 0.0	13.8 ± 0.4	119.4 ± 6.5
85	17.2 ± 0.9	20.3 ± 2.2	17.2 ± 2.6	152.5 ± 0.9
86	>100	>100	76.3 ± 4.0	460.0 ± 0.0

Compounds	Epimastigote IC$_{50}$ (μM) Average ± SD	Trypomastigote EC$_{50}$ (μM) Average ± SD	Promastigote IC$_{50}$ (μM) Average ± SD	Vero cells CC$_{50}$ (μM) Average ± SD
87	10.2 ± 2.7	25.6 ± 4.4	2.4 ± 0.0	28.3 ± 3.6
88	5.5 ± 0.9	19.1 ± 3.4	2.0 ± 0.2	21.8 ± 0.3
89	65.2 ± 4.4	74.2 ± 4.2	17.4 ± 1.1	46.9 ± 0.5
90	2.8 ± 0.9	7.6 ± 0.4	2.9 ± 0.0	27.1 ± 0.1
91	1.8 ± 0.4	20.0 ± 2.1	1.3 ± 0.2	24.4 ± 1.1
92	5.4 ± 0.1	19.5 ± 1.8	1.4 ± 0.2	29.4 ± 4.6
93	2.5 ± 0.1	17.9 ± 2.1	0.5 ± 0.0	36.0 ± 0.7
PC1	6.5±0.7	34.5±7.6		
PC2			0.06 ± 0.0	3.7 ± 0.31

PC1 (positive control 1): Benznidazole; PC2 (positive control 2): Amphotericin B.

Compounds **75-86** were synthesized on the basis of our previous work. The result of these compounds is very crucial compared to that reported previously, where we observed potency for compounds having electron withdrawing moieties (ZIA et al., 2014). Here we explored different electron donating and withdrawing substituted moieties including halogens, which were not explored in our previous study. Compounds **87-93**, also having different electron withdrawing groups with substituted modification, and a different alkyl group at alpha position next to carbonyl were synthesized and evaluated for their anti-parasitic potential. Mono arylidene intermediate having electron donating substitution enhances their potency when their diaryl system supplied with electron donating group and vice versa for electron withdrawing group. Among all electron donating groups the contribution of methoxy is higher than other donating groups. Monoaryliende compounds having methoxy substitution enhance the potency further by methoxy substitution in their diaryl system. Compounds **75** having three methoxy substitution has potent activity in this

series showing IC_{50} 6.1 ± 1.0 μM against epimastigote form of *Trypanosoma cruzi*. Compound **76** has two methoxyl substitutions and was found second potent compounds (IC_{50} 9.7 ± 0.8 μM) amongs all compounds derived from compound **73**. Our result is in agreement with that reported previously regarding substitution of methoxy upon activity (APONTE et al., 2008). There was no such a contributing effect observed for other electron donating species.

The halogen substitutions on compound **73** play no significant contributing effect upon activity. The effect of electro negativity was studied in compounds **77**, **80** and **83**. In all three cases the halogen is substituted at ortho position. Compounds **83** possessing flouro substitution has better activity (IC_{50} 15.2 ± 1.8 μM) for epimastigote form of *T. cruzi* than compound **5** (IC_{50} 17.8 ± 1.0 μM), which is chloro substituted, and further compound **77** is better activity than compound **78** (IC_{50} 21.7 ± 3.4 μM) having bromo substituted aromatic ring B. For promastigote form of *L. amazonensis* compound **77** (IC_{50} 19.5 ± 2.1 μM) shows better activity than compound **78** (IC_{50} 21.7 ± 3.6 μM) and compound **83** (IC_{50} 32.2 ± 3.6 μM). The results show the effect of electronegative elements substitution on aromatic ring B, obtained from intermediate compound **73**.

Through the results of unsymmetrical alkanones derived from compound **74** against epimastigote form of *Trypanosoma cruzi*, it was observed that halogen substitution has significant effect on activity. Compound **74** has no prominant activity, while second aldol reaction introduces huge activity to it. In compounds **87-93** the ketone length as well as the substitution on aromatic ring has modified. Intermediate **74** has *para* chloro substitution and ethyl group next to corbonyl. The nature and activity completely change by such a modification. Electron withdrawing effect of substituted moiety on aromatic ring is more crucial. All compounds of this series are potent except **89** due to *para* aldehydic group. The most potent compound is **91** having IC_{50} 1.8 ± 0.4 μM against

epimastigote and EC$_{50}$ 20.0 ± 2.1 µM against trypomastigote form of *T. cruzi* while IC$_{50}$ of 1.35 ± 0.2 µM against promastigote form of *L. amazonensis*. Both compounds **91** and **92** has bromo substitution on aromatic ring B, having different position of substitution. *Ortho* substituted bromo on aromatic ring has more potent effect than *para* substituted aromatic position. May be the bulkness of bromo interacts with aromatic hydrogens and pull the ring B out of the plane. Electron donating effect has also prominent in compound **88** and **90** but weaker than withdrawing effect upon activity. Methylenedioxy moiety has good effect for activity due to its special donating effect, and its occurance in most natural products.

The most active compounds against *T. cruzi* epimastigote were **75**, **88**, **90**, **91**, **92** and **93** which exhibited an IC$_{50}$ value of 6.1, 5.5, 2.8, 1.8, 5.4 and 2.5 µM respectively, which are more potent than benznidazole. Compounds **77-82**, **84**, **85**, **87**, **88**, **90**-**93** were found potent against trypomastigotes of *T. cruzi* showing EC$_{50}$ values in the range of 7.6-27.0 µM, greater than control drug benznidazol. All compounds active for epimastigote form were also found active for trypomastigote form except compound **75**, which was found potent for epimastigote form of *T.cruzi* while not for trypomastigote form. In all other potent compounds we observed perfect inhibition correlation for both form. The compounds **75**, **81**, **87**, **88**, **90**, **91** and **92** were active against promastigotes *Leishmania amazonensis* showing IC$_{50}$ in the range of 0.51 - 8.2 µM. Our compounds are good Michael acceptors, so it rapidly and specifically depleting thiol levels in trypanosomes by forming an adduct. This adduct may ultimately be responsible for the highly potent trypanocidal activity of the unsymmetrical alkanones. The results suggest that unsymmetrical synthetic analogous of curcumin has potential to be used for the treatment of leishmaniasis and

Chagas' disease. The compounds were also evaluated for cytotoxicity against Vero cell, showing that the active substances were more toxic against the parasite than for the normal cell line (table 3.5).

3.9 Molecular Docking of compounds 73-93

3.9.1 Optimization of ligands

Compounds **73-93** were screened for their stability and optimized energy using force field UFF, by advanced semantic chemical editor software Avogadro (HANWELL et al., 2012). The optimization calculations resulted possible best conformation and best stable structure of compounds. The selection of compounds for docking was carried by analyzing the optimization energy, and lowest energy conformation as best possible structure. The planarity of compounds affords modification in the result of different substitution on ortho, meta and para position. The maximum bulky interaction was observed between alkyl next to carbonyl and ortho substituent on aromatic ring. Compounds **75-86** are derived from compounds **73** and afford alpha methyl at C-2 of the 1,4-pentadienyl-3-one chain next to carbonyl, while compounds **87-93** obtained from compound **74** possess alpha ethyl at C-2 of the 1,4-pentadienyl-3-one chain. The molecular geometries that resulted from these calculations shows that the presence of the methyl or ethyl group at C-2 of the 1,4-pentadienyl-3-one chain disturbs the first enone *pi* system (1-en-3-one), while the second part, formed by the ring-B bound to C-5 and the 4-en-3-one, is planar with *p*-orbitals. All compounds (**87-93**) having ethyl at C-2 create maximum repulsion between aromatic ring A and ethyl, and in the result ring A

pushed out of the plane, while compounds **75-86** having methyl at C-2 create less repulsion in comparison (FIGURE 3**.**7).
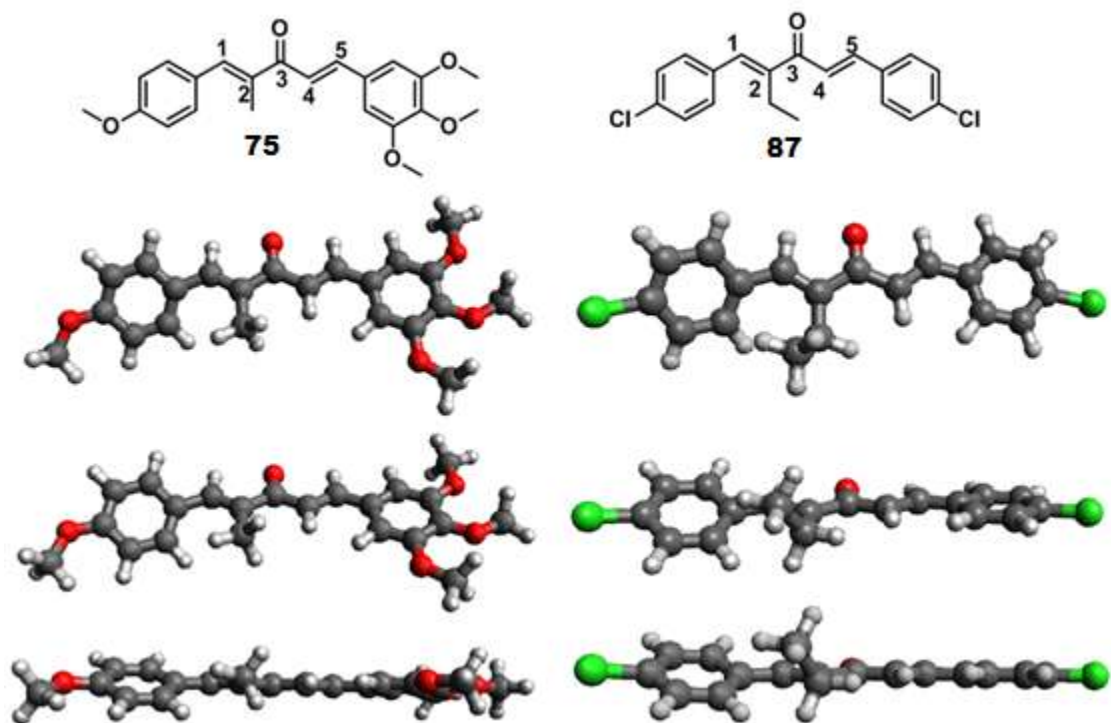
Figure 3.7 - Planarity loses by the repulsion of alkyl group at C-2 and ring A, in case of ethyl the planarity loss is maximum compared to methyl, calculated by Avogadro 1.1.1.

3.9.2 *In-silico* interaction studies

Compounds **73-93** were screened for their binding possibility to enzyme trypanothione reductase *Pdb* code 1BZL and the output obtained were tabulated in Table 3.4. Calculation of active site was performed on the basis of crystallized ligand in its crystal structure. Discovery studio (DASSAULT SYSTÈMES BIOVIA, 2015) computational tool were used to calculate centroid of the active site. The amino acids which participate actively are Gly-12, Gly-14, Ser-15, Gly-16, Asp-36, Val-37, Ser-47, Ala-48, Gly-51, Thr-52,

Cys-53, Val-56, Cys-58, Lys-61, Gly-126, Gly-128, Ala-160, Ser-161, Gly-162, Arg-288, Arg-291, Gly-326, Asp-327, Met-333, Leu-334, Thr-335, Pro-336, Ala-338. All Compounds **73-93** have interaction with amino acid in the active sites of 1BZL, depend on the structure and pharmacophoric sites (TABLE 3.6).

Table 3.6 - Docking results of compounds **73-93** docked on to trypanothione reductase (1BZL).

Compounds	Binding energy (kcal mol^{-1})	Inhibition constant (Temp = 298.15 k) ki μM	Calculated RMS from reference (Å)
73.	-4.42	289.19	20.39
74.	-4.66	381.00	21.44
75.	-4.07	586.21	19.65
76.	-4.63	757.37	19.54
77.	-5.83	53.35	20.76
78.	-4.70	358.40	22.63
79.	-4.80	163.79	21.38
80.	-4.80	304.18	22.57
81.	-4.20	830.18	23.75
82.	-4.49	507.83	23.18
83.	-4.44	556.92	23.06
84.	-5.04	201.16	20.60
85.	-4.95	233.57	20.73
86.	13.66	0.00	22.12
87.	-5.58	81.67	21.05
88.	-4.94	240.3	20.37
89.	-4.89	259.48	20.32
90.	-5.31	128.83	21.87
91.	-5.52	90.46	20.91
92.	-5.70	65.92	21.48
93.	-7.48	3.28	21.89

Compound **93**, which is most potent one, has interaction with amino acids Cys-53 and Cys-58 by forming H-bond between oxygen of compound with nitrogen of amino acid by distance of 3.12 and 3.17Å respectively. Nitrogen of nitro group in compound **93** forms H-bond interaction with Gly-326 by distance 3.09Å, and also exhibit interaction with N of Gly-16 by distance of 2.88Å. Interaction with N of Ser-15 by distance of 3.26Å was also observed. Moreover *pi*-hydrogen interactions of aromatic ring of compound **93** with Oxygen of Ser-15 by distance of 3.69Å, Thr-335 by distance of 3.9Å, and with Lys-61 by distance of 2.89Å was also formed (FIGURE 3.8).
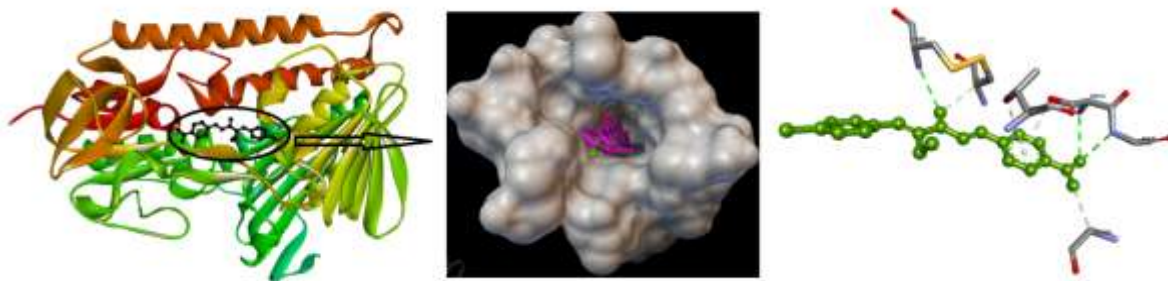
Figure 3.8 - Active site amino acids in protein 1BZL interaction with compound **93**, the compound seem perfectly fit in the active cavity.

Similarly compound **90**, which is also potent compound in series, revealed that Oxygen of carbonyl forms 2-hydrogen bonding interaction with same amino acid Thr-335 by distance of 2.58 and 2.81Å. The oxygen of methylene dioxy group is involved in hydrogen interaction and showing strong H-bond interation neibouring nitrogen of amino acids Ser-15 and Gly-16 by distance H-bond distances of 3.10 Å and 2.68Å respectively (FIGURE 3.9).
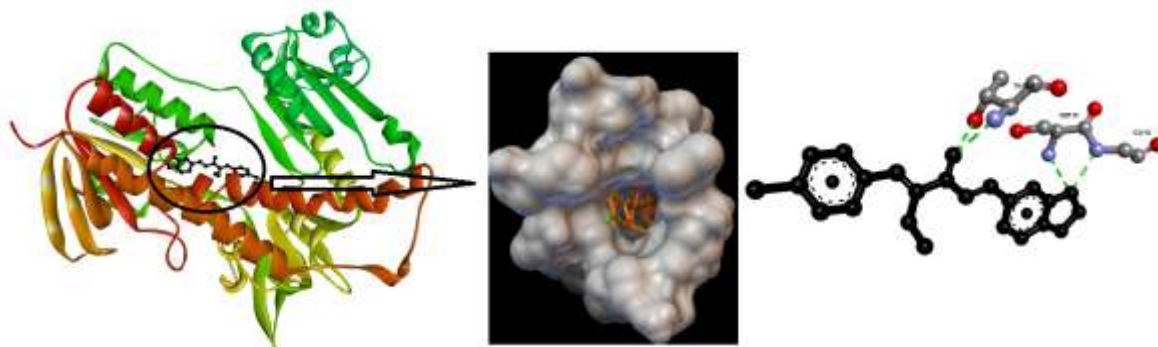
Figure 3.9 - Active site amino acids in protein 1BZL interaction with compound **90**, the compounds seem perfectly fit in the active site.

Compound **92** exhibits hydrogen bonding interaction with Thr-335 (3.14 Å) along with *pi*-hydrogen interaction of aromatic moiety with Gly-14 (3.8 Å). Compounds exhibiting potency *in-silico* was also active in wet lab experiment. Compound **86**, which does not have any *in-vitro* activity, was shown to have no interaction *in-silico*. The docking result is in agreement with *in-vitro* assay results except compound **84**, which show great inhibition *in-silico* than wet lab experiment. Compound **84** afford two chloro atoms may activate the double bonds and also play role to create non-planarity in compound. This may be one of the possible reasons of its *in-silico* interaction with active site residues.

3.9.3 Studies on molecular orbital's by computational analysis

The highest occupied molecular orbital (HOMO) and lowest unoccupied molecular orbital (LUMO) for compounds **73-93** were analyzed by Gaussian (HEHRE; DITCHFIELD; POPLE, 1972). The energy of HOMO is the capacity of a compound to lose electron, and therefore consider equal to the ionization potential. While on the other hand, energy of LUMO describes the capability of

a compound to gain electrons. Therefore, the negative of the energy of LUMO is taken as electron affinity.

The frontier orbital's of the global minimum configurations for the unsymmetrical alkanones were calculated (FIGURE 3.10). In the case of compounds **73** and **74**, the HOMO has dominating contributions from the benzene ring bearing the OCH_3 and chloro group substitution and from the adjacent C=C bond. In the case of the compound **75** and **76**, the HOMO has dominating contributions from the benzene ring B bearing the more OCH_3 and from the adjacent C=C bond whereas the LUMO has dominating contributions from the benzene ring A possessing only one OCH_3 group. Compounds **77**-**85** possessing halogen on ring B which tend to decrease electron density on aromatic ring by inductive potential. Due to this phenomena in compounds **77-88** the HOMO has dominating contributions from the benzene ring A bearing the OCH_3 group and from the adjacent C=C bond whereas the LUMO has dominating contributions from the benzene ring B, the adjacent C=C bond and the C=O bond. Compound **86** consist of three aromatic moieties, two terminal having p-methoxy substitution and having more HOMO contribution than middle one, which contribute for LUMO along with adjacent two C=C bonds. In compound **87**, **89**, **91-93**, the HOMO has major contributions from aromatic ring A, the adjacent double bond and the C=O bond, whereas the LUMO has influensive contribution from aromatic ring B and adjacent double bond. Compounds **88** and **90** possess electron donating group at ring B, so their HOMO and LUMO contribution differentiate from the rest. In case of compounds **88** and **90** HUMO has major contribution from aromatic ring B and a little from adjacent double bond, while LUMO has principal contribution from ring A, the adjacent C=C and the C=O bonds (FIGURE 3.10).
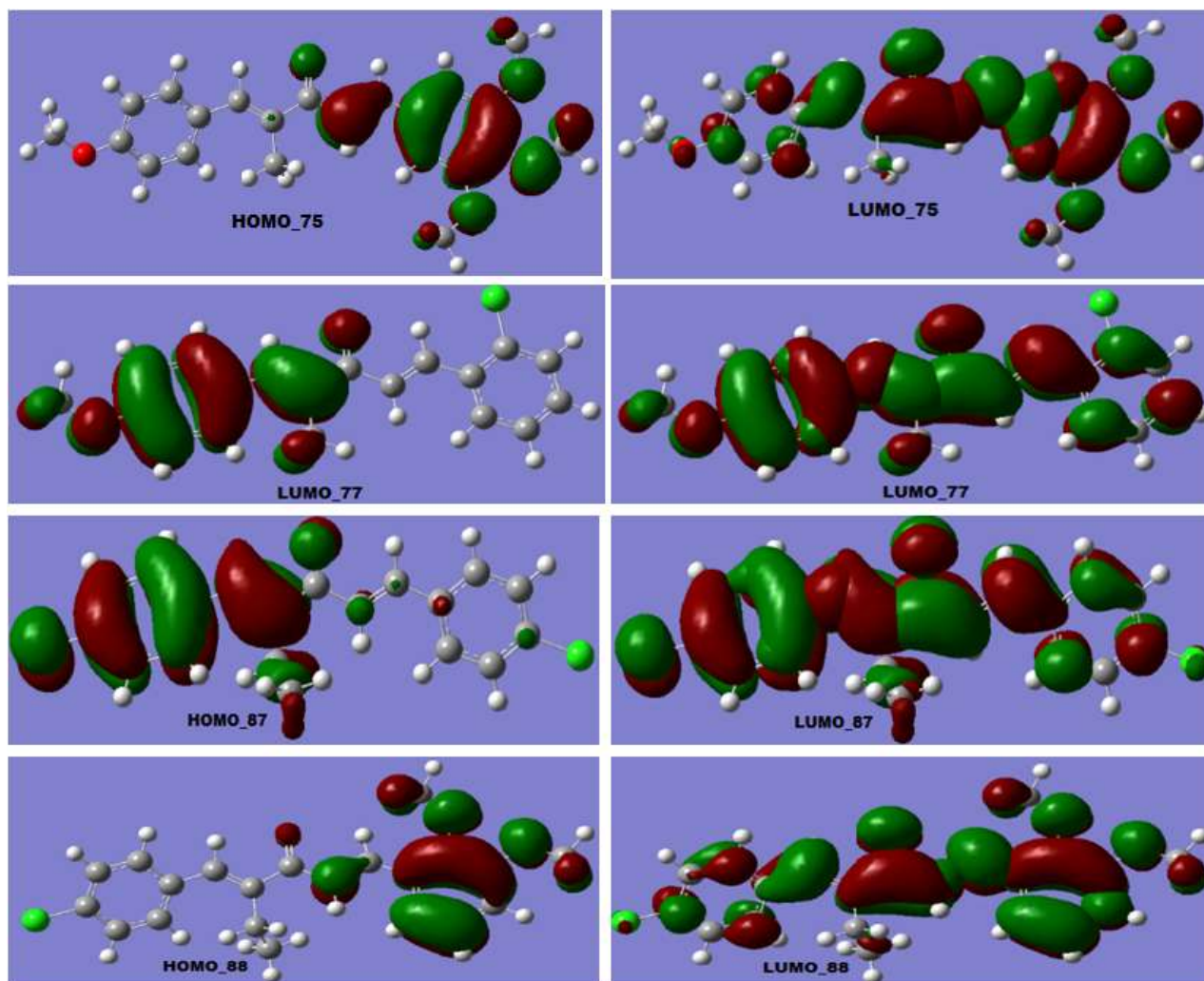
Figure 3.10 - Electronic distributions for compound **75**, **77**, **87** and **88**. Semi-empirical calculations were performed using the Gaussian software package with the semi empirical CAM-B3LYP/6-31G(d,p) method and full geometric optimization.

3.10 Synthesis of compounds 94-126

To explore more the alkyl group on C-2 different curcuminoids were synthesized having p-nitro group or electron with drawing group on aromatic

ring A. The effect of biological activity was studied. Compounds **94** were synthesized by the condensation of with acetone using gaseous HCl as catalyst. After crystallization and purification it was treated to hydrogen gas on Pd/C to obtain compound **95** having C=C bond being reduced. Compound **95** on reaction with nitrobenzaldehyde in basic medium yielding compound **96** having two aryl system separated by five inter ring carbon spacer (SCHEME 3.6).
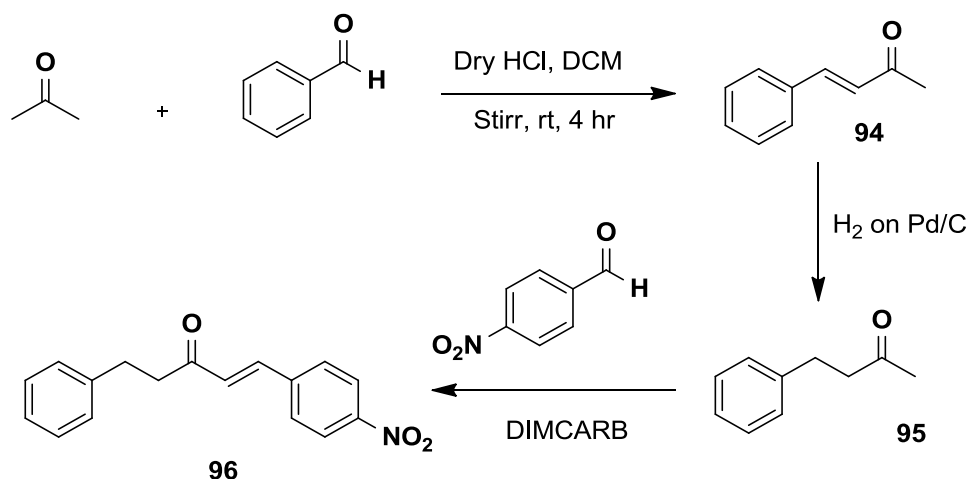
Scheme 3.6 - Synthesis of compounds **94-96**, compound **96** having two aryl moieties with one nitro group.
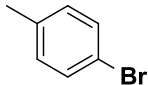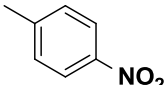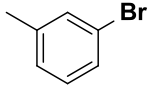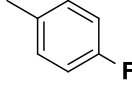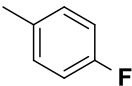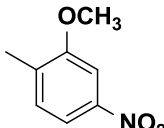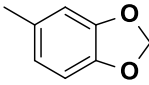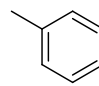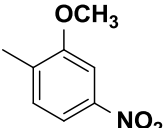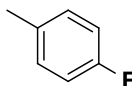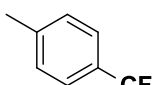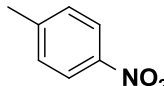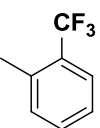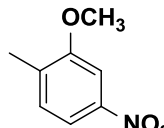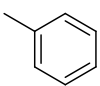
Further for the synthesis of unsymmetrical nitro curcuminoids analogous the condensation of *p*-nitrobenzaldehyde, *p*-triflourobenzaldehyde and o-triflourobenzaldehyde with 2-butanone were carried using gaseous HCl as catalyst and obtaining compounds **97-99**. Intermediate compounds **97-99** were isolated and recrystallized from ethanol and characterized. Then the intermediate compounds **97-99** yields compounds **100-114** by treating with various aromatic aldehydes in base catalyzed condition. The compounds **100-106** were synthesized from the reaction of compound **97** with different aldheydes. Similarly compounds **107-110** were synthesized from 98 and **111-**

114 from compound **99**. The targeted diarylpentanoids were synthesized to see the effect of different electron donating and with drawing substitution on aromatic rings. Previously symmetrical diarylpentatanoids with nitro group was found to have potency to treat chagas (ZIA et al., 2014). In this investigation we focused to prepared unsymmetrical diarylpentanoids of various substitution patterns with nitro substitution, to explore more the effect of different aryl groups upon activity (SCHEME 3.7 and TABLE 3.7).

97. $R_1 = NO_2$, $R_2 = H$,
98. $R_1 = CF_3$, $R_2 = H$,
99. $R_1 = H$, $R_2 = CF_3$,

100-114
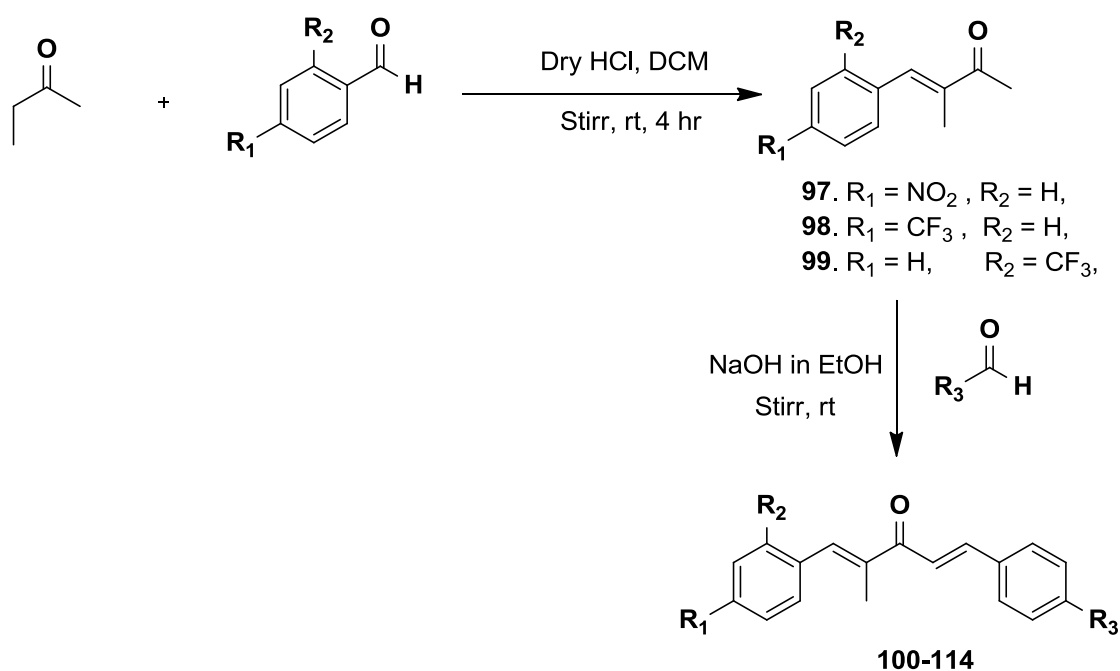
Scheme 3.7 - Synthesis of intermediate compounds **97, 98** and **99** and their unsymmetrical diaryl analogues. Compounds **100-106** are derived from **97** while **107-110** is derived from intermediate **98** and **111-114** from **99.**

Table 3.7 – Substitution variation of 2nd aryl system on compounds **97**, **98**, **99**.

Compounds	R	Compounds	R
100		108	
101		109	
102		110	
103		111	
104		112	
105		113	
106		114	
107			

The synthesis was continued to see the effect of alkyl group on C-2. The intermediate compounds **97**, **115** and **116** with methyl, ethyl and butyl

substitution were synthesized having one aryl group by the direct acid catalysis. Then compounds **117-122** were synthesized from compounds **97, 115** and **116** by the reaction of benzaldehyde and nitro benzaldehyde (SCHEME 3.8). The compounds **117-122** were synthesized to explore the activity of compounds **117** and **118** which was synthesized previously showing potent anti-parasitic activity. Compounds **117** and **118** have methyl group on C-2, while this group is modified to ethyl in compounds **118-120**, and to butyl in compounds **121** and **122**. This series give more accurate information of the role of alkyl group on C-2.
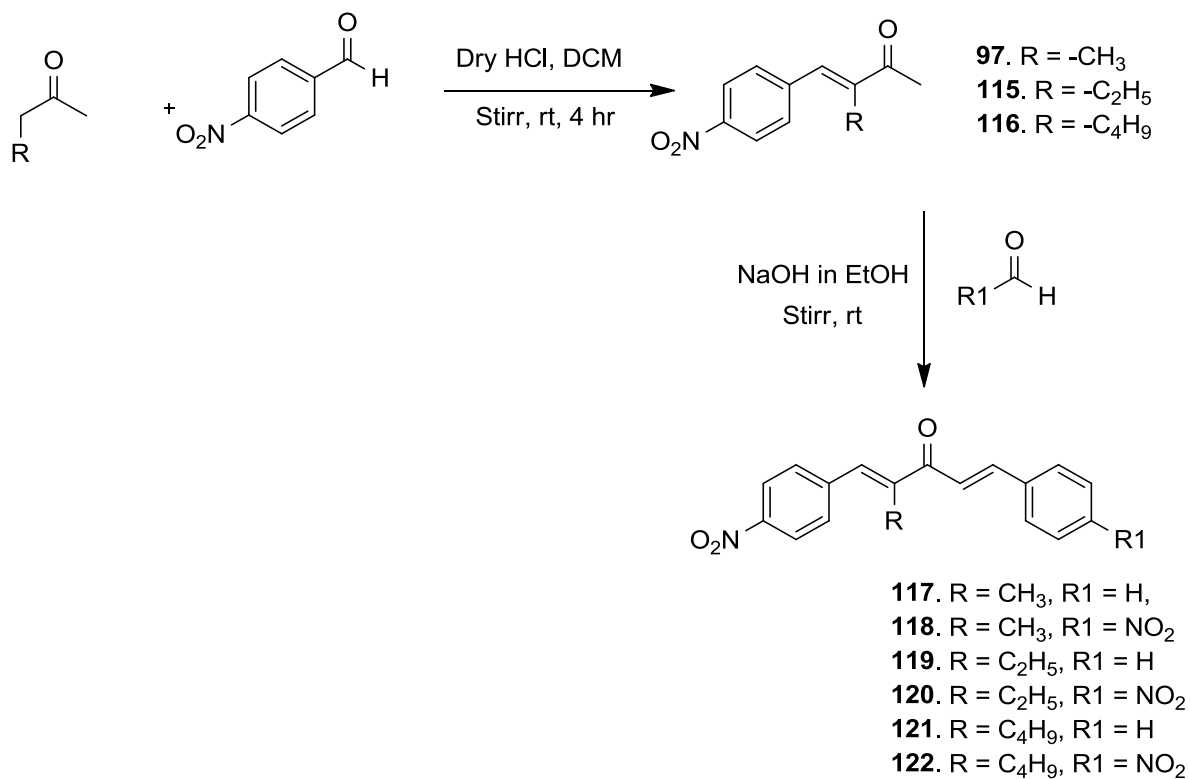
Scheme 3.8 - The synthesis of compounds with modification of alkyl groups on C-2 position, of curcuminoids.

The compounds **117** and **118** has potent activity with IC$_{50}$ 3.5 and 1.8 against epimastigote of *Trypansoma cruzi,* and also interfere in the redox system of *T. cruzi* by increasing reactive oxygen and nitrogen species by altering mitochondrial function and finally causing the death of parasite (ZIA et al., 2014) (BIDÓIA et al., 2016). Compounds **117** and **118** has *p*-nitro group on mono aryl system and methyl group on C-2, which is modified to *p*-triflouro group and butyl group on C-2 by yielding compounds **123** and **124** (SCHEME 3.9).
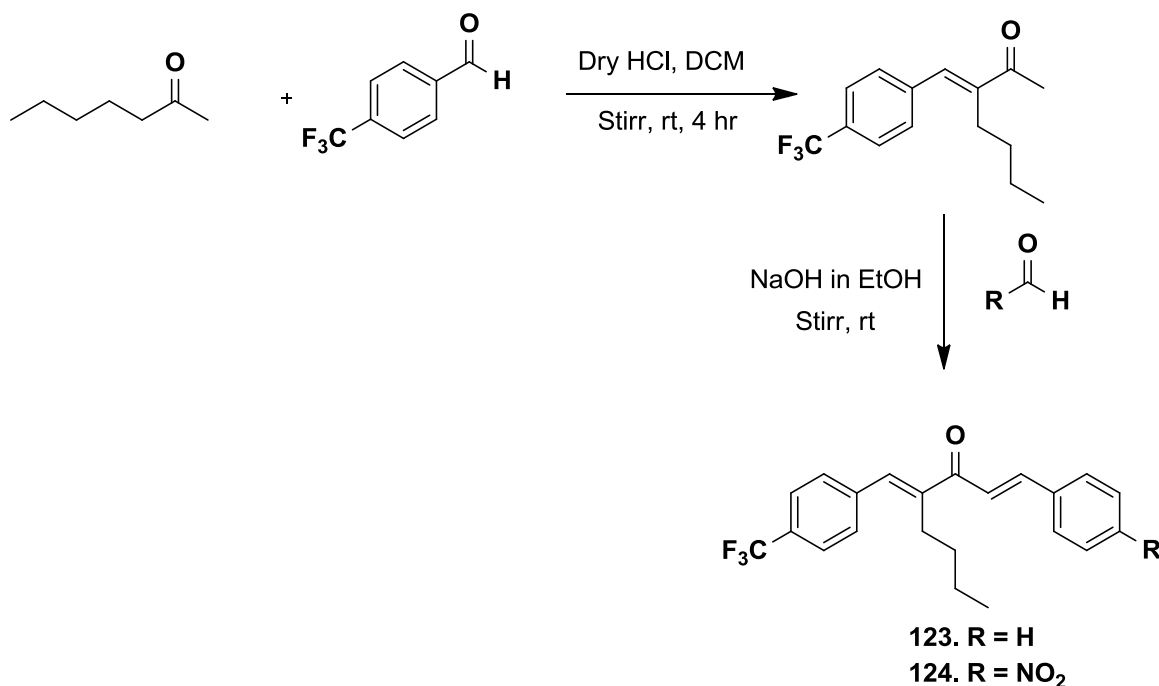
Scheme 3.9 - Synthesis of compounds **123** and **124** having *p*-triflouro and methyl group on C-2.

The catalyst also affects the mode of reaction. HCl gas always gives thermodynamic product while ionic liquid DIMCARB prefer kinetic product. The reaction of nitro benzaldehyde with 2-heptanone in acidic medium give product **116** while in DIMCARB it yield compounds **125** and **126** which is

considered the kinetic products (SCHEME 3.10) Compound **126** is the dehydrated form of compound **125** having instauration in the result of elimination reaction.
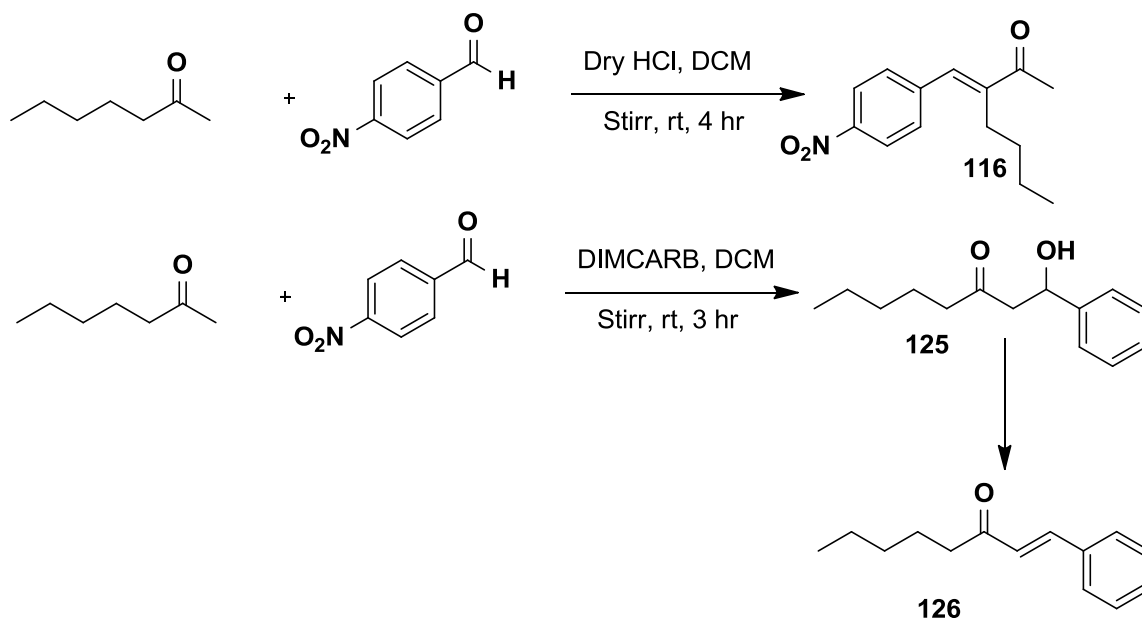
Scheme 3.10 - The synthesis of compound **125** and **126** by the reaction of 2-heptanone and *p*-nitro benzaldehyde in the presence of ionic liquid DIMCARB.

NMR data of compound **94** show the presence of double bond (=CH) signal was appeared at δ_H 7.47 as singlet. Three aromatic signals displayed at δ_H 6.95 and 7.41 having spin coupling constant of approximately 16 Hz. ^{13}C NMR spectra of **94** showed signals for methyl groups at δ_C 12.9, and six peaks from δ_C 113-159 for eight carbons. The characteristic peak appeared at δ_C 200.2 is due to carbonyl carbon. Compound **95** exhibits NMR spectra of compound **95** having same group only the shifting of signal take place due to C=C bond reduction. Compounds **96** having 2 aryl systems so having aromatic signals between δ_H 7-8, methyl signal in δ_H 2.0. The reaction of *p*-nitrobenzaldehyde,

p-triflouro and o-triflour benzaldehyde with 2-butanone yields compounds **97**, **98**, **99**, **115** and **116** having the characteristic signals of C=C bond in range of δ_H 6-7. Compounds **22** have ethyl and **23** has butyl group on C-2, comparing to **97**, **98** and **99** having methyl on C-2. The ^{13}C NMR show the C=O signal near δ_C 200, confirming the formation of these compounds. Further compounds **100-114** and **117-122** were produced by reacting compounds **97, 98, 6, 115** and **116** with different aldehydes having electron donating and electron withdrawing moieties. It was successfully completely characterized by NMR. One double bond and aromatic moiety has added, so ^1H NMR has two more doublet for -CH=CH- having coupling constant of approximately 16 Hz which is characteristic of H-H trans coupling system. The aromatic signals appeared at δ_H 6.5-7.8 depend on the substitution attached to it. Compounds **100-106** were prepared from the reaction of compound **97** with different aldehyde, while compounds **107-110** is derived from compound **98** and compounds **111-114** is produced from compound **99**. Compounds **117-122** are synthesized by the reaction of **97**, **115** and **116** with benzaldehyde and nitro benzaldehyde separately. These compounds were characterized by ^1H NMR and ^{13}C NMR having similar spectral signals. The quartet appearance is due to the coupling of CH_2 with neighboring CH_3 group. Compounds **123** and **124** having butyl group on C-2 only differentiation of signals occurs in up-field region due to butyl contribution. Other signals remain the same comparing with signals of that of other compounds derived from **97**, **98**, **99**, **115** and **116**. Compound **125** showing the signal of hydroxyl near δ_H 4, while the disappearance of it and appearance of C=C bond between 6-7 ppm confirm their formation.

3.11 Biological Evaluation of compounds 94-126

3.11.1 Antiproliferative assay

The unsymmetrical curcuminoids (**94-126**) were evaluated for their anti-parasitic potential against epimastigote and trypomastigote of *T. Cruzi* and promastigote of *L. amazonesis* (TABLE 3.8). Moreover, the results showed that the compounds were more toxic against the parasites than to Vero cells (kidney epithelial cells from African green monkey). This research opened a way to explore the promising activity of diarylheptanoids (**94-122**) for the development of effective drugs for the treatment of parasitic diseases.

Table 3.8 – Anti-parasitic and cytotoxic activities of diarylalkanones **94-122.**

S.No	*L. amazonensis* Promastigotes IC_{50} (μM)	*T. cruzi* Epimastigotes IC_{50} (μM)	Vero cells CC_{50} (μM)
94	>100	>100	113.5 ± 8.2
95	>100	>100	292.7 ± 74.6
96	23.0 ± 0.3	>100	29.2 ± 7.6
97	>100	82.2 ± 7.42	266.0 ± 12.73
98	>100	>100	266.7 ± 28.3
99	>100	4.1 ± 0.6	509.1 ± 101.2
100	3.2 ± 0.9	>100	<10
101	3.8 ± 0.5	>100	31.7 ± 5.3
102	23.7 ± 1.8	4.6 ± 2.1	27.0 ± 3.3
103	5.0 ± 1.8	3.0 ± 1.4	27.6 ± 6.0
104	4.9 ± 1.2	>100	27.0 ± 4.2
105	5.7 ± 1.4	3.5 ± 0.7	<10

S.No	L. amazonensis Promastigotes IC$_{50}$ (μM)	T. cruzi Epimastigotes IC$_{50}$ (μM)	Vero cells CC$_{50}$ (μM)
106	5.8 ± 0.0	3.3 ± 0.0	<10
107	29.9 ± 4.8	24.7 ± 0.4	32.2 ± 5.9
108	3.1 ± 0.8	14.0 ± 5.7	26.2 ± 4.0
109	30.6 ± 4.6	>100	28.1 ± 4.9
110	5.8 ± 1.5	11.6 ± 3.7	30.5 ± 4.5
111	24.9 ± 4.1	33.2 ± 4.5	38.2 ± 2.6
112	4.0 ± 0.5	4.5 ± 2.1	27.2 ± 1.8
113	5.8 ± 1.2	4.7 ± 1.0	41.9 ± 4.0
114	3.9 ± 0.3	3.2 ± 0.2	12.6 ± 1.8
115	20.8 ± 3.4	3.3 ± 2.4	35.5 ± 3.9
116	72.2 ± 3.1	>100	138.5 ± 5.4
117	13.4 ± 1.98	3.45 ± 0.35	47.3 ± 4.2
118	3.4 ± 0.07	1.75 ± 0.21	43.0 ± 4.24
119	20.3 ± 1.1	3.8 ± 1.2	27.6 ± 6.0
120	3.4 ± 0.0	>100	29.7 ± 4.3
121	3.5 ± 0.2	>100	37.2 ± 5.5
122	3.6 ± 0.0	>100	157.7 ± 38.1
123	7.6 ± 0.9	3.0 ± 0.1	26.1 ± 5.1
124	17.6 ± 0.8	24.7 ± 1.9	192.4 ± 5.5
125	80.9 ± 7.6	>100	30.4 ± 7.2
126	>100	>100	189.0 ± 33.4
PC1		6.5±0.7	
PC2	0.06 ± 0.00		

PC1 (positive control 1): Benznidazole; PC2 (positive control 2): Amphotericin B Define IC50

All compounds were synthesized on the basis of our previous work, where we observed potent activity for curcuminoids containing *p*-nitro group (ZIA et al., 2014). Here we explored different electron donating and withdrawing substituted moieties including nitro as crucial part, which were crucial for exploring the importance of nitro for activity. Compounds with ethyl and butyl on C-2 were also synthesized to see its importance of methyl on C-2. All synthesized products were evaluated for their anti-parasitic potential. Mono arylidene intermediate having electron donating substitution enhances their potency when their diaryl system supplied with electron donating group and vice versa for electron withdrawing group. Among all electron donating groups the contribution of methoxyl is higher than other donating groups. The compounds where the nitro on second aryl system was replaced by other electron withdrawing groups along with one electron donating group (-O-CH$_2$-O) maintained their activities, comparing to compounds **117** and **118**. Monoarylidene compounds having methoxy substitution enhance the potency further by methoxy substitution in their diaryl system. Compounds **98** have no active and their derivitization also do not show interesting activity, while compound **99** is potent and its all derivatives also show good activity except compound **111** which show decrease in activity. Other compounds **112**, **113** and **114** show potent activities due to electron with drawing substitution on second aromatic ring. Compound **115** and **116** possesses mono aryl system with *p*-nitro system and alkyl group next to carbonyl. Compound **115** formed by the reaction of 2-pentanone with p-nitrobenzaldehude while **116** by the reaction of 2-heptanone with *p*-nitrobenzaldehyde. Compounds **115** is potent due to less alkyl chain near C=O showing IC$_{50}$ 3.3 ± 2.4 µM. Its reaction with benzaldehyde yields compound **119** which maintain the activity showing the inhibition of IC$_{50}$ 3.8 ± 1.2 with a little decrease from the parent compound.

91

Compound **120** having p-nitro on second aryl system but not exhibiting activity may be due to the contribution of ethyl system in this case which play a role in the disturbing the planarity. Other compounds **121** and **122** do not show any activity due to the same reason of *p*-nitro on second aryle system. The result become understandable by studying the activity of compounds **123** and **124** which contain *p*-trifluoro on first aryl system while compound **121** has only benzene with no substitution while **122** has *p*-nitro substitution on ring B. Compounds **123** is active showing the inhibition IC_{50} 3.0 ± 0.1, while there is decrease of activity in case of **124**, where *p*-nitro group is attached on second aryl system. The larger alkyl chain on C-2, like ethyl and butyl decrease the activity and it affect more in case of *p*-nitro on second aryl group, where complete loss of activity occurs. Also when the α,β-unsaturated carbonylic system is disturbed, the activity also diminishes just like in case of compounds **125** and **126**. So the study shows the effect of activity on the result of substitution effect on C-2, and replacement of *p*-nitro group by other electron with drawing moieties. The results suggest that unsymmetrical synthetic analogous of curcumin with *p*-nitro has potential to be used for the treatment of leishmaniasis and Chagas' disease. The compounds were also evaluated for cytotoxicity against Vero cell, showing that the active substances were more toxic against the parasite than for the normal cell line.

3.11.2 Molecular Docking

3.11.2.1 Optimization of ligands

Compounds were screened for their stability and optimized energy using force field UFF, by advanced semantic chemical editor software Avogadro

(HANWELL et al., 2012). The optimization calculations resulted possible best conformation and best stable structure of compounds. The selection of compounds for docking was carried by analyzing the optimization energy, and lowest energy conformation as best possible structure. The planarity of compounds affords modification in the result of different substitution on ortho, meta and para position. The maximum bulky interaction was observed between alkyl next to carbonyl and ortho substituent on aromatic ring. Compounds derived from **97, 98** and **99** yielded compounds **100-114** and afford alpha methyl at C-2 of the 1,4-pentadienyl-3-one chain next to carbonyl , while compounds **119** and **120** possess alpha ethyl at C-2 of the 1,4-pentadienyl-3-one chain and compounds **121** and **122** possessing butyl at C-2 of the 1,4-pentadienyl-3-one chain. The molecular geometries that resulted from these calculations shows that the presence of the methyl, ethyl or butyl group at C-2 of the 1,4-pentadienyl-3-one chain disturbs the first enone *pi* system (1-en-3-one), while the second part, formed by the ring-B bound to C-5 and the 4-en-3-one, is planar with *p*-orbital's. All compounds (**100-114**) having methyl at C-2 create repulsion between aromatic ring A and ethyl, and in the result ring A pushed out of the plane, while compounds **19-20** having ethyl at C-2 create more repulsion in comparison, and maximum repulsion were observed for compounds 28 and 29 having butyl group on C-2 of 1,4-pentadienyl-3-one system. (FIGURE 3.11). Any alkyl group on C-2 significantly affects the structure of compounds which further affect its biological potential. In case of methyl on C-2, minimum repulsion with ring A, give potency to compounds **102, 104, 106, 112, 113, 114, 117** and **118.**
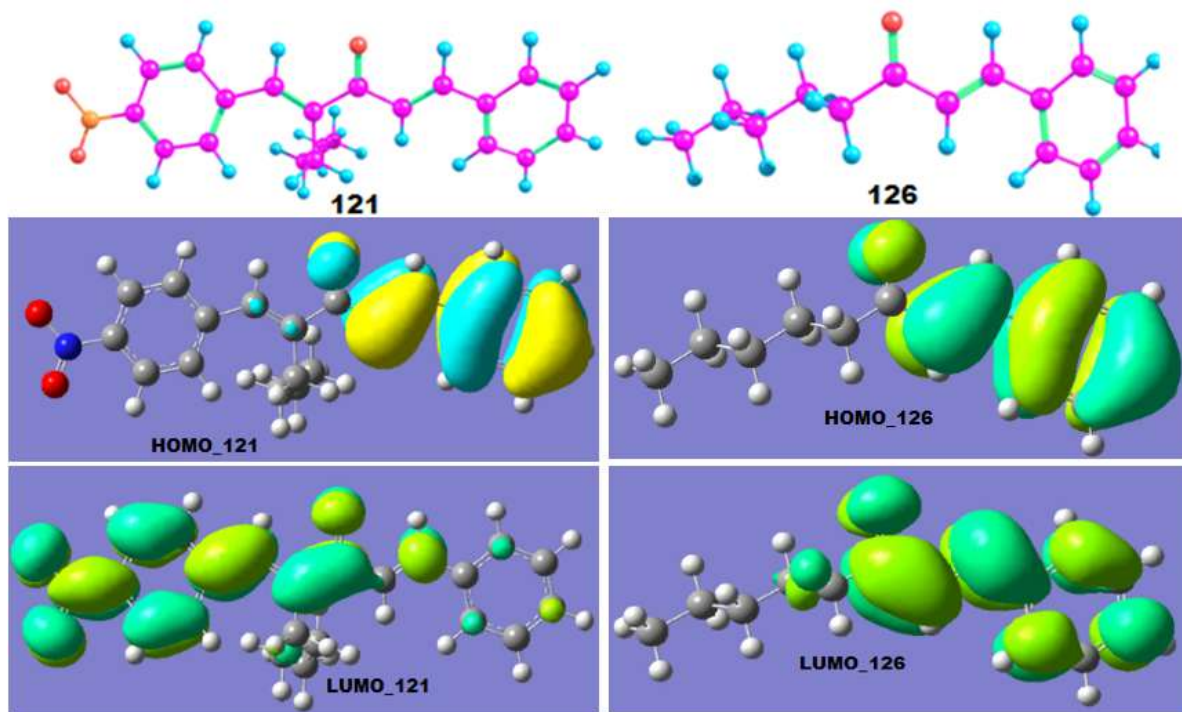
Figure 3.11 - Planarity loses by the repulsion of alkyl group at C-2 and ring A, in case of ethyl the planarity loss is maximum compared to methyl, calculated by Avogadro 1.1.1.

3.11.2.2 *In-silico* interaction studies

Active compounds were screened for their binding possibility to enzyme trypanothione reductase *Pdb* code 1BZL. Calculation of active site was performed on the basis of crystallized ligand in its crystal structure. Discovery studio (DASSAULT SYSTÈMES BIOVIA, 2015) computational tool were used to calculate centroid of the active site. The amino acids which participate actively are Gly-12, Gly-14, Ser-15, Gly-16, Asp-36, Val-37, Ser-47, Ala-48, Gly-51, Thr-52, Cys-53, Val-56, Cys-58, Lys-61, Gly-126, Gly-128, Ala-160, Ser-161, Gly-162, Arg-288, Arg-291, Gly-326, Asp-327, Met-333, Leu-334, Thr-335, Pro-336, Ala-338. Active compounds have interaction with amino

acid in the active sites of *1BZL*, depend on the structure and pharmacophoric sites.

Compound **106**, which is most potent one has interaction with amino acids H-bonding between nitro group and Cys-58 and Lys-61 by distance of 2.94 Å and 1.66 Å. H-bonding between fluoro group and Gly-51, Gly-14 and Gly-16 by distance of 3.35 Å, 2.89, 3.67, 3.59 Å. *Pi*-donar hydrogen bonding between aromatic ring and Gly-16 by distance of 2.47 Å (FIGURE 3.12).
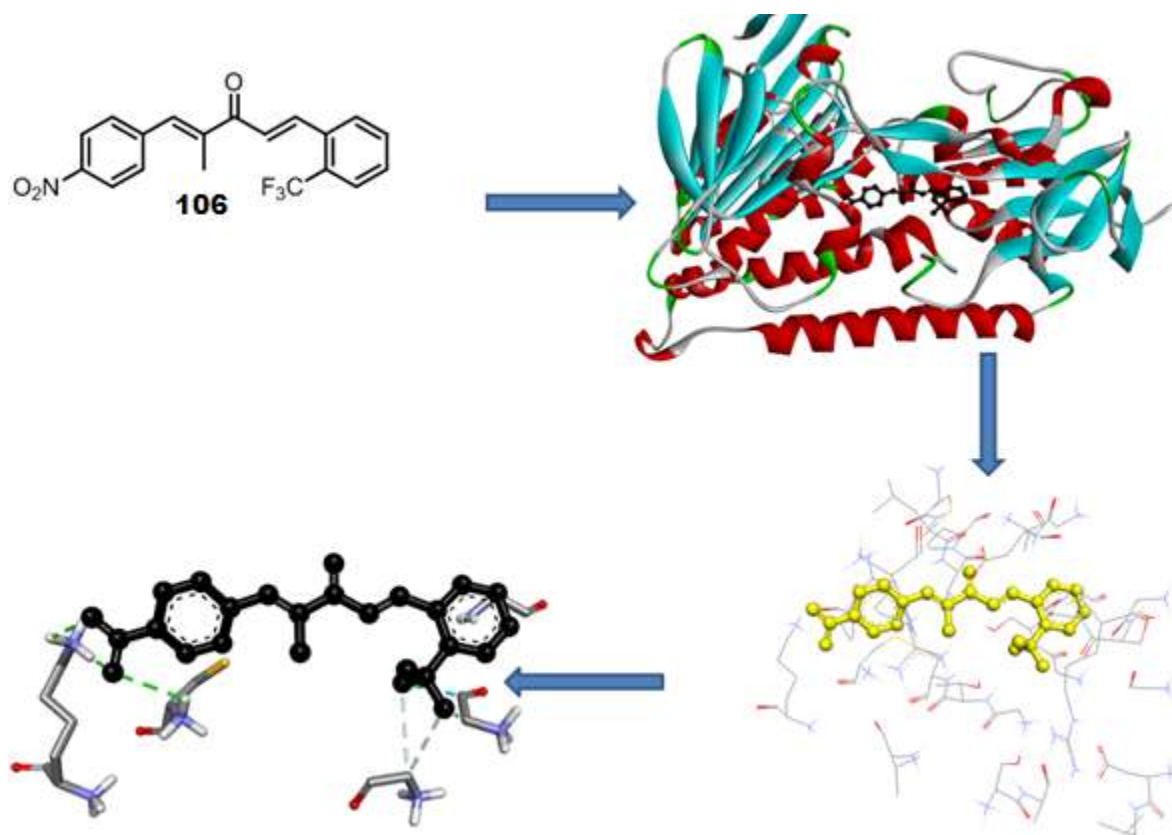
Figure 3.12 - Active site amino acids in protein 1BZL interaction with compound **106**, the compound seem perfectly fit in the active cavity.

Similarly compound **111**, which is also less potent compound in series, revealed that Oxygen of carbonyl forms 2-hydrogen bonding interaction with Thr-335 by distance of 2.58 and 2.81Å. The oxygen of methylene dioxy group

is involved in hydrogen interaction with nitrogen of Ser-15 and Gly-16 by distance of 3.10, 2.68Å (FIGURE 3.13). But the second aryl system is unable to inter to the active site cavity due to butyl group interference, so less interaction leading to less potent compounds.
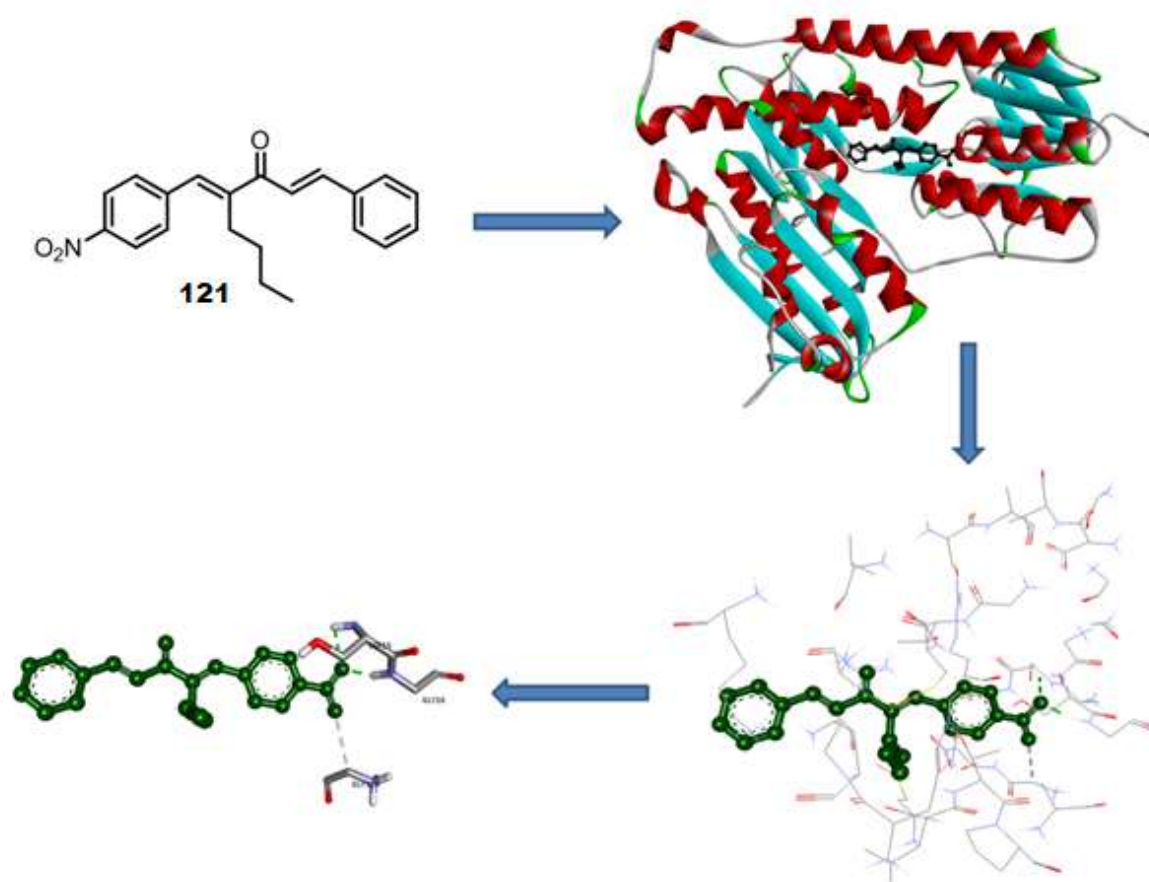
Figure 3.13 - Active site amino acids in protein 1BZL interaction with compound **121**, the compounds seem perfectly fit in the active site.

3.12 Synthesis of Monoarylidene products

The use of DIMCARB was introduced to synthesized unsymmetrical curcuminoids from symmetrical ketones. The reaction of aldehydes with

ketones in conventional acidic or basic condition yield symmetrical diaryl alkanones (FIGURE 3.11). Several methodologies have been reported for the synthesis of symmetrical diaryl alkanone (SHETTY et al., 2015). Also, attempts have been made to control the reaction and to obtain monoarylidene product, which can further be utilized as an intermediate for the preparation of unsymmetrical diaryl alkanone.

127. R = H
128. R = OCH3
129. R = Cl
130. R = Br
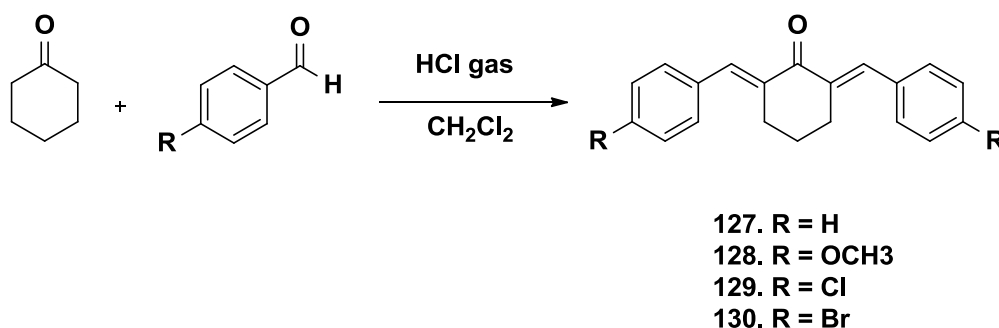
Scheme 3.11 - Synthesis of symmetrical diaryl alkanone.

Unsymmetrical diaryl alkanones are promising building blocks for pronounced pharmacological chemistry (ZIA et al., 2014). But they cannot be synthesized by aldol or claisen Schmidt condensation when symmetrical ketones are used for reaction. Unfortunately different inorganic acid and base catalysts let to symmetrical bisarylidene alkanones even when using adjusted stoichiometric ratio of aldehydes and ketones. Microwave method with Al_2O_3 and $NaNO_3$ also yield symmetrical bis aryl alkanones products.

There was a need of controlling the reaction in monoarylidene step, for further synthesis of unsymmetrical diaryl alkanone (FIGURE 3.14). Amine based catalyst is the best option to deal with this challenge. There is a limited literature which show the synthesis of monoarylidene alkanone using the amine

based catalyst DIMCARB. Preparation of the monoarylidene adducts usually requires two steps, i.e. aldol addition followed by a separate elimination. The challenge to synthesize monoarylidene cyclic and acyclic alkanones required different methods investigation. Previously Christopher R. Strauss *et al.* used this ionic liquid successfully for the synthesis of monoarylidene cyclic and acyclic alkanones,(KREHER UP; et al., 2003) but DIMCARB was used as a solvent and as reaction medium. We focused to optimize these reactions, which were performed successfully by catalytic amount of DIMCARB. The modification reduced the quantity of DIMCARB and also the chance of side products. DIMCARB is an adduct of CO_2 and Me_2NH, both of which are gaseous under ambient conditions. We also replaced the chlorinated solvent previously used by Christopher R. Strauss and his collogues by green solvent ethanol and water (50:50) (TABLE 3.9). It was observed that the reaction is more efficient in green solvent rather than dichloromethane. The conversion in model reactions in ethanol water mixture was 100, while the reaction in dichloromethane showed 92 percent conversion. Different bases were checked for this reaction. DIMCARB and DBU (1,8-Diazabicycloundec-7-ene) were found excellent for this type of conversion. Other bases did not give any products or give very less yield.
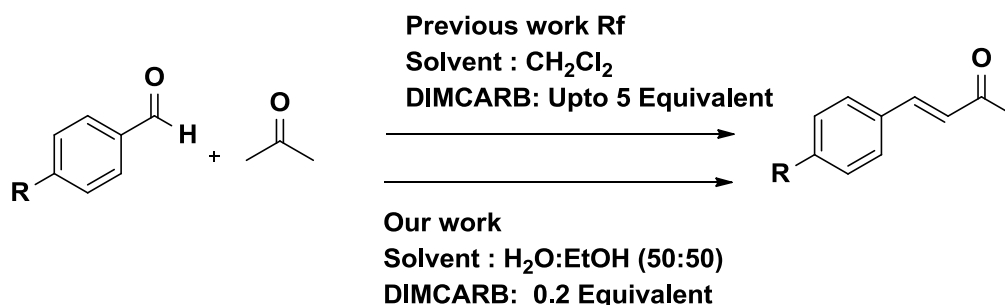
Figure 3.14 - Synthesis of monoarylidene alkanone.

The targeted unsymmetrical diarylalkanones were focused to synthesis due to its carbon moiety which look like those of the curcuminoids (1,7-diarylheptanes) and the chalcones (1,3-diarylpropanes). Curcuminoids are very important bioactive natural products found in many plant species. The promising structures of unsymmetrical biarylalkanone analogs exhibits important biological activity such as antitumor, anti-nematodal, anti-cancer, antioxidant, antifungal, antimitotic, anti-viral, anti-HIV, chemoprotective, anti-inflammatory, antimicrobial, antibacterial, antimalarial, anti-tubercular, anti-tubulin, anti-parasitic, neuro-protective and Anti-Metastatic.

Our initial efforts focused on carrying the synthesis of monoarylidene alkanones and unsymmetrical diarylalkanones. Our model reaction of nitro benzaldehyde with cyclopentanone rapidly gives hydrated intermediary and after some time *E1cb* mechanism produces dehydrated monoarylidene product. The reaction carried in ethanol water mixture (50:50) with 20 mole percent of DIMCARB at room temperature ends in 2 hours. Mild reaction conditions, shorter reaction time, cost-effectiveness, operational simplicity and high yields make this transformation a method of alternative for the straightforward preparation of various monoarylidene products. Comparing with previous methods (KREHER UP; et al., 2003) highlighted herein, a solution is offered to carry mild and green alternative for this key transformation. We observed that the use of water play an important role in the mechanism, by converting keto form of ketone to its respective enol form for reaction. We stir aldehyde with DIMCARB in water:ethanol mixture for 5 minutes, which produce reactive imine specie. The addition of ketone adapts its enolic form, which readily attack on imine to give dehydrated product first and hydrated product later. The substrate scope was analyzed for this reaction in the developed condition. Different cyclic, acyclic ketones, electron donating and withdrawing substituted

aromatic aldehydes were used (TABLE 3.12, and 3.13). It was observed that electron with drawing aldehydes take less time to form imine then electron donating. HPLC analysis shows that both products are interconvert able to each other. We isolated both products and were characterized by spectroscophic and spectrometric analysis. To date, no reported procedure for monoarylidene alkanones makes use of such a very mild and green environment and leads to such a high product yields. Isolated products were treated with aldehyde in basic condition and unsymmetrical diaryl alkanones were obtained in good to excellent yield.

Table 3.9: Table of selected bases.
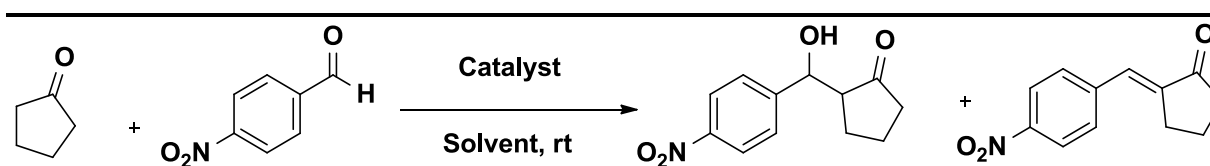
Entry	Base	Conversion %
1	Pyridine	No reaction
2	DMF	No reaction
3	Diisopropylethylamine	No reaction
4	DIMCARB (0.2 equivalent)	100
6	DBU (0.2 equivalent)	100
8	N,N-dimethylamine (0.2 equivalent)	100

It was experimented that DIM, DBU and *N,N*-dimethyl amine utilized all the starting material at 0.2 equivalent. So it means all three act as a catalyst. DIMCARB yields *N,N*-dimethyl amine which carry the reaction. So it was concluded that liquid crystal DIMCARB is the source of reactive *N,N*-dimethyl amine. Further the reaction was carried in different solvent to see the effect of solvent on reaction (TABLE 3.10). There was no reaction observed in water due to the less solubility of aldehyde. It was observed that using dichloromethane only 92 percent of aldehyde was converted into products. Ethanol water mixture (50:50) converts 100 percent of aldehyde into product. It is a green solvent so was selected for further reactions.

Table 3.10 - Table of selected solvents for the synthesis of mono arylidene alkanone.

Entry	Solvent	Conversion (%)
1	CH_2Cl_2	91
2	H_2O	ND
3	CH_3OH	96
4	CH_3CH_2OH	92
5	CH_3CH_2OH/H_2O (1:1)	100
6	CH_3CN	100

Conversion was calculated by HPLC analysis.

The catalytic quantity was also calculated for modal reaction. It was observed that 100 percent conversion ocurred at all catalytic quantity (TABLE 3.11). We carried further reaction with 20 mol percent due to effectiveness. For some aldehyde 10 mole percent was not effective so we did all reaction by 20 mole percent of DIMCARB. The reaction with 20 mole percent of aldehyde was so cleared that most of the time there was no need of column chromatography for purification. Un-reacted reactant in case of less reactive aldehyde was removed during work up procedure by extraction with saturated solution of sodium meta bisulphate.

Table 3.11 - Table of catalytic quantity of DIMCARB for the synthesis of mono arylidene alkanone.
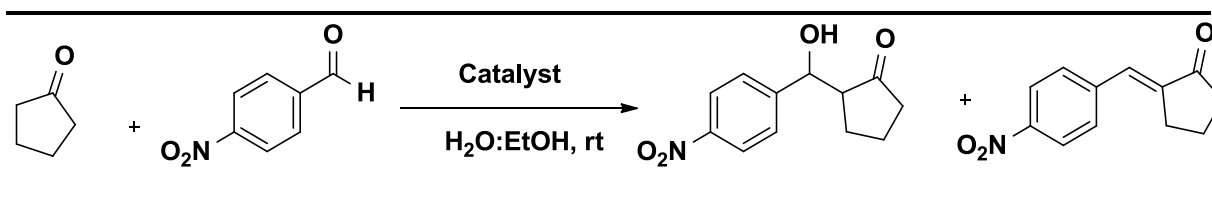
Entry	Quantity (Mole percent)	Conversion%
1	10	50
2	20	100
3	30	100
4	40	100
6	50	100

Conversions were calculated by HPLC

The speed of reaction for A11K10 is also investigated. It was observed that 100 percent conversion was not obtained in dichloromethane by DIM using 1 equivalent. The graph has recorded by interval. The HPLC analysis was done after 10, 60, 120, 180, 240 minutes. Even after 240 minutes 92 percent conversion occurred. By catalyzing the reaction with 20 mole percent of DIMCARB in ethanol water (50:50) mixture, the reactant was converted 100 percent even after 60 minutes of reactions (FIGURE 3.15).
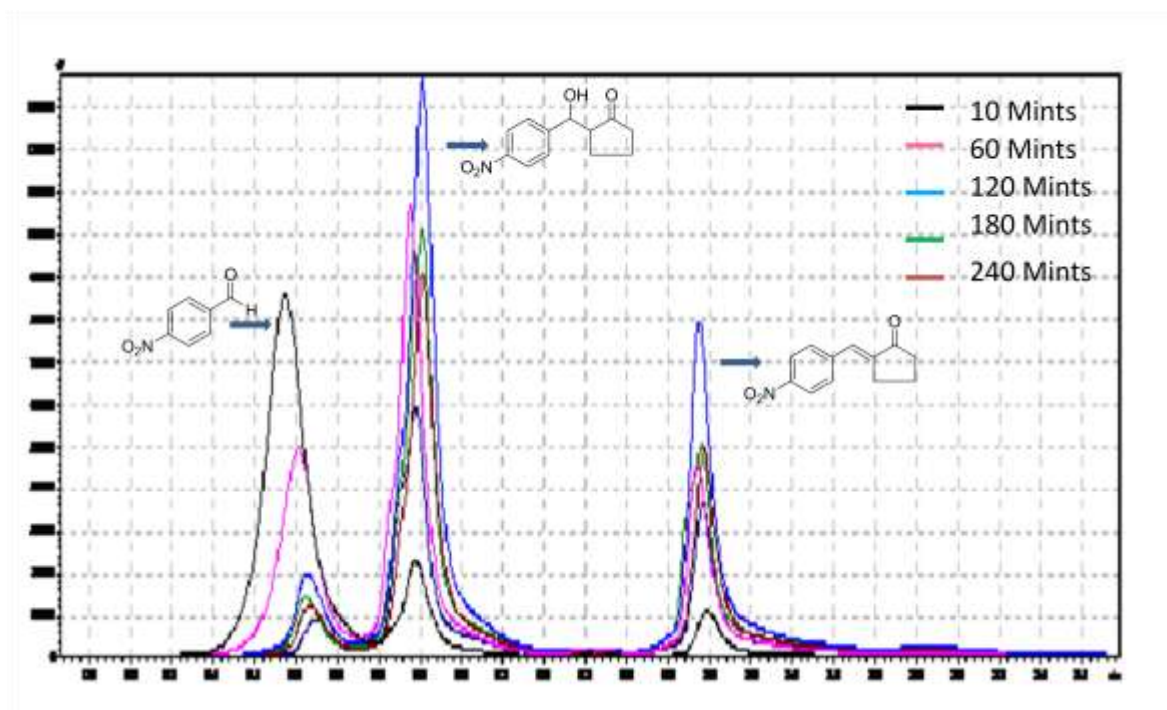
Figure 3.15 - Kinetic study of the modal reaction in CH_2Cl_2.

Table 3.12 - Synthesis of mono arylidene products using acetone and cyclopentanone with aldehydes.
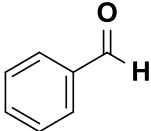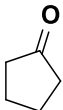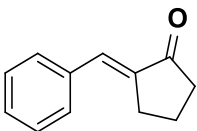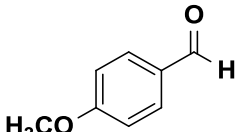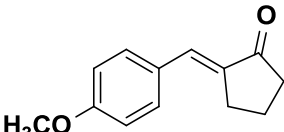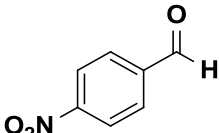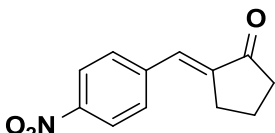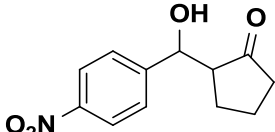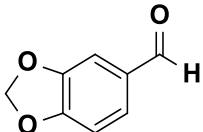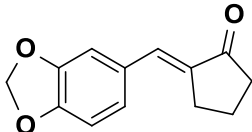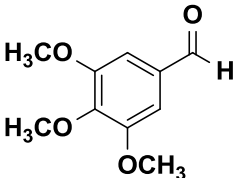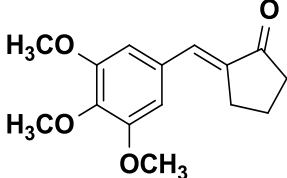
Entry	Aldehyde	Ketone	Products	Time (h)	Yield%
					DIM
131				5	75
132				8	72
133				1	30
134				1	60
135				8	40
136				18	60

TABLE 3.12 - Continued
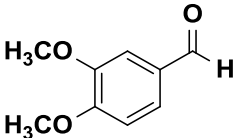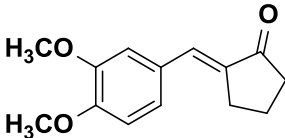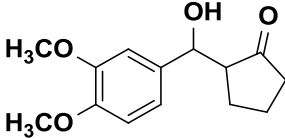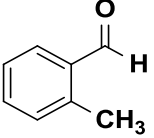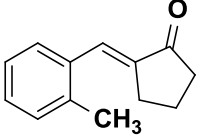
	Aldehyde	Product	Time	Yield
137	H₃CO, H₃CO-benzaldehyde	H₃CO, H₃CO-arylidene cyclopentanone	12	40
138		OH, H₃CO, H₃CO-aryl hydroxyl cyclopentanone		44
139	2-methylbenzaldehyde	2-methyl arylidene cyclopentanone	10	78

Table 3.13: Synthesis of Mono-arylidene derived from cyclohexanone and aldehydes.
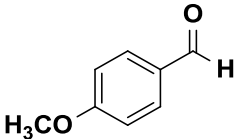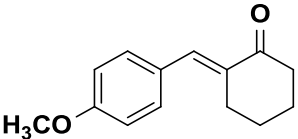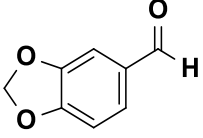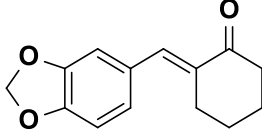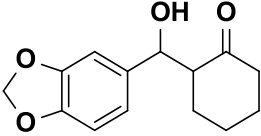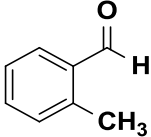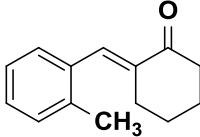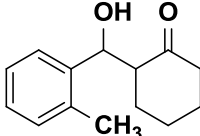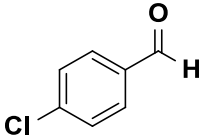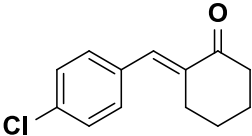
Entry	Aldehyde	Ketone	Products	Time	Yield%
					DIM
140	H₃CO-benzaldehyde		H₃CO-arylidene cyclohexanone	4	87
141	methylenedioxy benzaldehyde		methylenedioxy arylidene cyclohexanone	10	39

TABLE 3.13 - Continued

142			40
143		12	75
144		12	25
145		5	80

Different ketones were used to check the validity of the chemical method used for the synthesis of mono arylidene products.

3.13 Reaction Mechanism

The reaction was further evaluated by mass spectrometer LC-MS to study the mechanism of reaction. The reaction is catalysed by *N,N*-dimethyl amine produced by DIMCARB. For this study we select moderate reactive aldehyde,

anisaldehyde and cyclohexanone to explore its mechanism. *N,N*-dimethyl amine produced by DIMCARB first react with aldehyde yielding iminium species **i**, which further react with enolic form of cyclohexanone **ii** to yield intermediate **iii.** Compound **iv** were produced in the result of E1CB mechanism of intermediate compound iii. Compound iii was observed stable as its enolic form did not process further reaction (FIGURE 3.16). The production **of** *N,N*-dimethyl amine from ionic liquid and its attack on the aldehydic moiety is also explained.

The attack of *N-N*-dimethyl amine on aldehyde yield iminuim compound **i**. The reaction of compound **i** with **ii** follows Micheal mechanism. We have explored the mechanism of this reaction with HCl and NaOH, which follow Aldolic pathway. In this case it is difficult to control reaction and get monoarylidene product, because enol formation takes place at both alpha corbon and leading to symmetrical bis aryl alkanones (FIGURE 3.17). DIMCARB totally modify the mechanism of reaction and become more selective for monoarylidene compounds.
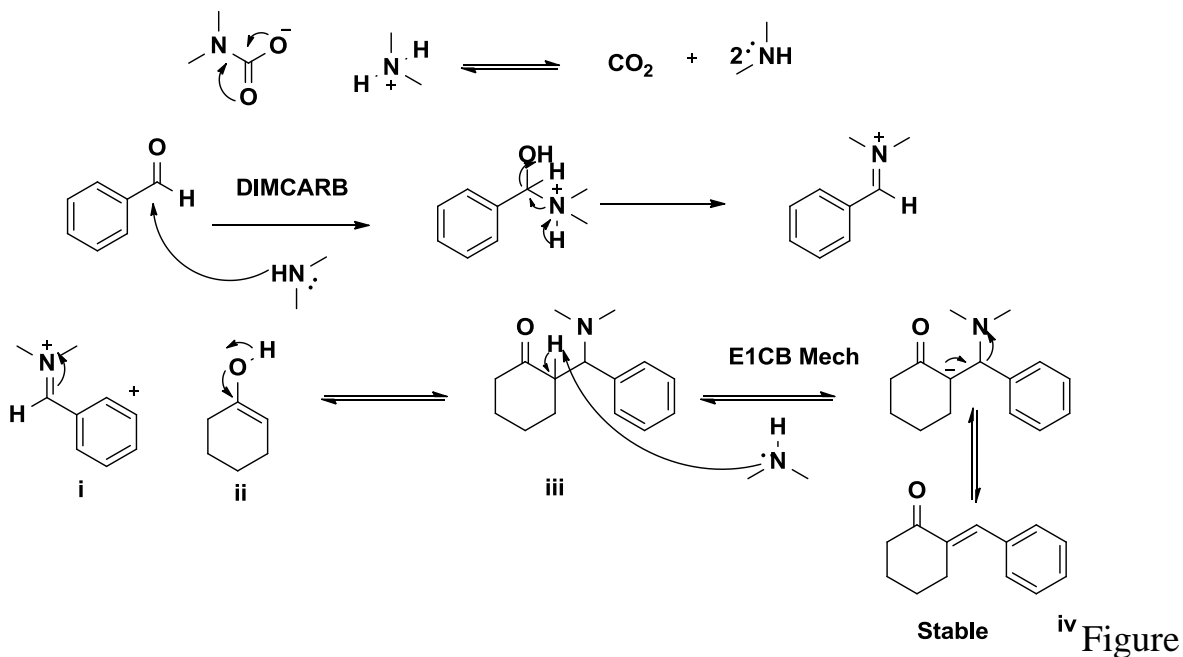
Figure 3.16 – Synthetic scheme of mono arylidende intermediate.
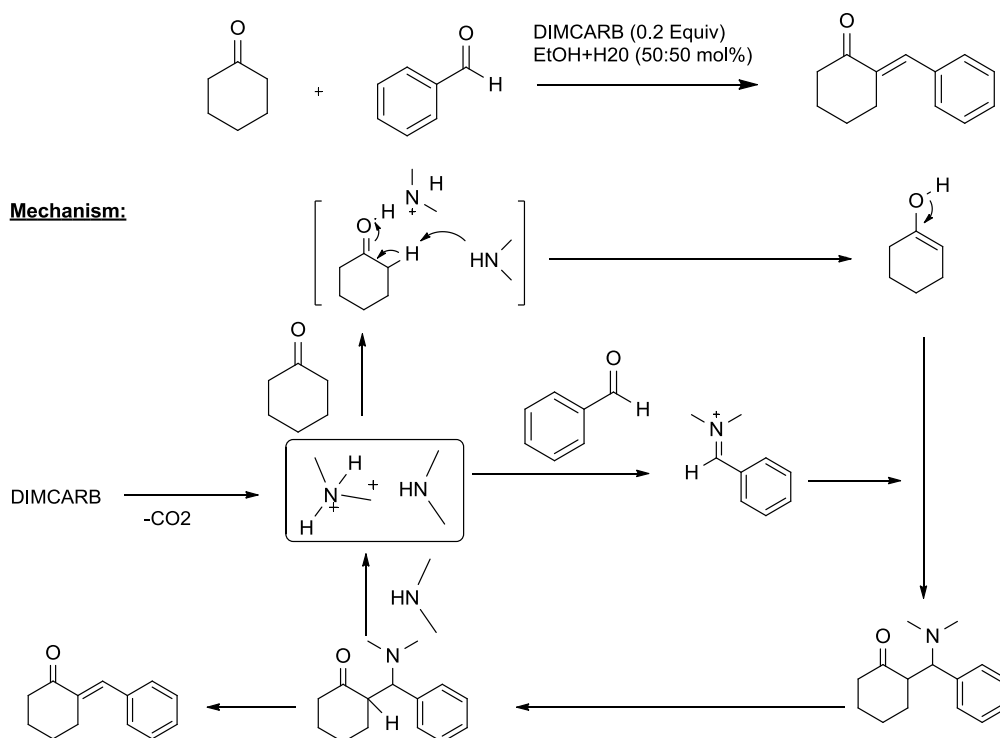
Figure 3.17 – Catalytic cycle of DIMCARB for the formation of mono arylidene intermediate.

The reaction was further optimized for the synthesis of unsymmetrical monocarbonylic analogues of curcumin. One pot synthesis was carried by the addition of one molar equivalent of aldehyde in reaction mixture after completion the synthesis of monoarylidene product. NaOH were dissolved in ethanol and were added in the reaction mixture. The diarylidene alkanone (unsymmetrical monocarbonylic analogues of curcumin) were synthesized in good yield. There is limited literature about the synthesis of unsymetrical diarylidene compounds. Braga *et al.* synthesized symmetrical bis arylmethylidene cycloalkanone by catalyzing the reaction with NaOH in ethanol (S.F.P. BRAGA et al., 2014). This method fails to produce unsymmetrical bis arylmethylidene cycloalkanone. Efficient synthesis of unsymmetrical bis arylmethylidene cycloalkanone could be obtain in good yield by catalyzing the reaction with DIMCARB for the synthesis of monoarylidene product, and then this product can be used as an intermediate for the synthesis of unsymmetrical bis arylmethylidene cycloalkanone (SCHEME 3.12). The products can be obtained even doing the reaction in one Pot.
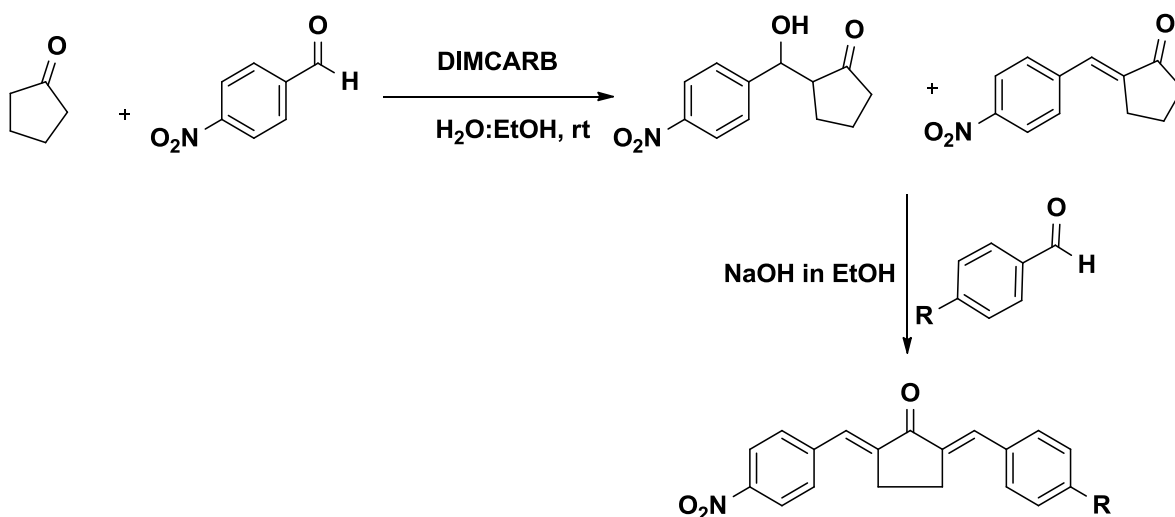
Scheme 3.12 - Synthesis of unsymmetrical bis arylmethylidene cycloalkanone.

109

3.14 Biological evaluation of monoarylidene products

Biological activity of mono arylidene products represents some interesting result. The biological activities of compounds **127-147** are reported (TABLE 3.14). Compounds **127-145** there was some mono arylidene compounds exhibited potent activities. Compounds **134** show potent activity and inhibit epimastigote of *Trypanosoma cruzi* and exhibit IC_{50} 1.8 ± 1.7 µM. The hydroxyl group next to aryl system play a vital role in activity, because by the elimination of hydroxyl and introduction of C=C bond diminishes activity. So electron withdrawing group with hydroxyl next to aryl system is the reason of activity. It may be due to the affinity of OH toward hydrogen bonding with amino acids in the active site of protein. Compounds **135** and **136** are possessing electron donating substituent on aryl system, mainly methoxy and methandioxy substitution, which also show strong tendency toward hydrogen bonding in the active site of protein. Compound **139** having *p*-chloro substitution on aryl system exhibited IC_{50} 1.8 ± 0.3, and found potent.

Table 3.14: Anti-parasitic activity of mono arylidene products prepared by DIMCARB.

S.No	Code	*L. amazonensis* Promastigote IC_{50} (µM)	*T.cruzi* Epimastigote IC_{50} (µM)	Vero cells CC_{50} (µM)
127	A1K8A1	2.8 ± 0.2	18.4 ± 0.2	40.6 ± 4.4
128	A2K8A2	33.3 ± 3.1	63.6 ± 2.0	177.9 ± 12.3
129	A13K8A13	3.6 ± 0.4	16.2 ± 4.5	32.1 ± 1.7
130	A14K8A14	4.2 ± 0.3	29.3 ± 6.8	58.0 ± 5.3
131	A1K10	>100	>100	610.4 ± 32.4
132	A2K10	>100	95.0 ± 7.1	280.0 ± 9.4
133	A11K10_a	>100	>100	236.7 ± 33.0

S.No	Code	*L. amazonensis* Promastigote IC$_{50}$ (µM)	*T.cruzi* Epimastigote IC$_{50}$ (µM)	Vero cells CC$_{50}$ (µM)
134	A11K10_b	78.1 ± 16.8	1.8 ± 1.7	>1000
135	A5K10	>100	1.8 ± 0.4	201.3 ± 45.3
136	A6K10	>100	3.8 ± 1.8	337.6 ± 62.6
137	A9K10_a	>100	>100	564.4 ± 154.0
138	A9K10_b	>100	>100	766.7 ± 188.6
139	A31K10	>100	1.8 ± 0.3	281.3 ± 65.0
140	A2K8	54.0 ± 4.2	54.8 ± 3.3	193.6 ± 6.5
141	A5K8_a	>100	>100	571.4 ± 40.4
142	A5K8_b	>100	>100	503.5 ± 83.5
143	A31K8_a	>100	>100	275.6 ± 60.3
144	A31K8_b	>100	>100	>1000
145	A13K8	41.4 ± 8.1	67.7 ± 13,5	34.5 ± 6.4

3.15 Synthesis of compounds 146-157

The search for novel anti-parasitic compounds continued, and several curcuminoids having methoxy on mono aryl system were synthesized. The monoarylidene cycloadduct (**146**) were synthesized by the reaction of cyclohexanone with anisaldehyde in the presence of DIMCARB as a catalyst in 87 % yield. Monoarylidene cyclo adduct cannot be synthesized by the aldol condensation, because the reaction of aldehyde with cycloalkanone give symmetrical bis-(arylmethylidene)-cycloalkanones even the reaction is carried at room temperature and controlled environment (SCHEME 3.13). So the use of DIMCARB is an interesting methodology for obtaining selectively monoarylidene cyclo adduct, further second step leading to get unsymmetrical bis-(arylmethylidene)-cycloalkanones. The synthesis of compounds (**147-157**) was carried in room temperature and all the starting materials were consumed in reaction times and no unreacted starting materials were recovered. Comparing our synthesis to reported one it is observed that using catalyst Al$_2$O$_3$
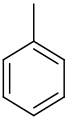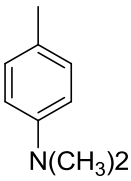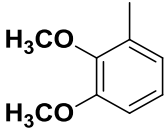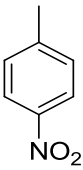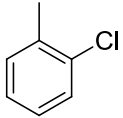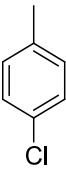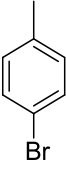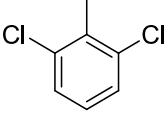
in microwave the symmetrical bis-(arylmethylidene)-cycloalkanones products were obtained (ESMAEILI et al., 2005). Compounds (**147-157**) were obtained in good yields (80-94%) under base catalyzed aldol condensation of (**146**) with various aldehydes as outlined (TABLE 3.15). The advantages of this synthetic methodology are that the compounds can be obtained in a crystalline nature by simple and rapid steps in good to excellent yield from readily available starting materials.
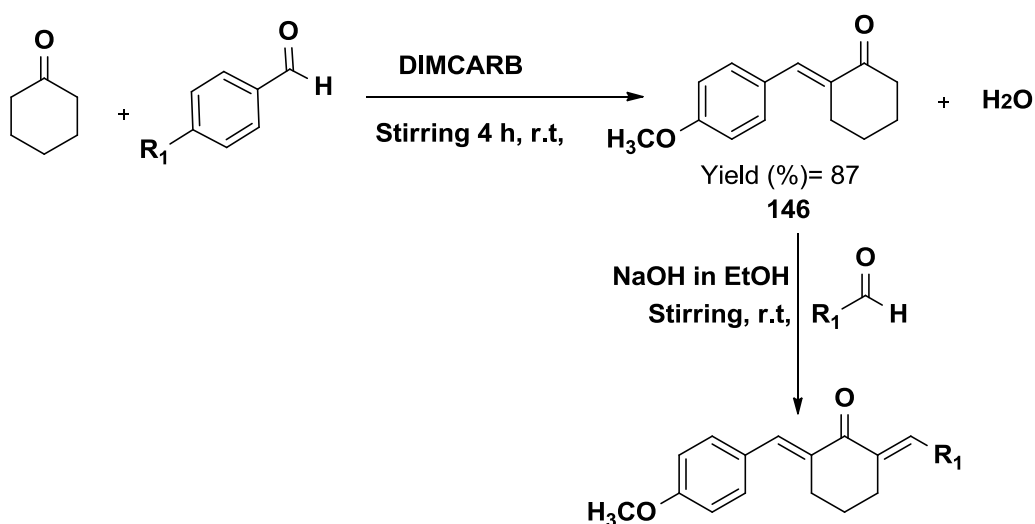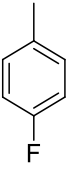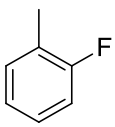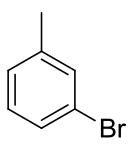
Scheme 3.13 - Synthesis of monoarylidene cycloadduct.

Table 3.15 - Synthesis of asymmetrical bis-(arylmethylidene)-cycloalkanones

Entry	R1	Time (h)	Yield (%)
147		4	85
148	N(CH$_3$)2	6	82
149	H$_3$CO / H$_3$CO	5	80
150	NO$_2$	2	89
151	Cl	3	80
152	Cl	2.5	86
153	Br	2	82
154	Cl, Cl	2.5	88

Entry	R1	Time (h)	Yield (%)
155		1.5	94
156		2	80
157		2	81

^{1}H NMR spectra of compound **146** show four specific signals of four methylene groups in the shielded region at δ_H 1.7 - 2.9, which is the evidence that among five methylene of cyclohexanone one is involved in the reaction, whereas one =CH signal was showed at δ_H 7.67 as singlet; Additionally, two aromatic signals having integration for four protons were detected at δ_H 7.41and 6.93, which confirm the aromatic moiety has added to cyclohexanone ^{13}C NMR spectrum of **146** showed four signals at δ_C 23.2 - 55.3, and six peaks from δ_C 113.9 - 159.9 for eight carbons, with two of these peaks having double intensity for aromatic carbons. The typical peak at δ_C 201.5 is due to carbonyl carbon. The reaction of **146** with various aldehydes gave products **144-157** in 80–94 % after re-crystallization from ethanol. All these reactions were carried in basic medium in ethanol, and their progress was monitored by TLC. The reaction time varied for each product and depended on the nature and reactivity of the aldehyde used. Thus, as expected, electron donating groups at various positions in the benzene rings increases the reaction time, while electron withdrawing groups decreases reaction time. The spectra of all compounds **147-157** are

similar except some signals in aromatic regions due to different substitution at different position on second benzene ring. The presence of a two broad singlet at de-shielded region δ_H 7.00 and 8.00, clearly showed two =CH signals which confirm that the second reaction did occur. The structures of all compounds were further identified using mass spectrometry, UV-Vis analysis.

3.16 Biological Evaluation of compounds 146-157

Initially, the *in vitro* anti-protozoal activities of the synthesized compounds were assayed against *T. cruzi* and *L. amazonensis*. The values are summarized in Table (TABLE 3.16). Eleven compounds (**146, 147, 149, 151-157**) displayed *in vitro* trypanocidal activity with IC_{50} values ranging from 5.2 to 55 µM (TABLE 3.16). There was a correlation between leishmanicidal and trypanocidal activity. All compounds active against *T. cruzi* were also active against *L. amazonesis*. Compound **149** were found more potent in the series. The potent activity may be due to the electron donating effect of methoxy substitution on aromatic ring like that present in curcumin. Recently it is investigated that methoxyl group in curcuminoids analogues play an important role in the biological activity by binding with amino acids aspartine, histidine, lysine, thrombin and serine in the active site of enzymes (GUPTA SC, PRASAD S; PATCHVA S; INDIRA PK, 2011). Singh and Misra also investigated through distance mapping of active site that methoxy is crucial for interaction with catalytic residues of thioredoxin (SINGH; MISRA, 2009). In addition, the compounds were evaluated against Vero cells. The results showed

that the active compounds were more toxic against the parasites than for the cell tested.

The mono arylidene cycloadduct was not considerably active in the bioassays, indicating that the second reaction is significant since it leads groups that contribute to bioactivity. The second reaction of aldehyde with mono arylidene cyclo adducts gives various products having electron donating and electron attracting groups on aromatic ring. It was observed that substitution has a great impact upon activity. The electron donating groups attached to aromatic ring increases the activity, while electron withdrawing group decreases it. Our results also prove the study reported by Aanandhi *et al.* (MV et al., 2009), and Suryawanshi *et al.* (SURYAWANSHI et al., 2013). The mechanism of drugs acting against parasites have been studied by many researcher around the world (RAINEY P, SANTI DV, 1983). We studied how our potent compounds interact with parasite. These potent compounds were evaluated against different enzymes target of *T. cruzi* like arginase and GAPDH, but our compounds showed no inhibition of these target (results not shown here). Later during other studies, we discovered that our compounds are good Michael acceptors. Thus enzyme having Michael reaction chances like those cysteine-containing ones may be the target. We observed that the best target our compounds may inhibit is trypanothione reductase, as found in other studies in the literature (S.F.P. BRAGA et al., 2014) So we did *in-silico* docking calculation against this enzyme.

Table 3.16 - Antiparasitary and citotoxicity activities of cyclo alkanone **73-85** Benznidazole and Amphotericin B.

Compounds	Epimastigote of *T. cruzi* IC$_{50}$ (µM)	Trypomastigote of *T. cruzi* EC$_{50}$ (µM)	Promastigote of *L. amazonesis* IC$_{50}$ (µM)	Vero cell CC$_{50}$ (µM)
146	54.8 ± 3.3	>100 ± 0.0	54.0 ± 4.2	193.6 ± 6.5
147	20.6 ± 1.7	>100 ± 0.0	11.8 ± 1.4	290.6 ± 9.4
148	>100 ± 0.0	>100 ± 0.0	91.0 ± 7.1	392.3 ± 7.7
149	5.2 ± 0.8	27.4 ± 3.6	8.9 ± 0.7	401.2 ± 8.8
150	>100 ± 0.0	>100 ± 0.0	>100 ± 0.0	435.0 ± 5.0
151	26.6 ± 4.0	>100 ± 0.0	13.0 ± 1.4	237.6 ± 6.8
152	21.6 ± 0.4	>100 ± 0.0	17.8 ± 2.5	401.2 ± 8.8
153	55.0 ± 3.0	>100 ± 0.0	17.3 ± 2.4	250.0 ± 2.7
154	20.5 ± 3.7	54.2 ± 0.9	5.2 ± 0.1	231.9 ± 9.7
155	21.0 ± 3.0	>100 ± 0.0	10.8 ± 3.1	378.1 ± 6.6
156	13.6 ± 2.5	>100 ± 0.0	9.0 ± 1.4	269.5 ± 8.3
157	20.2 ± 3.3	>100 ± 0.0	5.7 ± 0.8	30.0 ± 3.9
PC1	6.5±0.7	34.5 ± 7.6		
PC2			0.06 ± 0.00	

PC1: Benznidazol, PC2: Amphotericin B, Average ± SD

3.17 Molecular Docking of compounds 146-157

To identify how the ligands interact with trypanothione reductase (TR), docking studies were carried out for all our molecules. The interaction of each pose is then evaluated using the Glide Score (GScore) function. This score function takes into account the van der Waals energy, the Coulomb energy,

lipophilic contact term and hydrogen-bonding energy among other terms (SHERMAN W; et al., 2006; FRIESNER, R et al., 2006). In order to validate the theoretical results with the experimental ones, the dissociation constant Kd, was calculated from the GScore function and the docking studies were extended to two reference drugs used in the leishmaniasis and chagas treatment: amphotericin B and benznidazole (TABLE 3.17). The amphotericin B drug has the lowest GScore value (and lowest Kd) and benznidazole has the worse one compare to all our molecules, which is in accordance with the experimental inhibition studies. Among the 5 molecules with better GScore are compound **154**. These compounds are also among the 5 with better experimental IC_{50}. The docking results for **154**, amphotericin B and benznidazole compounds are shown in table (TABLE 3.18).

Non covalent interactions like hydrogen, halogen and van der Waals interactions play an important role in the stabilization of ligand-receptor complexes in biological systems. The van der Waals (vdW) interaction contacts can be classified as good, bad and non suitable contacts depending on the atom distances and on the atomic van der Waals radii. It is well established and accepted that the stabilization of a ligand-receptor complex is highly dependent on the number of good van der Waals interactions. The hydrogen and halogen interaction can be seen as a Coulombic interaction between polar donor bond and an acceptor atom. They are weak interactions (compare to ionic or covalent) and are inside the interval of thermal fluctuations in biological systems. The latter imply that they can be switched on or off in biological processes permitting fast reactions and molecular recognitions. Accordingly to the donor-acceptor mean distance, the hydrogen bond interaction can be classified as very strong (1.2 - 1.5Å), strong (1.5 - 2.2Å), moderate (2.2 - 3.2Å)

and weak (3.2 - 4.0Å). Table 2.18 shows the van der Waals contacts, the hydrogen bonds, the halogen bonds and the docking scores for the molecules with the lowest experimental IC_{50} and the best theoretical score from docking studies **154**.

Compounds make 54 van der Waals contacts and 3 hydrogen contacts with the TR structure. The van der Waals contacts are concentrated between the aromatic rings and the residues Ala160(2), Ile325(4), Phe45(12), Trp127(12), Trp164(12), Val37(12). The 3 hydrogen bonds are between the oxygen from the cyclohexane ring, located in the middle of the molecule, with the residues Ser47 (1, moderate) and Thr52 (2, strong). On the other hand, the **154** ligand makes 31 contacts with the TR structure distributed as 26 good vdW contacts, 3 hydrogen bonds and 2 halogen bonds, been 13 vdW contacts between the methoxy phenyl ring and residues Phe199 (6) and Ile200 (7), 3 vdW contacts between the cyclohexane ring at the center of ligand and residue Cys53 (3) and 10 vdW contacts between the di-halogenated aromatic ring with residues Ala160 (4), Ala338 (3) and Ile325 (3). The 3 hydrogen bonds are between the oxygen attached to the cyclohexane ring and residues Ser163 (2, one strong and one moderate) and Thr52 (moderate) whereas the halogen bonds are between the dihalogenated ring and residues Cys53 (weak) and Val328 (moderate). In both cases, these contacts are spread over the ligands structure (FIGURE 3.18). This distribution of contacts over the whole structure **154** is responsible for the complex stability and the good docking scores.

From docking studies, the theoretical IC_{50} found for compounds **154** and **157** were a little lower than the calculated for **149**, which were found the most active in the anti-parasitic bioassays. **154** and **157** have electron withdrawing groups at second aromatic ring (from second aldehyde). Maybe these groups

make these two compounds more reactive and they are reduced by other enzymes, such as those co-acting with NADH, before hitting the target in the parasite. Compound **149** possesses electron donator groups maybe less reactive against reducing enzymes, resulting in more of it getting to the target TR.

Table 3.17 - Docking scores of compounds **146-157** amphotericin B and benznidazole.

Compounds	IC_{50} (μM)	Glide Score (kcal/mol)	Kd	H-Bond
146	54.0	-7.86138	1.87E-06	3
147	11.8	-9.13451	2.21E-07	3
148	91.0	-9.11385	2.29E-07	4
149	8.9	-9.27467	1.75E-07	6
150	120.0	-8.81497	3.78E-07	3
151	13.0	-9.24603	1.84E-07	2
152	17.8	-9.65754	9.20E-08	5
153	17.3	-9.62981	9.64E-08	3
154	5.2	-10.1012	3.94E-08	3
155	10.8	-9.31534	1.63E-07	4
156	9.0	-9.14575	2.17E-07	2
157	5,7	-8.82743	3.70E-07	5
Amphotericin B	0.06	-10.3831	2.45E-08	
Benzonidazole		-5.18318	1.59E-04	2

Table 3.18 **-** Docking results: van der Waals contacts, hydrogen bonds and halogen contacts between ligands **154** and TR; docking parameters for it, amphotericin B and benznidazole.

van der Waals contacts		
	Number of contacts	Residues of TR
154	26	Ala160, Ala338, Cys53, Ile200, Ile325, Phe199
Hydrogen contacts		
	Residues of TR	Distances (Å)
154		
O7	Ser163	2.518 (moderate)
O7	Ser163	1.784 (strong)
O7	Thr52	2.388 (moderate)
Halogen contacts		
154	Residues of TR	Distances (Å)
Cl24	Cys53	3.417 (weak)
Cl25	Val328	2.575 (moderate)
TR-inhibitors docking score (GScore)[a]		
154	Amphotericin B	Benznidazole
-10.101	-10.383	-5.183
Dissociation constant (Kd)[b]		
154	Amphotericin B	Benznidazole
39.42 nM	24.50 nM	158.74 μM

[a]Lower score means more favorable binding between ligands and receptor.

[b]Calculated as Exp[GScore/RT] where R is the universal gas constant and T is the temperature (took as 298.15K).
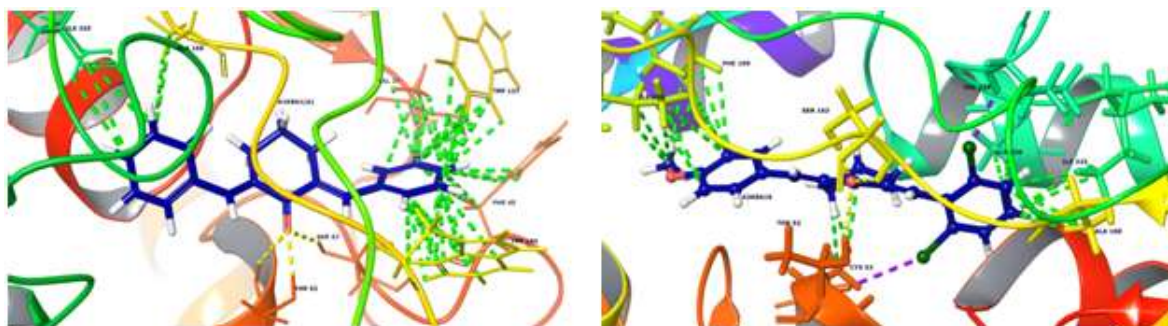
Figure 3.18 - Best poses of ligands **127** (left) and **154** (right) in dark blue interacting with TR structure. The good vdW contacts are represented in form of dashed-green lines, the hydrogen bonds are represented as dashed-yellow lines and the halogen bonds are represented as dashed-purple lines.

❖ 4

Experimental – Part 1

4   Experimental

Dibenzylideneacetones can be formed by the direct reaction of aldehyde (A1) with acetone using basic or acid catalysis. Acid catalysts used for cross-aldol condensation reaction include sulfuric, and Lewis acids. Generally, aldol condensation can be carried at room temperature or ethanol reflux condition. Dibenzylideneacetones and chalcones usually are more easily synthetized in one step by aldol condensation under basic catalysis. This procedure works very well for symmetric ketones and a variety of substituted aldehydes. However, only a few studies used non-symmetric ketones and different aldehydes to be attached to the ends of the alkyl chain spacer. These non-symmetric 1,5-diaryl-3-oxo-1,4-pentadienyls can be formed in two steps. Methyl-alkyl ketones are good for aldol condensation because of the easy regiochemistry control. Therefore, these ketones react with an appropriate aldehyde in acidic medium (thermodynamic enol formation), and then the dehydrated aldol is isolated. The second aldehyde is then added dropwise in cold ethanol solution, stirred, and the non-symmetric 1,5-diaryl-3-oxo-1,4-pentadienyl is formed. Using this methodology and combining different aldehydes with ketones, it is possible to generate a great molecular diversity, creating a library of compounds with 1,5-diarylpentane basic structures, which are still to be explored as to their bioactivities.

4.1 Chemistry

All chemicals were purchased from Organics, Sigma-Aldrich, Acros Chemicals and Fisher Scientific Ltd and used without further purification. The deuterated

solvents of Apolo were used for the NMR analysis. Thin layer chromatography (TLC) was prepared with precoated silica gel G-25-UV254 plates and detection was carried out at254 nm under UV, and by ceric sulphate in 10% H_2SO_4 solution. Mass spectra (ESI-MS) were measured in a Waters QuattroLC spectrometer. ^{1}H-NMR, ^{13}C-NMR and 2D experiments (gHSQC (^{1}H/^{1}H), gHMBC (^{1}H/^{13}C) and NOESY) were performed on a Brüker AVANCE 400 operating at 400.15 MHz and 100.62 MHz, respectively. $CDCl_3$ was used as solvent and tetramethylsilane (TMS) as internal reference. Compounds **45-65** were dissolved in organic solvents at about 10 mg mL^{-1} each and transferred into a 5-mm NMR tube. Chemical shifts (δ ppm) were measured with accuracy of 0.01 and 0.5 ppm for ^{1}H and ^{13}C NMR, respectively. Internal lock and tetramethylsilane (TMS) were used as internal reference. The UV-Vis spectra were recorded on a Perkin Elmer Lambda 25 spectrophotometer using 1 cm optical length quartz cuvettes at 25 °C and chloroform as solvent.

4.2 Synthetic detail

4.2.1 Compound (45)

Benzaldehyde (10 g, 90 mmol) and 2-butanone (1.36 g, 1.69 mL, 18.9 mmol) were taken in a 50 mL two - necked round bottom flask. Dry HCl gas was passed via the content of the flask at room temperature until it was saturated and red coloration appeared. The reaction mixture was stirred for 8 hrs. The crude product was diluted with toluene and washed with $NaHSO_3$ solution. The organic layer was separated, dried with anhydrous Na_2SO_4 and evaporated in

vacuo. The residue was distilled under reduced pressure to give pure compound, which was solidified by keeping in a refrigerator for 2 days.
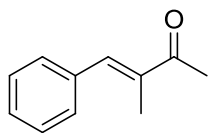
Percent yield: 52 %; Mp: 34-35 °C; ^{1}H NMR (400 MHz, CDCl$_3$) δ 7.52 (d, 1H, *J*=4 Hz, ArH), 7.41 (m, 3H, Ar H), 7.39 (m, 1H, CH=CCH$_3$), 7.32 (m, 1H, ArH), 2.47 (s, 3H, COCH$_3$), 2.06 (d, *J*=1.6 Hz, 3H, CH=CCH$_3$); ^{13}C NMR (400 MHz, CDCl$_3$) δ 129.71, 200.34, 139.68, 137.78, 135.92, 128.57, 128.47, 25.87, 12.94; HRMS ESI(+): calcd 161.09609; found 161.09623; UV-vis λmax (nm)[ε (mol^{-1} dm^3 cm^{-1})] in CH$_2$Cl$_2$: 278.

4.2.2 Compound (46):

Anisaldehyde (1 g, 7.3 mmol) and 2-butanone (1.05 g, 14.6 mmol) were taken in a 50 mL two - necked round bottomed flask. Dry HCl gas was passed via the content of the flask until it was saturated and coloration appeared. The reaction mixture was stirred for 8 hrs. The crude product was dilute with toluene and washed with NaHSO$_3$ solution. The organic layer was separated, dried with anhydrous Na$_2$SO$_4$ and evaporated with in vacuo. The residue was distilled under reduced pressure to give pure compound, which was solidified by keeping in a refrigerator for 24 hours.
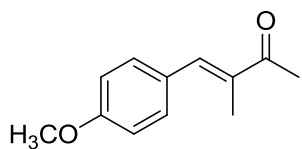
Percent yield: 67 %; Mp: Oil; ^{1}H NMR (400 MHz, CDCl$_3$) δ 7.47 (s, 1H, =CH), 7.40 (d, *J*=12 Hz, 2H, ArH), 6.93 (d, *J*=12 Hz, 2H, ArH), 3.85 (s, 3H, OCH$_3$), 2.45 (s, 3H, =CCH$_3$), 2.07 (d, *J*=1.6 Hz, 3H, COCH$_3$); ^{13}C NMR (400 MHz, CDCl$_3$) δ 131.58, 200.24, 159.92, 139.62, 135.83, 128.43, 113.97, 55.33, 25.78, 12.91;

HRMS ESI(+): calcd 191.10666; found 191.10722; UV-vis λmax (nm)[ε (mol^{-1} dm^3 cm^{-1})] in CH$_2$Cl$_2$: 308.

4.2.3 Compound (47):

N,N-Dimethylebenzaldehyde (1 g, 6.13 mmol) and 2-butanone (0.864 g, 12.26 mmol) were taken in a 50 mL two - necked round - bottomed flask. Dry HCl gas was passed via the content of the flask until it was saturated and coloration appeared. The reaction mixture was stirred for 8 hrs. The crude product was dilute with toluene and washed with NaHSO$_3$ solution. The organic layer was separated, dried with anhydrous Na2SO$_4$ and evaporated with vacuo. The residue when recrystalized in ethanol yield pure compound.
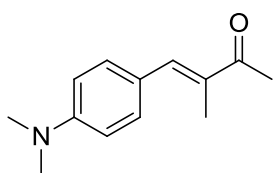
Percent yield: 48 %; Mp: 122-123 °C; ^{1}H NMR (400 MHz, CDCl$_3$) δ 7.45 (s, 1H, =CH), 7.41 (d, *J*=8Hz, 2H, ArH), 6.71 (d, *J*=12Hz, 2H, ArH), 3.02 (s, 6H, N(CH$_3$)$_2$, 2.44 (s, 3H, COCH$_3$), 2.10 (d, *J*=4 Hz, 3H, =CCH$_3$); ^{13}C NMR (400 MHz, CDCl$_3$) δ 200.16, 150.52, 140.74, 133.39, 131.87, 123.62, 111.69, 40.15, 25.71, 12.97; HRMS ESI(+): calcd 204.13829; found 204.13849; UV-vis λmax (nm)[ε (mol^{-1} dm^3 cm^{-1})] in CH$_2$Cl$_2$: 366.

4.2.4 Compound (48):
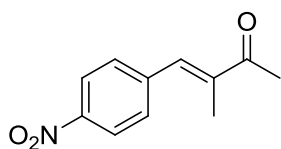
Percent yield: 61 %; Mp: 84-85 °C; ^{1}H NMR (400 MHz, CDCl$_3$) δ 8.27 (d, *J*=8 Hz, 2H, ArH), 7.55 (d, *J*=8 Hz, 2H, ArH), 7.52 (s, 1H, =CH), 2.49 (s, 3H, COCH$_3$), 2.06 (d, *J*=1.6 Hz, 3H, =CCH$_3$); 13C NMR (400 MHz, CDCl$_3$) δ 199.63, 147.30,

142.48, 140.64, 136.48, 130.24, 123.71, 25.99, 13.21; HRMS ESI(+): calcd 206.08117; found 206.08253; UV-vis λmax (nm)[ε (mol^{-1} dm^3 cm^{-1})] in CH$_2$Cl$_2$: 300.

4.2.5 Compound (49):

A Solution of compound **45** (50 mg, 3.125 mmole), and benzaldehyde (39.75 mg, 3.75 mmole) in ethanol (5 mL) was stirred for 5 minutes at room temperature and sodium hydro oxide solution in ethanol (4 mL, 50 mmole) was added and the stirring was continued for seven hours. The solvent evaporated in vacuo. Residue was dissolved in ethyl acetate, extraction with a NaHSO$_3$ solution, drying with Na$_2$SO$_4$, and concentration in vacuo the crude product which was collected as yellow precipitate and further purified by column chromatography and recrystallized from ethanol to give pure compound **49**.
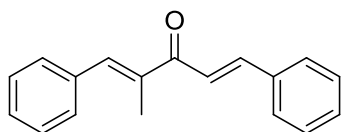
Percent yield: 51.4 %; Mp: 52-53 °C; ^{1}H NMR (400 MHz, CDCl$_3$) δ 7.67 (d, J=16 Hz, 1H, Ar-CH), 7.59 (m, 1H, ArH), 7.56 (m, 2H, ArH), 7.40 (m, 4H, ArH), 7.34 (s, 1H, Ar-CH), 7.28 (d, J=8 Hz, 1H, COCH), 6.92 (d, J=8 Hz, 2H, ArH), 3.85 (s, 3H, OCH$_3$), 2.19 (d, J=1.6 Hz, 3H, =C-CH$_3$); ^{13}C NMR (400 MHz, CDCl$_3$) δ 192.86, 161.42, 143.38, 138.66, 138.06, 133.31, 130.00, 129.73, 128.40, 127.86, 119.67, 114.37, 55.41, 13.93; HRMS ESI(+): calcd 249.12739; found 249.12827; UV-vis λmax (nm)[ε (mol^{-1} dm^3 cm^{-1})] in CH$_2$Cl$_2$: 313.

4.2.6 Compound (50):
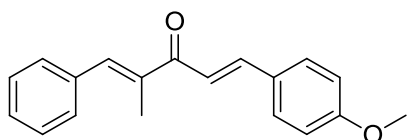
Percent yield: 57 %; Mp: 115-117 °C; ^{1}H NMR (400 MHz, CDCl₃) δ 7.67 (d, J=16 Hz, 1H, CH₃OAr-CH), 7.59 (m, 1H, ArH), 7.56 (m, 2H, ArH), 7.40 (m, 4H, ArH), 7.34 (s, 1H, Ar-CH), 7.28 (d, J=8 Hz, 1H, COCH), 6.92 (d, J=8 Hz, 2H, ArH), 3.85 (s, 3H, OCH₃), 2.19 (d, J=1.6 Hz, 3H, =C-CH₃); ^{13}C NMR (400 MHz, CDCl₃) δ 192.86, 161.42, 143.38, 138.66, 138.06, 133.31, 130.00, 129.73, 128.40, 127.86, 119.67, 114.37, 55.41, 13.93; HRMS ESI(+): calcd 279.13796; found 279.13878; UV-vis λmax (nm)[ε (mol^{-1} dm^3 cm^{-1})] in CH₂Cl₂: 340.

4.2.7 Compound (51):
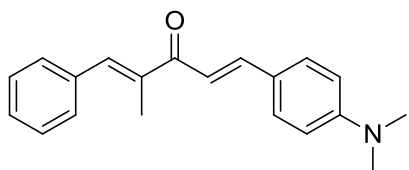
Percent yield: 68 %; Mp: 91-92 °C; ^{1}H NMR (400 MHz, CDCl₃) δ 7.68 (d, J=16Hz, 1H, =CH), 7.52 (d, J=8Hz, 2H, ArH, 7.40 (m, 4H, ArH), 7.31 (m, 1H, =CH), 7.19 (d, J=16Hz, 1H, =CH), 6.68 (d, J=8Hz, 2H, ArH), 3.04 (s, 6H, N(CH₃)₂, 2.19 (d, J=1.6 Hz, 2H, =CCH₃); ^{13}C NMR (400 MHz, CDCl₃) δ 193.09, 151.85, 144.55, 138.91, 137.04, 136.40, 130.14, 129.68, 128.40, 128.16, 122.91, 116.93, 111.68, 40.17, 14.10; HRMS ESI(+): calcd 292.16959; found 292.17099; UV-vis λmax (nm)[ε (mol^{-1} dm^3 cm^{-1})] in CH₂Cl₂: 414.

4.2.8 Compound (52):
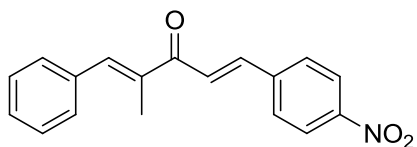
Percent yield: 50.5%; Mp: 138-140 °C; ^{1}H NMR (400 MHz, CDCl$_3$) δ 8.26 (d, *J*=8 Hz, 2H, ArH), 7.75 (d, *J*=12 Hz, 2H, ArH), 7.69 (d, *J*=16 Hz, 1H, =CH), 7.62 (s, 1H, =CH), 7.53 (d, *J*=16 Hz, 1H, =CH), 7.43-7.50 (m, 5H, ArH), 7.34 (t, 1H, ArH), 2.21 (d, *J*=1.6 Hz, 3H, =CCH$_3$); ^{13}C NMR (400 MHz, CDCl$_3$) δ 191.78, 148.38, 141.39, 1403.23, 139.92, 138.35, 135.61, 134.63, 129.84, 128.76, 125.67, 124.19, 123.98, 13.72; HRMS ESI(+): calcd 294.11247; found 294.11383; UV-vis λmax (nm)[ε (mol^{-1} dm^3 cm^{-1})] in CH$_2$Cl$_2$:300.

4.2.9 Compound (53):

A Solution of compound **46** (200 mg, 1.05 mmole), and benzaldehyde (133.9 mg, 1.26 mmole) in ethanol (5 mL) was stirred for 5 minutes at room temperature, added sodium hydro oxide solution in ethanol (4mL, 50 mole) and stirring was continued for two hours. The solvent was evaporated in vacuo. The residue was dissolved in ethyl acetate extracted with NaHSO$_3$ solution and dried with Na$_2$SO$_4$, solvent was evaporated in vacuo, the crude product was collected as a yellow precipitate which further purified by Column chromatography and recrystalized from ethanol to give compound **53**.
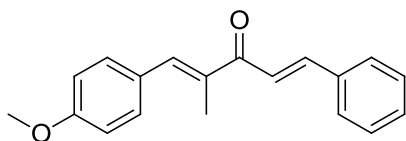
Percent yield: 51 %; Mp: 57-58 °C; ^{1}H NMR (400 MHz, CDCl$_3$) δ 7.67 (d, *J*=12 Hz, 1H, =CH), 7.61 (m, 2H, ArH), 7.56 (s, 1H, CH$_3$C=CH), 7.45 (m, 3H, ArH), 7.39 (m, 3H, =CH and ArH), 6.95 (d, *J*=8 Hz, 2H, ArH), 3.85 (s, 3H, OCH$_3$), 2.21 (d, *J*=1.6 Hz, 3H, =C-CH$_3$); ^{13}C NMR (400 MHz, CDCl$_3$) δ

192.62, 159.94, 143.03, 138.77, 136.64, 135.29, 131.65, 130.08, 128.89, 128.53, 128.22, 122.08, 114.01, 55.36, 13.84; HRMS ESI(+): calcd 279.13796; found 279.13880; UV-vis λmax (nm)[ε (mol^{-1} dm^3 cm$_{-1}$)] in CH$_2$Cl$_2$: 335.

4.2.10 Compound (54):
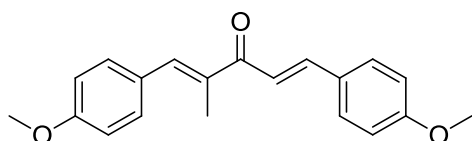
Percent yield: 91 %; Mp: 86-88 °C; ^{1}H NMR (400 MHz, CDCl$_3$) δ 7.65 (d, J=16, 1H, =CH), 7.56 (d, J=12 Hz, 2H, ArH), 7.53 (s, 1H, CH3C=CH), 7.44 (d, J= 8Hz, 2H, ArH), 7.30 (d, J=12 Hz, 1H, =CH), 6.95 (d, J=8 Hz, 2H, ArH), 6.92 (d, J=8 Hz, 2H, ArH), 3.85 (d, J=4 Hz, 6H, OCH$_3$), 2.20 (d, J=1.6 Hz, 3H, =C-CH$_3$); ^{13}C NMR (400 MHz, CDCl$_3$) δ 13.92, 55.35, 113.97, 114.34, 119.77, 127.99, 128.66, 129.92, 131.58, 136.77, 138.14 (1C, =C), 159.82, 161.31, 192.72; HRMS ESI(+): calcd 309.14852; found 309.14943; UV-vis λmax (nm)[ε (mol^{-1} dm^3 cm^{-1})] in CH$_2$Cl$_2$: 348.

4.2.11 Compound (55):
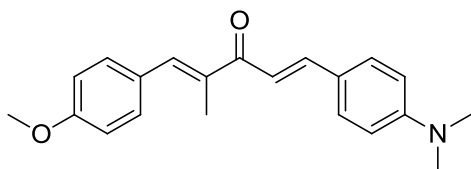
Percent yield: 93 %; Mp: 68-70 °C; ^{1}H NMR (400 MHz, CDCl$_3$) δ 7.66 (d, J=12 Hz, 1H, =CH), 7.50 (s, 1H, =CH), 7.49 (d, J=8 Hz, 2H, ArH), 7.41 (d, J=12 Hz, 2H, ArH), 7.20 (d, J=16 Hz, 1H, =CH), 6.92 (d, J=8 Hz, 2H, =CH), 6.65 (d, J=8Hz, 2H, ArH), 3.82 (s, 3H, OCH$_3$), 2.99 (s, 6H, N(CH$_3$)$_2$, 2.19 (d, J=1.6 Hz, 3H, =CCH$_3$); ^{13}C NMR (400 MHz, CDCl$_3$) δ 192.88, 159.67, 151.79, 144.13, 137.04, 136.97, 131.52, 130.09, 128.90, 122.99, 116.93, 113.94, 111.67, 55.33, 40.14, 14.10;

HRMS ESI(+): calcd 322.18016; found 322.18111; UV-vis λmax (nm)[ε (mol^{-1} dm^3 cm^{-1})] in CH$_2$Cl$_2$: 413.

4.2.12 Compound (56):
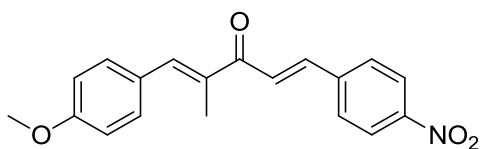
Percent yield: 69.3%; Mp: 145-146 °C; ^{1}H NMR (400 MHz, CDCl$_3$) δ 8.25 (d, *J*=12 Hz, 2H, ArH), 7.74 (d, *J*=12 Hz, 2H, ArH), 7.66 (d, *J*=16 Hz, 1H, =CH), 7.59 (s, 1H, =CH), 7.54 (d, *J*=16 Hz, 1H, =CH), 7.47 (d, *J*=8 Hz, 2H, ArH), 6.97 (d, *J*= 8Hz, 2H, ArH), 3.87 (s, 3H, OCH$_3$), 2.22 (d, *J*=1.6 Hz, 3H, =CCH$_3$); ^{13}C NMR (400 MHz, CDCl$_3$) δ 191.60, 160.24, 148.29, 141.54, 139.99, 139.79, 136.38, 131.83, 128.70, 128.15, 125.84, 124.18, 114.10, 55.39, 13.72; HRMS ESI(+): calcd 324.12303; found 324.12449; UV-vis λmax (nm)[ε (mol^{-1} dm^3 cm^{-1})] in CH$_2$Cl$_2$: 348.

4.2.13 Compound (57):
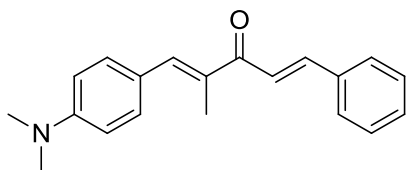
Percent yield: 67 %; Mp: 60-62 °C; ^{1}H NMR (400 MHz, CDCl$_3$) δ 7.68 (s, 1H, =CH), 7.61 (m, 2H, ArH), 7.56 (s, 1H, CH$_3$-C=CH), 7.47 (d, *J*=12Hz, 2H, =CH), 7.46 (d, *J*=0Hz, 2H, ArH), 7.39 (m, 2H, ArH), 6.73 (d, *J*=8 Hz, 2H, ArH), 3.04 (s, 6H, N(CH$_3$)$_2$), 2.24 (d, *J*=1.6 Hz, 3H, =CCH3); ^{13}C NMR (400 MHz, CDCl$_3$) δ 150.56, 142.24, 142.14, 140.14, 135.55, 134.21, 132.01, 129.83, 128.84, 128.13, 123.71, 122.39, 111.71, 40.17, 13.90; HRMS ESI(+): calcd 292.16959; found 292.17054; UV-vis λmax (nm)[ε (mol^{-1} dm^3 cm^{-1})] in CH$_2$Cl$_2$: 401.

4.2.14 Compound (58):
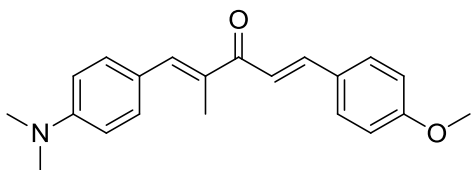
Percent yield: 79 %; Mp: 110-112 °C; ^{1}H NMR (400 MHz, CDCl$_3$) δ 7.62 (d, J= 16 Hz, 1H, =CH), 7.56 (d, J=8 Hz, 2H, ArH), 7.54 (s, 1H, CH3-C=CH), 7.45 (d, J= 8 Hz, 2H, ArH), 7.34 (s, J=16 Hz, 1H, =CH), 6.91 (d, J=8 Hz, 2H, ArH), 6.73 (d, J=8 Hz, 2H, ArH), 3.85(s, 3H, OCH$_3$), 3.03 (s, 6H, N(CH$_3$)$_2$), 2.23 (d, J=4 Hz, 3H, =CCH3); ^{13}C NMR (400 MHz, CDCl$_3$) δ 192.50, 161.10, 150.48, 142.13, 139.50, 134.37, 131.91, 129.80, 128.25, 123.85, 120.08, 114.28, 111.72, 55.39, 40.17, 13.98; HRMS ESI(+): calcd 322.18016; found 322.18115; UV-vis λmax (nm)[ε (mol^{-1} dm^3 cm^{-1})] in CH$_2$Cl$_2$: 401.

4.2.15 Compound (59):
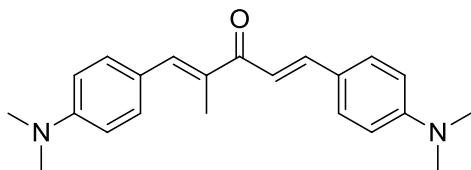
Percent yield: 60 %; Mp: 146-147 °C; ^{1}H NMR (400 MHz, CDCl$_3$) δ 7.63 (d, J=16 Hz, 2H, =CH), 7.63 (d, J=8 Hz, 2H, ArH), 7.44 (d, J=8 Hz, 2H, ArH), 7.30 (s, 1H, CH$_3$-C=CH), 6.73 (d, J=8 Hz, 2H, ArH), 6.68 (d, J=8 Hz, 2H, ArH), 3.03 (d, J=0 Hz, 12H, N(CH$_3$)$_2$), 2.23 (d, J=1.6 Hz, 3H, =CCH$_3$); ^{13}C NMR (400 MHz, CDCl$_3$) δ 192.81, 151.62, 150.34, 143.31, 138.51, 134.71, 131.76, 129.90, 124.18, 123.37, 117.39, 111.90, 111.75, 40.20, 14.11; HRMS ESI(+): calcd 335.21179; found 335.21236; UV-vis λmax (nm)[ε (mol^{-1} dm^3 cm^{-1})] in CH$_2$Cl$_2$: 422.

4.2.16 Compound (60):
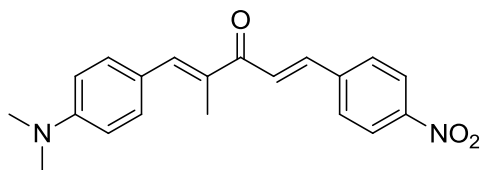
Percent yield: 57.6 %; Mp: 212-215 °C; ^{1}H NMR (400 MHz, CDCl$_3$) δ 1H NMR (400 MHz, CDCl$_3$) δ 8.25 (d, J=8 Hz, 2H, =CH), 7.74 (d, J=8 Hz, 2H, ArH), 7.62 (d, J=8 Hz, 2H, ArH), 7.58 (s, 1H, CH$_3$-C=CH), 7.48 (d, J=8 Hz, 2H, ArH), 6.73 (d, J=12 Hz, 2H, ArH), 3.05 (s, 6H, N(CH$_3$)$_2$), 2.25 (d, J=1.6 Hz, 3H, =CCH$_3$); ^{13}C NMR (400 MHz, CDCl$_3$) δ 191.30, 150.55, 148.13, 141.88, 141.40, 139.01, 133.81, 132.28, 128.61, 126.23, 124.14, 123.37, 111.68, 40.12, 13.80; HRMS ESI(+): calcd 337.15467; found 337.15621; UV-vis λmax (nm)[ε (mol^{-1} dm^3 cm^{-1})] in CH2Cl2: 418.

4.2.17 Compound (61):

Percent yield: 92 %; Mp: 100-101 °C; ^{1}H NMR (400 MHz, CDCl$_3$) δ 8.28 (d, J=8 Hz, 2H, ArH), 7.73 (d, J=16 Hz, 2H, ArH), 7.62 (m, 2H, ArH), 7.58 (d, J=12 Hz, 2H, =CH), 7.55 (s, 1H, CH$_3$C=CH), 7.42 (m, 3H, ArH), 7.36 (d, J=16 Hz, 2H, =CH), 2.19 (d, J=4 Hz, 3H, =CCH$_3$); ^{13}C NMR (400 MHz, CDCl$_3$) δ 14.13 (1C, =CCH3); 121.40 (1C, =C); 123.73 (2C, ArC); 128.40 (2C, ArC); 129.00 (2C, ArC); 130.25 (2C, ArC); 130.61 (1C, ArC); 134.79 (1C, =C); 135.25 (1C, =C); 141.55 (1C, ArC); 142.58 (1C, =C); 144.64 (1C, ArC); 147.25 (1C,ArC); 192.16 (1C, CO); HRMS ESI(+): calcd 294.11247; found 294.11339; UV-vis λmax (nm)[ε (mol^{-1} dm^3 cm^{-1})] in CH$_2$Cl$_2$: 308.

4.2.18 Compound (62):
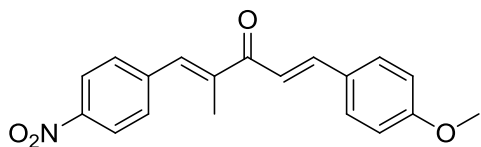
Percent yield: 63 %; Mp: 74-76 °C; ^{1}H NMR (400 MHz, CDCl$_3$) δ 8.27 (d, J=8 Hz, 2H, ArH), 7.71 (d, J=16 Hz, 1H, =CH), 7.58 (d, 4H, ArH), 7.52 (s, 1H, =CH), 7.26 (s, 1H, CH$_3$C=CH), 6.93 (d, J=8 Hz, 2H, ArH), 2.19 (d, J=1.6 Hz, 3H, =CCH$_3$), 1.59(s, 3H, OCH$_3$); ^{13}C NMR (400 MHz, CDCl$_3$) δ 192.23, 161.74, 147.17, 144.45, 142.76, 141.72, 134.62, 130.22, 130.21, 127.51, 123.72, 119.07, 114.46, 55.45, 14.23; HRMS ESI(+): calcd 324.12303; found 324.12500; UV-vis λmax (nm)[ε (mol^{-1} dm^3 cm^{-1})] in CH$_2$Cl$_2$: 316.

4.2.19 Compound (63):
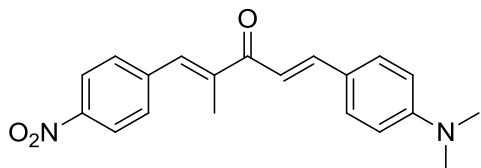
Percent yield: 61 %; Mp: 129-131 °C; ^{1}H NMR (400 MHz, CDCl$_3$) δ 8.26 (d, J=8 Hz, 2H, ArH), 7.71 (d, J= 16 Hz, 1H, =CH), 7.56 (d, J= 12 Hz, 2H, ArH), 7.52 (d, J=8 Hz, 2H, ArH), 7.48 (s, 1H, =CH), 7.12 (d, J=16 Hz, 1H, =CH), 3.68 (d, J=8 Hz, 2H, ArH), 3.05 (s, 6H, N(CH$_3$)$_2$), 2.19 (d, J=1.6 Hz, 3H, =CCH$_3$); ^{13}C NMR (400 MHz, CDCl$_3$) δ 192.43, 152.08, 147.02, 145.76, 143.10, 142.05, 133.63, 130.40, 130.19, 123.67, 122.51, 116.23, 111.83, 40.14, 14.42; HRMS ESI(+): calcd 337.15467; found 337.15678; UV-vis λmax (nm)[ε (mol^{-1} dm^3 cm^{-1})] in CH$_2$Cl$_2$:415.

4.2.20 Compound (64):

Percent yield: 65 %; Mp: 188-189 °C; ^{1}H NMR (400 MHz, CDCl$_3$) δ 8.31 (t, J=0 Hz, J=4 Hz, 1H, ArH), 8.29 (t, J=0 Hz, J=4 Hz, 2H, ArH), 8.23 (t, J=0 Hz, J=4 Hz, 1H, ArH), 7.74 (m, 3H, ArH and CH$_3$-C=CH), 7.60 (d, J=8 Hz, 3H, =CH and ArH), 7.49 (d, J=16 Hz, 1H, =CH), 2.21 (d, J=1.6 Hz, 3H, =CCH$_3$); ^{13}C NMR (400 MHz, CDCl$_3$) δ 191.20, 148.58, 147.44, 142.13, 141.31, 141.27, 140.95, 136.40, 130.31, 128.90, 125.01, 124.25, 123.81, 13.98; HRMS ESI(+): calcd 339.09955; found 339.09955. UV-vis λmax (nm)[ε (mol^{-1} dm^{3} cm^{-1})] in CH$_2$Cl$_2$:304.

4.2.21 Compound (65):
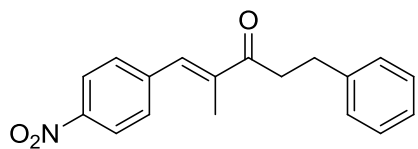
Percent yield: 69 %;; ^{1}H NMR (400 MHz, CDCl$_3$) δ 8.17 (d, J = 8.8 Hz, 2H), 7.42 (d, J = 8.5 Hz, 2H), 7.38 (s, 1H), 7.27 – 7.20 (m, 2H), 7.20 – 7.10 (m, 4H), 3.07 (t, J = 7.8 Hz, 2H), 2.93 (d, J = 7.3 Hz, 2H), 1.98 (d, J = 1.4 Hz, 3H); ^{13}C NMR (400 MHz, CDCl$_3$) 200.91, 147.39, 142.61, 141.31, 140.37, 135.71, 130.33, 128.70, 128.58, 126.36, 123.81, 39.80, 30.69, 13.54.

4.2.22 Compound (66):
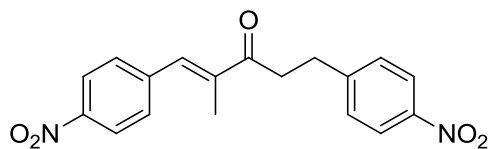
Percent yield: 72 %; ^{1}H NMR (400 MHz, CDCl$_3$) δ 8.26 (d, J = 8.8 Hz, 2H), 8.16 (d, J = 8.7 Hz, 2H), 7.52 (d, J = 8.7 Hz, 2H), 7.50 (s, 1H), 7.41 (d, J = 8.8 Hz, 2H), 3.19 (d, J = 6.7 Hz, 2H), 3.14 (d, J = 6.5 Hz, 2H), 2.06 (d, J = 1.4 Hz, 3H). ^{13}C NMR (400 MHz, CDCl$_3$) δ 199.52, 148.98,

147.39, 146.60, 142.17, 140.00, 135.87, 130.23, 129.38, 123.80, 123.74, 38.79, 29.99, 13.43.

4.2.23 Compound (67)
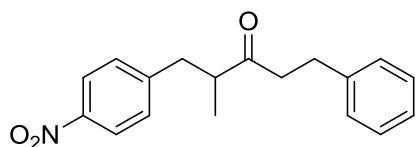
Percent yield: 30 %; ^{1}H NMR (400 MHz, CDCl$_3$) δ 8.09 (d, J = 8.7 Hz, 2H), 7.25 − 7.14 (m, 5H), 7.10 (d, J = 6.8 Hz, 2H), 3.06 (dd, J = 13.4, 7.6 Hz, 1H), 2.88 − 2.73 (m, 4H), 2.69 − 2.52 (m, 2H), 1.08 (d, J = 7.0 Hz, 3H). ^{13}C NMR (400 MHz, CDCl$_3$)δ 211.95, 147.62, 146.20, 140.84, 129.76, 128.47, 128.30, 126.17, 123.64, 47.88, 43.43, 38.41, 29.51, 16.68.

4.2.24 Compound (68):
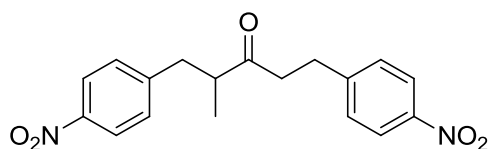
Percent yield: 39 %; ^{1}H NMR (400 MHz, CDCl$_3$) δ 8.10 (dd, J = 8.8, 1.1 Hz, 4H), 7.29 (dd, J = 8.8, 3.8 Hz, 4H), 3.09 (dd, J = 13.5, 7.6 Hz, 1H), 3.00 − 2.81 (m, 4H), 2.71 − 2.57 (m, 2H), 1.11 (d, J = 7.0 Hz, 3H). ^{13}C NMR (400 MHz, CDCl$_3$) δ 211.00, 148.84, 147.49, 146.61, 146.49, 129.81, 129.26, 123.66, 123.64, 47.76, 42.48, 38.34, 29.15, 16.70.

4.2.25 Compound (69):
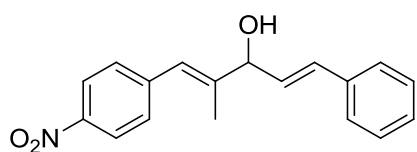
Percent yield: 72 %; ^{1}H NMR (400 MHz, CDCl$_3$) δ 8.10 (d, J = 8.9 Hz, 2H), 7.37 − 7.30 (m, 4H), 7.29 − 7.22 (m, 2H), 7.21 − 7.14 (m, 1H), 6.63 (d,

$J = 15.1$ Hz, 2H), 6.18 (dd, $J = 15.9$, 6.7 Hz, 1H), 4.78 (d, $J = 6.7$ Hz, 1H), 1.85 (d, $J = 1.3$ Hz, 3H). ^{13}C NMR (400 MHz, CDCl$_3$)δ145.92, 144.27, 142.95, 136.08, 131.78, 129.39, 129.19, 128.46, 127.84, 126.39, 123.50, 123.29.

4.2.26 Compound (70):
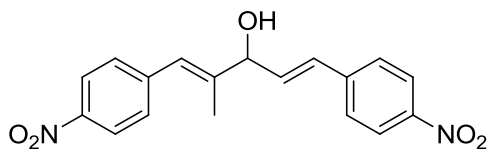
Percent yield: 76 %; ^{1}H NMR (400 MHz, CDCl$_3$) δ 8.22 (dd, $J = 8.8$, 4.2 Hz, 4H), 7.57 (d, $J = 8.7$ Hz, 2H), 7.47 (d, $J = 8.6$ Hz, 2H), 6.84 (d, $J = 15.9$ Hz, 1H), 6.76 (s, 1H), 6.47 (dd, $J = 15.9$, 6.0 Hz, 1H), 4.97 (d, $J = 5.9$ Hz, 1H), 1.97 (d, $J = 1.3$ Hz, 3H). ^{13}C NMR (400 MHz, CDCl$_3$) δ 147.29, 146.45, 144.12, 142.97, 142.54, 134.34, 129.75, 129.48, 127.28, 124.76, 124.20, 123.70, 77.67, 14.61;

4.2.27 Compound (71):
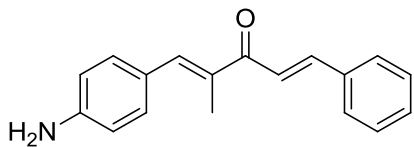
Percent yield: 90 %; ^{1}H NMR (400 MHz, CDCl$_3$) δ 7.28 − 7.23 (m, 2H), 7.21 − 7.14 (m, 1H), 7.12 (dd, $J = 7.8$, 0.9 Hz, 2H), 6.94 (d, $J = 8.4$ Hz, 2H), 6.73 (d, $J = 8.4$ Hz, 2H), 2.83 (ddd, $J = 10.9$, 10.2, 4.7 Hz, 3H), 2.77 − 2.65 (m, 2H), 2.57 (ddd, $J = 17.2$, 8.6, 6.4 Hz, 1H), 2.47 (dd, $J = 13.4$, 7.2 Hz, 1H), 1.03 (d, $J = 6.9$ Hz, 3H). ^{13}C NMR (400 MHz, CDCl$_3$)δ 213.65, 142.75, 141.35, 131.03, 129.92, 128.54, 128.44, 126.11, 116.30, 48.61, 43.78, 38.53, 29.66, 16.36.

4.2.28 Compound (72):
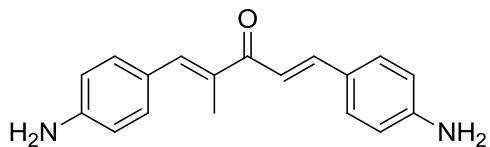
Percent yield: 92 %; ^{1}H NMR (400 MHz, CDCl$_3$) δ 6.90 (dd, J = 8.3, 7.1 Hz, 4H), 6.60 (dd, J = 8.4, 1.8 Hz, 4H), 3.62 (s, 4H), 2.83 (dd, J = 13.3, 7.1 Hz, 1H), 2.79 – 2.59 (m, 4H), 2.58 – 2.49 (m, 1H), 2.45 (dd, J = 13.4, 7.2 Hz, 1H), 1.02 (d, J = 6.8 Hz, 3H). ^{13}C NMR (400 MHz, CDCl$_3$) δ 214.07, 144.50, 144.28, 131.24, 129.70, 129.59, 129.08, 115.37, 115.29, 48.52, 43.99, 38.37, 28.76, 16.19.

4.2.29 Compound (73):
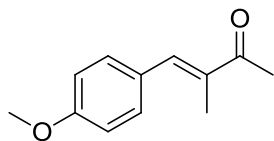
Percent yield: 67 %. m.p: Oil. ^{1}H NMR (400 MHz, CDCl$_3$), δ ppm: 7.47 (1H, s, =CH); 7.40 (2H, d, J=12 Hz, ArH); 6.93 (2H, d, J=12 Hz, ArH); 3.85 (3H, s, OCH3); 2.45 (3H, s, =CCH3); 2.07 (3H, d, J=0 Hz, COCH3). ^{13}C NMR (400 MHz, CDCl$_3$), δ ppm: 200.24 (1C, CO); 159.92 (1C, =C); 139.62 (1C, =C); 135.83 (1C, ArC); 131.58 (2C, ArC); 128.43 (1C, ArC); 113.97 (2C, ArC); 55.33 (1C. OCH3); 25.78 (1C, COCH3); 12.91 (1C, =CCH$_3$). HRMS ESI(+): calcd for C$_{12}$H$_{15}$O$_2$ (M+H)$^+$ 191.0994, found 191.1072.

***4.2.30* Compound (74):**
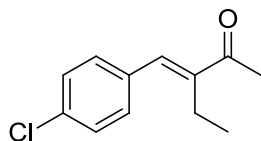
Percent yield**:** 82. m.p: oil. ^{1}H NMR (400 MHz, CDCl$_3$), δ ppm: 7.37 (s, 1H); 7.31 (dd, J = 16.8, 8.2 Hz, 4H); 2.46 (q, J = 7.4 Hz, 2H); 2.40 (s, 3H); 1.06 (t, J = 6.7 Hz, 3H). ^{13}C NMR (400 MHz, CDCl$_3$), δ ppm: 199.69 (1C, CO); 144.39 (1C, =C); 137.84 (1C, =C); 134.41 (1C, ArC); ArC), 134.15 (1C, ArC); 130.48 (2C, ArC);

128.75 (2C, ArC); 26.07 (1C. CH_2-CH_3); 19.55 (1C, CH_3); 13.65 (1C, CH_3).
HRMS ESI(+): calcd for $C_{12}H_{13}ClO_2$ (M+H)$^+$ 209.0655, found 209.0611.

4.2.30 Compound (75):
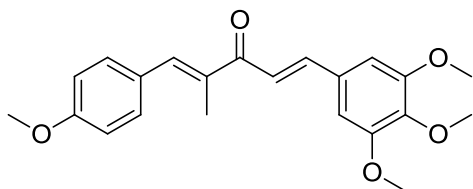
Percent yield: 84. m.p: 96-98 °C. ^{1}H NMR (400 MHz, CDCl$_3$) δ ppm: 7.59 (d, J = 15.6 Hz, 1H); 7.53 (s, 1H); 7.46 (d, J = 8.7 Hz, 2H); 7.28 (d, 2H); 6.96 (d, J = 8.9 Hz, 2H); 6.83 (s, 2H); 3.92 (s, 6H); 3.89 (s, 3H); 3.86 (s, 3H); 2.21 (d, J = 1.3 Hz, 3H). ^{13}C NMR (400 MHz, CDCl$_3$) δ ppm: 192.71 (1C, CO); 159.93 (1C, ArC); 153.43 (1C, =C); 143.27 (1C, =C); 140.08 (1C, =C); 138.63 (1C, =C); 136.67 (1C, ArC); 131.59 (2C, ArC); 130.78 (1C, ArC); 129.92 (1C, ArC); 128.51 (1C, ArC); 121.53 (1C, ArC); 114.34 (2C, ArC); 114.01 (1C, ArC); 106.45 (1C, ArC); 61.00 (2C, OCH$_3$); 56.25 (1C, OCH$_3$); 55.36 (1C, OCH$_3$); 13.95 (1C, CH$_3$). HRMS ESI(+): calcd for $C_{22}H_{24}O_5Na$ (M+Na) 391.1624, found 391.1519.

4.2.32 Compound (76):
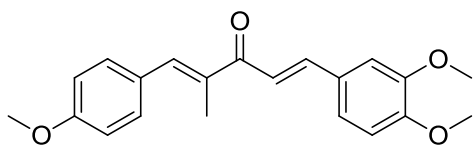
Percent yield: 85. m.p: oil. ^{1}H NMR (400 MHz, CDCl$_3$) δ ppm: 7.66 (d, J = 15.6 Hz, 1H); 7.55 (s, 1H); 7.47 (d, J = 8.7 Hz, 2H); 7.30 (d, J = 15.4 Hz, 1H); 7.22 (dd, J = 8.4, 1.9 Hz, 1H); 7.15 (d, J = 1.9 Hz, 1H); 6.98 (d, J = 8.8 Hz, 2H); 6.91 (d, J = 8.3 Hz, 1H); 3.96 (s, 3H); 3.94 (s, 3H); 3.87 (s, 3H); 2.22 (d, J = 1.3 Hz, 3H). ^{13}C NMR (400 MHz, CDCl$_3$) δ 192.78 (1C, CO); 159.85 (1C, ArC); 151.05 (1C, =C); 149.21 (1C, =C); 143.28

(1C, =C); 138.21 (1C, =C); 136.77 (1C, ArC); 131.56 (2C, ArC); 128.62 (1C, ArC); 128.25 (1C, ArC); 122.66 (1C, ArC); 120.10 (1C, ArC); 113.98 (2C, ArC); 111.13 (1C, ArC); 110.10 (1C, ArC); 56.00 (1C, OCH_3); 55.35 (1C, OCH_3); 13.95 (1C, CH_3). HRMS ESI(+): calcd for $C_{21}H_{22}O_4Na$ (M+Na) 361.1518, found 361.1413.

4.2.33 Compound (77):
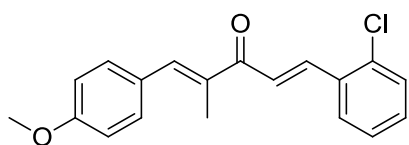
Percent yield: 79. m.p: 101 – 103 °C. ^{1}H NMR (400 MHz, $CDCl_3$) δ ppm: 8.04 (d, J = 15.7 Hz, 1H); 7.71 (dd, J = 6.4, 3.1 Hz, 1H); 7.56 (s, 1H); 7.46 (d, J = 8.7 Hz, 2H); 7.43 (d, J = 4.9 Hz, 1H); 7.37 (d, J = 15.7 Hz, 1H); 7.31 (dd, J = 6.1, 3.5 Hz, 2H); 6.96 (d, J = 8.8 Hz, 2H); 3.86 (s, 3H); 2.21 (d, J = 1.2 Hz, 3H). ^{13}C NMR (400 MHz, $CDCl_3$) δ 192.58 (1C, CO); 160.03 (1C, ArC); 139.40 (1C, =C); 138.84 (1C, =C); 136.43 (1C, =C); 135.19 (1C, =C); 133.73 (1C, ArC); 131.68 (2C, ArC); 130.17 (1C, ArC); 130.21 (1C, ArC); 128.44 (1C, ArC); 127.68 (1C, ArC); 127.01 (1C, ArC); 125.02 (1C, ArC); 114.03 (2C, ArC); 55.35 (1C, OCH_3); 13.78 (1C, CH_3). HRMS ESI(+): calcd for $C_{19}H_{17}ClO_2Na$ (M+Na) 335.0917, found 335.0807.

4.2.34 Compound (78):
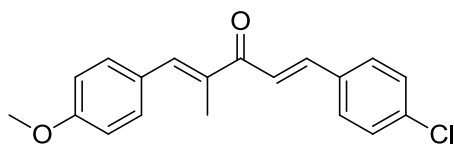
Percent yield: 83. m.p: 98 - 101 °C. ^{1}H NMR (400 MHz, $CDCl_3$) δ ppm: 7.63 (d, J = 15.6 Hz, 1H); 7.57 − 7.52 (m, 3H); 7.46 (d, J = 8.7 Hz, 2H); 7.39 (t, J = 12.1 Hz, 3H); 6.96 (d, J = 8.8 Hz, 2H); 3.86 (s, 3H); 2.20 (d, J

= 1.2 Hz, 3H). ^{13}C NMR (400 MHz, CDCl₃) δ ppm: 192.26 (1C, CO); 160.02 (1C, ArC); 141.53 (1C, =C); 139.00 (1C, =C); 136.58 (1C, =C); 135.90 (1C, =C); 133.73 (1C, ArC); 131.67 (2C, ArC); 129.36 (2C, ArC); 129.15 (2C, ArC); 128.43 (1C, ArC); 122.47 (1C, ArC); 114.03 (2C, ArC); 55.36 (1C, OCH₃); 13.81 (1C, CH₃). HRMS ESI(+): calcd for $C_{19}H_{17}ClO_2Na$ (M+Na) 335.0917, found 335.0805.

4.2.35 Compound (79):
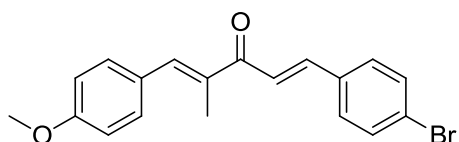
Percent yield: 90. m.p: 97.3 – 99.1 °C. ^{1}H NMR (400 MHz, CDCl₃) δ ppm: 7.61 (d, *J* = 15.6 Hz, 1H); 7.56 – 7.51 (m, 3H); 7.50 – 7.44 (m, 4H); 7.42 (d, *J* = 15.6 Hz, 1H); 6.96 (d, *J* = 8.8 Hz, 2H); 3.86 (s, 3H); 2.20 (d, *J* = 1.2 Hz, 3H). ^{13}C NMR (400 MHz, CDCl₃) δ ppm: 192.39 (1C, CO); 160.13 (1C, ArC); 141.73 (1C, =C); 139.18 (1C, =C); 136.71 (1C, =C); 134.36 (1C, =C); 132.25 (1C, ArC); 131.82 (2C, ArC); 129.73 (2C, ArC); 128.56 (2C, ArC); 124.37 (1C, ArC); 122.71 (1C, ArC); 114.17 (2C, ArC); 55.50 (1C, OCH₃); 13.94 (1C, CH₃). HRMS ESI(+): calcd for $C_{19}H_{17}BrO_2Na$ (M+Na) 379.0412, found 335.0268.

4.2.36 Compound (80):
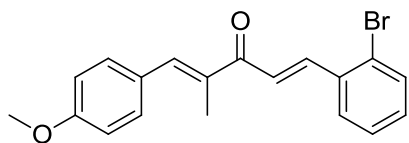
Percent yield: 87. m.p: 101.3 – 101.8 °C. ^{1}H NMR (400 MHz, CDCl₃) δ ppm: 7.77 (s, 1H); 7.62 – 7.54 (m, 2H); 7.51 (d, *J* = 7.2 Hz, 2H); 7.47 (d, *J* = 8.7 Hz, 2H); 7.42 (d, *J* = 15.6 Hz, 1H); 7.29 (d, *J* = 7.9 Hz, 1H); 6.97 (d, *J* = 8.8 Hz, 2H); 3.86 (s, 3H); 2.20 (d, *J* = 1.1 Hz, 3H). ^{13}C NMR (400 MHz, CDCl₃) δ ppm: 192.08 (1C, CO); 160.07 (1C, ArC); 141.17 (1C, =C); 139.26 (1C, =C);

137.46 (1C, =C); 136.51 (1C, =C); 132.78 (1C, ArC); 131.72 (2C, ArC); 130.57 (1C, ArC); 130.39 (1C, ArC); 128.39 (1C, ArC); 127.06 (1C, ArC); 123.30 (1C, ArC); 123.02 (1C, ArC); 114.04 (2C, ArC); 55.36 (1C, OCH$_3$); 13.75 (1C, CH$_3$). HRMS ESI(+): calcd for C$_{19}$H$_{17}$BrO$_2$Na (M+Na) 379.0412, found 335.0277.

4.2.37 Compound (81):
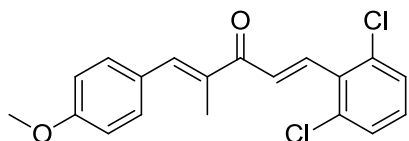
Percent yield: 88. m.p: 86.6 – 88.5 °C. ^{1}H NMR (400 MHz, CDCl$_3$) δ ppm: 7.69 (d, J = 16.1 Hz, 1H); 7.56 (s, 1H); 7.52 (d, J = 16.1 Hz, 1H); 7.46 (d, J = 8.7 Hz, 2H); 7.37 (d, J = 8.1 Hz, 2H); 7.23 – 7.15 (m, 1H); 6.96 (d, J = 8.8 Hz, 2H); 3.85 (s, 3H); 2.22 (d, J = 1.2 Hz, 3H). ^{13}C NMR (400 MHz, CDCl$_3$) δ ppm: 192.31 (1C, CO); 160.09 (1C, ArC); 140.10 (1C, =C); 136.28 (1C, =C); 135.99 (1C, =C); 135.04 (1C, =C); 133.16, (1C, ArC); 131.78 (2C, ArC); 130.76 (1C, ArC); 129.51 (2C, ArC); 128.76 (2C, ArC); 128.40 (1C, ArC); 114.03 (2C, ArC); 55.36 (1C, OCH$_3$); 13.75 (1C, CH$_3$). HRMS ESI(+): calcd for C$_{19}$H$_{16}$Cl$_2$O$_2$Na (M+Na) 369.0527, found 369.0387.

4.2.38 Compound (82):
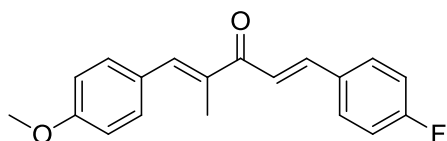
Percent yield: 92. m.p: 100-102 °C. ^{1}H NMR (400 MHz, CDCl$_3$) δ ppm: 7.65 (d, J = 15.7 Hz, 1H); 7.61 (dd, J = 8.7, 5.6 Hz, 2H); 7.54 (s, 1H); 7.46 (d, J = 8.7 Hz, 2H); 7.36 (d, J = 15.6 Hz, 1H); 7.10 (t, J = 8.6 Hz, 2H); 6.96 (d, J = 8.8 Hz, 2H); 3.86 (s, 3H); 2.20 (d, J = 1.2 Hz, 3H). ^{13}C NMR (400 MHz, CDCl$_3$) δ ppm: 192.37 (1C, CO);

166.04 (1C, ArC); 162.55 (1C, ArC); 159.97 (1C, ArC); 141.74 (1C, =C); 138.79 (1C, =C); 136.61 (1C, =C); 131.64 (1C, ArC); 130.09, (1C, ArC); 130.00 (2C, ArC); 128.47 (1C, =C); 121.76 (1C, ArC); 116.12 (1C, ArC); 115.90 (1C, ArC); 114.02 (2C, ArC); 55.36 (1C, OCH$_3$); 13.82 (1C, CH$_3$). HRMS ESI(+): calcd for C$_{19}$H$_{17}$FO$_3$Na (M+Na) 319.1213, found 319.1076;

4.2.39 Compound (83):

Percent yield: 83. m.p: 66.2 – 66.6 °C. ^{1}H NMR (400 MHz, CDCl$_3$) δ ppm: 7.76 (d, J = 15.9 Hz, 1H); 7.61 (td, J = 7.6, 1.5 Hz, 1H); 7.53 (d, J = 15.8 Hz, 2H); 7.45 (d, J = 8.7 Hz, 2H); 7.35 (dd, J = 13.5, 7.3 Hz, 1H); 7.21 – 7.06 (m, 2H); 6.95 (d, J = 8.8 Hz, 2H); 3.85 (s, 3H); 2.20 (d, J = 1.1 Hz, 3H). ^{13}C NMR (400 MHz, CDCl$_3$) δ ppm: 192.74 (1C, CO); 162.99 (1C, ArC); 160.19 (1C, ArC); 139.30 (1C, =C); 136.70 (1C, =C); 135.85 (1C, =C); 131.83 (2C, ArC); 131.41 (1C, ArC); 129.74 (1C, =C); 128.60 (1C, ArC); 124.93 (1C, ArC); 124.58 (1C, ArC); 123.58 (1C, ArC); 116.43 (1C, ArC); 114.15 (2C, ArC); 55.50 (1C, OCH$_3$); 13.92 (1C, CH$_3$). HRMS ESI(+): calcd for C$_{19}$H$_{17}$FO$_3$Na (M+Na) 319.1213, found 319.1071.

4.2.40 Compound (84)

Percent yield: 79. m.p: 119-121 °C. ^{1}H NMR (400 MHz, CDCl$_3$) δ ppm: 8.02 (d, J = 15.7 Hz, 1H); 7.61 (dd, J = 7.9, 1.1 Hz, 1H); 7.55 (s, 1H), 7.51 – 7.42 (m, 3H); 7.35 (d, J = 15.7 Hz, 1H); 7.24 (d, J = 8.0 Hz, 1H); 6.96 (d, J = 8.8 Hz, 2H); 3.86 (s, 3H); 2.21 (d, J = 1.2 Hz, 3H). ^{13}C NMR (400

MHz, CDCl$_3$) δ ppm: 192.42 (1C, CO); 160.26 (1C, ArC); 139.91 (1C, =C); 138.89 (1C, =C); 136.49 (1C, =C); 136.30 (C, ArC); 134.15 (1C, ArC); 131.88 (2C, ArC); 131.34 (1C, =C); 128.47 (1C, ArC); 127.56 (1C, ArC); 127.47 (1C, ArC); 126.27 (1C, ArC); 125.96 (C, ArC); 114.23 (2C, ArC); 55.51 (1C, OCH$_3$); 13.89 (1C, CH$_3$). HRMS ESI(+): calcd for C$_{19}$H$_{16}$Cl$_2$O$_2$Na (M+Na) 369.0527, found 369.0381.

4.2.41 Compound (85):
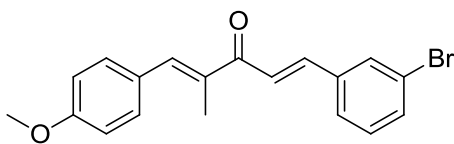
Percent yield: 88. m.p: 77-78 °C. ^{1}H NMR (400 MHz, CDCl$_3$) δ ppm: 7.77 (s, 1H); 7.59 (d, J = 15.7 Hz, 1H); 7.56 – 7.45 (m, 5H); 7.42 (d, J = 15.6 Hz, 1H); 7.29 (d, J = 7.9 Hz, 1H); 6.97 (d,

J = 8.8 Hz, 2H); 3.86 (s, 3H); 2.20 (d, J = 1.1 Hz, 3H). ^{13}C NMR (400 MHz, CDCl$_3$) δ ppm: 192.23 (1C, CO); 160.22 (1C, ArC); 141.32 (1C, =C); 139.41 (1C, =C); 137.61 (1C, =C); 136.66 (C, ArC); 132.93 (1C, ArC); 131.87 (2C, ArC); 130.72 (1C, =C); 128.56 (1C, ArC); 127.21 (1C, ArC); 123.46 (1C, ArC); 123.17 (1C, ArC); 114.19 (2C, ArC); 55.51 (1C, OCH$_3$); 13.90 (1C, CH$_3$). HRMS ESI(+): calcd for C$_{19}$H$_{17}$BrO$_2$Na (M+Na) 379.0412, found 379.0279.

4.2.42 Compound (86):
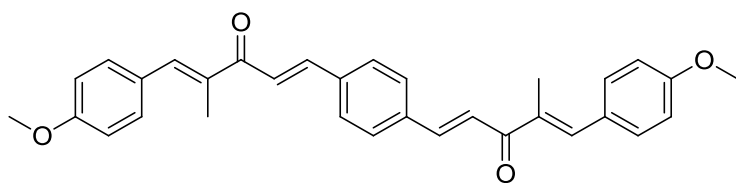
Percent yield: 76. m.p: 160-163 °C. ^{1}H NMR (400 MHz, CDCl$_3$) δ ppm: 7.71–7.63 (m, 6H); 7.57 (s, 2H); 7.51 – 7.44 (m, 6H); 6.97 (d, J = 8.8 Hz, 4H); 3.86 (s, 6H), 2.21 (d, J = 1.1 Hz, 6H). ^{13}C NMR (400 MHz, CDCl$_3$) δ ppm: 192.33 (2C,

CO); 160.02 (2C, ArC); 141.94 (2C, =C); 139.06 (2C, =C); 136.88 (2C, =C); 136.61 (4C, ArC); 131.71 (4C, ArC); 128.69 (2C, ArC); 128.44 (2C, =C); 122.85 (2C, ArC); 114.04 (4C, ArC); 55.37 (2C, OCH$_3$); 13.83 (2C, CH$_3$). HRMS ESI(+): calcd for C$_{32}$H$_{30}$O$_4$Na (M+Na) 501.2144, found 501.2010.

4.2.43 Compound (87):
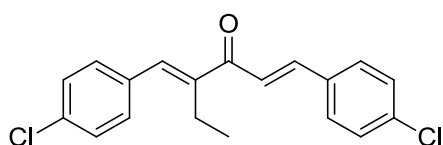
Percent yield: 80. m.p: 96-98 °C. ^{1}H NMR (400 MHz, CDCl$_3$) δ ppm: 7.63 (d, J = 15.7 Hz, 1H); 7.54 (d, J = 8.5 Hz, 2H); 7.42 (s, 1H); 7.39 – 7.29 (m, 7H); 2.64 (q, J = 7.5 Hz, 2H); 1.14 (t, J = 7.5 Hz, 3H). ^{13}C NMR (400 MHz, CDCl$_3$) δ ppm: 192.38 (1C, CO); 145.28 (1C, =C); 142.28 (2C, ArC); 136.75 (2C, ArC); 134.17 (1C, =C); 133.52 (1C,=C); 130.51 (2C, ArC); 129.44 (2C, ArC); 129.21 (2C, ArC); 128.86 (2C, ArC); 122.83 (1C, =C); 20.44 (1C, CH$_2$); 13.51 (1C, CH$_3$). HRMS ESI(+): calcd for C$_{20}$H$_{16}$Cl$_2$ONa (M+Na) 353.0578, found 353.0446.

4.2.44 Compound (88):
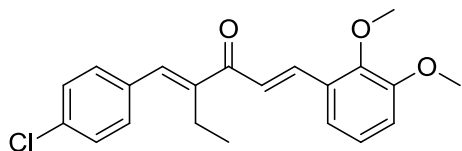
Percent yield: 86. m.p: 105-108°C. ^{1}H NMR (400 MHz, CDCl$_3$) δ ppm: 8.30 (d, J = 8.8 Hz, 2H); 7.71 (d, J = 15.6 Hz, 1H); 7.57 (d, J = 8.9 Hz, 2H); 7.24 (dd, J = 8.4, 1.9 Hz, 1H); 7.18 (d, J = 15.6 Hz, 1H); 7.15 (d, J = 2.0 Hz, 1H); 6.91 (s, 1H); 3.96 (d, J = 3.7 Hz, 6H); 2.67 (q, J = 7.5 Hz, 2H); 1.17 (t, J = 7.5 Hz, 3H). ^{13}C NMR (400 MHz, CDCl$_3$) δ 192.62 (1C, CO); 151.53 (1C, ArC); 149.31 (1C, =C); 147.98 (1C, =C); 144.90 (2C, =C); 142.69 (1C, ArC); 133.76 (1C, ArC); 129.77 (2C, ArC); 127.70 (1C, =C); 123.81 (2C, ArC); 123.15(1C, ArC); 120.31 (1C, ArC); 111.15 (1C, ArC); 110.09 (1C,

ArC); 56.02 (2C, OCH$_3$); 20.91 (1C, CH$_2$); 13.47 (1C, CH$_3$). HRMS ESI(-): calcd for C$_{21}$H$_{20}$ClO$_3$Na (M-H) 355.1179, found 355.1129.

4.2.45 Compound (89):
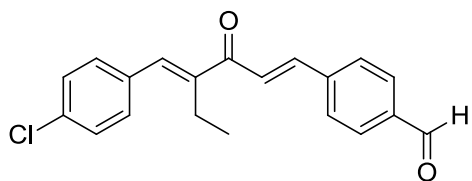
Percent yield: 85. m.p: 111-113°C. ^{1}H NMR (400 MHz, CDCl$_3$) δ ppm: 10.04 (d, J = 0.8 Hz, 1H); 8.05 (d, J = 1.1 Hz, 1H); 7.92 (d, J = 7.7 Hz, 2H); 7.76 (d, J = 8.1 Hz, 2H); 7.70 (d, J = 15.7 Hz, 1H); 7.47 (d, J = 8.9 Hz, 2H); 7.38 (d, J = 8.7 Hz, 3H); 2.65 (q, J = 7.4 Hz, 2H); 1.15 (t, J = 7.4 Hz, 3H). ^{13}C NMR (400 MHz, CDCl$_3$) δ ppm: 191.96 (1C, CO); 191.50 (1C, COH); 145.17 (1C, ArC); 141.80 (1C, =C); 140.78 (1C, =C); 137.43 (1C, =C); 137.13 (1C, ArC); 134.69 (1C, ArC); 134.01 (1C, ArC); 130.55 (2C, ArC); 130.12 (2C, ArC); 128.91 (2C, ArC); 128.70 (2C, ArC); 125.61 (1C, =C); 20.39 (1C, CH$_2$); 13.50 (1C, CH$_3$). HRMS ESI(-): calcd for C$_{20}$H$_{17}$ClO$_2$Na (M+H) 325.0917, found 325.1603.

4.2.46 Compound (90):
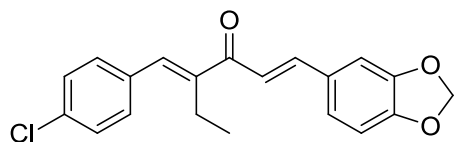
Percent yield: 82. m.p: oil. ^{1}H NMR (400 MHz, CDCl$_3$) δ ppm: 8.28 (d, J = 8.8 Hz, 2H); 7.65 (d, J = 15.7 Hz, 1H); 7.55 (d, J = 8.3 Hz, 2H); 7.44 (s, 1H); 7.39 − 7.35 (m, 1H); 7.00 (dd, J = 6.0, 3.2 Hz, 1H); 6.87 (d, J = 3.3 Hz, 1H); 6.79 − 6.76 (m, 1H); 6.10 (s, 2H), 2.63 (q, J = 7.5 Hz, 2H); 1.14 (t, J = 7.5 Hz, 3H). ^{13}C NMR (400 MHz, CDCl$_3$) δ ppm: 192.70 (1C, CO); 142.80 (1C, ArC); 139.24 (1C, =C); 134.79 (1C, =C); 129.95 (2C, ArC); 129.39 (1C, =C); 128.41 (1C, ArC); 126.53 (1C, ArC); 124.87 (1C, ArC);

123.93 (2C, ArC); 123.45 (1C, ArC); 122.12 (1C, ArC); 118.02 (1C, ArC); 110.21 (1C, =C); 101.65 (1C, ArC); 29.43 (1C, CH$_2$); 20.86 (1C, CH$_2$); 13.65 (1C, CH$_3$). HRMS ESI(+): calcd for C$_{20}$H$_{17}$ClO$_3$Na (M+Na) 363.0866, found 363.0729.

4.2.47 Compound (91):
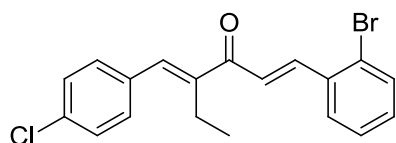
Percent yield: 82. m.p: 108-110 °C. ^{1}H NMR (400 MHz, CDCl$_3$) δ ppm: 8.28 (d, J = 8.8 Hz, 2H); 8.05 (d, J = 15.8 Hz, 1H); 7.70 (dd, J = 7.8, 1.7 Hz, 1H); 7.64 (dd, J = 8.0, 1.1 Hz, 1H); 7.55 (d, J = 8.4 Hz, 2H); 7.43 (s, 1H); 7.40 – 7.32 (m, 1H); 7.30 – 7.22 (m, 1H); 7.19 (d, J = 15.7 Hz, 1H); 2.64 (q, J = 7.5 Hz, 2H); 1.16 (t, J = 7.5 Hz, 3H). ^{13}C NMR (400 MHz, CDCl$_3$) δ ppm: 192.85 (1C, CO); 147.51 (1C, ArC); 143.27 (1C, =C); 142.56 (1C, =C); 135.09 (1C, =C); 133.72 (2C, ArC); 131.55 (1C, ArC); 129.94 (2C, ArC); 127.96 (1C, =C); 127.90 (2C, ArC); 125.97 (1C, ArC); 125.64 (1C, ArC); 123.99 (2C, ArC); 20.97 (1C, CH$_2$); 13.59 (1C, CH$_3$). HRMS ESI(+): calcd for C$_{19}$H$_{16}$ClBrONa (M+Na) 397.0073, found 396.9938.

4.2.50 Compound (92)
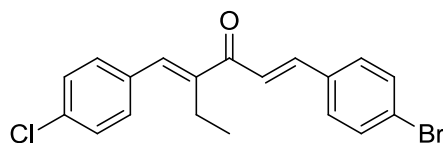
Percent yield: 86. m.p: 134-137 °C. ^{1}H NMR (400 MHz, CDCl$_3$) δ ppm: 8.28 (d, J = 8.8 Hz, 2H); 8.09 (d, J = 8.8 Hz, 1H); 7.66 (d, J = 15.7 Hz, 1H); 7.52 (dd, J = 19.9, 2.0 Hz, 3H); 7.47 – 7.43 (m, 2H); 7.31 (d, J = 15.7 Hz, 1H); 7.21 (d, J = 8.4 Hz, 1H); 2.64 (q, J = 7.5 Hz, 2H); 1.15 (t, J = 7.5 Hz, 3H). ^{13}C NMR (400 MHz, CDCl$_3$) δ ppm: 192.02 (1C, CO); 147.68 (1C, ArC); 144.27 (1C, =C); 143.18 (1C, ArC); 134.74 (1C, =C); 132.26 (2C, ArC);

129.80 (2C, ArC); 129.74 (2C, ArC); 129.19 (1C, A=C); 126.48 (1C, ArC); 123.85 (2C, ArC); 122.63 (1C, =C); 29.26 (1C, CH_2); 20.73 (1C, CH_2); 13.50 (1C, CH_3). HRMS ESI(+): calcd for $C_{19}H_{16}ClBrONa$ (M+Na) 397.0073, found 396.9938.

4.2.51 Compound (93):
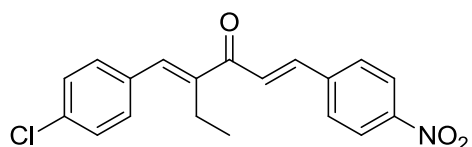
Percent yield: 88. m.p: 156-158 °C. ^{1}H NMR (400 MHz, $CDCl_3$) δ ppm: 8.25 (d, J = 8.8 Hz, 2H); 7.75 (d, J = 8.8 Hz, 2H); 7.69 (d, J = 15.7 Hz, 1H); 7.51 – 7.44 (m, 2H); 7.41 – 7.35 (m, 4H); 2.64 (q, J = 7.5 Hz, 2H); 1.14 (t, J = 7.5 Hz, 3H). ^{13}C NMR (400 MHz, $CDCl_3$) δ ppm: 191.69 (1C, CO); 148.53 (1C, ArC); 145.18 (1C, =C); 141.36 (1C, ArC); 140.59 (1C, =C); 137.94 (1C, ArC); 134.91 (1C, ArC); 134.00 (1C, ArC); 130.68 (2C, A=C); 129.06 (2C, ArC); 128.90 (2C, ArC); 126.19 (1C, =C); 124.269 (2C, ArC); 20.46 (1C, CH_2); 13.59 (1C, CH_3). HRMS ESI(+): calcd for $C_{19}H_{16}ClNO_3Na$ (M+Na) 364.0819, found 364.0689.

4.2.52 Compound (94):
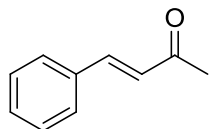
^{1}H NMR (400 MHz, $CDCl_3$) δ 7.49 – 7.43 (m, 2H), 7.34 (dd, J = 5.0, 2.8 Hz, 3H), 6.67 (d, J = 16.3 Hz, 1H), 2.32 (s, 3H). ^{13}C NMR (101 MHz, $CDCl_3$) δ 198.31 (1C), 143.39 (1C), 134.39 (1C), 130.50 (1C), 128.95 (2C), 128.25 (2C), 127.10 (1C), 27.44 (2C).

4.2.53 Compound (95):
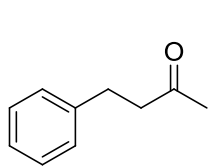
^{1}H NMR (400 MHz, CDCl$_3$) δ 7.29 (dtd, J = 4.2, 2.3, 1.1 Hz, 2H), 7.22 – 7.17 (m, 3H), 2.91 (t, J = 7.5 Hz, 2H), 2.81 – 2.72 (m, 2H), 2.14 (s, 3H). ^{13}C NMR (101 MHz, CDCl$_3$) δ 207.96 (1C), 141.01 (1C), 128.51 (2C), 128.31 (2C), 126.13 (1C), 45.18 (1C), 30.07 (1C), 29.75 (1C).

4.2.54 Compound (96):
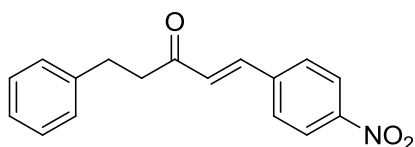
^{1}H NMR (400 MHz, CDCl$_3$) δ 8.24 (d, J = 11.2 Hz, 2H), 7.67 (d, J = 8.7 Hz, 2H), 7.57 (d, J = 16.2 Hz, 1H), 7.35 – 7.20 (m, 5H), 6.85 (d, J = 16.2 Hz, 1H), 3.05 (t, J = 3.4 Hz, 4H). ^{13}C NMR (101 MHz, CDCl$_3$) δ 198.68 (1C), 148.53 (1C), 140.84 (1C), 139.46 (1C), 124.17 (2C), 129.53 (1C), 128.86 (2C), 128.73 (2C), 128.42 (2C), 126.28 (1C), 124.17 (1C), 42.95 (1C), 29.95 (1C).

4.2.55 Compound (97):
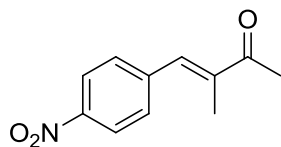
Percent yield: 61 %; Mp: 84-85 °C; ^{1}H NMR (400 MHz, CDCl$_3$) δ 8.27 (d, J=8 Hz, 2H, ArH), 7.55 (d, J=8 Hz, 2H, ArH), 7.52 (s, 1H, =CH), 2.49 (s, 3H, COCH$_3$), 2.06 (d, J=1.6 Hz, 3H, =CCH$_3$); 13C NMR (400 MHz, CDCl$_3$) δ 199.63, 147.30, 142.48, 140.64, 136.48, 130.24, 123.71, 25.99, 13.21; HRMS ESI(+): calcd 206.08117; found 206.08253; UV-vis λmax (nm)[ε (mol^{-1} dm^{3} cm^{-1})] in CH$_2$Cl$_2$: 300.

4.2.56 Compound (98):

^{1}H NMR (400 MHz, CDCl$_3$) δ 7.65 (d, J = 8.3 Hz, 2H), 7.50 (d, J = 8.7 Hz, 3H), 2.46 (s, 3H), 2.03 (d, J = 1.4 Hz, 3H). ^{13}C NMR (101 MHz, CDCl$_3$) δ 199.85 (1C), 139.51 (1C), 137.56 (1C), 129.72 (4C), 128.13(1C),125.32 (1C), 125.32 (1C), 25.80 (1C), 12.90 (1C).

4.2.57 Compound (99):

^{1}H NMR (400 MHz, CDCl$_3$) δ 7.70 (d, J = 7.1 Hz, 2H), 7.56 (t, J = 7.9 Hz, 1H), 7.42 (t, J = 7.7 Hz, 1H), 7.33 (d, J = 7.7 Hz, 1H), 2.44 (s, 3H), 1.82 (s, 3H). ^{13}C NMR (101 MHz, CDCl$_3$) δ 199.90 (1C), 139.99 (1C), 136.17 (1C), 134.64 (1C), 131.62 (1C), 130.35 (1C), 128.13 (1C), 126.00(1C), 125.97 (1C), 122.64 (1C), 25.69 (1C), 12.77 (1C).

4.2.58 Compound (100):

^{1}H NMR (400 MHz, CDCl$_3$) δ 8.28 (d, J = 8.8 Hz, 2H), 7.67 (d, J = 15.6 Hz, 1H), 7.59 (d, J = 8.5 Hz, 2H), 7.56 – 7.51 (m, 3H), 7.48 (d, J = 8.5 Hz, 2H), 7.36 (d, J = 15.6 Hz, 1H), 2.18 (d, J = 1.4 Hz, 3H). ^{13}C NMR (101 MHz, CDCl$_3$) δ 191.81 (1C), 147.29 (1C), 143.17 (1C), 142.45 (1C), 141.46 (1C), 135.52 (1C), 133.71 (1C), 132.24 (2C), 130.27 (2C), 129.75 (2C), 124.85 (1C), 123.75 (2C), 121.84 (1C), 14.08 (1C).

4.2.59 Compound (101):

¹H NMR (400 MHz, CDCl₃) δ 8.31 (d, *J* = 8.8 Hz, 2H), 7.80 (t, *J* = 1.8 Hz, 1H), 7.67 (d, *J* = 15.6 Hz, 1H), 7.64 – 7.60 (m, 2H), 7.58 (s, 1H), 7.57 – 7.51 (m, 2H), 7.39 (d, *J* = 15.6 Hz, 1H), 7.35 – 7.29 (m, 1H), 2.21 (d, *J* = 1.4 Hz, 3H). ¹³C NMR (101 MHz, CDCl₃) δ 191.64 (1C), 147.33 (1C), 142.73 (1C), 142.40 (1C), 141.40 (1C), 136.92 (1C), 135.75 (1C), 133.29 (2C), 130.69 (1C), 130.40 (1C), 130.29 (1C),127.28 (1C), 123.75 (2C), 123.12 (1C), 122.55 (1C), 14.03 (1C).

4.2.60 Compound (102):
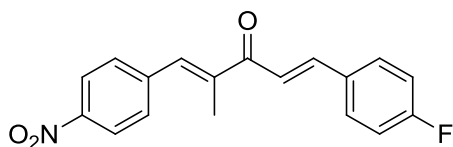
¹H NMR (400 MHz, CDCl₃) δ 8.25 (d, *J* = 8.9 Hz, 2H), 7.69 (d, *J* = 15.6 Hz, 1H), 7.65 – 7.57 (m, 3H), 7.55 (d, *J* = 11.3 Hz, 2H), 7.30 (d, *J* = 15.6 Hz, 1H), 7.09 (t, *J* = 8.6 Hz, 2H), 2.17 (d, *J* = 1.4 Hz, 3H). ¹³C NMR (101 MHz, CDCl₃) δ 191.92 (1C), 165.30 (1C), 162.80 (1C), 147.23 (1C), 143.27 (1C), 142.54 (1C), 141.48 (1C), 135.34 (1C), 130.31 (4C), 130 (1C), 123.72 (1C), 121.08 (1C), 116.26 (1C), 116.04 (1C), 14.09 (1C).

4.2.61 Compound (103):
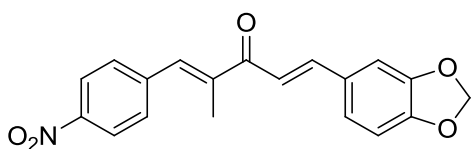
¹H NMR (400 MHz, CDCl₃) δ 8.28 (d, *J* = 8.7 Hz, 2H), 7.59 (ddd, *J* = 23.5, 15.4, 9.2 Hz, 5H), 7.00 (dd, *J* = 5.6, 3.2 Hz, 1H), 6.87 (dd, *J*

= 8.1, 5.5 Hz, 2H), 6.10 (s, 2H), 2.18 (d, J = 1.3 Hz, 3H). ^{13}C NMR (101 MHz, CDCl$_3$) δ 192.37 (1C), 148.02 (1C), 147.23 (1C), 146.64 (1C), 142.69 (1C), 141.58 (1C), 139.10 (1C), 135.36 (1C), 130.26 (2C), 123.97 (1C), 123.70 (2C), 123.35 (1C), 121.99 (1C), 117.92 (1C), 110.06 (1C), 101.52 (1C), 14.05 (1C).

4.2.62 Compound (104):
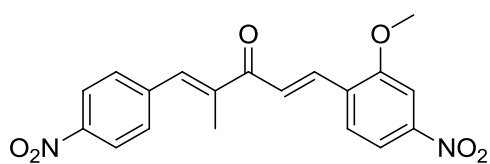
^{1}H NMR (400 MHz, CDCl$_3$) δ 8.26 (d, J = 8.8 Hz, 2H), 7.96 (d, J = 15.9 Hz, 1H), 7.85 (dd, J = 8.4, 1.9 Hz, 1H), 7.77 (d, J = 3.3 Hz, 1H), 7.72 (d, J = 8.5 Hz, 1H), 7.58 (d, J = 8.6 Hz, 2H), 7.52 (d, J = 15.9 Hz, 2H), 4.00 (s, 3H), 2.17 (d, J = 1.3 Hz, 3H). ^{13}C NMR (101 MHz, CDCl$_3$) δ 191.98 (1C), 158.61 (1C), 149.45 (1C), 147.33(1C), 142.35 (1C), 141.35 (1C), 137.24 (1C), 136.03 (1C), 130.25 (2C), 129.09 (1C), 125.58 (1C), 123.75 (2C), 115.87 (1C), 106.29 (1C), 56.30 (1C), 40.95 (1C), 14.01 (1C).

4.2.63 Compound (105):
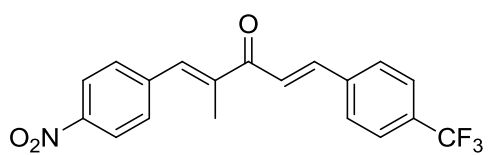
^{1}H NMR (400 MHz, CDCl$_3$) δ 8.28 (d, J = 8.8 Hz, 2H), 7.77 – 7.69 (m, 3H), 7.67 (d, J = 8.4 Hz, 2H), 7.60 (d, J = 8.8 Hz, 2H), 7.58 (s, 1H), 7.45 (d, J = 15.7 Hz, 1H), 2.19 (d, J = 1.4 Hz, 3H). ^{13}C NMR (101 MHz, CDCl$_3$) δ 191.62 (1C), 147.35 (1C), 142.41 (1C), 142.32 (1C), 141.35 (1C), 138.19 (1C), 135.98 (1C), 132.08 (1C), 131.76 (1C), 130.29 (2C), 128.46 (2C), 125.95 (1C), 125.92 (1C), 123.84 (2C), 123.66 (1C), 14.01 (1C).

4.2.64 Compound (106):
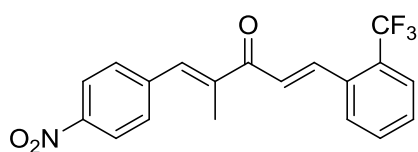
^{1}H NMR (400 MHz, CDCl$_3$) δ 8.28 (d, J = 8.8 Hz, 2H), 7.79 − 7.70 (m, 3H), 7.66 (d, J = 8.4 Hz, 2H), 7.60 (d, J = 8.6 Hz, 2H), 7.57 (s, 1H), 7.44 (d, J = 15.7 Hz, 1H), 2.19 (d, J = 1.4 Hz, 3H). ^{13}C NMR (101 MHz, CDCl$_3$) δ 191.61 (1C), 147.36 (1C), 142.41 (1C), 141.35 (1C), 142.32 (1C), 138.19 (1C), 135.97 (1C), 130.29 (2C), 128.46 (4C), 125.95 (1C), 123.85 (2C), 123.66 (1C), 30.91 (1C), 14.00 (1C).

4.2.65 Compound (107):
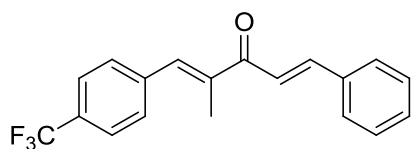
^{1}H NMR (400 MHz, CDCl$_3$) δ 7.74 (d, J = 15.7 Hz, 1H), 7.68 (d, J = 8.3 Hz, 2H), 7.65 − 7.61 (m, 2H), 7.55 (d, J = 8.7 Hz, 3H), 7.41 (dt, J = 13.5, 6.1 Hz, 4H), 2.18 (d, J = 1.4 Hz, 3H). ^{13}C NMR (101 MHz, CDCl$_3$) δ 192.39 (1C), 144.16 (1C), 140.38 (1C), 139.59 (1C), 136.47 (1C), 134.94 (1C), 130.45 (2C), 129.78 (2C), 128.97 (3C), 128.35 (2C), 125.41 (1C), 125.39 (1C), 121.61 (1C), 13.91 (1C).

4.2.66 Compound (108):
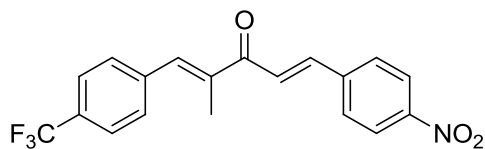
^{1}H NMR (400 MHz, CDCl$_3$) δ 8.24 (s, 2H), 7.76 (d, J = 11.4 Hz, 2H), 7.69 (d, J = 10.1 Hz, 2H), 7.65 − 7.48 (m, 4H), 2.18 (s, 3H). ^{13}C NMR (101 MHz, CDCl$_3$) δ 191.45 (1C), 148.48 (1C), 141.14 (1C), 140.85 (1C), 140.15 (1C), 139.20 (1C), 137.66 (1C),

129.83 (2C), 128.84 (2C), 126.00 (1C) , 125.51 (1C), 125.47 (1C), 124.90 (2C), 124.20 (2C), 13.76 (1C).

4.2.67 Compound (109):
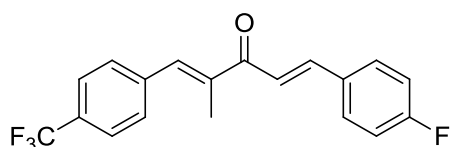
^{1}H NMR (400 MHz, CDCl$_3$) δ 7.69 (d, J = 12.3 Hz, 1H), 7.66 (d, J = 4.9 Hz, 2H), 7.59 (dd, J = 8.6, 5.4 Hz, 2H), 7.57 – 7.49 (m, 3H), 7.33 (d, J = 15.6 Hz, 1H), 7.07 (t, J = 8.6 Hz, 2H), 2.16 (d, J = 1.3 Hz, 3H). ^{13}C NMR (101 MHz, CDCl$_3$) δ 192.13 (1C), 165.23 (1C), 162.73 (1C), 142.82 (2C), 140.30 (1C), 139.54 (1C), 136.55 (2C), 130.24 (1C), 129.79 (2C), 125.37 (1C), 125 (1C), 121.25 (1C), 116.17 (2C), 115.95 (1C), 13.83 (1C).

4.2.68 Compound (110):
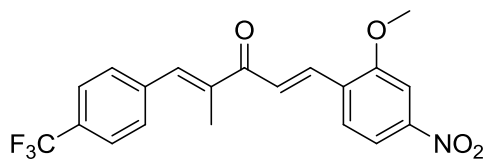
^{1}H NMR (400 MHz, CDCl$_3$) δ 7.95 (d, J = 15.9 Hz, 1H), 7.83 (d, J = 8.4 Hz, 1H), 7.75 (s, 1H), 7.72 (d, J = 8.5 Hz, 1H), 7.67 (d, J = 8.0 Hz, 2H), 7.61 – 7.49 (m, 4H), 4.00 (s, 3H), 2.16 (s, 3H). ^{13}C NMR (101 MHz, CDCl$_3$) δ 192.14 (1C), 158.55 (1C), 149.35 (1C), 140.22 (1C), 139.40 (1C), 137.28 (1C), 136.72 (1C), 130.39 (4C), 129.82 (1C), 128.96 (1C), 125.82 (1C), 125.81 (1C), 125.01 (1C), 115.83 (1C), 106.22 (1C), 56.24 (1C), 13.78 (1C).

4.2.69 Compound (111):
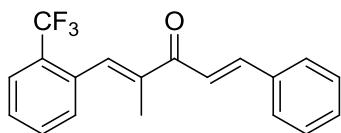
^{1}H NMR (400 MHz, CDCl$_3$) δ 7.78 – 7.72 (m, 3H), 7.64 – 7.60 (m, 2H), 7.58 (d, *J* = 7.6 Hz, 1H), 7.46 (d, *J* = 7.7 Hz, 1H), 7.43 – 7.38 (m, 4H), 7.35 (d, *J* = 15.8 Hz, 1H), 1.99 (d, *J* = 1.3 Hz, 3H). ^{13}C NMR (101 MHz, CDCl$_3$) δ 192.94 (1C), 144.33 (1C), 140.74 (1C), 134.85 (1C), 131.70 (1C), 130.47 (1C), 130.43 (1C), 128.97 (2C), 128.72 (3C), 128.25 (1C), 128.11 (1), 127.72 (1C), 126.047 (1C), 126.02 (1C), 121.86 (1C), 13.79 (1C).

4.2.70 Compound (112):
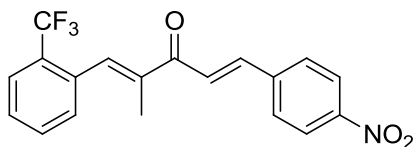
^{1}H NMR (400 MHz, CDCl$_3$) δ 8.26 (d, *J* = 8.7 Hz, 2H), 7.79 – 7.68 (m, 5H), 7.61 (t, *J* = 7.6 Hz, 1H), 7.48 (d, *J* = 7.7 Hz, 1H), 7.46 – 7.36 (m, 2H), 1.97 (d, *J* = 1.2 Hz, 3H). ^{13}C NMR (101 MHz, CDCl$_3$) δ 192.02 (1C), 148.49 (1C), 141.03 (1C), 140.54 (1C), 140 (1C), 135.98 (1C), 134.35 (1C), 131.77 (1C), 130.36 (1C), 128.80 (2C), 128.37 (1C), 126.82 (1C), 126.11 (1C), 125.53 (1C), 122.72 (2C), 122.72 (1C), 13.63 (1C).

4.2.71 Compound (113):
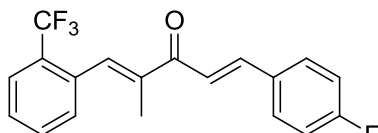
^{1}H NMR (400 MHz, CDCl$_3$) δ 7.73 (t, *J* = 12.1 Hz, 3H), 7.60 (dt, *J* = 7.5, 5.4 Hz, 3H), 7.48 – 7.39 (m, 2H), 7.27 (d, *J* = 15.7 Hz, 1H), 7.10 (t, *J* = 8.6 Hz, 2H), 1.99 (d, *J* = 1.2 Hz, 3H). ^{13}C NMR (101 MHz, CDCl$_3$) δ 192.73 (1C), 165.23 (1C), 162.73 (1C), 143.00 (1C), 140.68 (1C), 134.79 (1C),131.70 (1C),

131.18 (1C),130.70 (1C), 130.44 (1C), 130.25 (1C), 130.16 (1C), 128.12 (1C), 126.12 (1C), 126.03 (1C), 121.54 (1C), 116.18 (1C), 115.96 (1C), 13.73 (1C).

4.2.72 Compound (114):
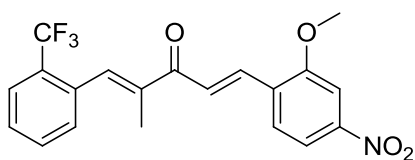
^{1}H NMR (400 MHz, CDCl$_3$) δ 7.92 (d, J = 16.0 Hz, 1H), 7.87 (dd, J = 8.5, 2.1 Hz, 1H), 7.78 (d, J = 2.1 Hz, 1H), 7.74 (d, J = 7.8 Hz, 2H), 7.70 (d, J = 8.5 Hz, 1H), 7.63 – 7.56 (m, 2H), 7.47 (t, J = 7.7 Hz, 1H), 7.40 (d, J = 7.7 Hz, 1H), 4.02 (s, 3H), 1.98 (d, J = 1.3 Hz, 3H). ^{1}H NMR (400 MHz, CDCl$_3$) δ 7.92 (d, J = 16.0 Hz, 1H), 7.87 (dd, J = 8.5, 2.1 Hz, 1H), 7.78 (d, J = 2.1 Hz, 1H), 7.74 (d, J = 7.8 Hz, 2H), 7.70 (d, J = 8.5 Hz, 1H), 7.63 – 7.56 (m, 2H), 7.47 (t, J = 7.7 Hz, 1H), 7.40 (d, J = 7.7 Hz, 1H), 4.02 (s, 3H), 1.98 (d, J = 1.3 Hz, 3H).

4.2.73 Compound (115):
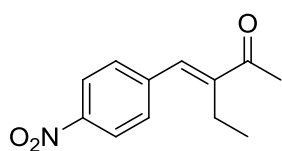
^{1}H NMR (400 MHz, CDCl$_3$) δ 8.24 (d, J = 8.9 Hz, 2H), 7.52 (d, J = 8.4 Hz, 2H), 7.45 (s, 1H), 2.47 (q, J = 7.5 Hz, 4H), 2.46 (s, 3H), 1.07 (t, J = 7.5 Hz, 3H). ^{13}C NMR (101 MHz, CDCl$_3$) δ 199.85 (1C), 144.51 (1C), 137.88 (1C), 134.50 (1C), 134.18 (1C), 130.49 (2C), 128.82 (2C), 26.15 (1C), 19.60 (1C), 13.69 (1C).

4.2.74 Compound (116):
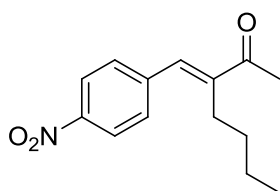
^{1}H NMR (400 MHz, CDCl$_3$) δ 8.12 (d, J = 8.4 Hz, 2H), 7.45 (d, J = 8.5 Hz, 2H), 7.41 (s, 1H), 2.35 (dd, J = 8.9, 6.9 Hz, 5H), 1.26 (ddt, J = 33.1, 14.1, 6.7 Hz, 4H), 0.74 (td, J = 7.1, 3.3 Hz, 3H). ^{13}C NMR (101 MHz, CDCl$_3$) δ 199.55 (1C), 147.10 (1C), 145.51 (1C), 142.53 (1C), 136.26 (1C), 129.79 (2C), 123.55 (2C), 31.14 (1C), 26.17 (1C), 26.07 (1C), 22.77 (1C), 13.63 (1C).

4.2.75 Compound (117):

Percent yield: 92 %; Mp: 100-101 °C; ^{1}H NMR (400 MHz, CDCl$_3$) δ 8.28 (d, J=8 Hz, 2H, ArH), 7.73 (d, J=16 Hz, 2H, ArH), 7.62 (m, 2H, ArH), 7.58 (d, J=12 Hz, 2H, =CH), 7.55 (s, 1H, CH$_3$C=CH), 7.42 (m, 3H, ArH), 7.36 (d, J=16 Hz, 2H, =CH), 2.19 (d, J=4 Hz, 3H, =CCH$_3$); ^{13}C NMR (400 MHz, CDCl$_3$) δ 14.13 (1C, =CCH3); 121.40 (1C, =C); 123.73 (2C, ArC); 128.40 (2C, ArC); 129.00 (2C, ArC); 130.25 (2C, ArC); 130.61 (1C, ArC); 134.79 (1C, =C); 135.25 (1C, =C); 141.55 (1C, ArC); 142.58 (1C, =C); 144.64 (1C, ArC); 147.25 (1C,ArC); 192.16 (1C, CO); HRMS ESI(+): calcd 294.11247; found 294.11339; UV-vis λmax (nm)[ε (mol^{-1} dm^3 cm^{-1})] in CH$_2$Cl$_2$: 308.

4.2.76 Compound (118):

Percent yield: 65 %; Mp: 188-189 °C; ^{1}H NMR (400 MHz, CDCl$_3$) δ 8.31 (t, J=0 Hz, J=4 Hz, 1H, ArH), 8.29 (t, J=0 Hz, J=4 Hz, 2H, ArH),

8.23 (t, *J*=0 Hz, *J*=4 Hz, 1H, ArH), 7.74 (m, 3H, ArH and CH_3-C=CH), 7.60 (d, *J*=8 Hz, 3H, =CH and ArH), 7.49 (d, *J*=16 Hz, 1H, =CH), 2.21 (d, *J*=1.6 Hz, 3H, =CCH$_3$); ^{13}C NMR (400 MHz, CDCl$_3$) δ 191.20, 148.58, 147.44, 142.13, 141.31, 141.27, 140.95, 136.40, 130.31, 128.90, 125.01, 124.25, 123.81, 13.98; HRMS ESI(+): calcd 339.09955; found 339.09955. UV-vis λmax (nm)[ε (mol^{-1} dm^3 cm^{-1})] in CH$_2$Cl$_2$:304.

4.2.77 Compound (119):
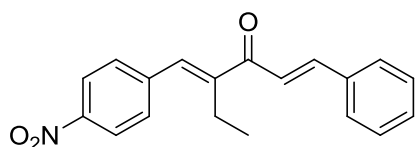
^{1}H NMR (400 MHz, CDCl$_3$) δ 8.25 (d, *J* = 8.8 Hz, 2H), 7.73 (d, *J* = 15.7 Hz, 1H), 7.62 (dd, *J* = 6.6, 2.9 Hz, 2H), 7.55 (d, *J* = 8.7 Hz, 2H), 7.47 − 7.34 (m, 5H), 2.65 (q, *J* = 7.5 Hz, 2H), 1.16 (t, *J* = 7.5 Hz, 3H). ^{13}C NMR (101 MHz, CDCl$_3$) δ 192.32 (1C), 147.65 (1C), 147.23 (1C), 144.52 (1C), 142.57 (1C), 134.60 (1C), 131.03 (1C),130.59 (1C), 129.85 (2C), 128.99 (2C), 128.42 (2C), 123.77 (2C), 122.22 (1C), 20.76 (1C), 13.52 (1C).

4.2.78 Compound (120):
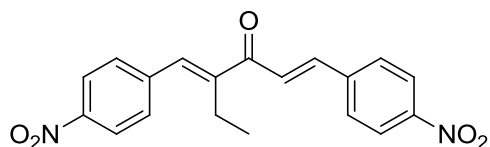
^{1}H NMR (400 MHz, CDCl$_3$) δ 8.33 − 8.24 (m, 4H), 7.75 (t, *J* = 12.1 Hz, 3H), 7.57 (d, *J* = 8.6 Hz, 2H), 7.53 − 7.41 (m, 2H), 2.65 (q, *J* = 7.5 Hz, 2H), 1.16 (t, *J* = 7.5 Hz, 3H). ^{13}C NMR (101 MHz, CDCl$_3$) δ 191.33 (1C), 148.58 (1C), 147.45 (1C), 142.09 (1C), 141.27 (1C), 140.94 (1C), 135.73 (1C),

129.84 (2C), 129.31 (1C), 128.89 (2C), 125.71 (1C), 124.24 (2C), 123.90 (2C), 20.64 (1C), 13.52 (1C).

4.2.79 Compound (121):
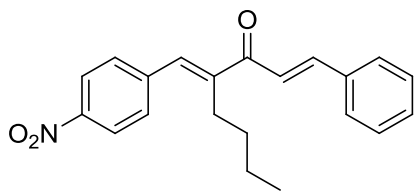
^{1}H NMR (400 MHz, CDCl$_3$) δ 8.27 (d, J = 8.8 Hz, 2H), 7.72 (d, J = 15.7 Hz, 1H), 7.62 (dd, J = 6.5, 3.0 Hz, 2H), 7.54 (d, J = 8.5 Hz, 2H), 7.42 (dd, J = 6.1, 2.6 Hz, 4H), 7.30 (d, J = 15.7 Hz, 1H), 2.67 – 2.55 (m, 2H), 1.55 – 1.43 (m, 2H), 1.37 (dq, J = 14.5, 7.1 Hz, 2H), 0.90 (t, J = 7.2 Hz, 3H). ^{13}C NMR (101 MHz, CDCl$_3$) δ 192.71 (1C), 147.24 (1C), 146.80 (1C), 144.67 (1C), 142.66 (1C), 134.76 (1C), 134.48 (1C), 130.62 (1C), 129.81 (2C), 129.00 (2C), 128.41 (2C), 123.80 (2C), 122.31 (1C), 31.06 (1C), 27.19 (1C), 22.90 (1C), 13.82 (1C).

4.2.80 Compound (122):
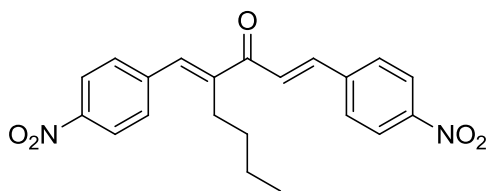
^{1}H NMR (400 MHz, CDCl$_3$) δ 8.33 – 8.23 (m, 4H), 7.81 – 7.70 (m, 3H), 7.56 (d, J = 8.7 Hz, 2H), 7.51 – 7.39 (m, 2H), 2.68 – 2.54 (m, 2H), 1.55 – 1.42 (m, 2H), 1.43 – 1.31 (m, 2H), 0.91 (t, J = 7.2 Hz, 3H). ^{13}C NMR (101 MHz, CDCl$_3$) δ 191.60 (1C), 148.59 (1C), 147.44 (1C), 146.51 (1C), 142.19 (1C), 141.30 (1C), 140.93 (1C), 135.75 (1C), 129.83 (2C), 128.89 (2C), 125.78 (1C), 124.24 (2C), 123.88 (2C), 31.08 (1C), 27.10 (1C), 22.89 (1C), 13.80 (1C).

4.2.81 Compound (123):
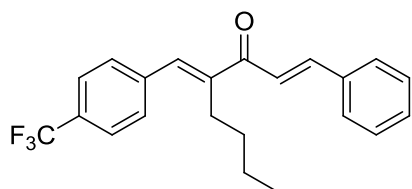
^{1}H NMR (400 MHz, CDCl$_3$) δ 8.02 (d, J = 7.8 Hz, 2H), 7.63 (d, J = 15.7 Hz, 1H), 7.57 (d, J = 8.1 Hz, 2H), 7.41 − 7.35 (m, 4H), 7.30 (dd, J = 5.0, 1.8 Hz, 2H), 7.26 (d, J = 2.2 Hz, 2H), 2.56 − 2.44 (m, 2H), 1.38 (dd, J = 16.7, 6.7 Hz, 2H), 1.31 − 1.22 (m, 2H), 0.81 (t, J = 7.3 Hz, 3H).

4.2.82 Compound (124):
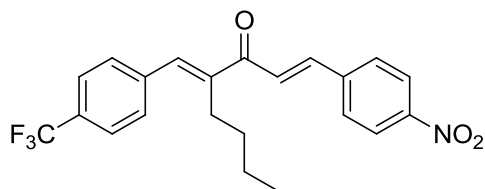
^{1}H NMR (400 MHz, CDCl$_3$) δ 8.27 (d, J = 8.8 Hz, 2H), 7.79 − 7.65 (m, 5H), 7.51 (d, J = 8.8 Hz, 3H), 7.45 (d, J = 15.7 Hz, 1H), 2.68 − 2.56 (m, 2H), 1.55 − 1.44 (m, 2H), 1.41 − 1.33 (m, 2H), 0.91 (t, J = 7.2 Hz, 3H). ^{13}C NMR (101 MHz, CDCl$_3$) δ 191.81 (1C), 148.51 (1C), 145.43 (1C), 140.99 (1C), 140.82 (1C), 140.68 (2C), 139.16 (1C), 137.03 (1C), 129.33 (2C), 128.84 (2C), 126.01 (1C), 125.57 (1C), 125.56 (1C), 124.22 (2C), 31.13 (1C), 26.95 (1C), 22.91 (1C), 13.82 (1C).

4.2.83 Compound (125):
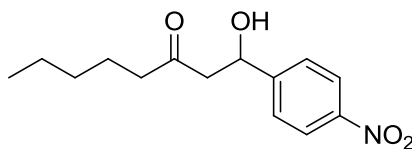
^{1}H NMR (400 MHz, CDCl$_3$) δ 8.12 (d, J = 8.8 Hz, 2H), 7.50 (d, J = 6.9 Hz, 2H), 5.28 − 5.17 (m, 1H), 3.69 (s, 1H), 2.84 − 2.76 (m, 2H), 2.41 (t, J = 7.4 Hz, 2H), 1.61 − 1.44 (m, 2H), 1.31 − 1.12 (m, 4H), 0.83 (t, J = 7.0 Hz, 3H). ^{13}C NMR (101 MHz, CDCl$_3$) δ 210.97 (1C), 150.57

(1C), 147.13 (1C), 126.45 (2C), 123.61 (2C), 68.96 (1C), 50.61 (1C), 43.57 (1C), 31.18 (1C), 23.13 (1C), 22.33 (1C), 13.81 (1C).

4.2.84 Compound (126):
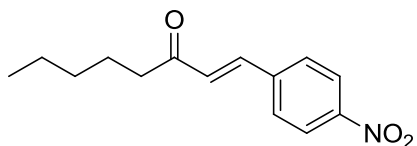
^{1}H NMR (400 MHz, CDCl$_3$) δ 8.16 (d, J = 8.8 Hz, 2H), 7.65 (d, J = 8.6 Hz, 2H), 7.51 (d, J = 16.2 Hz, 1H), 6.80 (d, J = 16.2 Hz, 1H), 2.66 − 2.59 (m, 2H), 1.62 (dd, J = 14.8, 7.4 Hz, 2H), 1.29 − 1.22 (m, 4H), 0.82 (t, J = 7.1 Hz, 3H). ^{13}C NMR (101 MHz, CDCl$_3$) δ 199.79 (1C), 148.37 (1C), 140.90 (1C), 138.97 (1C), 129.58 (1C), 128.76 (2C), 124.05 (2C), 41.35 (1C), 31.35 (1C), 23.71 (1C), 22.42 (1C), 13.87 (1C).

4.2.85 Compound (127):
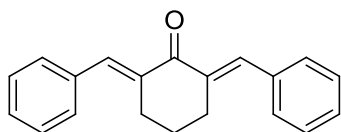
Percent yield: 86 %; Mp: 118-119 °C; ^{1}H NMR (400 MHz, CDCl$_3$) δ 7.82 (s, 1H), 7.47 (d, J = 7.4 Hz, 2H), 7.44 - 7.37 (m, 2H), 7.37 - 7.31 (m, 1H), 2.94 (td, J = 6.6, 2.0 Hz, 2H), 1.86 - 1.73 (m, 1H); ^{13}C NMR (400 MHz, CDCl$_3$) δ 190.5, 137.0, 136.3, 136.1, 130.5, 128.7, 128.5, 28.6, 23.1; HRMS-ESI(+): calcd 275.1430; found 275.1432; UV-Visλmax (nm) in CH$_3$OH: 320.

4.2.86 Compound (128):
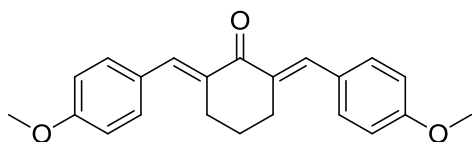
Percent yield: 87 %; Mp: 70-73 °C; ^{1}H NMR (400 MHz, CDCl$_3$) δ 7.52 (s, 1H), 7.42 (d, J = 8.8 Hz, 2H), 6.94 (d, J = 8.8 Hz, 2H), 3.86 (s, 3H), 2.87 (td, J = 6.4, 2.0 Hz, 2H), 2.55 (t, J = 6.7 Hz, 2H), 1.94 (dt, J = 13.0, 6.6 Hz, 2H), 1.84 – 1.75 (m, 2H); ^{13}C NMR (400 MHz, CDCl$_3$) δ 201.5, 159.9, 135.8, 134.4, 132.3, 128.3, 113.9, 55.3, 40.2, 28.9, 23.9, 23.3; HRMS- ESI(+): calcd 217.1223; found 217.1222; UV-Visλmax (nm) in CH$_3$OH: 316.

4.2.87 Compound (129):
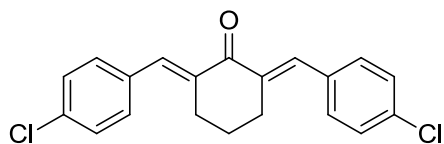
^{1}H NMR (400 MHz, CDCl$_3$) δ 7.64 (t, *J* = 1.7 Hz, 2H), 7.34 – 7.26 (m, 8H), 2.84 – 2.74 (m, 4H), 1.79 – 1.66 (m, 2H). ^{13}C NMR (400 MHz, CDCl$_3$) δ 189.85, 136.42, 135.78, 134.62, 134.31, 131.60, 128.69, 28.38, 22.81.

4.2.88 Compound (130):
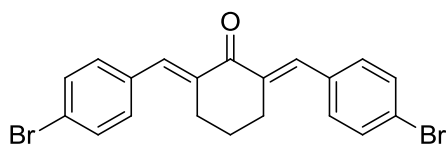
^{1}H NMR (400 MHz, CDCl$_3$) δ 7.72 (s, 2H), 7.55 (d, *J* = 8.5 Hz, 4H), 7.34 (d, *J* = 8.4 Hz, 4H), 2.98 – 2.83 (m, 4H), 1.87 – 1.76 (m, 2H). ^{13}C NMR (400 MHz, CDCl$_3$) δ 189.88, 136.53, 135.85, 134.74, 131.81, 131.66, 122.96, 28.38, 22.80.

4.2.89 Compound (131):

^{1}H NMR (400 MHz, CDCl$_3$) δ 7.63 – 7.52 (m, 2H), 7.47 – 7.37 (m, 3H), 7.37 – 7.30 (m, 1H), 3.06 – 2.89 (m, 12H), 2.71 – 2.58 (m, 1H), 2.38 – 2.30 (m, 1H), 1.84 – 1.63 (m, 2H).

4.2.90 Compound (132):

^{1}H NMR (400 MHz, CDCl$_3$) δ 7.43 (d, J = 8.6 Hz, 2H), 7.36 – 7.17 (m, 1H), 6.87 (d, J = 15.3 Hz, 2H), 3.77 (s, 3H), 2.95 – 2.80 (m, 2H), 2.32 (dd, J = 10.4, 5.2 Hz, 2H), 1.96 (dt, J = 15.1, 5.9 Hz, 2H). ^{13}C NMR (101 MHz, CDCl$_3$) δ 207.99 (1C), 160.49 (1C), 133.63 (1C), 132.24 (2C), 132.08 (1C), 128.14 (1C), 114.17 (1C), 55.34 (1C), 37.65 (1C), 29.40 (1C), 20.05 (1C).

4.2.91 Compound (133):

^{1}H NMR (400 MHz, CDCl$_3$) δ 8.24 (d, J = 8.8 Hz, 2H), 7.65 (d, J = 8.7 Hz, 2H), 7.37 (t, J = 2.8 Hz, 1H), 3.00 (td, J = 7.2, 2.8 Hz, 2H), 2.44 (t, J = 7.9 Hz, 2H), 2.08 (p, J = 7.6 Hz, 2H). ^{13}C NMR (101 MHz, CDCl$_3$) δ 207.35 (1C), 147.52 (1C), 141.94 (1C), 139.90 (1C), 130.80 (2C), 129.29 (1C), 123.87 (2C), 37.67 (1C), 29.41 (1C), 20.06 (1C).

4.2.92 Compound (134):

^{1}H NMR (400 MHz, CDCl$_3$) δ 8.18 (d, J = 8.8 Hz, 2H), 7.52 (d, J = 8.4 Hz, 2H), 5.41 (d, J = 2.8 Hz, 1H), 2.42 (ddd, J = 19.5, 15.7, 8.8 Hz, 2H), 2.10 – 1.96 (m, 2H), 1.76 – 1.68 (m, 2H). ^{13}C NMR (101 MHz, CDCl$_3$) δ 219.72 (1C), 150.44 (1C), 127.37 (1C), 126.37 (2C), 123.59 (2C), 70.37 (1C), 56.08 (1C), 38.98 (1C), 22.34 (1C), 20.35 (1C).

4.2.93 Compound (135):
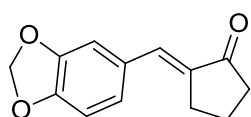
^{1}H NMR (400 MHz, CDCl$_3$) δ 7.29 (t, J = 2.4 Hz, 1H), 7.09 – 6.99 (m, 2H), 6.84 (d, J = 8.0 Hz, 1H), 6.00 (s, 2H), 2.92 (td, J = 7.2, 2.6 Hz, 2H), 2.38 (t, J = 7.9 Hz, 2H), 2.07 – 1.96 (m, 2H). ^{13}C NMR (101 MHz, CDCl$_3$) δ 208.15 (1C), 148.75 (1C), 148.07 (1C), 134.11 (1C), 132.42 (1C), 129.88 (1C), 126.47 (1C), 109.62 (1C), 108.69 (1C), 101.58 (1C), 37.75 (1C), 29.32 (1C), 20.15 (1C).

4.2.94 Compound (136):
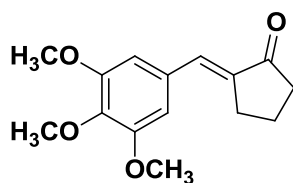
^{1}H NMR (400 MHz, CDCl$_3$) δ 7.43 (t, J = 2.7 Hz, 1H), 6.91 (s, 2H), 4.02 (s, 9H), 3.12 (td, J = 7.2, 2.7 Hz, 2H), 2.53 (t, J = 7.9 Hz, 2H), 2.18 (p, J = 7.6 Hz, 2H). ^{13}C NMR (101 MHz, CDCl$_3$) δ 207.79 (1C), 153.16 (2C), 139.36 (1C), 135.10 (1C), 132.46 (1C), 131.02 (1C), 107.84 (2C), 60.90 (1C), 56.10 (2C), 37.67 (1C), 29.22 (1C), 20.11 (1C).

4.2.95 Compound (137):
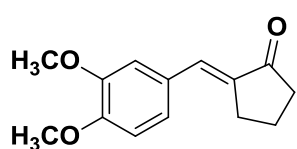
^{1}H NMR (400 MHz, CDCl$_3$) δ 7.24 (t, *J* = 2.6 Hz, 1H), 7.07 (dd, *J* = 8.4, 1.9 Hz, 1H), 6.99 (d, *J* = 1.9 Hz, 1H), 6.83 (d, *J* = 8.4 Hz, 1H), 3.84 (s, 3H), 3.83 (s, 3H), 2.88 (td, *J* = 7.2, 2.6 Hz, 2H), 2.31 (t, *J* = 7.9 Hz, 2H), 1.96 (p, *J* = 7.6 Hz, 2H). ^{13}C NMR (101 MHz, CDCl$_3$) δ 207.64 (1C), 150.10 (1C), 148.72 (1C), 133.74 (1C), 132.22 (1C), 128.37 (1C), 124.26 (1C), 113.07 (1C), 111.00 (1C), 55.78(1C), 55.74 (1C), 37.54 (1C), 29.09 (1C), 19.97 (1C).

4.2.96 Compound (138):
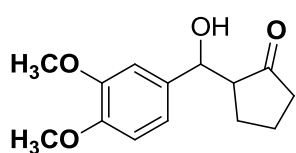
^{1}H NMR (400 MHz, CDCl$_3$) δ 6.95 (d, *J* = 1.7 Hz, 1H), 6.91 − 6.81 (m, 2H), 4.67 (d, *J* = 9.1 Hz, 1H), 3.91 (s, 3H), 3.89 (s, 3H), 2.50 − 2.39 (m, 2H), 2.27 (ddd, *J* = 19.4, 9.7, 5.9 Hz, 1H), 2.06 − 1.93 (m, 1H), 1.84 − 1.68 (m, 2H), 1.58 − 1.46 (m, 1H). ^{13}C NMR (101 MHz, CDCl$_3$) δ 180.17 (1C), 149.15 (1C), 148.78 (1C), 134.15 (1C), 119.02 (1C), 110.78 (1C), 109.36 (1C), 75.07 (1C), 55.89 (2C), 55.43 (1C), 38.79 (1C), 27.05 (1C), 20.41 (1C).

4.2.97 Compound (139):
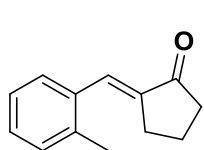
^{1}H NMR (400 MHz, CDCl$_3$) δ 7.61 (t, *J* = 2.7 Hz, 1H), 7.43 (dd, *J* = 7.4, 1.9 Hz, 1H), 7.30 − 7.16 (m, 3H), 2.89 (td, *J* = 7.2, 2.7 Hz, 2H), 2.50 − 2.33 (m, 5H), 1.99 (p, *J* = 7.5 Hz, 2H). ^{13}C

NMR (101 MHz, CDCl$_3$) δ 207.86 (1C), 138.86 (1C), 136.84 (1C), 134.31 (1C), 130.54 (1C), 129.76 (1C), 129.15 (1C), 128.65 (1C), 125.80 (1C), 38.03 (1C), 29.39 (1C), 20.49 (1C), 19.98 (1C).

4.2.98 Compound (140):
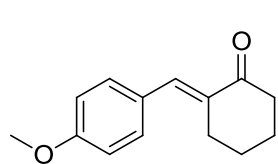
^{1}H NMR (400 MHz, CDCl$_3$) δ 7.50 (s, 1H), 7.40 (d, J = 8.8 Hz, 2H), 6.92 (d, J = 8.8 Hz, 2H), 3.84 (s, 3H), 2.84 (td, J = 6.4, 2.0 Hz, 2H), 2.52 (t, J = 6.7 Hz, 2H), 1.92 (dt, J = 13.0, 6.6 Hz, 2H), 1.84 – 1.73 (m, 2H). ^{13}C NMR (101 MHz, CDCl$_3$) δ 201.46 (1c), 159.94 (1c), 135.77 (1c), 134.39 (1c), 132.24 (2c), 128.24 (1c), 113.86 (2c), 55.27 (1c), 40.11 (1c), 28.95 (1c), 23.81 (1c), 23.23 (1c).

4.2.99 Compound (141):
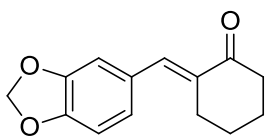
^{1}H NMR (400 MHz, CDCl$_3$) δ 6.82 (t, J = 4.9 Hz, 1H), 6.78 – 6.69 (m, 2H), 5.92 (s, 2H), 5.26 (d, J = 2.5 Hz, 1H), 2.60 – 2.49 (m, 1H), 2.47 – 2.28 (m, 2H), 2.12 – 1.99 (m, 1H), 1.92 – 1.75 (m, 2H), 1.75 – 1.60 (m, 2H), 1.60 – 1.47 (m, 1H). ^{13}C NMR (101 MHz, CDCl$_3$) δ 214.62 (1C), 147.52 (1C), 146.38 (1C), 135.70 (1C), 118.85 (1C), 107.94 (1C), 106.60 (1C), 100.90 (1C), 70.43 (1C), 57.31 (1C), 42.60 (1C), 27.89 (1C), 26.13 (1C), 24.81 (1C).

4.2.100 Compound (142):
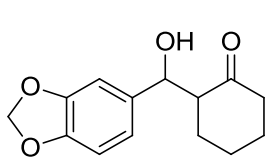
¹H NMR (400 MHz, CDCl₃) δ 6.82 (t, *J* = 4.9 Hz, 1H), 6.78 – 6.69 (m, 2H), 5.92 (s, 2H), 5.26 (d, *J* = 2.5 Hz, 1H), 2.60 – 2.49 (m, 1H), 2.47 – 2.28 (m, 2H), 2.12 – 1.99 (m, 1H), 1.92 – 1.75 (m, 2H), 1.75 – 1.60 (m, 2H), 1.60 – 1.47 (m, 1H). ¹³C NMR (101 MHz, CDCl₃) δ 214.62 (1C), 147.52 (1C), 146.38 (1C), 135.70 (1C), 118.85 (1C), 107.94 (1C), 106.60 (1C), 100.90 (1C), 70.43 (1C), 57.31 (1C), 42.60 (1C), 27.89 (1C), 26.13 (1C), 24.81 (1C).

4.2.101 Compound (143):
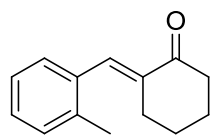
¹H NMR (400 MHz, CDCl₃) δ 7.55 (s, 1H), 7.30 – 7.10 (m, 4H), 2.72 – 2.63 (m, 2H), 2.56 (t, *J* = 6.7 Hz, 2H), 2.30 (s, 3H), 1.94 (dt, *J* = 13.1, 6.6 Hz, 2H), 1.78 – 1.67 (m, 2H). ¹³C NMR (101 MHz, CDCl₃) δ 202.01 (1C), 137.74 (1C), 137.45 (1C), 134.71 (1C), 134.07 (1C), 130.15 (1C), 128.98 (1C), 128.36 (1C), 125.36 (1C), 40.56 (1C), 28.79 (1C), 24.10 (1C), 23.72 (1C), 19.97 (1C).

4.2.102 Compound (144):
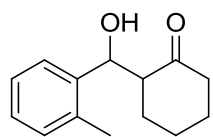
¹H NMR (400 MHz, CDCl₃) δ 7.50 (d, *J* = 8.4 Hz, 1H), 7.19 (dqd, *J* = 12.7, 7.5, 1.6 Hz, 4H), 5.61 (d, *J* = 2.1 Hz, 1H), 2.59 – 2.32 (m, 4H), 2.26 (s, 3H), 2.16 – 2.01 (m, 1H), 1.91 – 1.78 (m, 3H), 1.76 – 1.61 (m, 2H), 1.58 – 1.42 (m, 1H). ¹³C NMR (101 MHz, CDCl₃) δ 214.63 (1C), 139.48 (1C), 133.42 (1C), 130.22 (1C), 126.85 (1C), 126.63 (1C),

125.73 (1C), 67.22 (1C), 54.54 (1C), 42.64 (1C), 27.87 (1C), 26.18 (1C), 24.91 (1C), 19.03 (1C).

4.2.103 Compound (145):
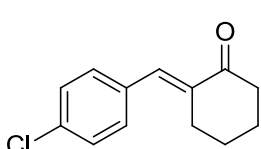
^{1}H NMR (400 MHz, CDCl$_3$) δ 7.72 (s, 1H), 7.38 (d, J = 1.1 Hz, 4H), 2.95 − 2.80 (m, 2H), 1.85 − 1.74 (m, 1H), 1.44 − 1.21 (m, 3H), 0.97 − 0.76 (m, 2H). ^{13}C NMR (101 MHz, CDCl$_3$) δ 189.85 (1C), 136.42 (1C), 135.78 (1C), 134.62 (1C), 134.31 (1C), 131.59 (2C), 128.69 (2C), 29.71 (1C), 28.38 (2C), 22.81 (1C).

4.2.104 Compound (146):
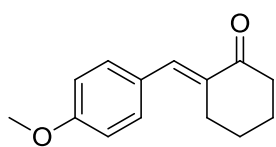
Percent yield: 87 %; Mp: 70-73 °C; ^{1}H NMR (400 MHz, CDCl$_3$) δ 7.52 (s, 1H), 7.42 (d, J = 8.8 Hz, 2H), 6.94 (d, J = 8.8 Hz, 2H), 3.86 (s, 3H), 2.87 (td, J = 6.4, 2.0 Hz, 2H), 2.55 (t, J = 6.7 Hz, 2H), 1.94 (dt, J = 13.0, 6.6 Hz, 2H), 1.84 − 1.75 (m, 2H); ^{13}C NMR (400 MHz, CDCl$_3$) δ 201.5, 159.9, 135.8, 134.4, 132.3, 128.3, 113.9, 55.3, 40.2, 28.9, 23.9, 23.3; HRMS- ESI(+): calcd 217.1223; found 217.1222; UV-Visλmax (nm) in CH$_3$OH: 316.

4.2.105 Compound (147):
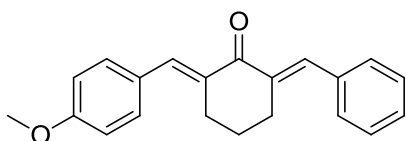
Percent yield: 85 %; Mp: 103-104 °C; ^{1}H NMR (400 MHz, CDCl$_3$) δ 7.81 (d, J = 7.8 Hz, 2H), 7.48 (d, J =

8.8 Hz, 4H), 7.42 (dd, J = 7.3, 5.8 Hz, 2H), 7.38 - 7.32 (m, 1H), 6.96 (d, J = 8.8 Hz, 2H), 3.86 (s, 3H), 3.00 - 2.87 (m, 4H), 1.87 - 1.75 (m, 2H); ^{13}C NMR (400 MHz, CDCl$_3$) δ 190.7, 160.5, 137.4, 136.9, 136,8, 134.6, 132.8, 132.7, 130.8, 129.1, 128.9, 128.8, 114.4, 55.8, 29.0, 28.8, 23.5; HRMS-ESI(+): calcd 305.1536; found 305.1534; UV-Visλmax (nm) in CH$_3$OH: 341.

4.2.106 Compound (148):
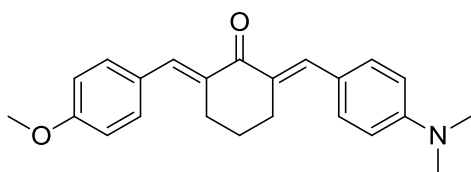
Percent yield: 82 %; Mp: 164-168 °C;^{1}H NMR (400 MHz, CDCl$_3$) δ 7.82 - 7.68 (m, 5H), 7.52 - 7.39 (m, 10H), 6.93 (d, J = 8.8 Hz, 6H), 6.81 (s, 4H), 3.84 (s, 8H), 3.03 (s, 12H), 2.97 - 2.87 (m, 10H), 1.87 - 1.74 (m, 5H);); ^{13}C NMR (400 MHz, CDCl$_3$) δ 189.9, 159.6, 137.6, 137.5, 136.5, 135.9, 134.7, 134.4, 132.6, 132.3, 132.2, 128.9, 113.9, 55.3, 28.7, 28.5, 23.0; HRMS- ESI(+): calcd348.1958; found 348.1960; UV-Visλmax (nm) in CH$_3$OH: 347.

4.2.107 Compound (149):
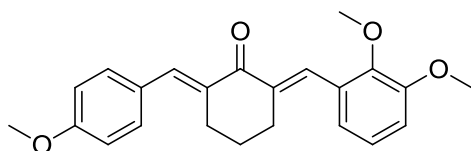
Percent yield: 80 %; Mp: 126-127 °C; ^{1}H NMR (400 MHz, CDCl$_3$) δ 7.94 (s, 1H), 7.80 (s, 1H), 7.48 (d, J = 8.7 Hz, 2H), 7.08 (t, J = 8.0 Hz, 1H), 6.99 - 6.90 (m, 4H), 3.90 (s, 3H), 3.87 (s, 3H), 3.84 (s, 3H), 2.94 (dd, J = 8.6, 3.7 Hz, 2H), 2.85 - 2.76 (m, 2H), 1.85 - 1.71 (m, 2H); ^{13}C NMR (400 MHz, CDCl$_3$) δ 190.4, 160.1, 153.0, 148.4, 137.8, 137.3, 134.4, 132.5, 132.1, 130.7, 128.9, 123.6, 122.3, 114.0, 112.8,

61.2, 56.0, 55.5, 28.9, 28.6, 23.3; HRMS-ESI(+): calcd 365.1746; found 365.1747; UV-Visλmax (nm) in CH$_3$OH: 341.

4.2.108 Compound (150):
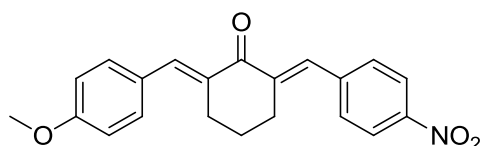
Percent yield: 89 %; Mp: 193-196 °C; ^{1}H NMR (400 MHz, CDCl$_3$) δ 8.25 (d, J = 8.7 Hz, 6H), 7.79 (s, 3H), 7.77 (s, 3H), 7.57 (d, J = 8.7 Hz, 6H), 7.47 (d, J = 8.7 Hz, 6H), 6.95 (d, J = 8.7 Hz, 7H), 3.85 (s, 9H), 2.99 - 2.93 (m, 6H), 2.93 - 2.86 (m, 6H), 1.83 (dt, J = 12.4, 6.3 Hz, 7H); ^{13}C NMR (400 MHz, CDCl$_3$) δ 189.7, 160.3, 147.1, 142.7, 139.5, 138.2, 133.5, 132.5, 130.7, 128.4, 123.6, 114.0, 55.4, 28.5, 28.4, 22.8; HRMS-ESI(+): calcd 350.1387; found 350.1388; UV-Visλmax (nm) in CH$_3$OH: 339.

4.2.109 Compound (151):
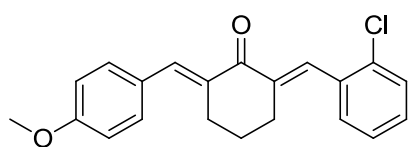
Percent yield: 80 %; Mp: 120-121 °C; $_1$H NMR (400 MHz, CDCl$_3$) δ 7.90 (s, 1H), 7.82 (s, 1H), 7.48 (d, J = 11.5 Hz, 2H), 7.45 (dd, J = 5.3, 3.9 Hz, 1H), 7.36 - 7.32 (m, 1H), 7.31 - 7.25 (m, 2H), 6.96 (d, J = 8.8 Hz, 2H), 3.87 (s, 3H), 2.95 (t, J = 6.3 Hz, 2H), 2.77 (t, J = 6.1 Hz, 2H), 1.86 – 1.76 (m, 2H); ^{13}C NMR (400 MHz, CDCl$_3$) δ 189.9, 160.0, 138.1, 137.6, 134.9, 134.6, 133.9, 133.1, 132.4, 130.5, 129.7, 129.3, 128.6, 126.2, 113.9, 55.3, 28.7, 28.1, 23.1; HRMS-ESI(+): calcd 339.1146; found 339.1148; UV-Visλmax (nm) in CH$_3$OH: 351.

4.2.110 Compound (152):
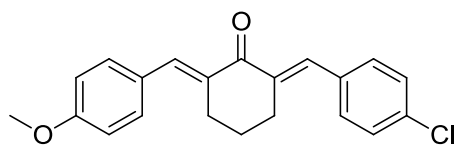
Percent yield: 86 %; Mp: 146-149 °C; ^{1}H NMR (400 MHz, CDCl$_3$) δ 7.77 (t, J = 1.9 Hz, 1H), 7.72 (t, J = 2.1 Hz, 1H), 7.46 (d, J = 8.7 Hz, 2H), 7.37 (dd, J = 5.3, 2.3 Hz, 4H), 6.94 (d, J = 8.8 Hz, 2H), 3.85 (s, 3H), 2.96 - 2.90 (m, 2H), 2.90 - 2.85 (m, 2H), 1.86 - 1.75 (m, 2H); ^{13}C NMR (400 MHz, CDCl$_3$) δ 190.1, 160.1, 137.3, 136.8, 135.1, 134.5, 134.4, 133.9, 132.4, 131.5, 128.6, 113.9, 55.4, 28.5, 28.4, 22.9; HRMS-ESI(+): calcd 339.1146; found 339.1141 ; UV-Visλmax (nm)in CH$_3$OH: 351.

4.2.111 Compound (153):
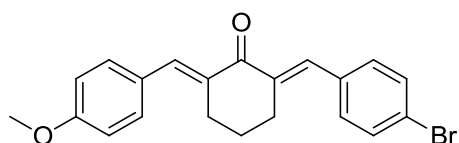
Percent yield: 82 %; Mp: 156-158 °C; ^{1}H NMR (400 MHz, CDCl$_3$) δ 7.77 (s, 1H), 7.69 (s, 1H), 7.52 (d, J = 8.5 Hz, 2H), 7.46 (d, J = 8.7 Hz, 2H), 7.31 (d, J = 8.4 Hz, 2H), 6.94 (d, J = 8.8 Hz, 2H), 3.84 (s, 3H), 2.92 (t, J = 6.1 Hz, 2H), 2.89 - 2.82 (m, 2H), 1.84 - 1.76 (m, 2H); ^{13}C NMR (400 MHz, CDCl$_3$) δ 190.1, 160.2, 137.5, 137.0, 135.2, 135.1, 134.0, 132.5, 131.9, 131.7, 128.7, 122.8, 114.1, 55.5, 28.7, 28.5, 23.0; HRMS-ESI(+): calcd 383.0641; found 383.0640; UV-Visλmax (nm) in CH$_3$OH: 344.

4.2.112 Compound (154):
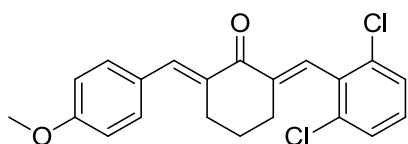
Percent yield: 88 %; Mp: 88-93 °C; ^{1}H NMR (400 MHz, CDCl$_3$) δ 7.75 (s, 1H), 7.47 (s, 1H), 7.40 (d, J = 8.7 Hz, 2H), 7.34 - 7.24 (m, 3H), 7.15 - 7.10 (m, 1H), 6.87 (d, J = 8.9 Hz, 2H), 3.78 (s, 3H), 2.86 (td, J = 6.4, 2.0 Hz, 2H), 2.44 - 2.27 (m, 2H), 1.71 (dt, J = 12.5, 6.3 Hz, 2H); ^{13}C NMR (400 MHz, CDCl$_3$) δ 189.1, 160.2, 140.5, 138.1, 134.5, 134.5, 133.8, 132.5, 130.9, 129.9, 129.2, 128.9, 128.6, 127.9, 113.9, 55.4, 28.8, 28.0, 22.5; HRMS-ESI(+): calcd 373.0757; found 373.0759; UV-Visλmax (nm) in CH$_3$OH: 355.

4.2.113 Compound (155):
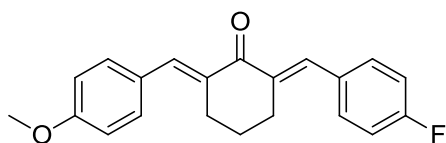
Percent yield: 94%; Mp: 124-125 °C; ^{1}H NMR (400 MHz, CDCl$_3$) δ 7.77 (s, 1H), 7.74 (s, 1H), 7.50 - 7.40 (m, 4H), 7.09 (t, J = 8.7 Hz, 2H), 6.94 (d, J = 8.8 Hz, 2H), 3.85 (s, 3H), 2.96 - 2.91 (m, 2H), 2.91 - 2.85 (m, 2H), 1.89 - 1.72 (m, 2H); ^{13}C NMR (400 MHz, CDCl$_3$) δ 190.3, 163.9, 160.2, 137.3, 136.2, 135.5, 134.2, 132.5, 132.4, 132.3, 128.8, 115.7, 115.5, 114.1, 55.5, 28.7, 28.5, 23.1; HRMS-ESI(+): calcd 323.1442; found 323.1439; UV-Visλmax (nm) in CH$_3$OH: 343.

4.2.114 Compound (156):
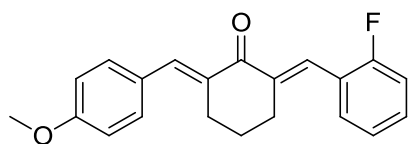
Percent yield: 80 %; Mp: 115-116 °C; ^{1}H NMR (400 MHz, CDCl$_3$) δ 7.81 (s, 1H), 7.78 (s, 1H), 7.46 (d, J = 8.8 Hz, 2H), 7.40 - 7.28 (m, 2H), 7.13 (dt, J = 17.4, 8.0 Hz, 2H), 6.94 (d, J = 8.8 Hz, 2H), 3.85 (s, 3H), 2.93 (t, J = 5.3 Hz, 2H), 2.82 - 2.75 (m, 2H), 1.83 - 1.74 (m, 2H); ^{13}C NMR (400 MHz, CDCl$_3$) δ 189.9, 162.2, 160.2, 138.7, 137.6, 134.1, 132.5, 130.9, 130.4, 130.3, 129.1, 128.8, 123.9, 115.9, 115.8, 114.1, 55.5, 28.9, 28.5, 23.1; HRMS-ESI(+): calcd 323.1442; found 323.1440; UV-Visλmax (nm) in CH$_3$OH: 348.

4.2.115 Compound (157):
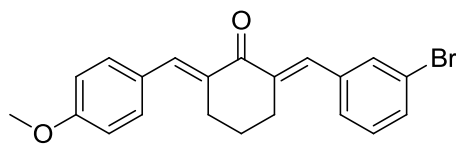
Percent yield: 81 %; Mp: 123-124 °C; ^{1}H NMR (400 MHz, CDCl$_3$) δ 7.80 (t, J = 2.0 Hz, 1H), 7.71 (t, J = 2.0 Hz, 1H), 7.61 (t, J = 1.7 Hz, 1H), 7.48 (dd, J = 8.6, 2.8 Hz, 3H), 7.38 (d, J = 7.8 Hz, 1H), 7.30 (d, J = 7.8 Hz, 1H), 6.97 (d, J = 8.8 Hz, 2H), 2.98 - 2.93 (m, 2H), 2.93 - 2.88 (m, 2H), 1.90 - 1.76 (m, 2H); ^{13}C NMR (400 MHz, CDCl$_3$) δ 190.1, 160.3, 138.3, 137.7, 137.6, 134.8, 134.0, 132.9, 132.5, 131.4, 130.0, 128.9, 128.7, 122.6, 114.1, 55.5, 28.7, 28.4, 23.1; HRMS-ESI(+): calcd 383.0641; found 383.0643; UV-Visλmax (nm) in CH$_3$OH: 341.

❖ 5

Conclusion and Perspectives

Part 1

5.1 Conclusion

We concluded that among synthetic newly designed unsymmetrical curcuminoids analogues many compounds were found more potent for epimastigote, trypomastigote form of *T. cruzi* than benznidazole. More specifically compounds having para nitro group were found more active. The nitro group make the double bonds inside curcuminoids analogus more reactive for nucleophile attack, so it is the medium of attack for potential cellular nucleophile like glutatione and trypanothione. The results showed that the compounds were more toxic against the parasites than Vero cells. Accordingly DFT and *in silico* studies were performed to recognize best conformers and the binding mode of these compounds. The structures of all compounds were confirmed by different spectroscopic techniques such as ^{1}H NMR, ^{13}C NMR and ESI-HRMS.

5.2 Perspective

- The enzyme target for potent compounds should be studied.
- The potent compound should be farwarded for clinical trials.
- More fruitfull modification should include in order getting more large and potent library for chagas disease.

Part 2

Chemoselective Green Biocatalytic Hydrogenation of α, β-Unsaturated Curcuminoids Analogues by Endophytic Fungus *Penicillium brasilianum.*

6 Chemoselective Green Biocatalytic Hydrogenation of α, β-Unsaturated Curcuminoids Analogues by Endo-Phytic Fungus *Penicillium brasilianum.*

6.1 Abstract

Selective asymmetric trans-bioreduction of C=C bond of curcuminoids were achieved by using whole cells of *Penicillium brasilianum* isolated from root bark of *Melia azedarch*. Different curcuminoids (**1-8**) analogues having different reductive moieties were evaluated and the result of biotransformation was compared with that of synthetic reduction. In this study different nitro substituted curcuminoids analogues were tested in order to see the diversity of biocatalyst. The whole cell of *Penicillium brasilianum* biocatalysed the substrate and chemo selectively reduces double bonds, while synthetic reducing agent Pd/C on H_2 reduces double bonds along with nitro groups present in compounds (**4-8**). This methodology selectively hydrogenates olefin functionalities without hydrogenolysis of aromatic carbonyls and nitro groups.

6.2 Introduction

In the last decades, biocatalysis has been the subject of extensive research due to its efficient and environmentally friendly methodology for the production of compounds with potential application to medical and industrial sectors (BARROS-FILHO et al., 2010). Bio catalysis of synthetic compounds is a powerful tool to produce natural products analogous combining biology and chemistry (GOSS; SHANKAR; FAYAD, 2012). The most extensively employed synthetic steps is the asymmetric reduction of activated C=C bonds

due to the generation of stereogenic centers (STUERMER et al., 2007). Therefore, biocatalytic reduction of activated alkenes to produce asymmetrical synthons is useful tool in either improving established synthetic pathways or creating novel methods (TOOGOOD; GARDINER; SCRUTTON, 2010).

Different enoate reductase from bacterial cell (HIRATA et al., 2009), (MATSUDA; YAMANAKA; NAKAMURA, 2009), plant cells (MATSUSHIMA et al., 2008), algal cells (SHIMODA; HIRATA, 2000) and fungal cell (KAWAI et al., 1996) has been used for the reduction of C=C bonds in α,β- unsaturated corbonylic system. *Nascimento et al and* André Porto *et al* used fungal whole cell to catalyze the reduction of double bonds in α, β-unsaturated corbonylic system (CÉSAR A. SCHAEFER, VANESSA D. SILVA, 2013). Pentaerythritol tetranitrate reductase from *Enterobacter cloacae* catalyze the asymmetric bioreduction of the C=C bond of α,β-unsaturated nitroalkenes (nitro in this case is activating group) (TOOGOOD et al., 2008). These enzymes contain $FMNH_2$, which play central role in reduction by providing hydride ion to α,β-unsaturated system (SCHEME 6.1), such FMN containing enzyme is also called old yellow enzyme (OYE). Asymmetric bio reduction by OYEs proceed in a step-wise manner with a mechanism similar to Michael-type conjugate addition of hydride to activated alkenes (RICHARD E. WILLIAMS AND NEIL C.BRUCE, 2002).
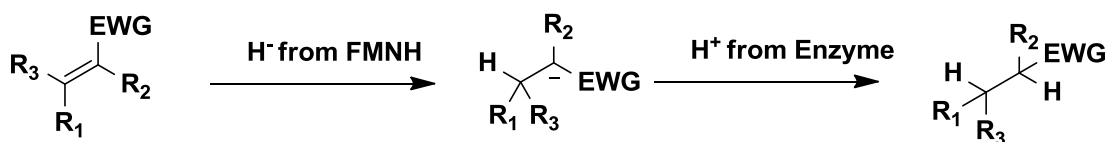
Scheme 6.1- Mechanistic reduction of C=C bond by OYE.

Literature survey suggest that isolated enzymes often lead to higher enantiomeric excesses (e.e.) (YANTO et al., 2011) because they avoid problems associated with competing catalysts of different stereo selective nature. Reduced cofactors must be regenerated *in situ* in a catalytic cycle or provide in stoichiometric amounts to maintain the catalytic activity. Mostly the co-factor is very expensive and sensitive against environmental factors. Thus, the use of whole living microbial cells is attractive because of their great diversity and its ability to be put to practical use (ISHIGE; HONDA; SHIMIZU, 2005). Whole microbial cell biocatalysis do not require the addition of exogenous cofactors because of their own cofactor regeneration systems.

Different researchers have reported the reduction of double bonds activated by electron withdrawing groups by using whole fungal cell. However we did not find any article of bio catalyzing the unsymmetrical curcuminoids analogues by *Penicillium* species. So we evaluated *Penicillium brasilianum* whole cell for its ability to biocatalyse chemo selectively C=C bonds, when other reactive moieties is present for reduction too. For this task we used **8** different di-α,β- unsaturated curcuminoids analogues having different *para* substitution on aromatic ring. Biocatalyst selectively reduces C=C bond, while synthetic reducing agent Pd/C on H_2 reduces C=C bond along with nitro groups. *Penicillium brasilianum* whole cell is crucial chemo selective biocatalyst to be applied for the reduction of double bonds in diverse system.

❖ 7

Objectives – Part 2

Objective

✓ The addition of interesting chemistry in natural products analogues.

✓ The study of whole cell fungal reactions.

✓ Isolation of biotransformed products.

✓ The exploration of enzymatic action of fungi for potencial modifications in functional groups.

❖ 8

Results and discussion –

Part 2

8 Results and discussion

8.1 Catalytic assymetrical reduction of curcuminoids 1-8.

The *P. brasilianum* is an unexplored source for fungal whole cells biotransformations. Our group has studied the oxidative potential of this fungi in bioconversions of 1-indanone for different enzymatic reactions (FILL et al., 2012). *P. brasilianum* is the most studied fungus in our group and many biologically important natural products has been isolated from it so. Researcher from Japan has also reported many important natural products produced by *P. brasilianum* (FUJITA et al., 2002). It is considered as enzyme factory due to its ability in the production of variety of natural products and its bio catalytic potential (PANAGIOTOU; OLAVARRIA; OLSSON, 2007). The ability of *P. brasilianum* to chemo selectively reduce double bonds were investigated by feeding different curcuminoids analogs having different substitution on aromatic rings. In the earlier investigation the biotransformation potential of *P. brasilianum* against curcuminoids analogous having no substitution (compound **1**), or having only one methoxy substitution on ring A or B (compounds **2** and **3**) were carried. The reduction of double bonds of these compounds (**1-3**) were successfully achieved and yielded compounds **1b-3b** and **3d**). In compound **3** the selective one bond reduction was also obtained (SCHEME 8.1).
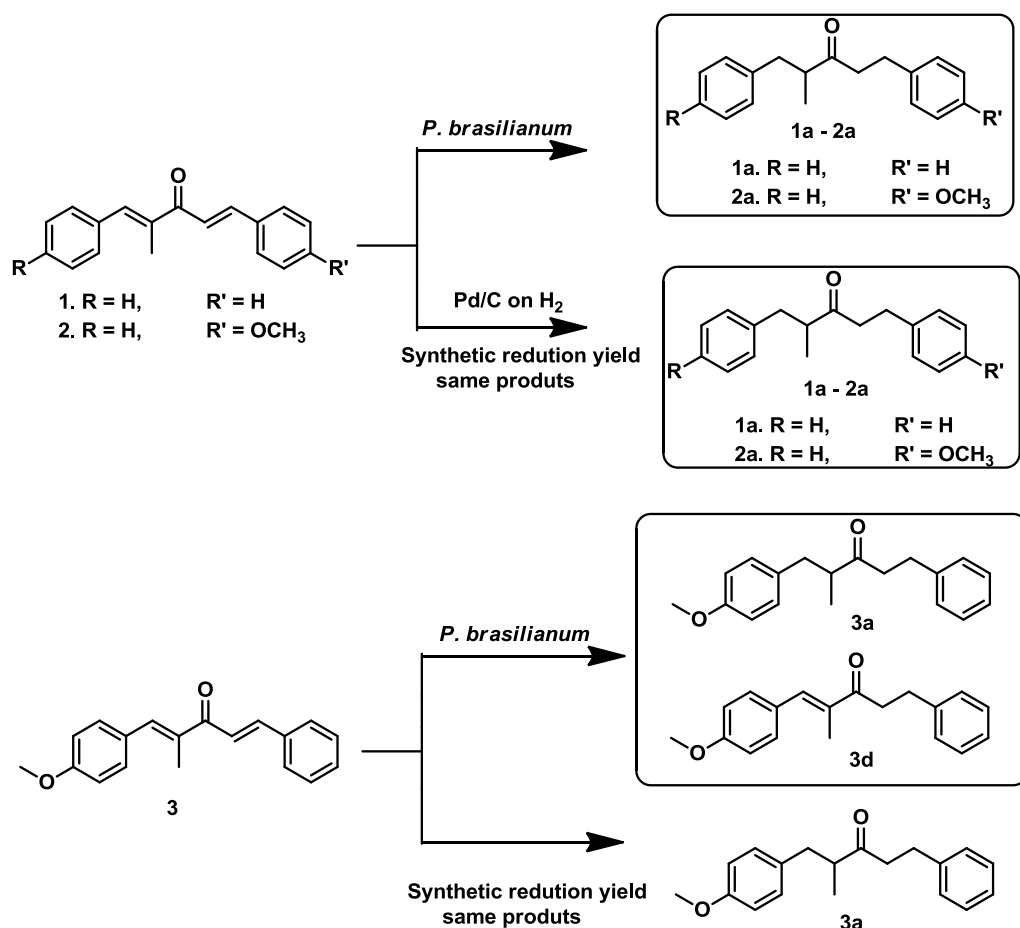
Scheme 8.1 - The reduction of compounds **1-3** by synthetic catalyst and biocatalytically by *Penicillium brasilianum.*

After these result we administered other curcuminoids moieties having more reductive groups on *para* position to see the selectivity of *P. brasilianum* for the reduction of activated C=C bonds (compounds **4-8**). After administrating and incubation, the curcuminoids analogs **4-8** was biotransformed to compounds **4a-8a** presented (SCHEME 8.2). All biotransformation products were isolated and purified, and their structure was established on the basis of ^{1}H NMR, ^{13}C NMR, HRMS. Simultaneously compounds **1-8** were also reduced by Pd/C on H$_2$ to see the difference between

biocatalytic and synthetic reduction. It was confirmed that synthetic reducing agent (H_2 on Pd/C) reduces both double bond along with nitro groups and yields compounds **4b-8b**. The synthetic reduced products was also isolated and purified through column chromatography, and their structure was established based on ^1H NMR, ^{13}C NMR, HRMS.
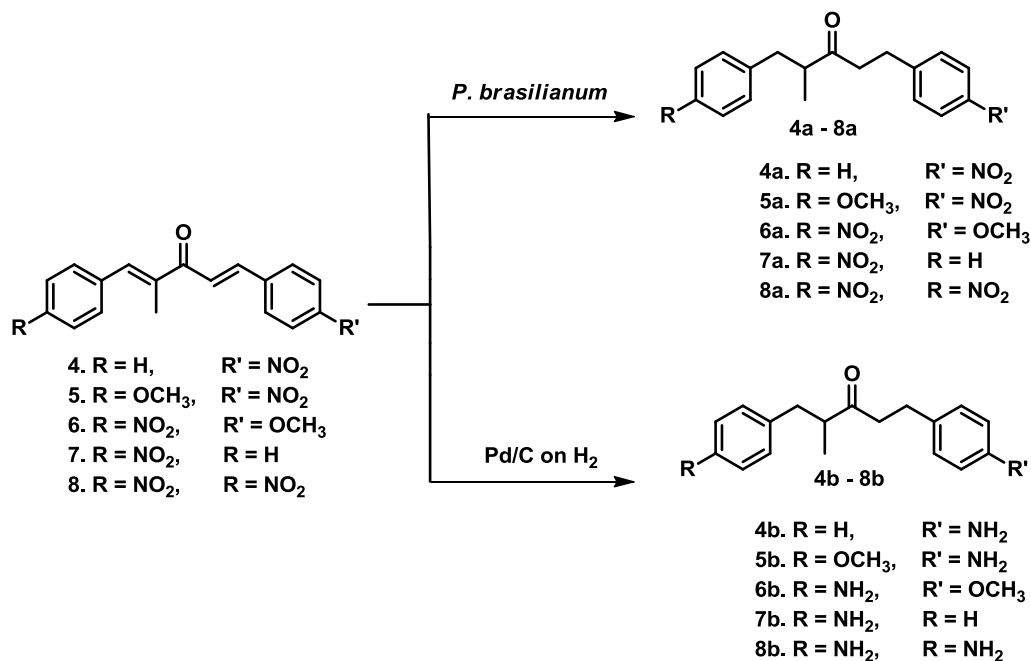
Scheme 8.2 - The reduction of compounds **4-8** by synthetic catalyst and biocatlytically by *Penicillium brasilianum.*

In compounds **1-8**, the presence of a pair of doublets nearly at δ 7.53 and 7.69, with a coupling constant of c.a. 16 Hz, typical for a *trans* two spins system. The methyl in all compounds **1-8** can be seen nearly δ 1.5-2. All compounds exhibits two aromatic doublet in aromatic area. Further the structures of all compounds were further established through FTIR, UV/ Vis, XRD and mass spectrometric analysis, which was reported previously (ZIA et al., 2014).

Compounds **1-8** has been reduced chemo selectively by *P. brasilianum.* Biocatalytically only both double bonds were reduced by whole cell of fungus. The resultant biotransformed products **1a-8a** were obtained in quantities **1a** (29 mg), **2a** (5 mg), **3a** (5 mg), **4a** (29 mg), **5a** (19 mg), **6a** (3 mg) **7a** (23 mg) and 8a (27 mg) respectively per 100 mg of substrate.

Compound **1** is characterized by ^{1}H NMR and ^{13}C NMR. ^{1}H NMR of **1** was confirmed because the double bonds signals in ^{1}H NMR which is disappeared in **1a**. Compound **1** exhibits two double bonds signals at δ 7.53 and at δ 7.69 having coupling constant 16 Hz which is typical for *trans* spin system and one broad singlet at δ 7.62. The mentioned 3 signals in **1a**, two doublets and one broad singlet disappeared. The signals of reduced methylene appeared at δ 2.5-2.9 having integration of seven protons, which perfectly matches with that reduce product **1a**. The ^{13}C NMR spectra of **1** exhibit double bonds signals at δ 135-140, which is disappear and new four signals appeared in **1a** at δ 29.27, 39.46, 43.04 and 48.37 respectively. NMR analysis completely confirms the structure of biotransformed products **1a**.

Other biotransformed products **2a, 3a and 3d** were characterized by ^{1}H NMR in comparison with their substrate. Biotransformed products **2a, 3a and 3d** have basic skeleton having only different substitution on aromatic moiety so can be characterized in the same format from its ^{1}H NMR spectra. Substrate **2 and 3** having two spin doublet signals for E-isomer at δ 7.4-7.7, which is disappeared in all reduced products and new methylene signals, appeared at δ 2.3-2.9, which is typical prominent signals for reduced biotransformed products **2a and 3a**. In **3d** only one double bond is reduced so C=C bond next to ring B reduced leaving C=C bond next to ring A un-reduced. Computational DFT analysis shows that C=C bond next to ring A contain methyl in vicinity and

having more electron density compared to C=C bond next to ring B. The electrophile facilitate its attack on C=C bond next to ring B due to its LUMO contribution (FIGURE 8.1) that's also the advantage of biocatalyst that can differentiate the two double bonds.
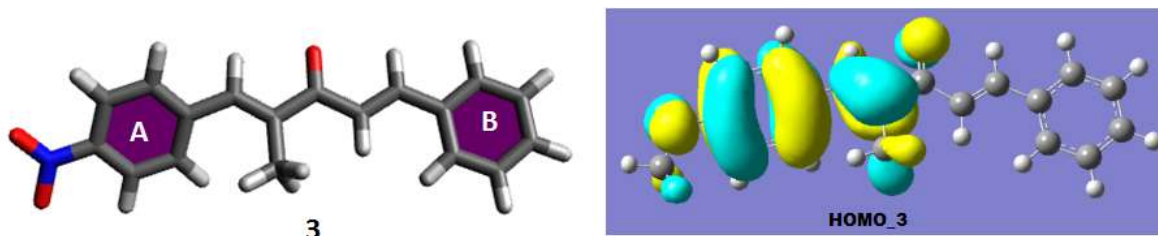

Figure 8.1 - HOMO analysis of compound **3** calculated by applying semi-empirical calculations using the Gaussian software package with the semi empirical B3LYP/6-31G(d,p) method and full energy optimization.

Compounds **4-8** were also selectively reduced to **4a-8a** by *Penicillium brasilianum.* In all reduced compounds (**4a-8a**), the hydrogen signals of C=C bonds disappeared leading to the appearance of methylene signal near δ 2-3. Which confirms the reduction of C=C in these moieties.

Literature survey suggest that fungal specie consist of a class of enzyme named old yellow enzyme (OYE), which involves in the reduction mechanism (TOOGOOD; GARDINER; SCRUTTON, 2010), representing different ecology and lifestyle and involve in many enzymatic process (NIZAM et al., 2014). Most of these OYE are flavine dependent enzymes which are oxidized to FMN during enzymatic reaction leading proton transfer for the reduction of substrate. The possible mechanism of enzymatic reduction of compounds **1-8** is shown (FIGURE 8.2).
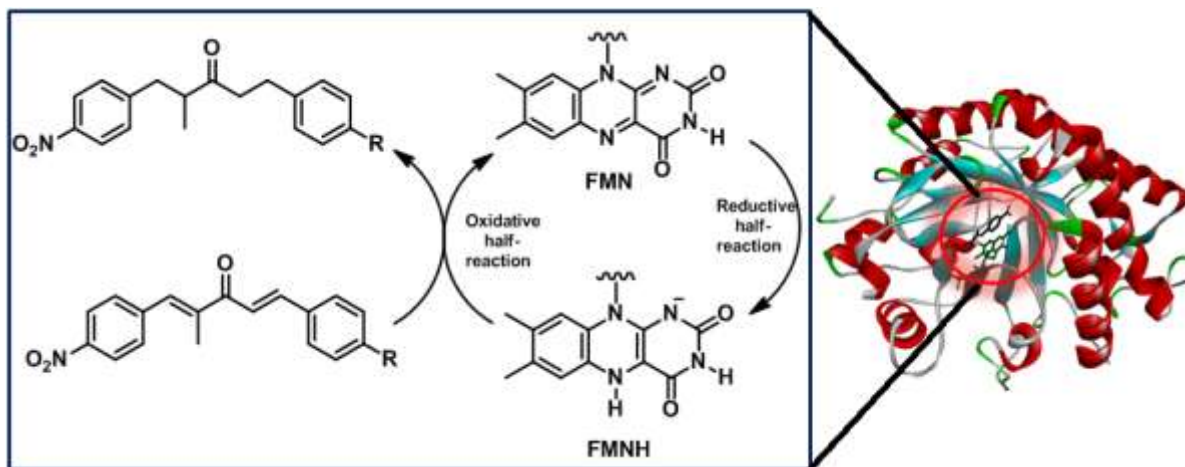
Figure 8.2 - Biocatalytic reduction of compounds **1** and **2** by *P.brasilianum* old yellow enzyme. FMNH is used as co-factor and hydrogen donor.

Alternatively compounds **1-8** were reduced by utilizing synthetic important reducing agents Pd/C on H_2. It is reported that aromatic carbonyls are simply reduced to form methylene compounds through benzyl alcohol as an intermediate under Pd/C-catalyzed hydrogenation (LAROCK, 1999), and it is difficult to achieve the selective hydrogenation of an olefin while leaving the aromatic carbonyl group intact. We were trying to reduce the two double bonds of curcuminoids selectively for our further research, and we successfully avoid reduction of carbonyl by Pd/C on H_2. Sajiki *et al.* reported the reduction of chalcone by Pd/C on H_2 in methanol, but reducing double bond, the reduction of carbonylic compounds were also produced (MORI et al., 2006). The reduction of nitro groups occurred even using less amount of catalyst and low temperature. Transition-metal-catalyzed hydrogenations have been used to a number of chemical transformations of functional groups (LAROCK, 1999). Chemo selective hydrogenation amongst some reducible functionality has been one of the most important subjects in the field of synthetic chemistry. We have

reported a chemo selective hydrogenation of curcuminoids (**1-8**) without reduction of nitro and carbonylic groups by using biocatalytic approach using *P. brasilianum* as biocatalyst.

Synthetic reduced compounds **1b-3b** was characterized on the basis of spectroscopic and spectrometric analysis and by comparison with compounds **1a-3a**. Compounds **4b-8b** was completely characterized by ^{1}H NMR, and was supported by ^{13}C NMR and mass analysis. When nitro group reduced to NH_2 group (**4b-8b**), the signal of vicinal aromatic positions shielded and the shift to δ 7. The aromatic signals for 2-aromatic hydrogen appear at δ 8.0-8.2 when there is *para*-nitro substitution on aromatic ring, and shifted to shielded area δ 7.0-7.2 when *para* nitro group reduces (FIGURE 8.3)
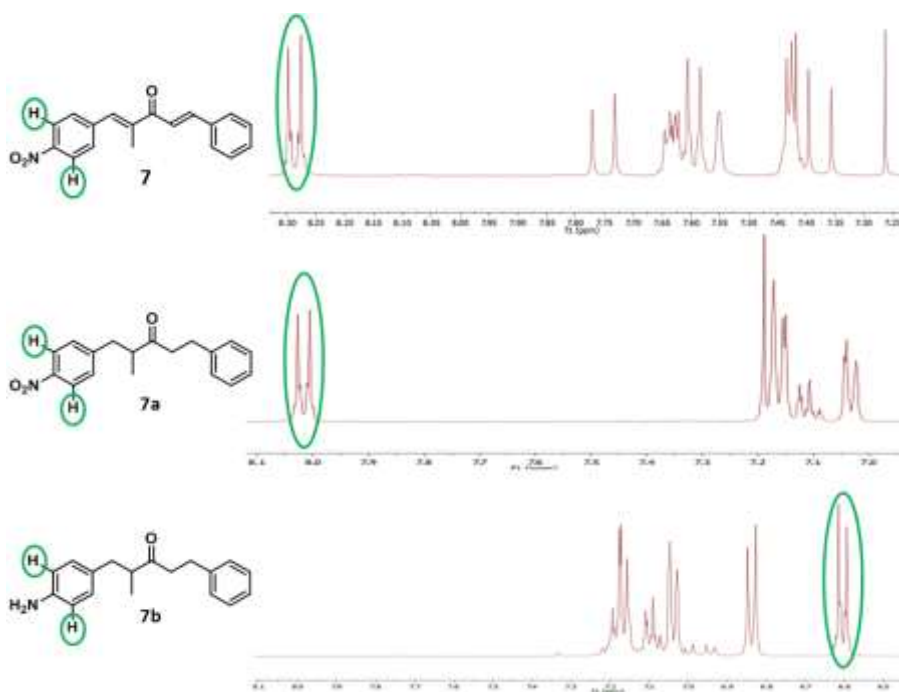
Figure 8.3 - Comparison of ^{1}H NMR spectra of compound 7, 7a and 7b. Para substituted groups on ring A (NO₂, NH₂) influence the shift of NMR signals of adjacent hydrogens (meta hydrogens).

Reduced form was also characterized on the basis of their mass analysis. Fragmentation pattern of both compound **7** and **7a** can differentiate clearly between the two reduce form. Compound **7** produces prominent fragment ion at m/z 136.04, while **7a** produces the same ion at m/z 106.07 due to nitro group's reduction (FIGURE 8.4). So mass spectral analysis confirms the reduction of nitro groups in all Pd/C on H_2 reduced products.
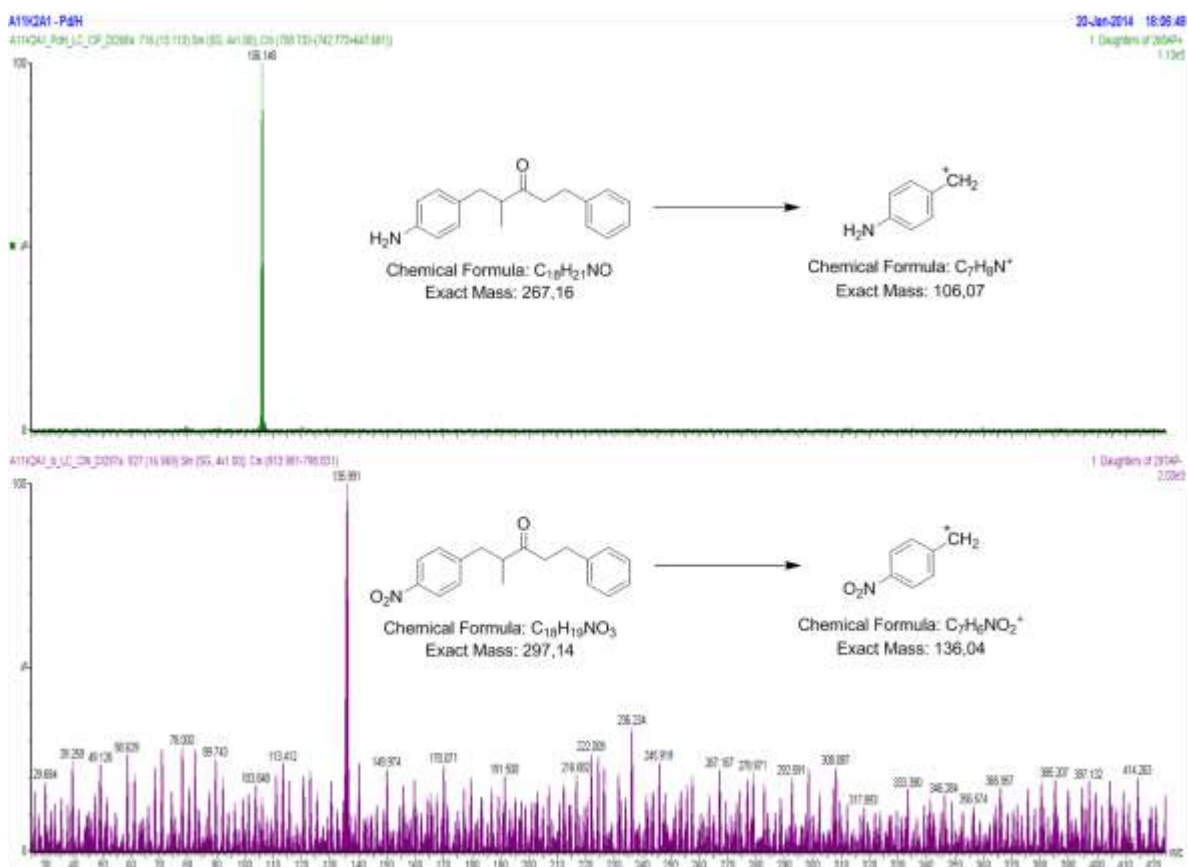
Figure 8.4 - Mass spectral analysis of 4c and 4d.

8.2 Chiral Analysis

The reduction of compounds **1-8** either by Pd/C on H2 or by biocatalytic method produces chiral compounds. The fungus is selective than synthetic reducing agent (TABLE 8.1). It was also observed that biological reduction of α,β-disubstituted nitroalkenes proceeded with poor enantioselectivity (FRYSZKOWSKA et al., 2008).

Table 8.1- Yield of reduced products and its ee.

Entry	Product	R	R´	Time	ee(R/S)	Solvent
1	1a	H	H	15d	48:52	H_2O
2	2a	H	OCH_3	15d	nd	H_2O
3	3a	OCH_3	H	15d	36:54	H_2O
4	4a	H	NO_2	15d	nd	H_2O
5	5a	OCH_3	NO_2	15d	72:28	H_2O
6	6a	NO_2	OCH_3	15d	18:82	H_2O
7	7a	NO_2	H	15d	64:36	H_2O
8	8a	NO_2	NO_2	15d	39:61	H_2O
2	1b	H	H	1h	52:48	$C_4H_8O_2$
4	2b	H	OCH_3	1h	nd	$C_4H_8O_2$
5	3b	OCH_3	H	1h	47:53	$C_4H_8O_2$
6	4b	H	NH_2	1h	nd	$C_4H_8O_2$
7	5b	OCH_3	NH_2	1h	49:51	$C_4H_8O_2$
8	6b	NH_2	OCH_3	1h	48:52	$C_4H_8O_2$
9	7b	NH_2	H	1h	50:50	C_4H_8O
10	8b	NH_2	NH_2	1h	47:53	$C_4H_8O_2$

Enantiomeric excesses were determined by HPLC using Chiralcel OB-H column in-hexane/i-propanol, 95:5; 0.6 mL/min

Later we observed that our compounds feed to fungus also consist of two isomers so it's reducing products also racemic mixture. It was not possible to isolate isomers due to inter conversion of E and Z isomers of compounds **1-8** in the presence of light. Once we isolate pure isomer, it racemize again with time.

8.3 Computational DFT analysis

The highest occupied molecular orbital (HOMO) and lowest unoccupied molecular orbital (LUMO) for compound **1-8** (FIGURE 8.5)**,** were analyzed by Gaussian (HEHRE; DITCHFIELD; POPLE, 1972). It is noticeable that the charge density in HOMO is mainly localized on the ring A of compound **3, 4** and **5** with little charge density on one double bond, while LUMO has contributing effect from ring B and adjacent double bond. In compounds **2**, **6**, and **7**, the charge density in HOMO is major contribution on the ring B, adjacent double bond and a little on carbonyl. The energy of HOMO is the ability of a compound to lose electron, and therefore consider equal to the ionization potential. On the other hand, energy of LUMO describes the ability of a compound to gain electrons. Therefore, the negative of the energy of LUMO is taken as electron affinity. The nitro group on *para* position of aromatic ring activates the adjacent double bond for hydride attack, so compounds having nitro substitution are more susceptible to reduction so can be reduced by the action of enzyme OYE. The stability of all compounds were also calculated by Avogadro (HANWELL et al., 2012).
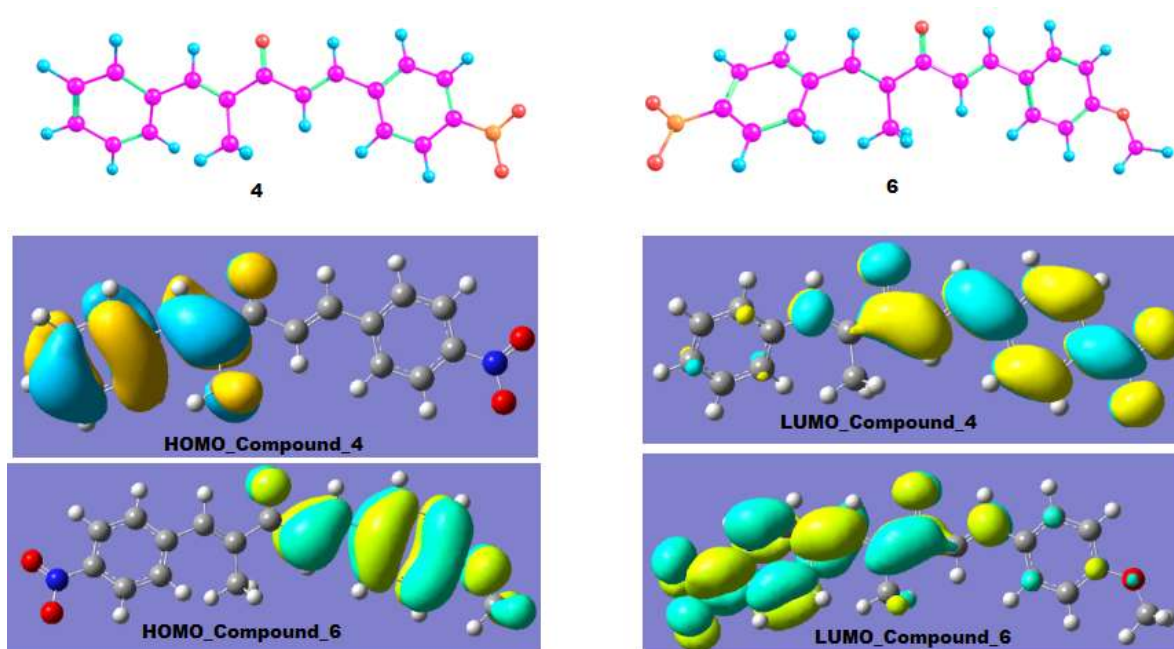
Figure 8.5 -Electronic distributions for for compound **4** and **6**. Semi-empirical calculations were performed using the Gaussian software package with the semi empirical B3LYP/6-31G(d,p) method and full geometric optimisation.

The total electron density distribution is a physical property of molecules. The electron density is typically showed as a comparison of the identified electron density with that predictable by spherical models of the atoms and is called deformation electron density. The HOMO and LUMO electron density was calculated by B3LYP/6-31G(d,p). The contour maps of electron density for compounds **4** and **6** are shown (FIGURE 8.6). It clearly explains the role of methyl in the distribution of electron density. The reduction of one double bond next to ring B in compound **3** can be explained on the basis of this calculation.
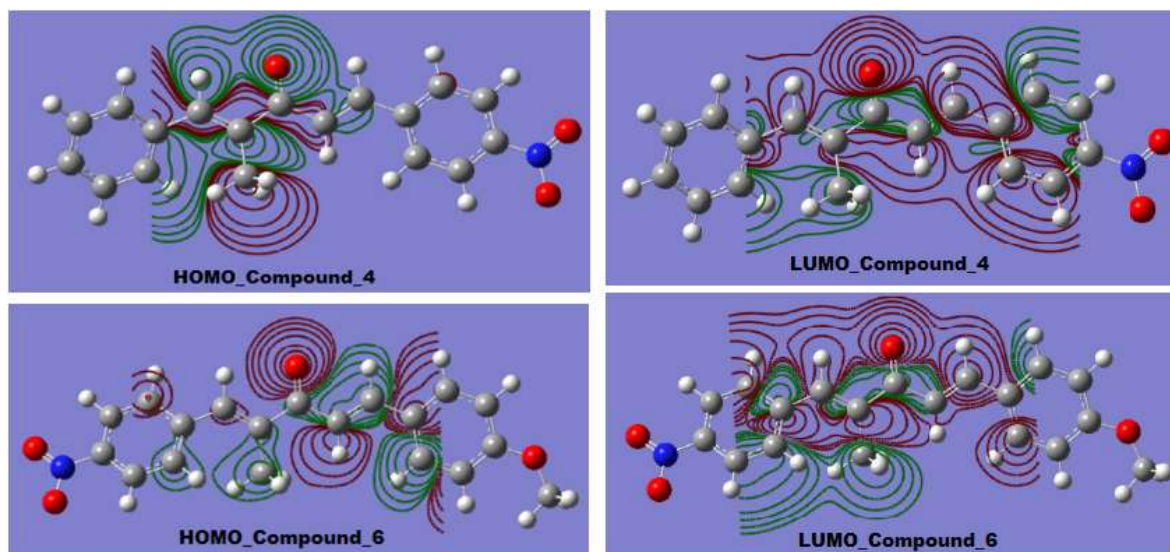
Figure 8.6 - Contour maps of electron density for HUMO and LUMO of 1b and 3b was calculated at the B3LYP/6-31G(d,p) level.

8.4 Molecular docking

Old yellow enzyme (OYE) is the class of flavin dependent enzyme carrying different hydrogenation reaction and can selectively reduce unsaturated double bonds. The sequence was modeled and the most stable active site where the binding energy is low was selected. The most active amino acids residues in active site consist of Ala-25, Pro-26, Thr-28, Gly-61, Gln-103, Arg-223, Gly-292, Gly-316 and Arg-317. The FMN was putted in the protein from reported old yellow enzyme from *Aspergillus fumigates* (pdb id: 4QNW). The FMN occupies the active site in our modeled protein and showing an interaction with active site residues. It shows Hydrogen bonding interaction with Pro-26, Thr-28, Gly-61, Gln-103, Arg-223, Gly-292, Gly-316 and Arg-317 by distance of 2.75, 2.58, 2.21, 1.87, 2.40, 1.74, 1.82, and 1.67 Å respectively.

The compounds **8** were docked with OYE and occupy the proximity with FMN with lowest binding energy. The modeled protein along with FMN and dock compound **8** is shown (FIGURE 8.7). Compound **8** was docked with OYE and it was found fitted well in the active site by forming hydrogen bonding with amino acid Lys-339, Phe-343 and Gly-316 by distance of 2.24, 3.05 and 2.35 Å respectively and showing binding energy -2.80 Kcal/mole. Two hydrogen bonding were observed between ligand and FMN by distance of 3.08 and 2.97 Å. The FMN act as hydride transfer, and then the compound gain hydrogen from solvent or enzyme leading to the reduction of C=C bond.
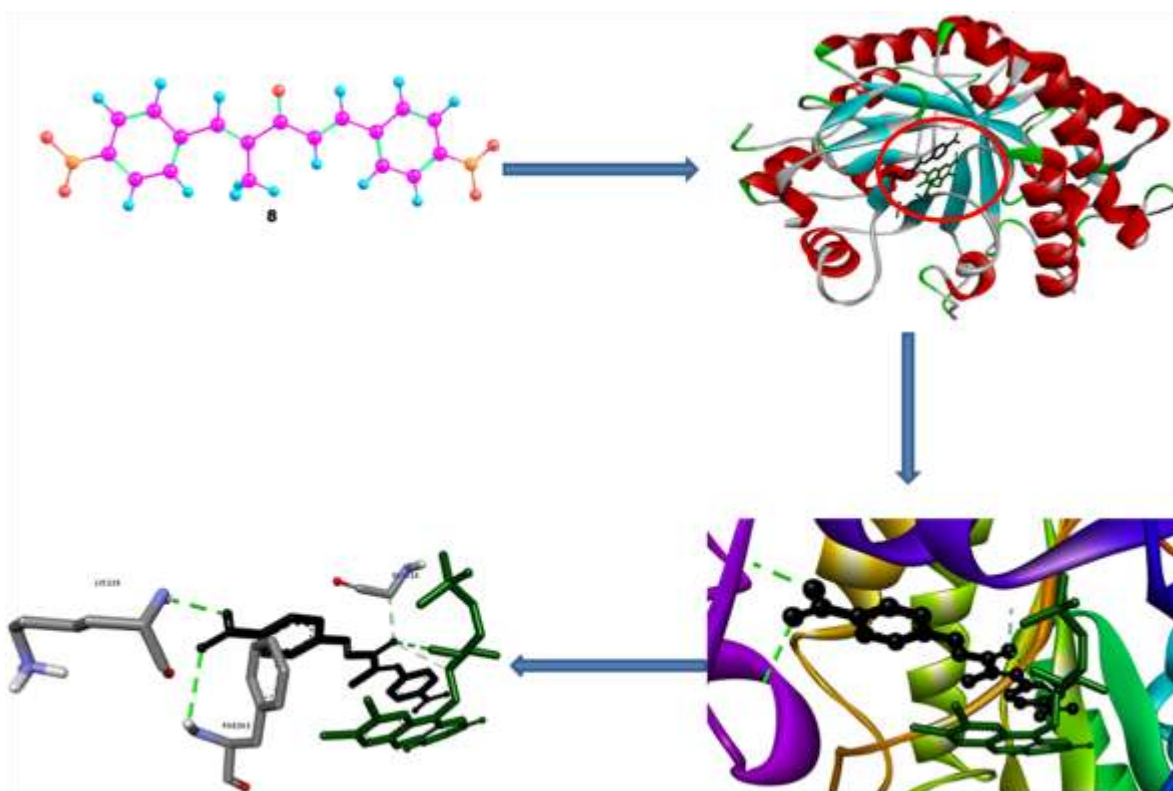
Figure 8.7 - Amino acid residues are shown in grey, the bound ligand in black and the flavin co factor in dark green. Hydrogen bonding interaction are depicted as green and grey, dashed lines

❖ 9

Experimental – Part 2

9 Experimental

9.1 Solvents and chemicals

Chemical for synthesis like 2-butanone, aldehydes, Hydrocholric acid were purchased from Sigma–Aldrich and used without further purification. All solvents used were of HPLC and analytical grade. The deuterated solvents of Apolo were used for the NMR analysis.

9.2 General Experimental Procedure

High resolution mass spectrometry analyses were obtained on a Thermo Scientific LTQ Orbitrap Velos Thermo with an ESI ion source. ^{1}H-NMR, ^{13}C-NMR and 2D experiments (gHSQC (^{1}H/^{1}H), gHMBC (^{1}H/^{13}C)) were performed on a Brüker AVANCE 400 operating at 400.15 MHz and 100.62 MHz, respectively. CDCl$_3$ was used as solvent and tetramethylsilane (TMS) as internal reference. Compounds were dissolved in organic solvents and transferred into a 5-mm NMR tube. Chemical shifts (δ ppm) were measured with accuracy of 0.01 and 0.5 ppm, respectively. Internal lock and tetramethylsilane (TMS) were used as internal reference.

9.2.1 Preparation of Substrate (1–8)

The reaction of benzaldehyde, p-methoxy benzaldehyde and p-nitro benzaldehyde with 2-butanone, using gaseous HCl as catalyst produces 4-aryl-3-methylbutenones, which on further reaction with the p-substituted aldehydes

under base catalyzed Aldol reactions, yields un-symmetrical compounds **1-8** (**FIGURE 9.1**).
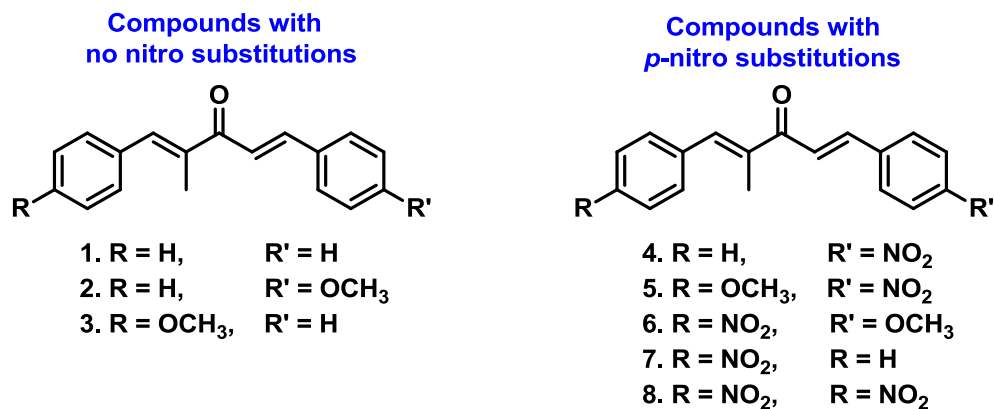
Figure 9.1- Chemical structure of substrates **1-8**.

9.2.2 Fungal whole cell

The procedure of fungus isolation has been reported by our group (SANTOS; M;; RODRIGUES-FO, 2002). *P. brasilianum* was deposited under the identification code LaBioMMi 024 at LaBioMMi (Laboratório de Bioquímica Micromolecular de Micro-organismos) of the Chemistry Department at Universidade Federal de São Carlos, Brazil.

9.2.3 Fermentation and extraction

The fungus was grown under shaking conditions (180 rpm) at room temperature for 3 days in 250 mL erlenmeyer flasks containing liquid medium (50 mL per flask) composed of glucose (26.7 g L^{-1}), NaNO$_3$ (3.0 g L^{-1}), K$_2$HPO$_4$ (1.0 g L^{-1}), MgSO$_4\cdot$7H$_2$O (0.5 g L^{-1}), KCl (0.5 g L^{-1}), FeSO$_4\cdot$7H$_2$O (0.01 g L^{-1}). After 3 days, substrates (**1-8**) were feed with 10 mg per flask and

shaking was continued for more 15 days. Each 10 flask were feed with same compounds. In total, 10 replicates were prepared for each substrate. Three flasks with culture and fungus but without the substrates were kept as negative control. The mycelium was separated by filtration and extractions were carried with ethanol (3×50 mL) per flask. Aqueous phase were extracted with ethyl acetate (3×50 mL) but did not afford significant biotransformed products. The organic solvent was concentrated under vacuum to afford a crude extract. TLC analysis suggested that mycelial extract afford biotransformed products, so all flask extract was combined. The crude was fractionated and selected fractions were loaded in column to yield pure reduced products, which is characterized by spectroscopic and spectrometric analysis.

9.2.4 Computational study

Computational calculations were performed using the tool Gaussian 03 package (FRISCH et al., 2004). Geometries of all the species investigated were optimized without any symmetry constraints, and the resulting structures were further assessed using vibrational frequency analysis to probe whether or not the structures represent true minimum-energy geometries. All the calculations were done using hybrid DFT functionals: B3LYP (PARR; YANG, 1989) . The approaches are subsequently referred to as B3LYP/6-31G*. For all the structures under investigation, the singlet states were studied. Molecular structures and frontier orbitals were visualized using Gauss view software.

9.2.5 *In-Silico* docking analysis

The sequence of OYE from *Penicillium brasilianum* was extracted and modeled by Swiss modal (Swiss-model is a fully automated protein structure homology modeling server) (JOHANSSON et al., 2012). Then the structure was visualized by discovery studio 4.1 (DASSAULT SYSTÈMES BIOVIA, 2015). The active site selection was made by castp, where the computation is based on the pocket algorithm of the alpha shape theory, and its core is the alpha shape API (DUNDAS et al., 2006). Also different random blind docking and analyzing their results and comparison with other OYE reported in literature, helps us to determine best active site.

The ligands **8** were drawn in Chemdraw converting to mol. format and then assigned with proper 2D orientation by chemcraft (chemcraft comprises a set of graphical tools for facilitating working with quantum chemistry computations) (ANDRIENKO,). Energy of the molecules was minimized using software Avogadro 1.1.1 (HANWELL et al., 2012) with MMFF94 force field. *In-silico* docking calculations were performed by Autodock tool 4.2 (MORRIS et al., 2009). Protein and ligands structure were converted to pdbqt file by MGL Tools 1.5.6 rc[3] by adding polar hydrogen's to both. After the calculation the interactions of complex protein-ligand conformations, were analyzed using Autodock Tools 4.2 (MORRIS et al., 2009) and Discovery studio 4.1 (DASSAULT SYSTÈMES BIOVIA, 2015).

❖ 10

Conclusion and Perspective

10.1 Conclusion

Biocatalysis is important tool to carry chemo-selective reduction of α, β-unsaturated corbonylic compounds in curcuminoids analogues. The Pd/C on H_2 reduces double bonds along with nitro groups. Biocatalysis using whole cell of *P.brasilianum* selectively reduces double bonds without carrying nitro group reduction. This result offers evidence of the presence of enoate reductase broadly called old yellow enzymes activity in this fungus for the first time.

10.2 Perspective

- Enoate reductase is useful enzyme which show the selectivity for the reduction of C=C bond, and so should be introduced to synthetic chemistry for the synthesis of natural products.
- More functional group should be evaluated in order to see the selectivity index for the reduction of C=C bond.

❖ **11**

References

References

ACCHE, R.; HSIRSAGAR, M. ; KAMBLE, S.; BANDGAR, B.; DHOLE, N.; SHISODE, K.; CHAUDHARI, A. Antioxidant and Anti-inflammatory Related Activities of Selected Synthetic Chalcones : Structure – Activity Relationship Studies Using Computational Tools. **Chem. Pharm. Bull.**, v. 56, n. 7, p. 897–901, 2008.

ACHANTA, G.; MODZELEWSKA, A.; FENG, L.; KHAN, S. R.; HUANG, P. A boronic-chalcone derivative exhibits potent anticancer activity through inhibition of the proteasome. **Molecular. pharmacol.**, v. 70, n. 1, p. 426–33, jul. 2006. Disponível em: <http://www.scopus.com/inward/record.url?eid=2-s2.0-33745276531&partnerID=tZOtx3y1>. Acesso em: 4 nov. 2014.

AGGARWAL, B. B. Prostate cancer and curcumin: Add spice to your life. **Cancer. Biol & Therapy.**, v. 7, n. 9, p. 1436–1440, 27 out. 2014. Disponível em: <http://www.scopus.com/inward/record.url?eid=2-s2.0-58149143164&partnerID=tZOtx3y1>. Acesso em: 31 dez. 2014.

AHER, R. B.; WANARE, G.; KAWATHEKAR, N.; KUMAR, R. R.; KAUSHIK, N. K.; SAHAL, D.; CHAUHAN, V. S. Dibenzylideneacetone analogues as novel Plasmodium falciparum inhibitors. **Bioorg. & Med. Chem. Lett.**, v. 21, n. 10, p. 3034–6, 15 maio 2011. Disponível em: <http://www.ncbi.nlm.nih.gov/pubmed/21493068>. Acesso em: 26 out. 2014.

AKSÖZ, B. E.; ERTAN, R.; ŞALKON, I.; ÖZELLIKLERI, Y. Chemical and Structural Properties of Chalcones I. **FABAD J. Pharm. Sci.**, v. 36, p. 223–242, 2011.

ANAND, P.; KUNNUMAKKARA, A. B.; NEWMAN, R. a; AGGARWAL, B. B. Bioavailability of curcumin: problems and promises. **Molecular. pharmaceutics.**, v. 4, n. 6, p. 807–18, 2007. Disponível em: <http://www.ncbi.nlm.nih.gov/pubmed/17999464>. Acesso em: 13 jul. 2014.

ANDRIENKO, G. A. **Chemcraft basics**. Disponível em: <http://www.chemcraftprog.com>.

APONTE, J. C.; VERÁSTEGUI, M.; MÁLAGA, E.; ZIMIC, M.; QUILIANO, M.; VAISBERG, A. J.; GILMA, R. H.; HAMMOND, G. B. Synthesis , Cytotoxicity , and Anti- Trypanosoma cruzi Activity of New Chalcones. **J. Med. Chem.**, v. 51, p. 6230–6234, 2008.

ATTAR, S.; O'BRIEN, Z.; ALHADDAD, H.; GOLDEN, M. L.; CALDERÓN-URREA, A. Ferrocenyl chalcones versus organic chalcones: a comparative study of their nematocidal activity. **Bioorg & Med. Chem.**, v. 19, n. 6, p.

2055–73, 15 mar. 2011. Disponível em: <http://www.ncbi.nlm.nih.gov/pubmed/21349727>. Acesso em: 1 nov. 2014.

BAIRWA, K.; GROVER, J.; KANIA, M.; JACHAK, S. M. Recent developments in chemistry and biology of curcumin analogues. **RSC. Adv.**, v. 4, p. 13946–13978, 2014.

BANDGAR, B. P.; GAWANDE, S. S.; BODADE, R. G.; TOTRE, J. V; KHOBRAGADE, C. N. Synthesis and biological evaluation of simple methoxylated chalcones as anticancer, anti-inflammatory and antioxidant agents. **Bioorg & Med. Chem.**, v. 18, n. 3, p. 1364–70, fev. 2010. Disponível em: <http://www.ncbi.nlm.nih.gov/pubmed/20064725>. Acesso em: 1 nov. 2014.

BARROS-FILHO, B. A.; NUNES, F. M.; DE OLIVEIRA, M. da C. F.; LEMOS, T. L. G.; DE MATTOS, M. C.; DE GONZALO, G.; GOTOR-FERNÁNDEZ, V.; GOTOR, V. Bioreduction of prochiral ketones by growing cells of Lasiodiplodia theobromae: Discovery of a versatile biocatalyst for asymmetric synthesis. **J Mol Cat B: Enzymatic**, v. 65, n. 1-4, p. 37–40, ago. 2010. Disponível em: <http://www.sciencedirect.com/science/article/pii/S1381117710000330>. Acesso em: 17 jun. 2015.

BASILE, V.; FERRARI, E.; LAZZARI, S.; BELLUTI, S.; PIGNEDOLI, F.; IMBRIANO, C. Curcumin derivatives: molecular basis of their anti-cancer activity. **Biochemical. pharmacol.**, v. 78, n. 10, p. 1305–15, 15 dez. 2009. Disponível em: <http://www.sciencedirect.com/science/article/pii/S0006295209005954>. Acesso em: 31 dez. 2014.

BHAGAT, S.; SHARMA, R.; CHAKRABORTI, A. K. Dual-activation protocol for tandem cross-aldol condensation: An easy and highly efficient synthesis of α,α′-bis(aryl/alkylmethylidene)ketones. **J. Mol. Cat. A: Chemical.**, v. 260, n. 1-2, p. 235–240, dez. 2006. Disponível em: <http://linkinghub.elsevier.com/retrieve/pii/S1381116906010119>. Acesso em: 6 nov. 2014.

BIDÓIA, D. L.; DESOTI, V. C.; MARTINS, S. C.; RIBEIRO, M. F.; ZIA, U.; FILHO, E. R.; NAKAMURA, T. U.; NAKAMURA, C. V.; SILVAA, S. O. Dibenzylideneacetones are potent trypanocidal compounds that affect the Trypanosoma cruzi redox system. **Antimicrob. Agents Chemo.**, v. 60, p. 890–903, 2016.

CÉSAR A. SCHAEFER, VANESSA D. SILVA, B. U. S. and M. da G. N. Use of Saccharomyces cerevisiae Yeasts in the Chemoselective Bioreduction of

(1E,4E)-1,5-Bis(4-Methoxyphenyl)-1,4-Pentadien-3-one in Biphasic System. **J. Braz. Chem. Soc**, v. 00, n. 00, p. 1–7, 2013.

CHANDRASEKAR, T.; PRAVIN, N.; RAMAN, N. Biosensitive metal chelates from curcumin analogues: DNA unwinding and anti-microbial evaluation. **Inorg. Chem. Comm.**, v. 43, p. 45–50, maio 2014. Disponível em: <http://www.sciencedirect.com/science/article/pii/S1387700314000665>. Acesso em: 7 dez. 2014.

CHANGTAM, C.; DE KONING, H. P.; IBRAHIM, H.; SAJID, M. S.; GOULD, M. K.; SUKSAMRARN, A. Curcuminoid analogs with potent activity against Trypanosoma and Leishmania species. **Eur. J. Med. Chem.**, v. 45, n. 3, p. 941–56, mar. 2010. Disponível em: <http://www.ncbi.nlm.nih.gov/pubmed/20004045>. Acesso em: 3 jan. 2015.

CHEN, M.; THEANDER, T. G.; CHRISTENSEN, S. B.; HVIID, L.; ZHAI, L. I. N.; KHARAZMIL, A. Licochalcone A , a New Antimalarial Agent , Inhibits In Vitro Growth of the Human Malaria Parasite Plasmodium falciparum and Protects Mice from P . yoelii Infection. **Antimicrob. Agents Chemother.**, v. 38, n. 7, p. 1470–1475, 1994.

CHENG, Z.-J.; LIN, C.-N.; HWANG, T.-L.; TENG, C.-M. Broussochalcone A, a potent antioxidant and effective suppressor of inducible nitric oxide synthase in lipopolysaccharide-activated macrophages. **Biochem. Pharmacol.**, v. 61, n. 8, p. 939–946, abr. 2001. Disponível em: <http://linkinghub.elsevier.com/retrieve/pii/S0006295201005433>.

DAS, B.; THIRUPATHI, P.; MAHENDER, I.; REDDY, K. R. Convenient and facile cross-Aldol condensation catalyzed by molecular iodine: An efficient synthesis of α,α'-bis(substituted-benzylidene) cycloalkanones. **J. Mol. Cat. A: Chemical**, v. 247, n. 1-2, p. 182–185, mar. 2006. Disponível em: <http://www.sciencedirect.com/science/article/pii/S1381116905008095>. Acesso em: 6 nov. 2014.

DAS, K. C.; DAS, C. K. Curcumin (diferuloylmethane), a singlet oxygen quencher. **Biochem. Biophys. Res. Comm.**, v. 295, n. 1, p. 62–66, jul. 2002. Disponível em: <http://www.sciencedirect.com/science/article/pii/S0006291X02006332>. Acesso em: 30 dez. 2014.

DAS, U.; ALCORN, J.; SHRIVASTAV, A.; SHARMA, R. K.; DE CLERCQ, E.; BALZARINI, J.; DIMMOCK, J. R. Design, synthesis and cytotoxic properties of novel 1-[4-(2-alkylaminoethoxy)phenylcarbonyl]-3,5-bis(arylidene)-4-piperidones and related compounds. **Eur. J. Med. Chem.**, v. 42, n. 1, p. 71–80, jan. 2007a. Disponível em:

<http://www.sciencedirect.com/science/article/pii/S0223523406002765>.
Acesso em: 31 dez. 2014.

DAS, U.; KAWASE, M.; SAKAGAMI, H.; IDEO, A.; SHIMADA, J.;
MOLNÁR, J.; BARÁTH, Z.; BATA, Z.; DIMMOCK, J. R. 3-(3,4,5-
Trimethoxyphenyl)-1-oxo-2-propene: a novel pharmacophore displaying potent
multidrug resistance reversal and selective cytotoxicity. **Bioorg & Med.
Chem.**, v. 15, n. 10, p. 3373–80, 15 maio 2007b. Disponível em:
<http://www.sciencedirect.com/science/article/pii/S0968089607002118>.
Acesso em: 31 dez. 2014.

DASSAULT SYSTÈMES BIOVIA. **Discovery Studio Modeling
Environment, Release 4.1**San DiegoDassault Systèmes, , 2015. .

DE CAMPOS-BUZZI, F.; PEREIRA DE CAMPOS, J.; POZZA TONINI, P.;
CORRÊA, R.; AUGUSTO YUNES, R.; BOECK, P.; CECHINEL-FILHO, V.
Antinociceptive effects of synthetic chalcones obtained from xanthoxyline.
Archiv der Pharmazie., v. 339, n. 7, p. 361–5, jul. 2006. Disponível em:
<http://www.ncbi.nlm.nih.gov/pubmed/16838282>. Acesso em: 1 nov. 2014.

DE, R.; KUNDU, P.; SWARNAKAR, S.; RAMAMURTHY, T.;
CHOWDHURY, A.; NAIR, G. B.; MUKHOPADHYAY, A. K. Antimicrobial
activity of curcumin against Helicobacter pylori isolates from India and during
infections in mice. **Antimicrob. Agents Chemother.**, v. 53, n. 4, p. 1592–7, 1
abr. 2009. Disponível em: <http://aac.asm.org/cgi/content/long/53/4/1592>.
Acesso em: 12 dez. 2014.

DIMMOCK, J. R.; DAS, U.; GUL, H. I.; KAWASE, M.; SAKAGAMI, H.;
BARÁTH, Z.; OCSOVSKY, I.; MOLNÁR, J. 3-Arylidene-1-(4-
nitrophenylmethylene)-3,4-dihydro-1H-naphthalen-2-ones and related
compounds displaying selective toxicity and reversal of multidrug resistance in
neoplastic cells. **Bioorg. & Med. Chem. Lett.**, v. 15, n. 6, p. 1633–6, 15 mar.
2005. Disponível em:
<http://www.sciencedirect.com/science/article/pii/S0960894X05001216>.
Acesso em: 31 dez. 2014.

DIMMOCK, J. R.; KANDEPU, N. M.; DAS, U.; ZELLO, G. A.; NIENABER,
K. H. Antimycobacterial arylidenecyclohexanones and related Mannich bases.
Pharmazie., v. 59, n. 7, p. 502–505, 2004. Disponível em:
<http://www.scopus.com/inward/record.url?eid=2-s2.0-
3242698945&partnerID=tZOtx3y1>.

DIMMOCK, J. R.; PADMANILYAM, M. P.; ZELLO, G. A.; WILSON
QUAIL, J.; OLOO, E. O.; PRISCIAK, J. S.; KRAATZ, H.-B.; CHERKASOV,
A.; LEE, J. S.; ALLEN, T. M.; SANTOS, C. L.; MANAVATHU, E. K.; DE

CLERCQ, E.; BALZARINI, J.; STABLES, J. P. Cytotoxic 1,3-diarylidene-2-tetralones and related compounds. **Eur. J. Med. Chem.**, v. 37, n. 10, p. 813–824, out. 2002. Disponível em: <http://www.sciencedirect.com/science/article/pii/S0223523402014022>. Acesso em: 31 dez. 2014.

DOLAI, S.; SHI, W.; CORBO, C.; SUN, C.; AVERICK, S.; OBEYSEKERA, D.; FARID, M.; ALONSO, A.; BANERJEE, P.; RAJA, K. "Clicked" sugar-curcumin conjugate: modulator of amyloid-β and tau peptide aggregation at ultralow concentrations. **ACS. chem. neurosci.**, v. 2, n. 12, p. 694–9, 21 dez. 2011. Disponível em: <http://www.pubmedcentral.nih.gov/articlerender.fcgi?artid=3369720&tool=pmcentrez&rendertype=abstract>.

DUNDAS, J.; OUYANG, Z.; TSENG, J.; BINKOWSKI, A.; TURPAZ, Y.; LIANG, J. CASTp: computed atlas of surface topography of proteins with structural and topographical mapping of functionally annotated residues. **Nucleic acids research**, v. 34, n. Web Server issue, p. W116–8, 1 jul. 2006. Disponível em: <http://www.pubmedcentral.nih.gov/articlerender.fcgi?artid=1538779&tool=pmcentrez&rendertype=abstract>. Acesso em: 26 jul. 2015.

EDDARIR, S.; COTELLE, N.; BAKKOUR, Y.; ROLANDO, C. An efficient synthesis of chalcones based on the Suzuki reaction. **Tetrahedron. Lett.**, v. 44, n. 28, p. 5359–5363, jul. 2003. Disponível em: <http://linkinghub.elsevier.com/retrieve/pii/S0040403903011407>.

ESMAEILI, A. A.; TABAS, M. S.; NASSERI, M. A.; KAZEMI, F. Solvent-Free Crossed Aldol Condensation of Cyclic Ketones with Aromatic Aldehydes Assisted by Microwave Irradiation. **Monatshefte fur Chemie - Chemical Monthly**, v. 136, n. 4, p. 571–576, 18 jan. 2005. Disponível em: <http://link.springer.com/10.1007/s00706-004-0256-9>. Acesso em: 26 out. 2014.

FERRARI, E.; PIGNEDOLI, F.; IMBRIANO, C.; MARVERTI, G.; BASILE, V.; VENTURI, E.; SALADINI, M. Newly synthesized curcumin derivatives: crosstalk between chemico-physical properties and biological activity. **J. Med. Chem.**, v. 54, n. 23, p. 8066–77, 8 dez. 2011. Disponível em: <http://www.ncbi.nlm.nih.gov/pubmed/22029378>.

FIALA, M.; LIU, P. T.; ESPINOSA-JEFFREY, A.; ROSENTHAL, M. J.; BERNARD, G.; RINGMAN, J. M.; SAYRE, J.; ZHANG, L.; ZAGHI, J.; DEJBAKHSH, S.; CHIANG, B.; HUI, J.; MAHANIAN, M.; BAGHAEE, A.; HONG, P.; CASHMAN, J. Innate immunity and transcription of MGAT-III and

Toll-like receptors in Alzheimer's disease patients are improved by bisdemethoxycurcumin. **Proc. Nat. Acad. Sci.**, v. 104, n. 31, p. 12849–54, 31 jul. 2007. Disponível em: <http://www.pubmedcentral.nih.gov/articlerender.fcgi?artid=1937555&tool=pmcentrez&rendertype=abstract>.

FILL, T. P.; DA SILVA, J. V.; DE OLIVEIRA, K. T.; DA SILVA, B. F.; RODRIGUES-FO, E. Oxidative potential of some endophytic fungi using 1-indanone as a substrate. **J Microbiol and Biotech**, v. 22, n. 6, p. 832–837, 2012.

FRANCESE, S.; BRADSHAW, R.; FLINDERS, B.; MITCHELL, C.; BLEAY, S.; CICERO, L.; CLENCH, M. R. Curcumin: A Multipurpose Matrix for MALDI Mass Spectrometry Imaging Applications. **Anal. Chem.**, v. 85, p. 5240–5248, 2013.

FRIESNER, R, A.; RB;, M.; MP;, R.; LL;, F.; JR;, G.; TA;, H.; PC;, S.; DT, M. Extra precision glide: docking and scoring incorporating a model of hydrophobic enclosure for protein-ligand complexes. **Journal of medicinal chemistry**, v. 49, n. 21, p. 6177–96, 19 out. 2006. Disponível em: <http://dx.doi.org/10.1021/jm051256o>. Acesso em: 7 ago. 2015.

FRISCH, M. J.; TRUCKS, G. W.; SCHLEGEL, H. B.; SCUSERIA, G. E.; ROBB, M. A.; CHEESEMAN, J. R.; MONTGOMERY, J, J. A.; VREVEN, T.; KUDIN, K. N.; BURANT, J. **GAUSSIAN 03, Revision D.01**Gaussian, Inc., Wallingford CT, , 2004. . Disponível em: <http://cheshirenmr.info/References.htm>.

FRYSZKOWSKA, A.; FISHER, K.; GARDINER, J. M.; STEPHENS, G. M. Highly enantioselective reduction of beta,beta-disubstituted aromatic nitroalkenes catalyzed by Clostridium sporogenes. **J org chem**, v. 73, n. 11, p. 4295–8, 6 jun. 2008. Disponível em: <http://dx.doi.org/10.1021/jo800124v>. Acesso em: 29 nov. 2015.

FUJITA, T.; MAKISHIMA, D.; AKIYAMA, K.; HAYASHI, H. New convulsive compounds, brasiliamides A and B, from Penicillium brasilianum batista JV-379. **Bioscie, biotech, and biochem**, v. 66, n. 8, p. 1697–1705, 2002.

GOEL, A.; KUNNUMAKKARA, A. B.; AGGARWAL, B. B. Curcumin as "Curecumin": from kitchen to clinic. **Biochem. pharmacol.**, v. 75, n. 4, p. 787–809, 15 fev. 2008. Disponível em: <http://www.ncbi.nlm.nih.gov/pubmed/17900536>. Acesso em: 17 nov. 2014.

GORMAN, A. A.; HAMBLETT, I.; SRINIVASAN, V. S.; WOOD, P. D.

Curcumin-derived transients: A pulsed laser and pulse radiolysis study. **Photochem. Photobiol.**, v. 59, n. 4, p. 389–398, 1994. Disponível em: <http://www.scopus.com/inward/record.url?eid=2-s2.0-0028408395&partnerID=tZOtx3y1>.

GOSS, R. J. M.; SHANKAR, S.; FAYAD, A. A. The Generation of "Unnatural" Products: Synthetic Biology Meets Synthetic Chemistry. **Nat prod rep**, v. 29, n. 8, p. 870–89, 1 ago. 2012. Disponível em: <http://pubs.rsc.org/en/content/articlehtml/2012/np/c2np00001f>. Acesso em: 27 out. 2015.

GUPTA SC, PRASAD S, J. H. K.; PATCHVA S, W. L.; INDIRA PK, A. B. Multitargeting by curcumin as revealed by molecular interaction studies. **Nat. Prod. Rep.**, v. 28, n. 12, p. 1937–1955, 2011.

HANWELL, M. D.; CURTIS, D. E.; LONIE, D. C.; VANDERMEERSCHD, T.; ZUREK, E.; HUTCHISON, G. R. Avogadro: An advanced semantic chemical editor, visualization, and analysis platform. **Jour. of Cheminformatics.**, v. 4, n. 8, p. 1–17, 2012.

HATHAWAY, B. An aldol condensation experiment using a number of aldehydes and ketones. **J. Chem. Edu.**, v. 64, n. 4, p. 367, abr. 1987. Disponível em: <http://pubs.acs.org/doi/abs/10.1021/ed064p367>.

HEHRE, W. J.; DITCHFIELD, R.; POPLE, J. A. Self—Consistent Molecular Orbital Methods. XII. Further Extensions of Gaussian—Type Basis Sets for Use in Molecular Orbital Studies of Organic Molecules. **J. Chem. Phy.**, v. 56, n. 5, p. 2257–2261, 1972. Disponível em: <http://link.aip.org/link/?JCP/56/2257/1&Agg=doi\nhttp://scitation.aip.org/content/aip/journal/jcp/56/5/10.1063/1.1677527>.

HIRATA, T.; MATSUSHIMA, A.; SATO, Y.; IWASAKI, T.; NOMURA, H.; WATANABE, T.; TOYODA, S.; IZUMI, S. Stereospecific hydrogenation of the CC double bond of enones by Escherichia coli overexpressing an enone reductase of Nicotiana tabacum. **J Mol Cat B: Enzymatic**, v. 59, n. 1-3, p. 158–162, jul. 2009. Disponível em: <http://www.sciencedirect.com/science/article/pii/S1381117709000484>. Acesso em: 17 jun. 2015.

HUANG, M. T.; LOU, Y. R.; MA, W.; NEWMARK, H. L.; REUHL, K. R.; CONNEY, A. H. Inhibitory effects of dietary curcumin on forestomach, duodenal, and colon carcinogenesis in mice. **Cancer Res.**, v. 54, n. 22, p. 5841–5847, 1994. Disponível em: <http://www.scopus.com/inward/record.url?eid=2-s2.0-0028073507&partnerID=tZOtx3y1>.

IRANPOOR, N.; KAZEMI, F. RuCI3 Catalyses Aldol Condensations of Aldehydes and Ketones. **Tetrahedron.**, v. 54, p. 9475–9480, 1998.

ISHIGE, T.; HONDA, K.; SHIMIZU, S. Whole organism biocatalysis. **Curr opin in chem bio**, v. 9, n. 2, p. 174–80, abr. 2005. Disponível em: <http://www.sciencedirect.com/science/article/pii/S1367593105000165>. Acesso em: 4 jun. 2015.

JIRÁSEK, P.; AMSLINGER, S.; HEILMANN, J. Synthesis of Natural and Non-natural Curcuminoids and Their Neuroprotective Activity against Glutamate-Induced Oxidative Stress in HT-22 Cells. **J. Nat. Prod.**, v. 77, n. 10, p. 2206–17, 24 out. 2014. Disponível em: <http://www.ncbi.nlm.nih.gov/pubmed/25313922>.

JOHANSSON, M. U.; ZOETE, V.; MICHIELIN, O.; GUEX, N. Defining and searching for structural motifs using DeepView/Swiss-PdbViewer. **BMC Bioinformatics**, v. 13, n. 1, p. 173, 2012. Disponível em: <http://www.biomedcentral.com/1471-2105/13/173>. Acesso em: 14 out. 2015.

JONATHAN, R. D.; MANIYAN, P. P.; GORDON, A. Z.; KURT, H. N.; THERESA, M. A.; CHERYL, L. S.; CLERCQ, E. De; BALZARINI, J.; ELIAS, K. M.; JAMES, P. S. Cytotoxic 2,6-bis(arylidene)cyclohexanones and related compounds. **Eur. J. Med. Chem.**, v. 35, n. 11, p. 967–977, nov. 2000. Disponível em: <http://www.sciencedirect.com/science/article/pii/S0223523400011739>. Acesso em: 31 dez. 2014.

JONATHAN, R. D.; MANIYAN, P. P.; GORDON, A. Z.; KURT, H. N.; THERESA, M. A.; CHERYL, L. S.; CLERCQ, E. De; BALZARINI, J.; ELIAS, K. M.; JAMES, P. S. Cytotoxic analogues of 2,6-bis(arylidene)cyclohexanones. **Eur. J. Med. Chem.**, v. 38, n. 2, p. 169–177, fev. 2003. Disponível em: <http://www.sciencedirect.com/science/article/pii/S0223523402014447>. Acesso em: 31 dez. 2014.

JONES, S.; THORNTON, J. M. Principles of protein-protein interactions. **Proc. Nat. Acad. Sci.**, v. 93, n. 1, p. 13–20, 9 jan. 1996. Disponível em: <http://www.pnas.org/cgi/content/long/93/1/13>. Acesso em: 8 fev. 2015.

KATSUYAMA, Y.; KITA, T.; FUNA, N.; HORINOUCHI, S. Curcuminoid biosynthesis by two type III polyketide synthases in the herb Curcuma longa. **J. biological. chem.**, v. 284, n. 17, p. 11160–70, 24 abr. 2009. Disponível em: <http://www.pubmedcentral.nih.gov/articlerender.fcgi?artid=2670121&tool=p mcentrez&rendertype=abstract>. Acesso em: 19 dez. 2014.

KAWAI, Y.; SAITOU, K.; HIDA, K.; DAO, D. H.; OHNO, A. Stereochemical control in microbial reduction. XXVIII. Asymmetric reduction of α,β-unsaturated ketones with Bakers' yeast. **Bull Chem Soc Japan**, v. 69, n. 9, p. 2633–2638, 1996.

KESERÜ, G. M.; NÓGRÁDI, M. **Structure and chemistry (part d)**. [s.l.] Elsevier, 1995. v. 17

KONIECZNY, M. T.; KONIECZNY, W.; SABISZ, M.; SKLADANOWSKI, A.; WAKIEĆ, R.; AUGUSTYNOWICZ-KOPEĆ, E.; ZWOLSKA, Z. Acid-catalyzed synthesis of oxathiolone fused chalcones. Comparison of their activity toward various microorganisms and human cancer cells line. **Eur. J. Med. Chem.**, v. 42, n. 5, p. 729–33, maio 2007. Disponível em: <http://www.ncbi.nlm.nih.gov/pubmed/17300856>. Acesso em: 4 nov. 2014.

KREHER UP; AE;, R.; CL;, R.; JL;, S.; STRAUSS CR. Direct Preparation of Monoarylidene Derivatives of Aldehydes and Enolizable Ketones with DIMCARB. **Org. Lett.**, v. 5, n. 17, p. 3107–3110, 2003. Disponível em: <http://pubs.acs.org/doi/abs/10.1021/ol0351145>.

KUMAR, S.; LAMBA, M. S.; MAKRANDI, J. K. An efficient green procedure for the synthesis of chalcones using C-200 as solid support under grinding conditions. **Green. Chem. Lett. and Rev.**, v. 1, n. 2, p. 123–125, jun. 2008. Disponível em: <http://www.tandfonline.com/doi/abs/10.1080/17518250802325993>. Acesso em: 1 nov. 2014.

KUMAR, S. S. D.; SURIANARAYANAN, M.; VIJAYARAGHAVAN, R.; MANDAL, A. B.; MACFARLANE, D. R. Curcumin loaded poly(2-hydroxyethyl methacrylate) nanoparticles from gelled ionic liquid--in vitro cytotoxicity and anti-cancer activity in SKOV-3 cells. **Eur. J. Pharm. Sci.**, v. 51, p. 34–44, 23 jan. 2014. Disponível em: <http://www.sciencedirect.com/science/article/pii/S0928098713003503>. Acesso em: 18 dez. 2014.

LAHTCHEV, K. L.; BATOVSKA, D. I.; PARUSHEV, S. P.; UBIYVOVK, V. M.; SIBIRNY, A. A. Antifungal activity of chalcones: a mechanistic study using various yeast strains. **Eur. J. Med. Chem.**, v. 43, n. 10, p. 2220–8, out. 2008. Disponível em: <http://www.ncbi.nlm.nih.gov/pubmed/18280009>. Acesso em: 27 out. 2014.

LAROCK, R. C. **Comprehensive organic transformations**. 2nd Editio ed. New York: Wiley-VCH, 1999.

LI, J. T. .; YANG, W. Z. .; WANG, S. X. .; LI, S. H. .; LI, T. S. . Improved

synthesis of chalcones under ultrasound irradiation. **Ultrasonics. Sonochem.**, v. 9, n. 5, p. 237–239, out. 2002. Disponível em: <http://linkinghub.elsevier.com/retrieve/pii/S1350417702000792>.

LUO, Z.; TIKEKAR, R. V; NITIN, N. Click chemistry approach for imaging intracellular and intratissue distribution of curcumin and its nanoscale carrier. **Bioconjugate. chem.**, v. 25, n. 1, p. 32–42, 15 jan. 2014. Disponível em: <http://www.ncbi.nlm.nih.gov/pubmed/24328059>.

MAI, C. W.; YAEGHOOBI, M.; ABD-RAHMAN, N.; KANG, Y. B.; PICHIKA, M. R. Chalcones with electron-withdrawing and electron-donating substituents: anticancer activity against TRAIL resistant cancer cells, structure-activity relationship analysis and regulation of apoptotic proteins. **Eur. J. Med. Chem.**, v. 77, p. 378–87, 22 abr. 2014. Disponível em: <http://www.ncbi.nlm.nih.gov/pubmed/24675137>. Acesso em: 24 out. 2014.

MANOHAR, S.; KHAN, S. I.; KANDI, S. K.; RAJ, K.; SUN, G.; YANG, X.; CALDERON MOLINA, A. D.; NI, N.; WANG, B.; RAWAT, D. S. Synthesis, antimalarial activity and cytotoxic potential of new monocarbonyl analogues of curcumin. **Bioorg. & Med. Chem. Lett.**, v. 23, n. 1, p. 112–6, 1 jan. 2013. Disponível em: <http://www.sciencedirect.com/science/article/pii/S0960894X12014473>. Acesso em: 24 dez. 2014.

MASCARELLO, A.; CHIARADIA, L. D.; VERNAL, J.; VILLARINO, A.; GUIDO, R. V. C.; PERIZZOLO, P.; POIRIER, V.; WONG, D.; MARTINS, P. G. A.; NUNES, R. J.; YUNES, R. A.; ANDRICOPULO, A. D.; AV-GAY, Y.; TERENZI, H. Inhibition of Mycobacterium tuberculosis tyrosine phosphatase PtpA by synthetic chalcones: kinetics, molecular modeling, toxicity and effect on growth. **Bioorg & Med. Chem.**, v. 18, n. 11, p. 3783–9, 1 jun. 2010. Disponível em: <http://www.ncbi.nlm.nih.gov/pubmed/20462762>. Acesso em: 1 nov. 2014.

MASUDA, T.; TOI, Y.; BANDO, H.; MAEKAWA, T.; TAKEDA, Y.; YAMAGUCHI, H. Structural Identification of New Curcumin Dimers and Their Contribution to the Antioxidant Mechanism of Curcumin. **J. Agric. Food. Chem.**, v. 50, n. 9, p. 2524–2530, abr. 2002. Disponível em: <http://www.scopus.com/inward/record.url?eid=2-s2.0-0037165538&partnerID=tZOtx3y1>. Acesso em: 30 dez. 2014.

MATSUDA, T.; YAMANAKA, R.; NAKAMURA, K. Recent progress in biocatalysis for asymmetric oxidation and reduction. **Tetra: Asymm**, v. 20, n. 5, p. 513–557, mar. 2009. Disponível em: <http://www.sciencedirect.com/science/article/pii/S095741660900144X>.

Acesso em: 17 jun. 2015.

MATSUSHIMA, A.; SATO, Y.; OTSUKA, M.; WATANABE, T.; YAMAMOTO, H.; HIRATA, T. An enone reductase from Nicotiana tabacum: cDNA cloning, expression in Escherichia coli, and reduction of enones with the recombinant proteins. **Bioorg chem**, v. 36, n. 1, p. 23–8, fev. 2008. Disponível em: <http://www.sciencedirect.com/science/article/pii/S0045206807000636>. Acesso em: 17 jun. 2015.

MIKSTACKA, R.; WIERZCHOWSKI, M.; DUTKIEWICZ, Z.; GIELARA-KORZAŃSKA, A.; KORZAŃSKI, A.; TEUBERT, A.; SOBIAK, S.; BAER-DUBOWSKA, W. 3,4,2′-Trimethoxy-trans-stilbene – a potent CYP1B1 inhibitor. **MedChemComm.**, v. 5, n. 4, p. 496, 2014. Disponível em: <http://xlink.rsc.org/?DOI=c3md00317e>. Acesso em: 8 fev. 2015.

MISHRA, S.; KAPOOR, N.; MUBARAK ALI, A.; PARDHASARADHI, B. V. V; KUMARI, A. L.; KHAR, A.; MISRA, K. Differential apoptotic and redox regulatory activities of curcumin and its derivatives. **Free. Radical. Biology. Medicine.**, v. 38, n. 10, p. 1353–60, 15 maio 2005. Disponível em: <http://www.sciencedirect.com/science/article/pii/S0891584905000407>. Acesso em: 17 dez. 2014.

MOJZIS, J.; VARINSKA, L.; MOJZISOVA, G.; KOSTOVA, I.; MIROSSAY, L. Antiangiogenic effects of flavonoids and chalcones. **Pharm. res**, v. 57, n. 4, p. 259–65, abr. 2008. Disponível em: <http://www.ncbi.nlm.nih.gov/pubmed/18387817>. Acesso em: 23 out. 2014.

MORI, A.; MIYAKAWA, Y.; OHASHI, E.; HAGA, T.; MAEGAWA, T.; SAJIKI, H. Pd/C-catalyzed chemoselective hydrogenation in the presence of diphenylsulfide. **Organ Lett**, v. 8, n. 15, p. 3279–3281, 2006.

MORRIS, G. M.; HUEY, R.; LINDSTROM, W.; SANNER, M. F.; BELEW, R. K.; GOODSELL, D. S.; OLSON, A. J. AutoDock4 and AutoDockTools4: Automated docking with selective receptor flexibility. **J of comput chem**, v. 30, n. 16, p. 2785–91, dez. 2009. Disponível em: <http://www.pubmedcentral.nih.gov/articlerender.fcgi?artid=2760638&tool=pmcentrez&rendertype=abstract>. Acesso em: 17 out. 2014.

MOTIUR, R. A. F. M. .; JEONG, B. S. .; KIM, D. H. .; PARK, J. K. .; LEE, E. S. .; JAHNG, Y. A facile synthesis of α,α′-bis(substituted-benzylidene)-cycloalkanones and substituted-benzylidene heteroaromatics: utility of NaOAc as a catalyst for aldol-type reaction. **Tetrahedron.**, v. 63, n. 11, p. 2426–2431, mar. 2007. Disponível em: <http://www.sciencedirect.com/science/article/pii/S0040402007000543>. Acesso em: 6 nov. 2014.

MURTHY, Y. L. N.; ACHARYULU, P. V. N.; DUBEY, P. K.; SUNDARI, T. T. Synthesis , Characterization and Bioevaluation of New Tetrahydroquinazolines. **J. Kor. Chem. Soc.**, v. 52, n. 3, p. 257–265, 2008.

MV, A. .; K, G. .; M, C. .; R.K, R. .; P, S. . Synthesis and characterization of some curcumin analogue as novel antileishmanial agent. **Rasayan J Chem**, v. 2, n. 2, p. 375–378, 2009. Disponível em: <http://rasayanjournal.co.in/vol-2/issue-2/23.pdf>.

NAKANO, T.; IRIFUNE, S.; UMANO, S.; INADA, A.; ISHII, Y.; OGAWA, M. Cross-condensation reaction of cycloalkanones with aldehyde and primary alcohols under the influence of zirconocene complexes. **J. Org. Chem.**, v. 66, n. 48, p. 2239–2244, 1987.

NIZAM, S.; VERMA, S.; BORAH, N. N.; GAZARA, R. K.; VERMA, P. K. Comprehensive genome-wide analysis reveals different classes of enigmatic old yellow enzyme in fungi. **Sci rep**, v. 4, p. 4013, 2014. Disponível em: <http://www.pubmedcentral.nih.gov/articlerender.fcgi?artid=3915301&tool=pmcentrez&rendertype=abstract>.

NOWAKOWSKA, Z. A review of anti-infective and anti-inflammatory chalcones. **Euro j med chem**, v. 42, n. 2, p. 125–37, fev. 2007a. Disponível em: <http://www.ncbi.nlm.nih.gov/pubmed/17112640>. Acesso em: 23 out. 2014.

NOWAKOWSKA, Z. A review of anti-infective and anti-inflammatory chalcones. **Eur. J. Med. Chem.**, v. 42, n. 2, p. 125–37, fev. 2007b. Disponível em: <http://www.ncbi.nlm.nih.gov/pubmed/17112640>. Acesso em: 23 out. 2014.

OUELLETTE, M.; DRUMMELSMITH, J.; PAPADOPOULOU, B. Leishmaniasis: drugs in the clinic, resistance and new developments. **Drug Resis Updates**, v. 7, n. 4-5, p. 257–266, out. 2004. Disponível em: <http://linkinghub.elsevier.com/retrieve/pii/S1368764604000652>. Acesso em: 19 nov. 2014.

PABON, H. J. J. A synthesis of curcumin and related compounds. **Recueil des Travaux Chimiques des Pays-Bas.**, v. 83, n. 4, p. 379–386, 2 set. 2010. Disponível em: <http://doi.wiley.com/10.1002/recl.19640830407>.

PADHYE, S.; AHMAD, A.; OSWAL, N.; DANDAWATE, P.; RUB, R. A.; DESHPANDE, J.; SWAMY, K. V.; SARKAR, F. H. Fluorinated 2-hydroxychalcones as garcinol analogs with enhanced antioxidant and anticancer activities. **Bioorg. & Med. Chem. Lett.**, v. 20, n. 19, p. 5818–21, 1 out. 2010. Disponível em:

<http://www.sciencedirect.com/science/article/pii/S0960894X10010978>. Acesso em: 6 nov. 2014.

PANAGIOTOU, G.; OLAVARRIA, R.; OLSSON, L. Penicillium brasilianum as an enzyme factory; the essential role of feruloyl esterases for the hydrolysis of the plant cell wall. **J of biotech**, v. 130, n. 3, p. 219–28, 30 jun. 2007. Disponível em: <http://www.sciencedirect.com/science/article/pii/S0168165607003215>. Acesso em: 18 jun. 2015.

PARR, R. G.; YANG, W. **Density-functional theory of atoms and molecules**. [s.l.] Oxford University Press, 1989.

PAVOLINI. Nuova sintesi della Curcumina. **Riv. Ital. Essenze. Profumi. Piante. Officinali.**, v. 19, p. 167–168, 1937.

PER, C.; CLAESON, U. P.; TUCHINDA, P.; REUTRAKUL, V. **Bioactive natural products**. [s.l.] Elsevier, 2002. v. 26

PETROV, O.; IVANOVA, Y.; GEROVA, M. SOCl2/EtOH: Catalytic system for synthesis of chalcones. **Cat. Comm.**, v. 9, n. 2, p. 315–316, fev. 2008. Disponível em: <http://linkinghub.elsevier.com/retrieve/pii/S1566736707002592>. Acesso em: 24 out. 2014.

QI, Z.; LIU, M.; LIU, Y.; ZHANG, M.; YANG, G. Tetramethoxychalcone, a chalcone derivative, suppresses proliferation, blocks cell cycle progression, and induces apoptosis of human ovarian cancer cells. **PloS. one.**, v. 9, n. 9, p. e106206, jan. 2014. Disponível em: <http://www.pubmedcentral.nih.gov/articlerender.fcgi?artid=4152132&tool=pmcentrez&rendertype=abstract>. Acesso em: 1 nov. 2014.

QIN, X.-Y.; CHENG, Y.; CUI, J.; ZHANG, Y.; YU, L.-C. Potential protection of curcumin against amyloid beta-induced toxicity on cultured rat prefrontal cortical neurons. **Neurosci. Lett.**, v. 463, n. 2, p. 158–61, 2 out. 2009. Disponível em: <http://www.sciencedirect.com/science/article/pii/S0304394009009860>. Acesso em: 28 dez. 2014.

QIN, X.-Y.; CHENG, Y.; YU, L.-C. Potential protection of curcumin against intracellular amyloid beta-induced toxicity in cultured rat prefrontal cortical neurons. **Neurosci. Lett.**, v. 480, n. 1, p. 21–4, 9 ago. 2010. Disponível em: <http://www.sciencedirect.com/science/article/pii/S0304394010006671>. Acesso em: 28 dez. 2014.

RAINEY P, SANTI DV. Metabolism and mechanism of action of formycin B

in Leishmania. **Proc. Nati Acad. Sci. USA**, v. 80, n. January, p. 288–292, 1983.

REDDY, M. V. B.; SU, C.-R.; CHIOU, W.-F.; LIU, Y.-N.; CHEN, R. Y.-H.; BASTOW, K. F.; LEE, K.-H.; WU, T.-S. Design, synthesis, and biological evaluation of Mannich bases of heterocyclic chalcone analogs as cytotoxic agents. **Bioorg. & Med. Chem.**, v. 16, n. 15, p. 7358–70, 1 ago. 2008. Disponível em: <http://www.ncbi.nlm.nih.gov/pubmed/18602831>. Acesso em: 4 nov. 2014.

RICHARD E. WILLIAMS AND NEIL C.BRUCE. "New uses for an Old Enzyme" – the Old Yellow Enzyme family of flavoenzymes. **Microbiology**, v. 148, p. 1607–1614, 2002.

ROJAS, J.; PAYÁ, M.; DEVESA, I.; DOMINGUEZ, J. N.; FERRÁNDIZ, M. L. Therapeutic administration of 3,4,5-trimethoxy-4'-fluorochalcone, a selective inhibitor of iNOS expression, attenuates the development of adjuvant-induced arthritis in rats. **Naunyn-Schmiedeberg's. arch. pharmacol.**, v. 368, n. 3, p. 225–33, set. 2003. Disponível em: <http://www.ncbi.nlm.nih.gov/pubmed/12904830>. Acesso em: 3 nov. 2014.

ROMANELLI, G.; PASQUALE, G.; SATHICQ, Á.; THOMAS, H.; AUTINO, J.; VÁZQUEZ, P. Synthesis of chalcones catalyzed by aminopropylated silica sol–gel under solvent-free conditions. **J. Molecular. Catalysis A: Chemical.**, v. 340, n. 1-2, p. 24–32, abr. 2011. Disponível em: <http://linkinghub.elsevier.com/retrieve/pii/S1381116911000926>. Acesso em: 1 nov. 2014.

ROUGHLEY, P. J.; WHITING, D. A. Experiments in the Biosynthesis of Curcumin. **J. Chem. Soc, Perkin. Transactions 1.**, p. 2379, 1 jan. 1973. Disponível em: <http://pubs.rsc.org/en/content/articlehtml/1973/p1/p19730002379>. Acesso em: 17 dez. 2014.

S.F.P. BRAGA; ALVES, É. V. P.; FERREIRA, R. S.; FRADICO, J. R. B.; LAGE, P. S.; DUART, M. C.; RIBEIRO;, T. G.; JÚNIOR, P. S.; ROMANHA, A. J.; TONINI, M. L.; STEINDEL;, M.; COELHO, E. F.; OLIVEIRA, R. B. Synthesis and evaluation of the antiparasitic activity of bis-(arylmethylidene) cycloalkanones. **Eur. J. Med. Chem.**, v. 71, p. 282–9, jan. 2014. Disponível em: <http://www.ncbi.nlm.nih.gov/pubmed/24321832>. Acesso em: 16 out. 2014.

SAHU, K. N. .; BALBHADRA, S. S. .; CHOUDHARY, J. V. .; KOHLI, D. Exploring Pharmacological Significance of Chalcone Scaffold: A Review. **Curr. Med. Chem.**, v. 19, n. 2, p. 209–225, 1 jan. 2012. Disponível em:

<http://www.eurekaselect.com/openurl/content.php?genre=article&issn=0929-8673&volume=19&issue=2&spage=209>.

SAIJUN, F.; PEIXUN, L. A Combined Experimental and Computational Study of Vam3, a Derivative of Resveratrol, and Syk Interaction. **Int. J. Mol. Sci.**, v. 15, p. 17188–17203, 2014.

SALEHI, P.; DABIRI, M.; ZOLFIGOL, M. A.; ALI, M.; FARD, B. Silica sulphuric acid as an efficient and reusable reagent for crossed aldol condensation of ketones with aromatic aldehydes under solvent free condition. **J. Braz. Chem. Soc.**, v. 15, n. 5, p. 773–776, 2004.

SALEHI, P.; KHODAEI, M. M.; ZOL, M. A.; KEYVAN, A. Solvent-Free Crossed Aldol Condensation of Ketones with Aromatic Aldehydes Mediated by Magnesium Hydrogensulfate. **Monatshefte. fur. Chemie.**, v. 133, p. 1291–1295, 2002.

SANTOS;, G. dos; M;, R.; RODRIGUES-FO, E. Meroterpenes from Penicillium sp found in association with Melia azedarach. **Phytochem**, v. 61, n. 8, p. 907–912, dez. 2002. Disponível em: <http://www.sciencedirect.com/science/article/pii/S0031942202003795>. Acesso em: 17 jun. 2015.

SASHIDHARA, K. V; KUMAR, A.; KUMAR, M.; SARKAR, J.; SINHA, S. Synthesis and in vitro evaluation of novel coumarin – chalcone hybrids as potential anticancer agents. **Bioorg. & Med. Chem. Lett.**, v. 20, n. 24, p. 7205–7211, 2010. Disponível em: <http://dx.doi.org/10.1016/j.bmcl.2010.10.116>.

SCHNEIDER, O. N.; GORDON, C. . Vanillin and ferulic acid are not the major degradation products of curcumin. **Trends. Mol. Med.**, v. 18, n. 7, p. 361–364, 2012. Disponível em: <http://www.ncbi.nlm.nih.gov/pmc/articles/PMC3739485/>.

SEBTI, S.; SOLHY, A.; SMAHI, A.; KOSSIR, A.; OUMIMOUN, H. Dramatic activity enhancement of natural phosphate catalyst by lithium nitrate. An efficient synthesis of chalcones. **Cat. Comm.**, v. 3, n. 8, p. 335–339, ago. 2002. Disponível em: <http://linkinghub.elsevier.com/retrieve/pii/S1566736702001371>.

SHARMA, A.; CHAKRAVARTI, B.; PRASAD, M.; SIDDIQUI, J. A.; KONWAR, R.; TRIPATHI, R. P. Synthesis and anti breast cancer activity of biphenyl based chalcones. **Bioorg & Med. Chem.**, v. 18, n. 13, p. 4711–4720, 2010. Disponível em: <http://dx.doi.org/10.1016/j.bmc.2010.05.015>.

SHEN, L.; JI, H.-F. The pharmacology of curcumin: is it the degradation

products? **Trend. molecular. med.**, v. 18, n. 3, p. 138–44, mar. 2012. Disponível em: <http://www.ncbi.nlm.nih.gov/pubmed/22386732>. Acesso em: 13 dez. 2014.

SHERMAN W; T;, D.; MP;, J.; RA;, F.; R., F. Novel Procedure for Modeling Ligand/receptor Induced Fit Effects. **J med chem**, v. 49, n. 2, p. 534–53, 26 jan. 2006. Disponível em: <http://pubs.acs.org/doi/pdf/10.1021/jm050540c>. Acesso em: 4 ago. 2015.

SHETTY, D.; KIM, Y. J.; SHIM, H.; SNYDER, J. P. Eliminating the heart from the curcumin molecule: monocarbonyl curcumin mimics (MACs). **Molecules.**, v. 20, n. 1, p. 249–92, jan. 2015. Disponível em: <http://www.pubmedcentral.nih.gov/articlerender.fcgi?artid=4312668&tool=pmcentrez&rendertype=abstract>. Acesso em: 19 mar. 2015.

SHI, W.; DOLAI, S.; RIZK, S.; HUSSAIN, A.; TARIQ, H.; AVERICK, S.; L'AMOREAUX, W.; EL LDRISSI, A.; BANERJEE, P.; RAJA, K. Synthesis of monofunctional curcumin derivatives, clicked curcumin dimer, and a PAMAM dendrimer curcumin conjugate for therapeutic applications. **Org. lett.**, v. 9, n. 26, p. 5461–4, 20 dez. 2007. Disponível em: <http://www.ncbi.nlm.nih.gov/pubmed/18020348>.

SHIGEO, T. .; YOICHI, S. .; KATSUSHI, M. .; YUKIHIRO, T. .; YOSHIHIKO, W. .; GISHO, H. .; MAMORU, T. .; TIKASHI, O. .; TORU, M. .; TOSHIAKI, U. .; MIKIO, S. .; NAOTAKA, N. .; WASUKE, K. .; YOSHIKI, K. .; YASUMASA, I. Influence of Natural and Synthetic Compounds on Cell Surface Expression of Cell Adhesion Molecules, ICAM-1 and VCAM-1. **Planta. Med.**, v. 67, p. 108–113, 2001.

SHIMODA, K.; HIRATA, T. Biotransformation of enones with biocatalysts — two enone reductases from Astasia longa. **J Molecul Cat B: Enzymatic**, v. 8, n. 4-6, p. 255–264, fev. 2000. Disponível em: <http://www.sciencedirect.com/science/article/pii/S1381117799000764>. Acesso em: 17 jun. 2015.

SHRIKHANDE, J. J.; GAWANDE, M. B.; JAYARAM, R. V. Cross-aldol and Knoevenagel condensation reactions in aqueous micellar media. **Cat. Comm.**, v. 9, n. 6, p. 1010–1016, mar. 2008. Disponível em: <http://www.sciencedirect.com/science/article/pii/S1566736707004372>. Acesso em: 6 nov. 2014.

SIMON, A.; ALLAIS, D. P.; DUROUX, J. L.; BASLY, J. P.; DURAND-FONTANIER, S.; DELAGE, C. Inhibitory effect of curcuminoids on MCF-7 cell proliferation and structure–activity relationships. **Cancer. Lett.**, v. 129, n. 1, p. 111–116, jul. 1998. Disponível em:

<http://www.sciencedirect.com/science/article/pii/S0304383598000925>.
Acesso em: 31 dez. 2014.

SINGH, D. V.; MISRA, K. Curcuminoids as inhibitors of thioredoxin
reductase: a receptor based pharmacophore study with distance mapping of the
active site. **Bioinformation**, v. 4, n. 5, p. 187–192, 2009.

SINGH, N.; PANDEY, J.; YADAV, A.; CHATURVEDI, V.; BHATNAGAR,
S.; GAIKWAD, A. N.; SINHA, S. K.; KUMAR, A.; SHUKLA, P. K.;
TRIPATHI, R. P. A facile synthesis of alpha,alpha'-(EE)-bis(benzylidene)-
cycloalkanones and their antitubercular evaluations. **Euro j med chem**, v. 44,
n. 4, p. 1705–9, abr. 2009. Disponível em:
<http://www.ncbi.nlm.nih.gov/pubmed/18952325>. Acesso em: 20 out. 2014.

SINGH, R. P.; AGARWAL, R. Mechanisms of action of novel agents for
prostate cancer chemoprevention. **Endocrine-related. Cancer.**, v. 13, n. 3, p.
751–78, out. 2006. Disponível em:
<http://www.scopus.com/inward/record.url?eid=2-s2.0-
33751081567&partnerID=tZOtx3y1>. Acesso em: 31 dez. 2014.

SOLOMON, V. R.; HU, C.; LEE, H. Hybrid pharmacophore design and
synthesis of isatin-benzothiazole analogs for their anti-breast cancer activity.
Bioorg. & Med. Chem., v. 17, n. 21, p. 7585–92, 1 nov. 2009. Disponível em:
<http://www.ncbi.nlm.nih.gov/pubmed/19804979>. Acesso em: 4 nov. 2014.

SOUMYANANDA, C. .; GOPA, D.; VISHNU, D. .; AMLAN, D. .; ASIM, P.
.; GOPAL, C. .; GAUTAM, B. .; PINAK, C. .; AVADHESHA, S. .;
BHABATARAK, B. Stable and Potent Analogues Derived from the
Modification of the Dicarbonyl Moiety of Curcumin. **Biochemistry.**, v. 52, n.
42, p. 7449–7460, 2013. Disponível em:
<http://pubs.acs.org/doi/abs/10.1021/bi400734e>.

SRINIVASAN, B.; JOHNSON, T. E.; LAD, R.; XING, C. Structure-activity
relationship studies of chalcone leading to 3-hydroxy-4,3',4',5'-
tetramethoxychalcone and its analogues as potent nuclear factor kappaB
inhibitors and their anticancer activities. **J. Med. Chem.**, v. 52, n. 22, p. 7228–
35, 26 nov. 2009. Disponível em:
<http://www.ncbi.nlm.nih.gov/pubmed/19883086>. Acesso em: 4 nov. 2014.

STOYANOV, E. V; CHAMPAVIER, Y.; BASLY, J. Efficient Liquid-Phase
Synthesis of 2 -Hydroxychalcones. **Bioorg. & Med. Chem. Lett.**, v. 12, p.
2685–2687, 2002.

STUERMER, R.; HAUER, B.; HALL, M.; FABER, K. Asymmetric
bioreduction of activated C=C bonds using enoate reductases from the old

yellow enzyme family. **Curr opin in chem bio**, v. 11, n. 2, p. 203–13, abr. 2007. Disponível em: <http://www.sciencedirect.com/science/article/pii/S1367593107000233>. Acesso em: 29 nov. 2015.

SUN, L.-P.; LI-XIN, G.; WEI-PING, M.; FA-JUN, N.; JIA, L.; HU-RI, P. Synthesis and biological evaluation of 2,4,6-trihydroxychalcone derivatives as novel protein tyrosine phosphatase 1B inhibitors. **Chemical. biol & drug. design.**, v. 80, n. 4, p. 584–90, out. 2012. Disponível em: <http://www.ncbi.nlm.nih.gov/pubmed/22805439>. Acesso em: 8 fev. 2015.

SURYAWANSHI, S. N.; KUMAR, S.; TIWARI, A.; SHIVAHARE, R.; CHHONKER, Y. S.; PANDEY, S.; SHAKYA, N.; BHATTA, R. S.; GUPTA, S. Synthesis and biological evaluation of a novel series of aryl S,N-ketene acetals as antileishmanial agents. **Bioorg & Med. Chem lett**, v. 23, n. 13, p. 3979–82, 1 jul. 2013. Disponível em: <http://www.sciencedirect.com/science/article/pii/S0960894X13004940>. Acesso em: 21 jul. 2015.

SUSRUTA, S.; DANILO, R. Interaction of Curcumin with PEO–PPO–PEO Block Copolymers: A Molecular Dynamics Study. **J. Phys. Chem. B.**, v. 117, n. 11, p. 3250–3257, 2013.

TEIMOURI;, F.; S;, H. K.; MIRI;, Z.; EFTEKHARI-SIS;, B.; AZIZIAN;, J. Ammonim chloride catalyzed aldol condensation: a facile synthesis of α, α-bis(substituted benzylidene) cycloalkanones. **J. Sci. I. A. U (JSIAU).**, v. 19, n. 72, p. 103–108, 2009.

TOMAR, V.; BHATTACHARJEE, G.; KAMALUDDIN; RAJAKUMAR, S.; SRIVASTAVA, K.; PURI, S. K. Synthesis of new chalcone derivatives containing acridinyl moiety with potential antimalarial activity. **Eur. J. Med. Chem.**, v. 45, n. 2, p. 745–51, fev. 2010. Disponível em: <http://www.ncbi.nlm.nih.gov/pubmed/20022412>. Acesso em: 2 nov. 2014.

TOOGOOD, H. S.; FRYSZKOWSKA, A.; HARE, V.; FISHER, K.; ROUJEINIKOVA, A.; LEYS, D.; GARDINER, J. M.; STEPHENS, G. M.; SCRUTTON, N. S. Structure-Based Insight into the Asymmetric Bioreduction of the C=C Double Bond of alpha,beta-Unsaturated Nitroalkenes by Pentaerythritol Tetranitrate Reductase. **Adv syn & cat**, v. 350, n. 17, p. 2789–2803, 17 nov. 2008. Disponível em: <http://www.pubmedcentral.nih.gov/articlerender.fcgi?artid=2854801&tool=pmcentrez&rendertype=abstract>. Acesso em: 29 nov. 2015.

TOOGOOD, H. S.; GARDINER, J. M.; SCRUTTON, N. S. Biocatalytic Reductions and Chemical Versatility of the Old Yellow Enzyme Family of

Flavoprotein Oxidoreductases. **ChemCatChem**, v. 2, n. 8, p. 892–914, 2010.

TUHIN, B.; SOUMITRA, G.; KARUNA, D.; VARSHA, G.; UDUPI, A. R. DEY, D.; SIDDHARTHA, P. S.; SURYANARAYANARAO, R.; N, V. Targeting Mycobacterium tuberculosis nucleoid-associated protein HU with structure-based inhibitors. **Nature. Chem.**, v. 5, p. 1–12, 2013.

V. LAMPE. Syntheee von Curoumin. **Ber. Dtsch. Chem. Ges.**, v. 51, p. 1347, 1918. Disponível em: <http://onlinelibrary.wiley.com/doi/10.1002/cber.19180510223/abstract;jsessio nid=220618EB4603CD34CDFC11B0C65697CB.f03t03>.

VALERO, G.; RIBÓ, J. M.; MOYANO, A. A Closer Look at Spontaneous Mirror Symmetry Breaking in Aldol Reactions. **Chemistry - A Eur. J.**, v. 20, p. 1–15, 24 out. 2014. Disponível em: <http://doi.wiley.com/10.1002/chem.201404497>. Acesso em: 26 out. 2014.

VENKATESAN, P.; RAO, M. N. A. Structure-activity relationships for the inhibition of lipid peroxidation and the scavenging of free radicals by synthetic symmetrical curcumin analogues. **J. Pharm. Pharmacol.**, v. 52, n. 9, p. 1123–1128, 2000. Disponível em: <http://www.scopus.com/inward/record.url?eid=2-s2.0-0033807753&partnerID=tZOtx3y1>.

W.M. WEBER, L.A. HUNSAKER, S.F. ABCOUWER, L.M. DECK, D. L. V. Anti-oxidant activities of curcumin and related enones. **Bioorg & Med. Chem.**, v. 13, n. 11, p. 3811–20, 1 jun. 2005. Disponível em: <http://www.ncbi.nlm.nih.gov/pubmed/15863007>. Acesso em: 26 out. 2014.

WU, J.-H.; WANG, X.-H.; YI, Y.-H.; LEE, K.-H. Anti-AIDS agents 54. A potent anti-HIV chalcone and flavonoids from genus Desmos. **Bioorg. & Med. Chem. Lett.**, v. 13, n. 10, p. 1813–1815, maio 2003. Disponível em: <http://linkinghub.elsevier.com/retrieve/pii/S0960894X03001975>. Acesso em: 2 nov. 2014.

WU, X.; TIEKINK, E. R. T.; KOSTETSKI, I.; KOCHERGINSKY, N.; TAN, A. L. C.; KHOO, S. B.; WILAIRAT, P.; GO, M.-L. Antiplasmodial activity of ferrocenyl chalcones: investigations into the role of ferrocene. **Euro. J. Pharm. sci**, v. 27, n. 2-3, p. 175–87, fev. 2006. Disponível em: <http://www.ncbi.nlm.nih.gov/pubmed/16269240>. Acesso em: 1 nov. 2014.

WYLLIE, S.; PATTERSON, S.; FAIRLAMB, A. H. Assessing the essentiality of Leishmania donovani nitroreductase and its role in nitro drug activation. **Antimicrob. Agents Chemo**, v. 57, n. 2, p. 901–6, fev. 2013. Disponível em: <http://www.pubmedcentral.nih.gov/articlerender.fcgi?artid=3553740&tool=p mcentrez&rendertype=abstract>. Acesso em: 5 jan. 2015.

YALLAPU, M. M.; KHAN, S.; MAHER, D. M.; EBELING, M. C.; SUNDRAM, V.; CHAUHAN, N.; GANJU, A.; BALAKRISHNA, S.; GUPTA, B. K.; ZAFAR, N.; JAGGI, M.; CHAUHAN, S. C. Anti-cancer activity of curcumin loaded nanoparticles in prostate cancer. **Biomaterials.**, v. 35, n. 30, p. 8635–48, out. 2014. Disponível em: <http://www.sciencedirect.com/science/article/pii/S0142961214007467>. Acesso em: 9 dez. 2014.

YANTO, Y.; WINKLER, C. K.; LOHR, S.; HALL, M.; FABER, K.; BOMMARIUS, A. S. Asymmetric bioreduction of alkenes using ene-reductases YersER and KYE1 and effects of organic solvents. **Organic Letters**, v. 13, n. 10, p. 2540–2543, 2011.

YIM-IM, W.; SAWATDICHAIKUL, O.; SEMSRI, S.; HORATA, N.; MOKMAK, W.; TONGSIMA, S.; SUKSAMRARN, A.; CHOOWONGKOMON, K. Computational analyses of curcuminoid analogs against kinase domain of HER2. **BMC. Bioinformatics.**, v. 15, n. 1, p. 261, jan. 2014. Disponível em: <http://www.scopus.com/inward/record.url?eid=2-s2.0-84906840208&partnerID=tZOtx3y1>. Acesso em: 31 dez. 2014.

YU, H.; HUANG, Q. Enhanced in vitro anti-cancer activity of curcumin encapsulated in hydrophobically modified starch. **Food. Chem.**, v. 119, n. 2, p. 669–674, 15 mar. 2010. Disponível em: <http://www.sciencedirect.com/science/article/pii/S0308814609008887>. Acesso em: 24 nov. 2014.

ZHAO, L.-M.; JIN, H.-S.; SUN, L.-P.; PIAO, H.-R.; QUAN, Z.-S. Synthesis and evaluation of antiplatelet activity of trihydroxychalcone derivatives. **Bioorg. & Med. Chem. Lett.**, v. 15, n. 22, p. 5027–9, 15 nov. 2005. Disponível em: <http://www.ncbi.nlm.nih.gov/pubmed/16169724>. Acesso em: 27 out. 2014.

ZIA, U. D.; FILL, T. P.; ASSIS, F. F. de; LAZARIN, D. B.; KAPLUM, V.; GARCIA, F. .; NAKAMURA, C. V.; OLIVEIRA, K. T.; FILHO, E. R. Unsymmetrical 1,5-diaryl-3-oxo-1,4-pentadienyls and their evaluation as antiparasitic agents. **Bioorg. & Med. Chem.**, v. 22, n. 3, p. 1121–7, 1 fev. 2014. Disponível em: <http://www.ncbi.nlm.nih.gov/pubmed/24398381>. Acesso em: 24 out. 2014.